BIOENGINEERED SKIN GRAFTS FOR CHRONIC WOUNDS USING 3-DIMENSIONAL HYBRID SCAFFOLDS MADE UP OF SILK FIBROIN, FIBRIN COMPOSITE AND AMNION

A THESIS PRESENTED BY

RASHMI R

TO

SREE CHITRA TIRUNAL INSTITUTE FOR
MEDICAL SCIENCES AND TECHNOLOGY
THIRUVANANTHAPURAM
INDIA

IN PARTIAL FULFILMENT OF THE
REQUIREMENTS FOR THE AWARD OF
DOCTOR OF PHILOSOPHY

2020

DECLARATION

I, **Rashmi R**, hereby certify that I had personally carried out the work depicted in the thesis entitled, ***"Bioengineered Skin Grafts for Chronic Wounds using 3-Dimensional Hybrid Scaffolds made up of Silk Fibroin, Fibrin Composite and Amnion",*** except where due acknowledgment has been made in the text. No part of the thesis has been submitted for the award of any other degree or diploma prior to this date.

Thiruvananthapuram — Rashmi R

Date: 07/08/2020 — Reg.No: 2016/PhD/13

SREE CHITRA TIRUNAL INSTITUTE FOR MEDICAL SCIENCES & TECHNOLOGY, BIOMEDICAL TECHNOLOGY WING,
POOJAPPURA, THIRUVANANTHAPURAM – 695012, KERALA, INDIA
(An Institute of National Importance under Govt. of India)
Phone-(91)0471-2520219 Fax-(91)0471-2341814
www.sctimst.ac.in

Dr. Lissy K Krishnan

Scientist G (Senior Grade) & Scientist-In-Charge
Division of Thrombosis Research,
Department of Applied Biology,
Biomedical Technology Wing, SCTIMST,
Poojappura -695012, Thiruvananthapuram, Kerala, India.
Email ID : lissykk@sctimst.ac.in, lissykrs@gmail.com

This is to certify that **Ms. Rashmi R,** in the Division of Thrombosis Research/Department of Applied Biology of this Institute has fulfilled the requirements prescribed for the PhD degree of the Sree Chitra Tirunal Institute for Medical Sciences and Technology, Thiruvananthapuram. The thesis entitled, **"Bioengineered skin grafts for chronic wounds using 3-dimensional hybrid scaffolds made up of silk fibroin, fibrin composite and amnion"** was carried out under my direct supervision. No part of the thesis was submitted for the award of any degree or diploma prior to this date.

* Clearance was obtained from the Institutional Ethics Committee / Institutional Animal Ethics Committee for carrying out the study.

Thiruvananthapuram
Date:

Dr. Lissy K Krishnan
(Research Guide)

The Thesis entitled

BIOENGINEERED SKIN GRAFTS FOR CHRONIC WOUNDS USING 3-DIMENSIONAL HYBRID SCAFFOLDS MADE UP OF SILK FIBROIN, FIBRIN COMPOSITE AND AMNION

Submitted by

RASHMI R

for the degree of

Doctor of Philosophy

of

SREE CHITRA TIRUNAL INSTITUTE FOR MEDICAL SCIENCES AND TECHNOLOGY, THIRUVANANTHAPURAM, INDIA

Is evaluated and approved by

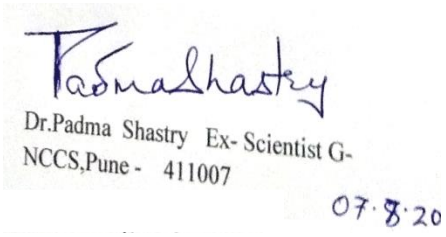

Dr. Lissy K Krishnan
(Research Guide)

Examiner's name
and Designation

Dedicated To My Family,

My Guide Dr. Lissy K Krishnan & My Teachers

ACKNOWLEDGEMENTS

It is with immense pleasure and gratitude that I acknowledge the help and support I have received during the entire tenure of my doctoral program. This program has not only helped me in building a scientific temper but has also helped me grow towards being a better person.

I have no words to express my deepest sense of gratitude and respect to my mentor Dr. Lissy K Krishnan, Scientist G, Senior Grade & Scientist-In-Charge, Division of Thrombosis Research, Department of Applied Biology, BMT wing, SCTIMST who offered unremitting support and encouragement throughout the course of study. She was always accessible and willing to help with her advices & suggestions and took momentous effort for the successful completion of this endeavour. I feel extremely fortunate to have had her as my mentor.

I express my sincere gratitude to my Doctoral Advisory Committee (DAC) members Dr. Kalliyana Krishnan V (Dental Products), Dr. Prashanth Varkey (Jubilee Mission Medical College and Research Institute, TCR) and Dr. Srinivas G (Biochemistry) for their timely suggestions and comments which helped in the improvement of the quality of this work. I also take this opportunity to thank Dr. Kalliyana Krishnan V who was also my M.Phil mentor, for teaching me the basics of polymer chemistry, synthesis & characterization and for his continuous support.

I am thankful to the present and former Directors of SCTIMST, Heads of BMT Wing and H.O.Ds of Applied Biology, SCTIMST for providing all the facilities to carry out this work. I am thankful to the present and former Deputy Registrar, Registrar, Dean, Associate Dean of Ph. D. and all members of Academic division & Director's office for their assistance. I also thank all the teaching faculties of my PhD course work.

I wish to thank Kerala State Council for Science, Technology & Environment (KSCSTE) for my research fellowship & SCTIMST for the Travel grant for attending TERMIS International Conference at Charlotte, North Carolina, USA. I would like to thank Technical Research Center for Biomedical Devices (TRC), SCTIMST for the internal project funding provided for PLGCFIBHA (TRC project : 8149) & AMFIBHA (TRC project : 8136) product development.

I whole heartedly thank Dr. Harikrishnan V S, Dr. Arya Anil, Dr. Aishwarya Lekshman, Mr. Manoj, Mr. Sunilkumar, Mr. Sarath, Mr. Pradeep (DLaboratory Animal Science) for Burn wound studies. Dr. Sachin J Shenoy, Mr Manoj and all other staffs (In Vivo Models and Testing) for helping in the Porcine Diabetic wound model studies. Dr. Sabareeswaran A, Ms. Sandhya, Mr. Joseph, Ms. Sreelakshmi (Experimental Pathology) for Histopathology processing and Cryostat training.

I sincerely thank Dr. Biman B Mandel and Ms. Dimple Chouhan (IIT, Guhawati) for providing silk fibroin for the study. I would like to thank Mr. Ranjith S Kartha, Ms. Priyanka Manoj, Mr. Anilkumar V and Ms. Deepa S (TRU) for providing fibrinogen concentrate and

thrombin, which plays a very important role in this study. I would also like to thank Dr. Rema from Gaureesha Hospital, Pattom for placenta & umbilical cord samples, Dr. Tara S (TRU) for training me in HA isolation, Dr. Jayakumar and staff (CVTS, SCTIMST), Dr. Maneesh Senan and staff (KIMS) for supplying adipose tissue & lipoaspirate samples & Blood Blank Division for PRP concentrates for PGF isolations.

I would like to thank Dr. Lizymol PP and all present & former members of DPL and POP for extending facility for polymer synthesis & related experiments, Mr. Ramesh Babu and Staff of Precision fabrication facility and Mr. Rajan for timely fabrication of templates for scaffolds and for burn wounds experiments and Ms. Sreedevi (EtO) & plasma sterilization facility staff of SCTIMST & SUT hospital for sterilization of samples.

I am thankful to Mr. Raj Krishna & Team for the IPR/Patent filing. I am thankful to Dr. Soumya Columbus for training me in electrospinning & Ms Jasmin Joseph for assisting in terpolymer synthesis, Dr. Vibha C and Dr. Deepu DR (Dental Products) for helping me in UTM, FT-IR & Micro-CT evaluations, Dr. Mohanan PV, Dr. Remya NS & team (Toxicology) for toxicological evaluations, Dr. Maya Nandkumar A, Mr Pradeepkumar SS and Ms. Sreeja KR (Microbial Technology) for sterility testing, Dr. Harikrishna Varma PR and Mr. Nishad (Bioceramics) for SEM and ESEM analysis, Mr. Hari, Dr. Radhakumary and Dr. Sasikala (LPA, Central Analytical Facility) for GPC & HPLC and TGA & DSC analysis, Dr.Anoop T and his students (Molecular Medicine) for nanodrop facility, Dr. SanthoshKumar TR and Mr Anurup (RGCB) for confocal analysis, Dr. Naresh Kasoju (Tissue Culture- confocal analysis demo), Ms. Indu and Ms. Arya (RGCB) for flow cytometric analysis and Dr. Umashankar PR & Mr. Premkumar (In Vivo Models and Testing) for training me in Microtome cutting.

I extend my thanks to Dr. Anugya Bhatt and Dr. Renjith P Nair for their guidance. The coorporation from all other colleagues of TRU Ms. Amita Ajit, Ms. Deepa S, Ms. Subha S, Ms. Renu Ramesh, Ms. Krishnapriya Chandrababu, Dr. Tara S, Dr. Unnikrishnan Sivan, Ms. Athulya Ramesh, Ms. Lakshmi TS, Ms. Riya Raju, Mr. Mejo C Korah, Dr. SuvanishKumar, Ms. Safeena, Ms. Rakhi, Ms. Athira, Ms. Karthika, Ms. Hima, Ms. Shilpa, Mr. Hari, Mr. Shibu, Ms. Usha, Ms. Bindhu, Mr. Arun, Mr. Vijith & Ms Gopika Ramesh (POP) are acknowledged. Cooperation from staff of various departments and library of the Institute is remembered. Cordial attitude and support from fellow labmates from other departments of our campus is fondly acknowledged.

I have no words to express my heartfelt gratitude and love to my family members who provided the most precious support. I owe my every thanks and gratitude to my parents Mr. Ramakrishnan PS & Mrs. Geetha TK for the burdens they took on them self and the sacrifices they made to ensure I could navigate through life with minimal difficulty. My grandmothers Chandramathi amma & Lakshmikutti amma, my sister, Ms. Roshni and my husband Mr. Jacob Raju & his family, with their constant love and encouragement have been the most comforting presence in my life. I dedicate this work & every success in my life to them. Finally yet importantly, I am indebted to the Divine spirit which has been a guiding force throughout my life.

TABLE OF CONTENTS

LIST OF FIGURES

LIST OF TABLES

LIST OF ABBREVIATIONS

HA	Hyaluronic acid
AM	Amniotic membrane
PLGC	Poly(L-Lactide-co-Glycolide-co-Caprolactone)
hADMSCs	Human adipose derived mesenchymal stem cells
HUVECs	Human umbilical vein endothelial cells
^{3}T-H	Tritiated thymidine
CD	Cluster of Differentiation
HBBS	Hank's balanced salt solution
FBS	Fetal bovine calf serum
PBS	Phosphate buffered saline
DMEM	Dulbecco's minimal essential medium
SD	Sodium deoxycholate
SDS	Sodium dodecyl sulphate
DAPI	4',6-diamidino-2-phenylindole
MTT	3-(4, 5-dimethylthiazol-2-yl)-2, 5-diphenyltetrazolium bromide
ESEM	Environmental scanning electron microscope
WVTR	Water vapour transmission rate
HPLC	High performance liquid chromatography
FT-IR	Fourier transform infrared spectroscopy
GPC	Gel permeation chromatography
M_n	Number average molecular weight
M_W	Weight average molecular weight
TGA	Thermo gravimetric analysis
DMA	Dynamic mechanical analysis
UTM	Universal testing machine
μ-CT	Micro computed tomography
DCM	Dichloromethane

LIST OF ANNOTATIONS

%	Percentage
*	Significance
<	Less than
>	Greater than
&	And
~	Around
Mg	Milligram
µg/ug	Microgram
ng	Nanogram
µL	Microlitre
mm	Millimeter
µm	Micrometer
nm	Nanometer
mM	Milli Molar
d	Days
min	Minutes
h	Hours
IU	International Unit

SYNOPSIS

Chronic wounds represent a significant burden to the quality of the patient's life and health care resources. Large sized acute and chronic wound regeneration is a major concern worldwide. According to WHO, about 11 million people seek medical treatment for curing chronic wounds and ~3,00,000 people die from burns each year. In India, > 10 lakh people are moderately or severely burnt every year. A further 6.5 million individuals suffer from chronic skin ulcers caused by diabetes mellitus, prolonged pressure or venous stasis. The global wound care market is expected to reach 20.4 billion by 2021 from 17.0 billion in 2016, expecting growth at a compound annual growth rate (CAGR) of 3.6 % from 2016 to 2021.

Currently, split-thickness autologous skin grafting is the clinical 'gold standard' treatment to restore the primary barrier function of skin. Formation of morbid, non-healing secondary injury in the case of diabetic patients, non-availability of required size, pain, scarring, slow healing, infection, high-cost and post operative complications are major limitations for following this treatment modality. Use of allograft is another option; but, facing major drawback of graft rejection, transmission of diseases and immune reactions due to inclusion of cadaveric components is a problem. Recent advances in tissue engineering using biocompatible materials have led to more complex biological skin equivalents that may yield better treatment options for patients. However, major hurdles, involving cell-based tissue engineering and associated cell-based therapies, are complicated regulatory and financial difficulties causing delayed clinical translation and commercialization. Such limitations have led to the quest of non-cellular dermal substitutes for regenerative medical applications in general and skin wound healing application in particular. Such products could be designed with capability to attract cells from neighbouring native tissue promoting cell adhesion and proliferation. Primary specification of such products should be minimal immune rejection, biodegradable- resorbed by body's natural proteolytic pathways, easy to apply, promote scar-less healing, stable during storage, and most importantly cost effective. Currently, such qualities are not met by any single commercial product. Hence an

absorbable and non-immunogenic matrix as skin substitute that can guide wound regeneration pose scope in the wound care product market.

Therefore, this study conceptualized design of a suitable combination scaffold meeting defined primary requirements and having biomimetic matrix for improved cell adhesion/migration supported by a mechanically strong, biocompatible scaffold. Hyaluronic acid (HA) and fibrin are components of normal or regenerating human skin and are considered as non-immunogenic and degradable matrix in this study. Three different compliant scaffolds were studied in parallel for supporting human derived FIB-HA matrix: electrospun terpolymer Poly(L-Lactide-co-Glycolide-co-Caproactone)/PLGC made of biodegradable FDA approved monomers - L-lactide, L-glycolide and Ɛ-caprolactone, a processed human derived biological matrix such as amniotic membrane/ amnion (AM) and pure non-immunogenic but xenogenic biopolymer such as silk fibroin (SF). Performance of the combination scaffolds in the context of *in vitro* tissue engineering and *in vivo* skin regeneration was the major criteria evaluated. The evaluations emphasized on mechanisms and modulations of skin regenerations to qualify one or more products. Other aspects considered were availability of raw materials, cost-effective production and both microbial/toxicological safety.

The research thesis is divided into 5 major chapters. Chapter 1, introduces the topic of research with sufficient background about the skin biology, giving emphasis to homeostasis and wound healing. Problems of non-healing chronic wounds are highlighted briefly and current strategies employed for wound care are described with major limitations. The rationale for selecting the topic of research is elaborated and specific problem is defined. Based on these background, the developed research hypotheses states that ‘non-immunogenic and pliable skin substitutes with suitable physiochemical & biological properties may be fabricated by combining fibrin-HA matrix with natural/synthetic biomaterials and validated by *in vitro* dermal tissue construction followed by further evaluation *in vivo* in cell-free guided wound regeneration applications. To prove the hypothesis, four major objectives have been set which are listed below:

Objective 1: To design different hybrid scaffolds using AM / PLGC / SF in combination with biomimetic fibrin-HA based matrix for skin tissue engineering.

Objective 2: To validate suitability of AMFIBHA, PLGCFIBHA and SFFIBHA hybrid scaffolds for promoting dermal like tissue generation *in vitro* using stem cell (hADMSCs) derived fibroblasts.

Objective 3: To compose an injectable or insitu forming hydrogel system using SF and FIBHA for applications in different wound healing indications.

Objective 4: To establish suitability of suture-less application of developed hybrid scaffolds for guiding regeneration of large-sized wounds caused by full thickness burns in rabbits or acute excisions in diabetic porcine models.

The chapter also describes rationale for selection of materials with brief description of different biomaterials highlighting advantages of using these materials, based on previous study reports.

In chapter 2, current literature in the field of research topic has been reviewed extensively to understand various strategies adopted for wound healing. The reviewed topics include problems associated with healing chronic wounds, strategies adopted for development of skin substitutes for treating non healing wounds, skin substitutes available in the market and their limitations, desirable properties of scaffolds for skin tissue engineering, etc. The review highlights merits of fibrin, HA, AM, PLGC and SF in the context of use as tissue engineering scaffold. The principles of *in vitro/in vivo* evaluation methods that may be adopted for validating the effectiveness of tissue engineering scaffolds are also reviewed and discussed.

In chapter 3, description of materials, experimental protocols and instruments employed for the present study are included. This chapter is divided into different subsections. The processing steps involved in obtaining the components of the scaffold are described wherever necessary. SF was processed in the Department of Bioscience and Bioengineering, Indian Institute of Technology, Guwahati (IIT-G) and was obtained as gift for the study. Components of clinical grade fibrin sealant kit was obtained as gift from the Biotherapeutics Development facility of the Institute.

Processing of human AM, purification and characterisation of HA from human umbilical cord, synthesis and electrospinning of PLGC scaffold are part of the study are described in detail. Details of AMFIBHA, PLGCFIBHA and SFFIBHA fabrication and physico-chemical characterization of the components and final product are described. The *in vivo* degradation of the synthetic hybrid scaffold PLGCFIHBA is also described. The evaluation of the hybrid scaffolds were done with human adipose tissue derived mesenchymal stem cells (hADMSCs) derived fibroblasts. Isolation of hADMSCs, differentiation into fibroblasts, isolation of human umbilical vein endothelial cells (HUVEC), their utilization for *in vitro* tissue engineering by long terms culture on developed scaffolds and the analysis for validation of engineered tissue are described. The hybrid scaffolds are evaluated *in vivo* in full thickness rabbit burn and porcine diabetic, wound models. The details of rabbit burn wound model and diabetic porcine model is described with details of tissue analysis carried out to establish regeneration. The cellular and molecular level skin tissue analysis protocols carried out for comparison of skin regeneration in terms of inflammation, epithelisation, angiogenesis, collagen organisation and skin appendages development are also described.

In chapter 4, the results are discussed in the light of defined research hypothesis, objectives and other published literature related to the topic of research. The results obtained during this study are substantiated by illustrations like figures, tables and graphs are presented. First part includes scaffold characterization data which include physic-chemical analysis such as mechanical properties, porosity, water vapour transmission rate (WVTR), swelling properties and micrographs showing gross and structural properties. In the second part, data presented include results of hADMSC and EC characterisation, induction of hADMSC into fibroblasts and characterisation of differentiated cells for its their dermal function, long terms culture and analysis of engineered dermal tissue for cell proliferation, cell phenotype grown and extracellular matrix deposited on scaffolds. The characteristics of the hydrogel system developed is also discussed which is used to encapsulate co-culture system of fibroblast and endothelial cells (EC) to induce angiogenesis in *in vitro* engineered dermal substitute. The *in vivo* results presented include *in vivo* degradation of the

synthetic hybrid scaffold and the results of rabbit burn and porcine diabetic wound models. Histological and immunochemical evidence for tissue regeneration demonstrating epithelialization, angiogenesis, ECM deposition, and skin appendage development are presented. The advantages of all three scaffolds for applications in *in vitro* tissue engineering has been discussed. Also the merits of scaffolds for use as suture-less cell-free skin substitute for guiding cell migration and tissue regeneration has been discussed.

In chapter 5, results of the study are summarised and conclusions are drawn. To summarize, all the three hybrid scaffolds showed appropriate characteristics for skin tissue engineering. The hydrogel system showed promising characteristics which can be used as an injectable system for delivering cells to wound site. The *in vivo* data also proved guided wound regeneration in the presence of the hybrid scaffold in terms of epithelialisation, angiogenesis, ECM organization and skin appendages development. The comparative results between the different scaffolds are given. The limitations of the study have been identified and future prospects are proposed in this chapter to address the gap and clinical use of the developed technology. The citations are listed in the bibliography section. Other supporting documents like acknowledgements, abbreviations and their explanations, table of contents, list of figures & tables are also mentioned.

CHAPTER 1

1. INTRODUCTION

Chronic non-healing wound is a worldwide health problem that has devastating consequences for patients and contributes key costs to healthcare systems and people (Maja *et al.,* 2018). Up to two per cent of the population in developed countries suffers from chronic wounds. Each year, more than 305 million acute, traumatic and burn wounds are recorded and treated globally. That's more than nine times the total number of people around the world living with cancer. In the United States, medical care spends at least US $ 32 billion and as much as $ 96.8 billion annually on wound treatment (Global wound dressing's market 2018-2022 report). India being a diabetes capital, incidence of diabetic ulcers is growing alarmingly. Burns account for 1 % of the global burden of diseases and about 7 million burn incidents occur annually in India alone making burn injuries the second largest group of injuries after road accidents (Muguregowda *et al.,* 2018, Sivamuthu, 2019).

In the event that there are no pharmacological agent available to promote wound healing, use of stem cells for regeneration of chronic wounds have been attempted by many researchers. However, cell based therapies face problems like poor survival of transplanted cells, difficulty in cell proliferation, lack of signals in the wound site for differentiation of stem cells into functional cell types of skin tissue and poor cell homing from neighboring native tissue due to degenerating environment at the chronic wound site etc.; therefore, cell based therapy is still at its infancy. Tissue engineering is considered a more appropriate technology which aims growing tissue on biocompatible scaffolds by long term *in vitro* culture of cells so that the tissue construct could be transferred upon maturation and sutured to the wound site. However, it takes a long time for cells to grow and mature into full thickness skin with all cell types. Other than lacking stem cells required for continuous skin homeostasis process, the *in vitro* grown tissue cannot be non-immunogenic or patient specific, difficultly to store as an off-the shelf product and the tissue need to be sutured and integration with surrounding tissue with vascular connectivity is a major challenge. Therefore, the *in vivo* guided tissue engineering is

considered as a better option in this study. Before standardizing such a technology, it is important to comprehend about the normal anatomy and physiology of skin, wound healing process, chronic wounds and current treatment strategies and their limitations.

1.1. Anatomy and physiology of the normal skin

Skin or the integument is the largest organ of the body, covering about 1.5 - 2 m^2 and comprising approximately 16 % of the total body mass of an average human being. It is continuous, with the mucous membranes lining the body's surface with thickness ranging from about 0.5 to 4 mm. The primary function of the skin is to provide a barrier between the body and the external environment protecting against a range of noxious assaults like UV radiation, mechanical, chemical and biological insults like allergens and microorganisms. Its physical strength and elasticity provide optimal mechanical support; semi-permeability to allow effective exchange of gases and moisture; removal of waste materials and prevention of fluid and electrolytes loss; and act as an important periphery sensing organ through its receptors in touch with the environment sensing stimulation in the form of temperature, pressure, and pain. The skin incorporates all major support systems; blood, muscle and innervation as well as plays important role in immune-surveillance, thermoregulation, melanogenesis, endocrine function and excellent adaptability and self-repairing potential. Together, these help to maintain the homeostasis of the mammalian body and manifests a perfect endeavor of nature (Benson, 2011 & Tobin, 2006).

The skin has a twofold origin: a superficial layer, the epidermis, derived from surface ectoderm, and a deep, thick layer, the dermis, derived from mesenchyme. Skin has an anatomically and functionally distinct layered architecture comprising of more than 8 different types of cells in three distinct layers (Mc Lafferty *et al.*, 2012). They are organized from top to bottom as: a) the epidermis (and its associated appendages, pilosebaceous follicles and sweat glands); b) the dermis, separated from the epidermis by the dermal epidermal junction, and c) the hypodermis.

The upper epidermis layer (0.1 - 0.2 mm) comprises mainly of keratinocytes and also harbors a number of other cell populations, such as melanocytes,

langerhan's cells, merkel cells, etc to form a well stratified, continually differentiating non-vascularized tissue that provides vital barrier function of skin (Kanitakis, 2002). Depending on the stage of keratinocyte differentiation, epidermis can be subdivided into 4-5 distinct cellular strata- the basal cell layer (stratum basale or stratum germinativum), the squamous cell layer (stratum spinosum), the granular cell layer (stratum granulosum) and the cornified or horny cell layer (stratum corneum) (James *et al.,* 2006 & Murphy, 1997). As the self-renewing population of keratinocytes in lowermost stratum basale progressively matures, they undergo changes in morphology, lose their nuclei, and fuses to form stratified keratinized layers that are routinely desquamated from skin surface and provide for the renewal of the outer epidermis. Specialized lipids and intercellular junctions in epidermis viz. desmosomes, adherens junctions, tight junction, and gap junction contribute to barrier function of skin and control evaporative water loss (Bazzoni & Dejana, 2002). Keratinized proteins that are abundant in uppermost stratum corneum protect the underlying tissue against mechanical and chemical insults.

Below the epidermis lies the dermis, the rich connective tissue matrix that stabilizes skin against mechanical forces and play significant roles in wound healing (Schultz *et al.,* 2005). The interface between the epidermis and dermis is formed by a porous basement membrane zone that allows the exchange of cells and fluid and holds the two layers together (James *et al.,* 2006). The dermal-epidermal junction acts as support for the epidermis, establishes cell polarity and direction of growth, directs the organization of the cytoskeleton in basal cells, provides developmental signals, and functions as a semi permeable barrier between layers. The thickness of dermis varies according to the location of skin. Collagen, mostly type I and III, represents 70 % of the skin‘s dry weight constitutes the major portion of ground substance and is a major stress-resistant material of the skin which provides appreciable tensile strength to tissue (Kolarsick, 2011). Elastin, on the other hand, though make up only a minor proportion of bulk tissue, play key role in providing resilience and suppleness to skin. These proteins are further inter/intra molecularly cross-linked and associated with proteoglycans to form macromolecular complexes that meet up specific physiological requirements (Starcher *et al.,* 2005). The cellular

components of dermis include fibroblasts, monocytes or macrophages, and mast cells. The dermal layer supports abundant vasculature, lymphatics, cutaneous nerves, sensory receptors, and appendages (eg: hair follicles sweat glands, sebaceous, apocrine, and eccrine glands), that contribute to important skin functions such as sensation, contractility, lubrication and thermoregulation. In fact the epidermal layer being devoid of a vascularized network, rely on dermal capillaries for nutrient supply. The dermis interacts with the epidermis collaborate during development in the morphogenesis of the dermal-epidermal junction and epidermal appendages and interact in repairing and remodeling the skin as wounds are healed (Chu, 2008).

The epidermis and dermis are connected by a specialized acellular fibrous extracellular matrix (ECM) element called basement membrane that comprises of various two layers- the basal lamina and reticular lamina (Chan,1997). These layers are attached to each other via anchoring fibrils (type VII collagen fibers) and microfibrils (fibrillin). The basal lamina can be further be differentiated into two layers- upper lamina lucida and lower lamina densa (Briggaman, 1975 & Douglas, 1993). The matrix proteins actively regulate the epidermal mesenchymal interactions and are essential for secure attachment of epidermis and dermis. In adddition, the basement membrane also controls keratinocyte behavior by influencing cellular polarity, proliferation, migration and differentiation (Leblond, 1989).

The hypodermis forms a subcutaneous tissue of fat and connective tissue that houses larger blood vessels and nerves. This layer varies in thickness depending on the skin site and from person to person. The main cell types are fibroblasts, macrophages and adipocytes (the hypodermis contains 50 % of body fat). Fat serves as padding and insulation for the body (James *et al.*, 2006).

1.2. Wound

Wounds are breaches in the structure of the skin which leads to compromised health and immunity. It is defined as disruption of cellular, anatomical, and functional continuity of a living tissue. It may be produced by physical, chemical, thermal, microbial, mechanical or immunological insult to the tissue or for many reasons,

including disorders, acute trauma, chronic wounds, or even surgical interventions. Wounding affects all the functions of the skin ie protection, regulation and sensation.

Wounds are generally classified into two categories acute and chronic wounds, based on the healing response. Acute wounds are caused by trauma, lacerations, burns (wounds with tissue loss) or surgery (without tissue loss) healing proceeds in an orderly and timely restoring the anatomical and functional property of the injured site; whereas chronic wounds are the outcomes of diseases such as diabetes, tumors, etc and take long time to heal (more than 12 weeks in the range 4 weeks up to more than 3 months). Chronic wounds fail to regenerate naturally, and often heal by fibrotic tissue formation with compromised structure, function and mechanical properties (Meaume, 2002 & Thakur *et al.,* 2011). Wounds are also classified by the layers involved: a) superficial wounds involve only the epidermis, b) partial thickness wounds – involve injured epidermis and a fully or partially intact dermis, contain healing pre-cursors and are conveniently healed by re-epithelialization (Wooldridge, 1980) and c) full thickness wounds, being fully depleted of dermis and skin appendages, have to rely on granulation tissue formation prior to re-epithelialization. Based on their appearance, wounds are again classified into: epithelializing (clean, medium to high exudates), granulating (clean, exudating), slough-covered and necrotic (dry) wounds. Based on the causative aetiologies, the wound healing society classifies chronic wounds into four categories: pressure ulcers, diabetic ulcers, venous ulcers and arterial insufficiency ulcers (WHS, 2006).

However, if the wound size is large (> 4 cm diameter) the wound fails to regenerate naturally and often heals by non-functional fibrotic tissue formation. It also takes significantly higher time for wound closure that makes the lesion highly prone for bacterial infestation that often leading to morbidity. Other factors like wound drying, tissue death or signs of circulation impairment, presence of pathology etc can influence the healing time and create a complex wound, thus making wound care and management a great clinical challenge (Swaim *et al.,* 2001).

1.3. Biology of wound healing

The wound healing process is classically defined as a series of continuous, sometimes overlapping and interactive process involving soluble mediators, blood cells, ECM, and parenchymal cells. Wound healing is a process whereby an injured tissue is repaired, resulting in regeneration of its cell lining with the reorganization of the deep tissue components into scar. The healing response involves consecutive cascade of biological events : haemostasis, inflammation, proliferation, epithelialization, maturation, wound contraction and ECM reorganization of the scar tissue (Li *et al.*, 2007) (Figure 1).

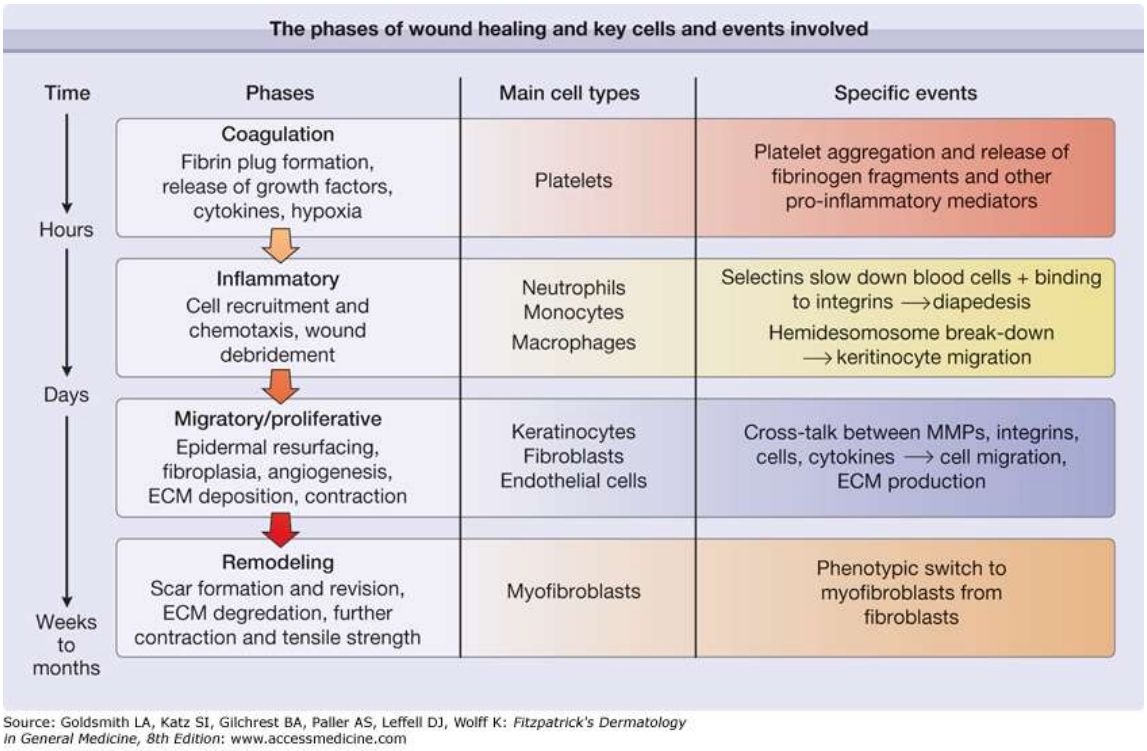

Figure 1. Phases of wound healing

1.4. Impairment of wound healing

Skin regenerate continuously and homeostasis take place with the help of stem cells that reside in the skin. In the event of small sized acute wounds, regeneration of skin takes place in short span of time due to the regenerative ability of skin. Acute wounds heal through the routine processes of inflammation, tissue formation, and

remodelling, which occur in a timely fashion. But when the wound size increases and the local environment are not favourable, healing gets delayed. Prolonged delay in any of these reparative processes of wound healing may result in the formation of a chronic wound (Singer & Clark, 1999).

Chronic wounds are characterized by prolonged inflammation with excessive levels of proinflammatory cytokines, proteases such as matrix metallo proteases (MMPs), elastase and plasmin, reactive oxygen species (ROS), persistent infection, decreased activity of TIMPs, α1- protease inhibitor and α2 – macroglobulin, senescent cell populations with impaired proliferative and secretory capacities, aberrant cellular phenotypes ,defective MSCs, neuropathy and impaired angiogenesis (Mast & Schultz, 1996, Lobmann *et al.,* 2002). Evidence of collagen degradation in chronic wounds has largely been correlated with levels of MMP. MMP activity has been reported to be elevated by 30 fold in chronic wounds (Trengove *et al.,* 1999). Thus, the milieu for wound healing is lost in the case of chronic wounds and do not close without interventions. There is no effective therapeutic option available to enhance the healing or for conditioning the milieu. Despite the magnitude of the problem, years of investigation and significant resources invested in research, the exact pathophysiology of these wounds is not clear.

1.5. Current strategies for treating chronic wounds

Most of the minor wounds are healed by simple contraction and growth of the cells inside the wound. However, the large skin wounds take much longer to heal and hence are more prone to possibilities such as inflammation, infection, scar formation, etc., which marks in the formation of chronic wounds. The incidence of chronic wounds is expected to increase as the population ages. The impact of chronic wounds on the health and quality of life of patients and their families should not be underestimated. Various pathologic conditions result in chronic wound development, including arterial or venous insufficiency, diabetes, undue skin pressure, presence of a foreign body, inflammation, immunocompromised status of the body and infection. It is extremely important to incorporate these factors while engineering various grafts in the field of skin tissue regeneration.

Conventional therapeutic options available for boosting wound regeneration are limited. Immediate wound coverage is one of the keystones of wound management. Standard wound care involves patient and wound assessments, offloading, debridement of necrotic and infected tissue, treatment with antibiotics, and regular wound dressing changes, hyperbaric oxygen therapy, ultrasound and electromagnetic therapy, vacuum-assisted closure therapy (VAC therapy), etc. Currently, autologous skin grafting is the clinical 'gold standard' treatment to restore the primary barrier function of skin. Unfortunately, this procedure has drawbacks like donor site morbidity, formation of secondary injury in the case of diabetic patients, extended healing periods, size limitations especially in large body surface area, prolonged medication and high cost. Another option is the use of allografts, where commercially available skin allografts face major drawback of graft rejection as many constructs contain cadaveric components provoking immune reactions and are also associated with transmissible diseases. Hence these limitations have led to the search for alternatives and development of advanced substitutes (Lesher *et al.,* 2011). However, most of them are costly and result in relatively poor cosmetic outcomes. Furthermore, cell therapies have complicated regulatory and financial hurdles to overcome, prior to commercialization. Ideally, bio-artificial skin should be cost-effective, readily available, non-toxic, slowly biodegradable and highly compatible.

1.6. Development of biocompatible skin substitutes

Among the tissue engineered organs, skin was the first engineered organ that went from laboratory research to patient care (Rheinwald *et al.,* 1989). Skin substitutes are heterogeneous group of wound coverage materials that aid in would closure and replace the functions of the skin, either temporarily or permanently, depending on the product characteristics. These substances are alternatives to the standard wound coverage in circumstances when standard therapies are not desirable.

Tissue-engineered skin substitutes are classified into three categories (i) on the basis of material: biological, synthetic and bio-synthetic; (ii) on the basis of covering time: temporary and permanent and (iii) on the basis of the layer :

epidermal, dermal and bilayered skin substitutes. Over the last two decades, significant improvement has been done for the development of bio-engineered skin and various bio-engineered skin substitutes are commercially available for clinical application. Tissue-engineered skin includes cells delivered on their own, cells delivered within two or three-dimensional (2 / 3-D) biomaterials, biomaterials for replacement of the skin's dermal layer (both with and without cells), and biomaterials to support the replacement of both the epidermis and dermis. However, the selection of suitable bio-material, fabrication technique, identification of cell lines and physiological condition for the regeneration of neo-skin tissue is an active area of research. A suitable biomaterial is crucial in the development of functional engineered tissues. Engineering skin substitutes by tissue engineering approach has relied upon the creation of 3-D scaffolds as ECM analog to guide cell adhesion, growth, and differentiation to form skin-functional and structural tissue. The fabrication methodologies for 3-D scaffolds involve freeze-drying, phase separation, self-assembly, particle leaching, decellularized matrix, radiation crosslinking, electrospinning, photo-polymerization processes, microfluidic assembly, 3-D bioprinting and extrusion-based techniques such as 3-D fiber deposition. Till date, in the market, a lot of tissue engineered products (scaffolds) are available such as Integra and Biobrane (bio-synthetic); Alloderm, SureDerm and GraftJacket (allogeneic); OrCel, Apligraf, Matriderm, Permacol and Oasis (xenogeneic), etc. Extensive research has been done on the fabrication of bioengineered skin and to overcome the limitation of the commercially available products.

1.7. Major concerns of the current skin substitutes

Recent advances in tissue engineering have led to complex biological skin equivalents that may yield suitable wound treatment options for patients. Majority of these products are generally comprised of a polymer scaffold seeded with human fibroblasts/keratinocytes or a combination of both; cultured *in vitro* prior to application. Most biological based products contain bovine, porcine, or human constituents and thus have chance of disease transmission apart from religious and ethical considerations (Enoch *et al.,* 2006). Poor angiogenesis and scar formation are the other major concern (Metcalfe & Ferguson, 2007). Mostly such products do not

have the capability to attract cells from neighbouring native tissue, promote cell adhesion and proliferation, are prone to immune rejection, do not get resorbed by body's natural proteolytic pathways, not easy to apply, and often promote scar upon healing, are not available as off the shelf stable product, and most importantly are very expensive. While *in vitro* tissue engineering faces many hurdles, *in vivo* guided tissue engineering matrices are of great advantage.

1.8. Definition of problem

In order to develop suitable skin substitute, major strategy that can be employed is to use components of natural wound healing matrix. The advantages of such biomimetic properties of easily obtainable matrix components may be exploited for fabricating skin substitutes. However, natural biological materials alone may not have the required mechanical strength to be used as skin substitutes. The skin substitute should have required mechanical strength to prevent wound contraction and at the same time possess many different biological functions to promote cell migration, proliferation, regeneration of complete tissue including dermal compartment and epidermal compartment. The matrix components included should have the ability to signal tissue maturation, angiogenesis, development of hair follicle and other skin appendages. In order to achieve the suppleness and mechanical strength including elasticity, the deposition of collagen and elastin by the dermal fibroblast in a regulated manner may be induced by the matrix components included in the skin substitute. When biological molecules selected as constituents of the skin substitutes, to prevent adverse immune response, human origin molecules are preferable. For clinical translation of the substitute, the parameters to be considered are ease of application and the degradation of the substitute for easy replacement by the regenerating tissue. In order to improve the mechanical properties of the skin substitute, biological molecules may be combined with synthetic or natural biomaterials that have better mechanical properties. In either case, the biomaterial used should be biodegradable so that it is replaced by the regenerating tissue. The biomaterial degradation products should not cause any immune reaction and also get eliminated by body's natural clearance mechanism. So several such requirements need to be addressed to develop a suitable skin substitute. Also, as the requirement of

skin substitute is for different indications such as chronic burn wounds, diabetic wounds or acute surgical wounds, different types of substitutes may be required, depending on the nature and pathophysiology of the wound.

1.9. Development of hypothesis

The natural wound healing matrix in physiology includes fibrin and other matrix components including hyaluronic acid (HA). Exogenous fibrin with other ECM components can also favor the wound healing process when the wound is not able to regenerate by natural physiological process. It can facilitate the growth of collagen-producing fibroblasts and is completely absorbable (Michel *et al.,* 1990). Exogenous fibrin promotes hemostasis which will stabilize the substitute, facilitate graft nutrition by serum imbibition (plasmatic circulation) with subsequent in-growth of vascular buds (neovascularization) and promote angiogenesis. Fibrin sealant acts as a template for cellular migration and proliferation and accelerates wound healing. It has added advantage in wound healing and regeneration along with the adhesive property even after lyophilisation. In 2004, Krishnan *et al* demonstrated that when clotted fibrin is lyophilized, it forms a porous wafer and acts as an excellent hemostat which arrest bleeding (Krishnan *et al.,* 2004). Similar effect was seen in acute skin wounds; when the fibrin was allowed to degrade in the natural process, skin regeneration was optimal and the regenerated skin showed normal skin architecture. HA is a naturally occurring glycosaminoglycan (GAG) found in the human skin ECM. HA is considered as one of the key players in the tissue regeneration process which has been proven to modulate inflammation, cellular migration and angiogenesis, which are the main phases of wound healing via specific HA receptors like CD 44, and toll like receptors (Litwiniuk *et al.,* 2016). The water attracting property of HA produces swelling pressure in ECM allowing the rapid diffusion of water-soluble molecules. When given exogenously, it may absorb the exudates from the injured tissue and retain the moisture to support various processes in wound healing which include proteolytic degradation of provisional matrix to increase cell migration and tissue remodeling. It is also a free radical scavenger and an inflammatory regulator. It has pro-angiogenic properties stimulating blood vessel growth and can facilitate the growth and movement of fibroblasts, controls matrix

hydration and osmoregulation (Anilkumar *et al.,* 2011). However, the fibrin-HA wafer did not have the required compliance for application to larger wounds with uneven planes. Therefore, the necessity for combining other biomaterials with fibrin-HA wound healing matrix was recognized.

1.9.1 Biomaterial selection

Three different biomaterials may be considered for combining with fibrin-HA. Each of these candidate material has certain advantages based on which they are selected. The selected biomaterials are synthetic polymer such as poly (L-Lactide-co-Glycolide-co-Caprolactone) / PLGC, decellularized human amniotic membrane / amnion (AM), natural material such as silk fibroin (SF). Each one of them has unique properties and specific advantages for use as component of skin substitute.

Amniotic membrane / Amnion (AM): The wound healing property of AM has been explored and the decellularized AM has been a major attraction in the wound care industry. This biomaterial with wound regeneration potential can be prepared from human placental tissues by decellarization of AM. In the physiological environment, AM degrades into non-toxic and non-immunogenic end products and aids in wound regeneration. U.S. Food and Drug Administration (FDA) have approved several amnion based products and are available in the international market for clinical use. AM based products are dehydrated/decellularized/cryopreserved/injectable membranes like Amniograft, Graftjacket, AmnioFix, EpiFix (MiMedx, AmnioExcel (Derma Sciences), Surgenex, Neox (Amniox Medical), Bioplex (NovastepInc) for wound healing. But a combination product is not available. The major reason for the popularity of AM is due to the presence of various inherently present ECM molecules and growth factors (GFs) that are able to promote skin regeneration. However, the decellularized AM is extremely thin and it is difficult to handle for positioning on the wound bed. Also, it has no hemostatic property as in the case of fibrin and is not able to arrest micro bleeding and tissue exudation. Therefore, by combining decellularized and dried AM with fibrin-HA, a ready to use lyophilized skin substitute with combined properties of both may be developed for suitable application as skin substitute.

Synthetic polymer: Monomers employed in the synthesis of terpolymer Poly (L-Lactide-co-Glycolide-co-Caprolactone) / (PLGC) - L-lactide, glycolide and ε-caprolactone are U.S.FDA approved. In the physiological environment, PLGC degrade into amino acids- lactic acid and glycolic acid, and caprolactone. All the three monomers released from PLGC degrade in the physiological environment into CO_2, O_2, and water. Due to the non-toxic and non-immunogenic nature of the end products, U.S.FDA has approved copolymers synthesized using these monomers for clinical use. For this product, the terpolymer is synthesized using a fast degrading monomer glycolide, moderately degrading L-lactide and long degrading caprolactone. The monomer ratio may be selected to achieve moderate rate of degradation so that no acidic pH of the degradation products glycolic acid and lactic acid will adversely affect the wound healing process. The PLGC may be dissolved in organic solvent and using the technique of electrospinning, fibrous and porous 3-D mats with pliable and compliance to match mechanical properties of native skin for soft tissue substitution can be fabricated.

Natural polymer: Silk fibroin (SF) as a biomaterial began centuries ago, with its use as sutures for wound treatment. In recent years, silk from *Bombyx mori* (silkworm) has been utilized extensively in tissue engineering applications due to its biocompatibility, robust mechanical performance, tunable degradation, ease of processing, sufficient supply, and ease of acquisition from the mature sericulture industry. Due to their excellent performance, SF-based biomaterials have been found suitable for a variety of applications, including wound protection, drug delivery and other biomedical applications (Kundu *et al.,* 2014). SF devices whether native, dissolved or reconstituted do not typically contain cell-binding domains such as those found in collagen, fibronectin, and many other ECM components. SF is hydrophobic due to the β-sheet-rich crystalline network of the core fibroin protein. These two factors couple to severely limit the capacity of native host cells to bind to and interact with implanted silk devices, as neither inflammatory cells like macrophages or reparative cells like fibroblasts are able to attach strongly, infiltrate and resorb the SF devices. This can be solved by the use of other components like fibrin and HA in the composite scaffold.

1.9.2. Hypothesis

The hypothesis of the study is that 'non-immunogenic and pliable hybrid material with suitable physiochemical properties may be developed by combining fibrin-HA matrix with either synthetic or natural biomaterials for composing skin substitutes suitable for both *in vitro* and *in vivo* skin tissue engineering validated by *in vitro* dermal tissue construction followed by further evaluation *in vivo* in cell-free guided wound regeneration applications'.

1.10. Objectives of the study

The major goal of the study is to develop a range of skin substitutes using human fibrin and HA as the important constituents in combination with diverse biomaterials, to identify the most suitable product for clinical use in various indications. To prove the hypothesis, four major objectives have been set which are listed below:

Objective 1: To design different hybrid scaffolds using AM / PLGC / SF in combination with biomimetic fibrin-HA based matrix for skin tissue engineering.

Specific objective 1: To prepare different biomaterials - AM, PLGC & SF for fabrication of hybrid scaffolds and analyze its physico-chemical properties.

Specific objective 2: To fabricate hybrid scaffolds using AM / PLGC / SF in combination with fibrin-HA matrix and analyze its physico-chemical properties.

Objective 2: To validate suitability of AMFIBHA, PLGCFIBHA and SFFIBHA hybrid scaffolds for promoting dermal like tissue generation *in vitro* using stem cell derived fibroblasts.

Specific objective 1: To isolate & characterize human adipose derived mesenchymal stem cells (hADMSCs) for induction to fibroblasts and analyze the dermal functions of the differentiated cells.

Specific objective 2: To validate the dermal tissue generation on AMFIBHA, PLGCFIBHA and SFFIBHA hybrid scaffolds using long term cultures upon seeding ADMSC derived fibroblasts for *in vitro* tissue engineering.

Objective 3: To compose an *in situ* forming / injectable hydrogel system using SF and FIBHA for applications in different wound healing indications.

Specific objective 1: To fabricate cell (fibroblast) encapsulated hydrogel for culture and evaluation as *in vitro* engineered dermal substitute.

Specific objective 2: To encapsulate fibroblast and endothelial *cells* (ECs) and co-culture to induce angiogenesis in *in vitro* engineered dermal substitute.

Objective 4: To establish suitability of suture-less application of the developed hybrid scaffolds and *in situ* forming / injectable hydrogel system for guiding regeneration of large-sized wounds caused by full thickness burns in rabbits or acute excisions in diabetic porcine models.

Specific objective 1: To standardize rabbit burn wound and porcine streptozotocin induced diabetic model.

Specific objective 2: To evaluate potential of AMFIBHA, PLGCFIBHA and SFFIBHA based skin substitutes for guided skin tissue regeneration in 28 d in terms of wound closure, epithelialization, angiogenesis and ECM deposition & organization.

CHAPTER 2

2. LITERATURE REVIEW

Skin substitutes with hemostatic and self-adhesive properties are of great advantage in the management of chronic wounds. The major objective of the study is to design non-immunogenic and pliable skin substitutes with suitable physiochemical & biological properties by combining fibrin-HA matrix with natural/synthetic biomaterials and to validate for *in vitro* dermal tissue construction followed by *in vivo* evaluation in cell-free guided wound regeneration as an off-the-shelf product. Fibrin and HA has been identified as the key ingredient for the skin substitutes developed in this study. Their fragile and non-pliable nature is a drawback. Therefore, combination of fibrin-HA with three distinct biomaterials with unique physicochemical and biological properties with favourable pliability is attempted in this study which in turn will compensate the limitations of each other. The fabricated hybrid scaffold could either be used for *in vitro* tissue engineering or *in vivo* guided tissue regeneration. Therefore, this chapter reviews the strategies used for healing chronic wounds and their limitations, the rationale for selecting biomaterials and methods to evaluate *in vitro* and *in vivo*.

2.1. Skin tissue engineering

Tissue engineering is an interdisciplinary field that applies the principles of engineering and life sciences towards the development of biological substitutes that restore, maintain, or improve tissue function or a whole organ (Langer & Vacanti, 1993). Regardless of the application, the key components for effective tissue engineering are reliable cell source, 3-D scaffold with ECM-like architecture, signalling molecules such as GFs for directing cell differentiation and adhesive proteins for better cell growth.

With the advent of tissue-engineered skin replacements revolutionized the therapeutic potential for recalcitrant wounds and for wounds that are not acquiescent to primary closure. Due to the structural and functional complexity of the skin organ, engineering skin equivalents to normal skin has been challenging. Engineering of biologic skin substitutes has progressed over time from individual applications of skin cells, or biopolymer scaffolds, to combinations of cells and scaffolds for treatment, healing, and closure of acute and chronic skin wounds. Two major approaches, *in vitro* and *in vivo*, have been utilized to develop engineered tissue. The *in vitro* method creates organs in tissue culture or bioreactors for implantation and replacement of diseased or damaged tissue. In contrast, the *in vivo* or guided tissue engineering approach attempts to create an acellular biomaterial that contains clues conductive for tissue cell recruitment into the biomaterial and inductive of cell differentiation to form the needed tissue. Guided tissue regeneration is achieved by designing the material so that only the desired types of cells enter the area and regenerate new tissue. In skin wound care, the scaffold ideally covers the wound initially, and as the regeneration takes place it is gradually degrades. Ideally, tissue-engineered skin replacements should facilitate faster healing and promote the development of a new tissue that bears a close structural and functional resemblance to the uninjured host tissue (Clark *et al.*, 2007).

The production of an engineered tissue *in vitro* requires the use of cells to populate matrices and produce matrix resembling that of the native tissue. The cell sources can be: keratinocytes, fibroblasts, melanocytes, ECs etc, stem cells, skin stem cells, etc. The main successes in this field have come from the use of primary cells, taken from the patient, and used in conjunction with scaffolds to produce tissue for re-implantation. However, culture of these autologous cells takes time, which limits their usefulness, and donor site insufficiency is a problem for patients with large skin defects. Moreover, immune rejection becomes a major problem when an allogeneic source of cells is used. Therefore, these cells are not the best choice for tissue engineering or regenerative medicine. In addition, mature cells from an autologous or allogeneic source are mostly terminally differentiated and, thus, have lost the ability to form new tissues via proliferation and differentiation (Atala, 2012).

Bone marrow-derived MSCs are suboptimal for clinical use due to the required highly invasive aspiration procedure and the decline in both their proliferation and differentiation potential with increasing senescence. Zuk *et al.*, (2002) introduced ADMSCs, a multipotent, undifferentiated, self-renewing progenitor cell population isolated from adipose tissue that is morphologically and phenotypically similar to the MSCs. They have their capacity of paracrine secretion of a broad selection of cytokines, chemokines, and GFs make them highly clinically attractive. More specific, of particular interest are the anti-apoptotic, anti-inflammatory, pro-angiogenic, immunomodulatory, and anti-scarring effects that have been demonstrated for ADMSCs, which make these cells promising candidates for cellular therapy in regenerative medicine (Frese *et al.*, 2016). Differentiation of ADMSC into fibroblasts, keratinocytes and endothelial cells are already proven (Unni *et al.*, 2014) (Table 1).

Source	Inducers	Lineage	Reference
Human adipose-tissue derived stem cells (hADMSCs)	Fibrin-based niche with gelatin (0.2 %), HA (100 μg/mL) (PGF (20 μg/mL), laminin V (25 μg/mL) and EGF (250 ng/mL) along with conditioned medium and cocktail of BMP-4, hydrocortisone, insulin and EGF.	Keratinocytes	Unni *et al.*, 2014; Colazzo *et al.*, 2012
	Fibrin-based niche with gelatin (0.2 %), HA (100 μg/mL), PGF (50 μg/mL), laminin V (25 μg/mL) and EGF (250 ng/mL) along with conditioned medium and L-ascorbic acid (50 μg/mL), IGF-2 (60 ng/mL)	Fibroblasts	
	KGF (10 ng/mL), EGF (20–30 ng/mL) HGF (10 ng/mL)	Keratinocytes	
	Air-liquid interface culture	Keratinocytes	
	Fibrin gel or pellet culture + ascorbate	Keratinocytes	
	Self-assembly culture system	Keratinocytes & Fibroblast	
	VEGF supplementation	Keratinocytes & Endothelial cells	
	Shear stress exposure	Keratinocytes & Endothelial cells	

Table 1. hADMSC induction into skin cells

However, major hurdles involving cell-based tissue engineering and associated cell-based therapies are their complicated regulatory and financial difficulties causing delayed clinical translation and commercialization.

GFs are currently delivered to the wound either topically or by subcutaneous injections. But, their effectiveness is limited due to their short half-life and the presence of proteases in the chronic wound microenvironment. Becaplermin (Regranex™), a recombinant human-PDGF, is the only GF approved by FDA for the treatment of diabetic foot ulcers (Enoch *et al.,* 2006). To overcome this, gene therapy approach was tried to deliver GFs at the wound site, for example PDGF lentiviral vectors were successfully transfected into the regenerating dermis of diabetic wound which enhanced angiogenesis and collagen deposition (Lee *et al.,* 2005), plasmid expressing TGF- β 1 was injected in the wound bed and the results were highly promising (Lee *et al.,* 2004). But the genetic modification is of concern when using gene therapies. Choi *et al.,* (2013) reported regeneration of hair follicles and micro-vessels in full thickness wounds in rat models when treated using placenta derived ECM containing bioactive molecules like EGF, bFGF, TGF-β, PDGF, IGF-1 and VEGF. VEGF incorporated into PLA scaffolds to provide a controlled release of angiogenic signals from a scaffold (Kanczler *et al.,* 2007), bFGF attached to alginate beads enhanced wound healing, etc.

Another crucial factor in tissue engineering is the selection and fabrication of a suitable scaffold. Scaffold serves as an ECM analogue for the cell adhesion, migration, proliferation and tissue regeneration in three dimensions. Biodegradable scaffolds enable the gradual replacement of the scaffold material with host tissue thereby avoiding long term immune responses. Major requirements for a tissue engineered scaffold are optimum porosity characteristics, suitable degradation properties and appropriate mechanical stability while good biocompatibility criteria. Several natural and synthetic polymeric biomaterials are used as scaffolds for skin tissue engineering. The naturally-derived polymers, commonly used natural polymers for skin tissue engineering include proteins of natural extracellular matrices such as collagen, elastin, GAGs, alginate, chitosan, silk fibroin and fibrin (Chen *et al.,* 2002). The natural polymers closely mimic natural cellular environment, thereby

facilitating cell-scaffold interaction. The natural polymers are preferred more, as the synthetic polymers lack the biological cues for cell recognition and proliferation and natural remodelling. But the major limitation of the natural polymers is its poor mechanical strength, availability, unstable material, and batch-to-batch variation in properties and faster degradation. The mechanical strength, degradation rate and porosity of synthetic polymer scaffold can be tailored by selecting appropriate polymer and fabrication technique. Different scaffold fabrication methods include solvent casting/particulate leaching, freeze-drying (lyophilization), gas foaming, electrospinning, bioprinting etc.

Electrospinning is an efficient technique to produce nano and micro diameter fibers by manipulating polymer concentration and various process parameters (Li *et al.*,2002). Electrospun scaffolds have several advantages over the scaffolds synthesised by conventional fabrication techniques. The nano and micro architectural fibers mimic the ECM of the tissue and have the properties like controlled evaporative water loss, excellent oxygen permeability, and enhanced fluid drainage ability due to the porosity of the nanofibrous sheets (Bhattarai *et al.*, 2004, Sundaramurthi *et al.*, 2014). The solid nanofibers are collected onto a static / dynamic grounded collector. The fiber dimensions as well as pore dimensions can be appropriately varied to regulate the regenerative process. Depending upon the cells involved, the fibrous structure can be designed to yield optimum pore size along with the required mechanical properties. In addition to that, integration of cells (Stankus *et al.*, 2006), GFs (Sahoo *et al.*, 2010) can also be done.

2.2. Skin substitutes

Skin substitutes are constantly evolving and new products are often being produced and approved for clinical use. An ideal skin substitute should completely replicate the biology, anatomy and physiology of natural skin. To date, an ideal skin substitute does not exist. But the skin substitutes are required to possess some essential properties and meet certain requirements. Skin substitutes should be ideally be sterile, non-toxic, evoke minimal inflammatory reactivity, easy to handle and apply to the wound site, provide vital barrier function with appropriate water flux, should

readily adhere and have appropriate physical and mechanical properties; undergo controlled degradation. They should adhere to wound surface rapidly and easy to handle, agile to conform to irregular wound surfaces, relatively inexpensive, and facilitate angiogenesis. They should also have a long shelf-life with low storage requirements and stress resistance in engineered skin substitutes. When biomaterials are used for substitutes, they should be biodegradable, repairable, non-toxic, non-immunogenic, and non-inflammatory with low risk of disease transmission. Easy availability, long-shelf life, and user-friendliness make an ideal engineered substitute (MacNeil, 2007; Metcalfe *et al.,* 2007). Additionally, they should incorporate into the host with minimal scar and pain, facilitate tissue generation with angiogenesis and must be cost-effective. The ultimate goal of the skin tissue engineering is to satisfy most if not all of these criteria when producing novel and smart skin replacement therapies (Metcalfe and Ferguson, 2007). Till date, in the market, a lot of tissue engineered products (scaffolds) are available and extensive research has been done on the fabrication of bioengineered skin and to overcome the limitation of the commercially available products.

Majority of commercially available and clinically approved tissue engineered skin-substitutes are cellular therapy, acellular ECM constructs and composite cell-seeded matrix. Skin substitutes can be classified into different types based on cellularity - acellular/cellular, layering - single layer/bilayer, layers to be substituted - epidermis/dermis/both, materials used - natural/synthetic/composite, and durability - temporary (biodegradable)/permanent (non-biodegradable) (Metcalfe & Ferguson, 2007, Shevchenko *et al.,* 2010). Some of the commercially available skin substitutes are: EpiDex, Epibase, Bioseed-S, My Skin, Epicel, Cellspray, Laserskin, Cryoceal (autologous epidermal), Hyalomatrix, Pelnac, Hyalograft 3D, Dermagraft, MyDerm, TransCyte (autologous dermal), Apligraf, OrCel, StrataGraft (allogenic), Matriderm, Ezderm (xenogeneic), denovoSkin, Permaderm (composite skin substitutes), etc. They are also classified into three groups: Class I, temporary, impervious, dressing materials; Class II, single layer, durable, skin substitutes; and Class III, composite skin substitutes (Kotler *et al.,* 2018). FDA regulates products commonly referred to as skin substitutes under one of four categories depending on the product's origin and

composition: human-derived products regulated as human cells, tissues, and cellular and tissue-based products (HCT/Ps); human- and human/animal-derived products regulated through premarket approval (PMA) or as a humanitarian use device (HUD) obtained through a humanitarian device exemption (HDE); or as animal-derived products and synthetic products regulated under the 510(k) process (AHRQ report, 2012). *In vivo* studies have shown the importance of a dermal bed for successful full-thickness wound epithelialization (Wood *et al.,* 2007).

2.3. Limitations of currently available skin substitutes

Although increased healing rates of burn and/or chronic wounds can be observed with current engineered constructs, several intrinsic shortcomings exist, like reduced vascularization, poor mechanical integrity, failure to integrate, scarring, and immune rejection (Vig *et al.,* 2017). Scar is a major concern during full thickness wound healing resulting in functional, mechanical and aesthetic problems. None of the presently available skin substitutes can replicate the normal anatomy of skin after wound healing. In the case of epidermal grafts, they are fragile and therefore difficult to handle. They lack the ability to make differentiated structures/skin appendages like hair follicles, sweat glands, sebaceous glands, nerves, lymphatics, and blood vessels.

Most tissue-engineered skins are created by expanding cells in the laboratory on biomaterial scaffolds. Majority of the tissue engineered skin replacements utilizes normal skin cells - allogenic fibroblast and keratinocytes. Harvesting autologous cells from the normal skin may lead to donor site morbidity. The allogenic cells do not engraft permanently into the skin due to the inability to revascularize eventually dies and gets sloughed away from the host tissue (Griffiths *et al.,* 2004). Allografts or xenografts may induce immune rejection and may carry infectious agents including prion (Nunery, 2001). Another limitation of using cells is the delay involved in cell culture. The development of engineered skin is a time consuming process involving 2-3 weeks of cell culture before it is ready for grafting. They are not readily scalable for manufacturing and are difficult to store and transport. Technical advances in cell

and tissue culture protocols are required to overcome cell growth issues of skin substitutes. Autologous stem cells have the advantage of rapid proliferation but a suitable source of stem cells and a niche for the *in vitro* expansion is a major challenge. Such limitations have led to the quest of non-cellular dermal substitutes for regenerative medical applications in general and skin wound healing application in particular.

2.4. *In vivo* / guided skin tissue engineering

In guided tissue engineering, the scaffold should be able to attract cells from the surrounding native tissue, which may include mature dividing cells like fibroblasts and stem cells. The scaffold could be a skin substitute consisting of a biodegradable material acting as mechanical support matching native skin properties and biomimetic matrix with capability to promote cell migration, adhesion, spreading and proliferation. The cells that migrate and grow may have the potential to synthesize and deposit ECM and the stem cell may participate in the continuous homeostasis process throughout the lifespan. If a hybrid scaffold with appropriate mechanical strength to prevent wound contraction and required biological cues for cell growth, the scaffold could play an important role in wound healing by substituting the lost ECM. Therefore, scaffold design should consider specification such that it mimics ECM having capability to attract cells from neighboring native tissue, promote cell adhesion and proliferation, be a reservoir of GFs, provide cell adhesion molecules with cues for cell growth and the microenvironment for tissue regeneration, be non-immunogenic, be resorbed by body's natural proteolytic pathways promoting scar-less healing, should be easy to apply, stable during storage, and most importantly cost effective would be appreciated. There are many efforts across the world to design an optimum composition and many products are available in market. Currently, the products available in the market do not meet many of the defined requirements. For standardizing a novel scaffold composition, it is important to understand the normal anatomy and physiology of skin, wound pathology, normal wound healing and current treatment strategies and its limitations. The heterogeneity of chronic wound pathology makes it difficult for any one product to be universally applicable for types of wounds. Therefore, once the problem is properly understood,

one or more products may be designed for selected end use depending on the study outcome.

2.5. Biomaterials identified for the study

2.5.1. Fibrin: a versatile scaffold for tissue engineering applications

Fibrin is a critical blood component responsible for hemostasis, which has been used extensively as a biopolymer scaffold in tissue engineering. It formed from fibrinogen and thrombin during blood coagulation. The fibrinogen molecule is composed of two sets of three polypeptide chains named α, β, and γ which are joined together by six disulfide bridges. Fibrin is formed after thrombin-mediated cleavage of fibrinopeptide A from the α chains and fibrinopeptide B from the β chains, with subsequent conformational changes and exposure of polymerization sites. This generates the fibrin monomer that has a great tendency to self-associate and form insoluble fibrin. Further, the blood coagulation factor XIIIa is a transglutaminase that rapidly cross-links γ chains in the fibrin polymer by introducing intermolecular ε-(γ-glutamyl) lysine covalent bonds between the lysine of one γ-chain and glutamine of the other. This covalent cross-linking produces a stable fibrin network that is resistant to protease degradation (Horan *et al.*, 2001) (Figure 2).

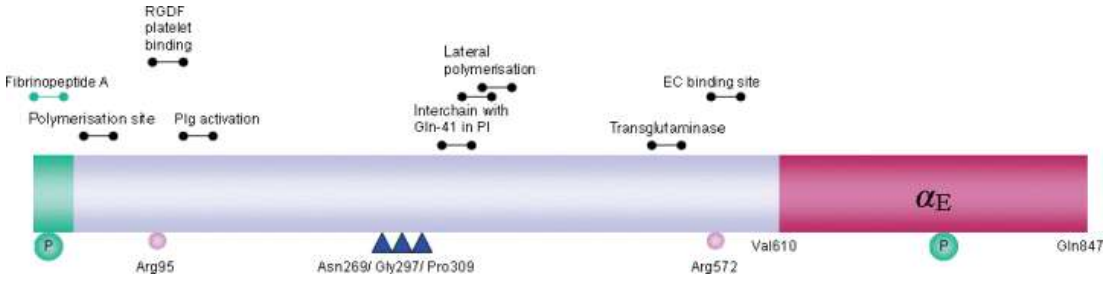

Figure 2. Fibrinogen structure (Laurens *et al.*, 2006)

Fibrin glue is usually obtained after the fractionation of pooled plasma and consists primarily of two components - enriched fibrinogen (also known as cryoprecipitate) and thrombin. The cryoprecipitate often contains factor XIIIa and fibronectin in addition to fibrinogen, while the thrombin component sometimes contains $CaCl_2$ and antifibrinolytic drugs (Clark, 2000). Fibrinogen can be isolated

from cryoprecipitation of fresh-frozen plasma or stored plasma (freezing at -80° C for 12 h, thawing for several hours at 4 °C, centrifugation, supernatant discarded and yellow precipitate of fibrinogen is resuspended in small volume of the plasma supernatant) (Spotnitz *et al.,* 1987), by using cell saver equipment (centrifugal blood concentrator) that concentrates the blood by removing plasma from whole blood by physical separation of cellular components by the centrifugal field is based on the differences in density and particle size (Koster *et al.,* 2001), chemical precipitation of fibrinogen using agents such as ethanol, polyethylene glycol, or ammonium sulfate (Silver *et al.,* 1995) or by chromatographic method in which plasma is passed through a column containing ligand like heparin, protamine, insolubilized fibrin, and fibrin monomer with high affinity immobilized to a matrix such as agarose and is eluted out (Burnouf *et al.,* 2001). Fibrin glue can be prepared either from allogeneic pooled plasma such as commercially available Tissucol/Tisseel, Beriplast (CSL Surgery), Crosseal (Ethicon Inc., USA), Evicel (Johnson & Johnson, Somerville, NJ, USA) have been approved by the FDA for clinical use as hemostatic agents and Quixil, or from autologous plasma that is collected from the patient prior to surgery and processed using devices such as Cryoseal FS (Thermogenesis, Rancho Cordova, CA, USA) or Vivostat which has added advantage of reduced possibility of viral transmission and prion infection and is cost-effective (Chen *et al.,* 2010). The most widely used forms of fibrin scaffolds are fibrin hydrogels, fibrin glue, and fibrin microbeads (FMBs) (Ahmed *et al.,* 2008). It is biocompatible, biodegradable, and less immunogenic material widely used as sealant, drug delivery vehicle and matrix component for tissue engineering.

During wound healing, plasma derived fibrin/fibronectin-rich clot acts as a natural provisional matrix or scaffold for the migration of leukocytes, fibroblasts, endothelial cells and keratinocyte cells into the wound space and each contributes to the wound healing process. The fibrin constitutes a provisional ECM, composed of 95 % fibrin and many other components, mainly fibronectin, SPARC/osteonectin, thrombospondin and vitronectin. In addition, GFs such as FGF-2 and VEGF bind specifically to fibrinogen and fibrin, suggesting that fibrinogen is not only important for hemostasis, but also for homeostasis. Fibrin contains multiple adhesive sites

including RGD sequences that engage integrins on the cell surface. Fibrin and fibrinogen functions as bridging molecule for many types of cell–cell interactions and provides a critical provisional matrix in which cells can proliferate, organize, and carry out specialized functions. Literature suggests that fibrin plays a major role in wound angiogenesis (Laurens *et al.*, 2006). Fibrin can also modulate the activity of monocytes and macrophages and therefore plays an important role in the transition rate between wound inflammation and tissue repair (Flick *et al.*, 2004). Once fibroblasts and EC express the proper integrin receptors, they invade the fibrin/fibronectin-rich clot in the wound space and start synthesizing a permanent ECM.

Exogenous fibrin scaffold mimic the final steps of the blood coagulation cascade, forming a stable, physiological fibrin clot that assists homeostasis and wound healing which in turn will help in migration and proliferation of inflammatory cells, ECs, stromal cells, angiogenesis, collagen synthesis, wound contraction, re-epithelialization and in cell-cell and cell-matrix interactions occurring during tissue remodeling. Degradation of the fibrin sealant occurs *in vivo* by proteolysis and phagocytosis of the course of 10 -15 d. Fibrin is rapidly degraded by plasmin, neutrophil elastase and proteolytic enzymes into its degradation products like fibrinopeptides A and B are chemo-attractant for neutrophils, monocytes and macrophages; D-dimers induce secretion of IL-1β and IL-6 by mononuclear cells; fragment E induces secretion of IL-1β and IL-6 by mononuclear cells; fragment β15-42 is chemo-attractant for neutrophils and fibroblasts and stimulate cell migration, inflammation, ECM deposition, fibroblast proliferation and angiogenesis. Fibrin can also be utilized as a printable hydrogel to establish specific cell patterns in the three-dimensional construct. Major drawbacks of using fibrin alone are low mechanical strength, gel shrinkage and rapid degradation rates which can be controlled by cross-linking or by combining fibrin with other artificial scaffolding material.

2.5.2. Hyaluronic acid / Hyaluronan (HA)

HA is a linear naturally synthesized non-sulfated GAG of the human skin which provides visco-elasticity and hydrophilicity. Native HA has a very high molar mass, usually in the order of millions of daltons (105-107 Da) before being progressively degraded into smaller fragments in the ECM. It is available in almost all body fluids and tissues, such as the synovial fluid, the vitreous humor of the eye, umbilical cord, hyaline cartilage, tendons, ligaments and connective tissues etc. HA is synthesized by HA synthases (HAS) on the cell membrane and forms long filaments (500 nm- 10 μm), hyaluronan which interacts with cell surface receptors, mainly CD-44 and RHAMM (receptor for hyaluronan mediated mobility), but also toll-like receptors TLR-4 and TLR-2, and inter cellular adhesion molecule-1 (ICAM-1). The interaction of hyaluronan with its receptor induces very important events in the wound repair process: modulation of inflammation, chemotaxis, cell migration, collagen secretion, and angiogenesis. The high molecular weight HA has a certain anti-inflammatory effect, and low molecular weight HA oligomers have been shown to promote angiogenesis. The abundance of hyaluronan in fetal skin is likely one of the factors which permits to the early gestation fetal skin wound to heal without scar formation. Similarly, the over-expression of hyaluronan synthase-1 is able to induce regenerative wound repair in C57Bl/6 mice (Price *et al.,* 2007).

HA is biocompatible, biodegradable, nontoxic and non-immunogenic polymer with high water affinity. The water attracting property of HA produces swelling pressure in ECM allowing the rapid diffusion of water-soluble molecules. Decreasing HA content during aging imply a shrinkage accounting for dried and wrinkled appearance of aged skin (Fleischmajer *et al.,* 1972). HA have excellent biocompatibility, hydrophilicity, limited immunogenicity and unique viscoelasticity properties. HA, as well as its degradation products that are generated in the wounds, are capable to activate specific responses in all the cells involved in the process; in particular, fibroblast proliferation and new vessel formation have been extensively studied. Anilkumar *et al.,* (2011) showed wound healing and skin tissue regeneration efficacy of HA-fibrin sheets in rabbit acute wounds. They suggest that HA introduced to the wound bed in dry state absorb the exudates from the injured tissue

and retain the wound moisture to support various processes in wound healing. The major limitation of HA-fibrin sheet is its poor mechanical and handling property.

2.5.3. Amniotic membrane / amnion (AM) for wound healing

Human AM has been used clinically in a variety of applications for over the past 100 years and produced a significant amount of data in multiple areas of medicine. AM is the innermost foetal membrane, up to 0.5 mm thick and avascular. AM has five layers: epithelium, basement membrane, compact layer, fibroblast layer and spongy layer. Epithelium is the inner layer, and it is facing amniotic fluid, whereas the outer, spongy layer is connected to the vascular chorion. AM is not only a intricate network of macromolecules produced and assembled by surrounding cells, but also numerous GFs and other soluble molecules. The major ECM components of AM basement membrane are collagen I, III, IV α1, α2, α5 and α6 chains, collagens type VII, XV, XVI, XVII and XVIII, laminin α3, β1, β2, β3, γ1 and γ2 chains, laminin-111 and laminin-332, nidogen-1 and nidogen-2, fibronectin, fibulin-2, fibrillin-2, perlecan and agrin, whereas RT-PCR and ELISA analysis detected EGF, KGF, HGF, basic FGF and TGF-α, -β1 and -β2 (Koizumi *et al.*, 2000, Dietrich Ntoukas *et al.*, 2012, Dusko Ilic *et al.*, 2016).

AM is an attractive method of grafting for wounds as it has unique properties, including anti-inflammatory effects, bacteriostatic, angiogenic, wound protection, decreased scarring, and pain reduction properties, as well as epithelialization initialization capacities. Also it is reported that AM contain some immunoregulatory factors, including HLA-G and FAS ligand making it immunoprivileged (Kubo *et al.*, 2001). AM expresses many neurotrophic and angiogenic factors: endothelin-2 and -3, vascular endothelial growth factor, vascular endothelial growth factor-B, Tie-2 angiopoietin receptor, ephrin-A2, ephrin receptors A2, B1, B3, B4, B5, neuropilin-2, nerve growth factor receptor, and semaphorin-F19 as well as erythropoietin and its receptor that contribute to healing of wounds. Furthermore, AM is widely available and less costly than other bioengineered skin substitutes (ElHeneidy *et al.*, 2016)

Its clinical usage ranges from wound coverage for burn victims to healing of the conjunctiva after pterygium repair (Jaianand *et al.*, 2017). In 1910, Davis was the first to introduce the use of human AMs as a skin graft. Shortly thereafter, in 1913, Sabella used AMs as a permanent coverage over wounds in burns patients. In 1952, Douglas was the first to report the use of AMs as a temporary biological dressing in the coverage of burns. There have been several successful reports of AMs used in patients with extensive burns and venous ulcers, where they have been demonstrated to be safe, easy to use, and extremely beneficial in allowing fast re-epithelialization of denuded skin (Venetia and Elena, 2009). Maral et al demonstrated accelerated re-epithelialization after covering split thickness skin graft with AM in rats. Loeffelbein *et al* demonstrated accelerated formation of basement membrane in wounds treated with AM that might be due to the release of GFs. Mermet *et al* reported that AM graft applied on chronic leg ulcers healing occurred in all patients. Pesteil *et al* used cryopreserved AM in eight patients with resistant vascular ulcers. Tolerance to the graft was excellent with healing of six out of eight patients with significant improved pain. Alsina-Gibert and Pedregosa-Fauste used AM for four refractory ulcers with a mean 81.93 % reduction of ulcer size after 16 weeks. Litwiniuk *et al* suggested the potential role of matrix metalloproteinase inhibitors present in radiation-sterilized amnion dressing in healing of out of 25 patients with chronic venous ulcers. Sheikh *et al* used dehydrated amnion to provoke healing of chronic wounds in four patients and healed wounds did not recur on long-term follow-up. A similar study was done by Zelen *et al* who used dehydrated AM in diabetic foot ulcers with complete healing of 37 out of 40 ulcers (ElHeneidy *et al.*, 2016). AM can be an ideal graft for chronic refractory ulcers, diabetic foot ulcers, fistulas, ocular defects, venous leg ulcers, wounds in preparation for skin grafting or as a biological dressing when there is a limited supply of skin graft, etc. It has been widely reported to be used in the treatment of burn wounds, leg ulcers, skin graft donor site dressings, chronic and acute wound care management for scar tissue reduction, diabetic ulcers, ocular defects, fistulas and venous ulcers (Gajiwala *et al.*, 2004, Loeffelbein *et al.*, 2014, Garoufalis *et al.*, 2018).

Although AM seemed to be an ideal natural wound dressing, preservation and risks associated with the human tissue donation have limited its use in clinical practice and its commercial availability. It took years for regulatory bodies to recognize the applicability of human AM in clinical practice and act on its manufacturing and distribution. In 1997, U.S.FDA announced a proposed approach to all human cells, tissues or cellular or tissue-based products, including previously unregulated cells and tissues. The act became effective on May 25, 2005, and today, in the USA, the manufacturing and distribution of HAM as a Human Cellular and Tissue Based Product (HCT/P) is regulated by the US FDA under 21 Code of Federal Regulations (CFR) Part 1271 and Section 361 of the Public Health Service Act. In order to be used for therapeutic purposes, the cellular components of AM should be removed. Since AM contains a variety of growth promoting proteins and factors, it was not exactly clear how decellularization procedures would affect the properties of AM as a biological scaffold. However, in spite of having lower levels of these soluble factors, denuded AM supported better cellular growth as a scaffold than the intact AM, suggesting that the ECM components and not soluble factors are playing the crucial role. However, ECM is rich in signalling molecules that are released and/or exposed during the process of *in vivo* degradation, and soluble molecules may play bigger roles than anticipated. Currently, there are several methods used for removal of the cellular components and each method has a slightly different effect on the basement membrane structural integrity. There are currently five manufacturers of commercial AM products tested in clinical trials for cutaneous wounds (Ilic *et al.,* 2016). The poor mechanical and handling characteristics of AM make it difficult to use on wounds of different dimensions.

2.5.4. Silk fibroin for wound healing

Silk fibroin (SF) has been intensively explored for tissue engineering and regenerative medicine applications due to its excellent biological and mechanical properties. Silk is a natural protein polymer which has been approved for medical use by the U.S.FDA. Silk fibers are obtained from diverse sources such as spiders, silkworms, scorpions, mites and flies. Among them, silk of silkworms is a good

source for the development of biomedical device. Silk is composed of two major proteins; SF and sericin. Sericin is the glue-like protein that wraps around the SF. The SF of *B. mori* has a diameter of 10 - 25 μm and consists of two chains i.e. a light chain (approximately 26 kDa) and a heavy chain (390 kDa) linked with a disulphide bond. SF is processed from mulberry silk after removal of the outer silk sericin which may potentially elicit an immunological response when it is associated with fibroin (Kundu *et al.,* 2008). SF processes excellent biocompatibility, controllable biodegradability, remarkable mechanical strength, and low immunogenicity and its bio-integrable materials enhancing collagen production and fibroblast and keratinocytes proliferation and migration. SF has also been explored as a biomaterial for skin repair due to its hemostatic properties, low inflammatory potential, and permeability to oxygen and water vapor. Moreover, silk protein was found to be safe under acute dermal toxicity, acute dermal irritation, and skin sensitization (Padol *et al.,* 2011).

SF in different morphologic forms, such as hydrogels, sponges, films, electrospun nanofiber mats, tubes and hydrocolloid dressings, have been successfully used for therapeutic use as wound dressings to induce the healing process. It has been reported that the SF nanofibers promote the adhesion of human keratinocytes and fibroblasts as well as enhance the deposition of type I collagen *in vitro*. Ouyang, Zou and co-workers from China conducted randomized single-blind parallel controlled clinical trial with 71 patients demonstrated that the SF film significantly reduces the time for wound healing and incidence of adverse events in comparison to commercial dressing (Zhang *et al.,* 2017). Dimple *et al* has shown non-mulberry SF in deposition and regulation of ECM towards accelerated wound healing, enhanced re-epithelialization, highly vascularized granulation tissue and higher wound maturity. SF alone lack cell binding sites, hence functionalization with other proteins or polymers enhance their efficiency. Functionalization of silk with other polymers like PVA-silk blended nanofibrous (Dimple *et al.,* 2019), curcumin loaded silk hydrogels, SF dressing with topical bioactive insulin (Li *et al.,* 2016), silk-elastin hydrogel, SF-chitosan wound dressing, EGF and silver sulfadiazine loaded for enhanced wound healing.

Three SF-based medical products have obtained regulatory approval for clinical use globally. They are SeriScaffold (Allergan Medical Inc.) from the U.S. FDA, TymPaSil (CG Bio Inc.) from the Ministry of Food and Drug Safety of South Korea and Sidaiyi (Suzhou Soho Biomaterial Science and Technology Co., Ltd) from the China FDA. SeriScaffold is a knitted silk mesh intended for hernia repair; TymPaSil is a SF patch used as a tympanic membrane; and Sidaiyi is a SF sponge-silicone two-layered scaffold indicated for skin wound healing (Khang *et al.,* 2017). Other SF based products include: fibroheal (Fibroheal Woundcare Pvt. Ltd, Bangalore, India).

2.5.5. Synthetic terpolymer for skin tissue engineering

Biodegradable polyesters such as poly lactic acid (PLA), poly glycolic acid (PGA) and poly (Ɛ-caprolactone) (PCL) and their copolymer scaffolds extensively used for skin tissue engineering applications (Kumbar *et al.*, 2008, Franco *et al.*, 2011). These polymers have gained FDA approval for human use. The ester bonds in these polymers are hydrolytically labile, and these polymers degrade by hydrolysis. The degradation products of PGA, PLA, and PCL are non-toxic; natural metabolites are eventually eliminated from the body in the form of carbon dioxide and water. Since these polymers are thermoplastics, they can easily be formed into a 3-D scaffold with desired microstructure, shape and dimension. PLA is more hydrophobic than PGA, and is more resistant to hydrolytic attack than PGA. For most applications the (l) isomer of lactic acid (LA) is chosen because it is preferentially metabolized in the body. PCL is semi crystalline aliphatic polyester and can be obtained by ring-opening polymerization of ε -caprolactone and is known for its long term degradation properties (Gunatillake & Adhikari, 2003)

The advantages of these polymers is that the degradation rate of these polymers can be tailored from several weeks to several years by altering crystallinity, initial molecular weight, and the copolymer ratio. Similarly the mechanical properties can also be tailored. They can also be processed with various techniques and consistently supplied in large quantities. Major limitations of polymer scaffolds

are their hydrophobic nature and lack of cell attachment sites (Mohammed *et al.,* 2016).

2.6. Development of hybrid 3-D scaffolds for *in vitro* and *in vivo* skin tissue engineering

3-D biodegradable and biomimetic porous scaffolds are ideal for skin tissue engineering. The development of new materials and the enhancement of existing materials to develop skin regeneration are wide areas of research. Natural polymers have great coincidence to natural ECM elements, particularly in biocompatibility and biodegradability. Combining a mechanically low natural biomaterial like AM and fibrin with other GAGs or proteins will enhance their bioactivity as well as handling characteristics. Combinations of natural and synthetic biomaterials or composite biomaterials combining two or three biomaterials as skin tissue engineering scaffolds may be a viable approach to fine tune the attractive regenerative properties, mechanical property, degradation kinetics and biocompatibility. Biocompatibility of the synthetic polymer scaffolds are found to be increased when it is hybridized with natural polymers like collagen, chitosan, gelatin, fibrin, fibronectin, HA, etc (Pankajakshan *et al.,* 2008, Chen *et al.,* 2005). Kumar & Krishnan (2002) have developed a method for producing stable fibrin coating along with other biomimetic ECM molecules on various synthetic biomaterials like poly(tetra fluoro ethylene) (ePTFE), dacron, PCL, etc. Incorporation of natural ECM components during the electro spinning of synthetic polymers by co-electrospinning of fibrin, collagen and chitosan with other synthetic polymers is also effective (Sreerekha *et al.,* 2013). These scaffolds have the combined advantages of both polymers with ECM-like architecture with added advantages for wound healing. It can cause enhanced cellular/tissue functions and regenerative outcomes, demonstrating the significance of the biomimetic materials for tissue engineering and regeneration.

2.7. Evaluation of tissue-engineered scaffolds

Tissue-engineered scaffolds are being developed to enhance restoration of the skin and improve the quality of wound healing. The skin equivalents, developed for

regeneration of chronic wounds, need to be tested for its efficacy in healing applications. Most important requirements are ability to match the properties of skin, biodegradability, biocompatibility and ability to heal the wound in the context of underlying pathological diseases like diabetes or burn. Several models have been used to study the wound healing process including *in silico, in vitro,* and *in vivo*.

In silico computational models may be helpful to understand cell growth and phases of wound healing in theory. They can also be used to design effective scaffolds and tissue substitutes that will aid in wound regeneration. The disadvantage of *in silico* models is that they lack biophysical characteristics of human skin and remain theoretical until confirmed biologically either by *in vitro* or *in vivo* models. Several mathematical equations have been used to assess the healing phases (Din *et al.,* 2017).

2.7.1. In vitro evaluation

It is mandatory that before the pre-clinical evaluation, *in vitro* evaluation has to be done to characterize and ensure the safety and efficacy of the scaffold for cell migration into the scaffold and growth. The cells should be characterized using specific markers and scaffold should be evaluated for cytocompatability, mechanical property, degradation rate, water vapour transmission and swelling properties (Ma *et al.,* 2003, Kumbar *et al.,* 2008). The tensile strength of human skin ranged between 3 -14 MPa (Jansen & Rottier, 1958) so the tensile strength of skin scaffold should be within this range. Poor mechanical properties and rapid degradation can cause graft instability and handling difficulty, scaffold degradation should balance with tissue generation. The ability of a scaffold to retain and preserve water is an important aspect to evaluate its property for skin tissue engineering (Ma *et al.,* 2003). The water vapour transmission rate (WVTR) for injured skin can range from 279 $g/m^2/d$ for first-degree burn to 5138 $g/m^2/d$ for a granulating wound (Lamke *et al.,* 1977). Recommended WVTR of a wound healing scaffold is 2000 to 2500 $g/m^2/d$, which is in the mid-range of water vapour loss rates from injured skin, may provide an adequate level of moisture without risk of wound dehydration (Mi *et al.,* 2001).

2.7.2. In vivo evaluation in animal model

Several animal models have been described in literature to study the impact of various therapies on wound healing. The most widely used models are pig, rabbit, rat and mice (Table 2). The pig has been used extensively for wound-healing studies because it has dermal structure somewhat similar to human skin (Lindblad, 2008). But the practical concern with the use of pigs is that the regulatory environment for these larger animals is more extensive. Rabbits are a potentially overlooked, manageable species for diabetes experiments (Wang *et al.,* 2010). Rabbit ear excision wound is a very useful experimental tool to assess tissue repair. By careful dissection of epidermis and dermis to the depth of the ear cartilage, one produces an ulcer-like lesion that has avascular base which is unable to close by contraction (Breen *et al.,* 2008). These properties differentiate the wound from most other small animal models and provide a greater resemblance to human wound closure.

Species	Thickness (mm)	Hair follicle density	Skin attachment	Wound healing mechanism	Cost
Human	2.97	Low	Tight	Re-epithelialization	N/A
Guinea Pig	1-2	High	Loose	Contraction	Medium
Mouse	0.70	High	Loose	Contraction	Low
Rat	2.09	High	Loose	Contraction	Low
Pig	2.5	Low	Tight	Re-epithelialization	High

Table 2. Comparative properties of skin in different species

Although animal skin does not resemble human skin, they have been developed and utilized in order to study the complexity of the healing process especially in chronic wounds. There is no one single appropriate model for a study to be conclusive; therefore, a combination of models should be employed. These models also come with their own distinct limitations particularly as they relate to translational potential to clinical practice. This is especially true for chronic wounds, for which no optimal preclinical model exists. In patients, chronic wounds are diverse with respect to (w.r.t) the wound type and microbial composition. Chronic

wounds result from a composite dysregulation of multiple local and systemic conditions that contribute to the wound healing process, including underlying conditions such as vascular disease, diabetes, and aging that are difficult to replicate in any given model. Therefore, multiple approaches exist to test wound healing effects of scaffolds, cells and GFs or its combinations.

The commonly used wound models are excisional wound models (full-thickness wounds) (Ansell *et al.,* 2014), incisional wound models where longitudinal incisional wound parallel to the midline on the dorsal side passing through epidermis, dermis and subcutaneous tissue down to the muscle is done, diabetic models induced by diabetogenic agents like alloxan, streptozotocin (STZ) which can be used for studying acute wound healing in diabetic animals but not suitable to study chronic skin ulcers as the etiology of the wound is significantly different (Wang *et al.,* 2010, Seaton *et al.,* 2015), radiation induced ulcer wounds, cutaneous ischemia reperfusion ulcers, ischemic skin wound model (Roy *et al.,* 2009), open skin ulcer model (Takeuchi *et al.,* 2017), skin fold chamber model (Schreiter *et al.,* 2017), burn wound models , infected wound model, para-biosis model, dead space wound model (Kumar *et al.,* 2013), denervated wound model, skin aging model (Lee *et al.,* 2014), etc. Although no single model is superior to the other, *in vivo* animal models will remain superior to *in vitro* models to study the complex wound environment (Davidson, 1998, William, 2008, Irena *et al.,* 2018).

2.7.3. Evaluation of regenerated skin after wound healing

Most constructs are first evaluated *in vitro* to assess, ie their biocompatibility and capacity to induce cell proliferation and/or differentiation. On the basis of these results, some constructs are further evaluated *in vivo*. Evaluation of *in vivo* healing requires the qualitative and quantitative analysis of chronic ulcers and wounds. A more systematic evaluation of tissue-engineered skin constructs in animal models is recommended to enhance the comparison of different constructs, thereby accelerating the trajectory to application in human patients. Regenerated skin can be evaluated by using different methods like macroscopic observations of wound for take rate of the construct, color (pigmentation, vascularization), signs of granulation

tissue or epithelialization, and the absence of signs of infection/inflammation or necrosis,etc planimetry, histopathology, immunohistochemical analysis, molecular analysis methods to assess gene expression levels and mRNA location, transillumination for blood vessel observation, *in situ/in vivo* imaging, electron microscopy, mechanical strength assessment, and microbiological sampling. An observer scar assessment scale (OSAS) containing a 1–10 scale to score for scar vascularity, pigmentation, thickness, relief, pliability, and surface area can be used (Chardack *et al.,* 1962).

Planimetry can be used to measure wound contraction and/or re-epithelialization by using a ruler or calliper manually to measure wound area, photographs to analyze wound contraction or by using transparent acetate wound perimeter tracing papers to trace the wounds edges, tattoo method, photogrammetry, weighing method, stereophotogrammetry, computer-assisted planimetry and in some cases, the software used to calculate the wound area is specified (Lammers *et al.,* 2011). Scar color determination by measuring the wavelengths of reflected light using tristimulus reflectance and narrow-band spectrophotometry, thickness of scar, measurement of surface irregularities or relief, etc. Epidermal barrier function of skin can be assessed by measuring stratum corneum/surface hydration, transepidermal water loss, epidermal pH and percutaneous penetration of different substances.

Tissue specimens at different time points in the healing process are accessed to understand the wound healing at molecular and cellular levels. This can be done by evaluating deposition of excessive ECM components, contraction, altered ECM remodelling, cells involved in these processes, like (myo)fibroblasts and proteins, like MMPs (Bonnans *et al.,* 2014). Depending on the structures of interest that have to be observed, different histological staining methods can be used. Since in most cases the skin regeneration process moves from the wound edges to the centre, comparable sampling positions are important when comparing different wounds. Standard histochemical staining techniques like hematoxylin - eosin (H & E) staining on tissue sections can be used to evaluate tissue cellularity, cell morphology, and architectural aspects such as presence and thickness of granulation tissue, thickness

of the epidermis or dermis and orientation of the collagen bundles, degradation of the biomaterial, ECM arrangement, vascularization, (extent of) re-epithelialization or epithelial gap, epithelial thickness and differentiation, and the presence of normal skin structures like rete ridges, papillary plexus, and appendages. H & E staining is also extremely useful in the identification and localization of different cell types involved in the wound healing process, like macrophages, granulocytes (polymorphonuclear leukocytes), lymphocytes, (foreign body multinuclear) giant cells, and fibroblasts (Chen *et al.,* 2005, Ma *et al.,* 2011, Anilkumar *et al.,* 2011). Signs of healing include minimal inflammation and complete restoration of normal skin structure, with normal collagen deposition and regularly distributed hair follicles, capillaries and glands. Alternative dyes were used to further distinguish between different tissue/biomaterial components. Richters *et al.* used an elastic-van gieson (EVG, also named verhoeff-van gieson) and trichrome-goldner staining to observe elastic fibers and collagen. Mallory's trichrome staining to distinguish scaffold polymer (white), tissue (red), and collagen deposition (green). Lamme *et al*. used herovici picropolychrome staining to distinguish scaffold collagen (highly crosslinked, red/purple) from newly formed collagen (blue). After 4 weeks, also the newly formed collagen started to stain red/purple. Windsor *et al.* used orcein to stain (scaffold) collagen and a periodic acid-schiff (glycogen) staining to observe basement membrane formation. Polarized light microscopy on Sirius red-stained sections was used to analyze the organization and orientation of collagen fibers in the wound bed. Images of these sections can be used for fourier analysis to quantify collagen bundle orientation and collagen bundle packing (Verhaegen *et al.,* 2009). One of the most pronounced differences between normal skin and scar tissue is the architecture of the collagen fibers. In scar tissue fiber thickness differs from normal skin and fibers are oriented more parallel to each other (Nayak *et al.,* 2006, Anilkumar *et al.,* 2011). Transmission electron microscopy (TEM) was used for a detailed examination of individual epidermal components and dermal elastic fiber, collagen, and fibroblast morphology.

Specific protein expression was analyzed in most studies by use of immunohistochemical techniques to observe the presence and location of specific

cell types and proteins like proliferation and differentiation of the epidermis, components of the dermal-epidermal basement membrane and/or blood vessels, proteins specific for dermal structures and cells, and general markers for cell migration and differentiation, collagen subtypes, components of the immune system (Balaji *et al.,* 2012, Choi *et al.,* 2013).

Quantification of histological data is also important. Lamme *et al*. used a semi-quantitative 1 - 5 scale to score for inflammation severity. Other studies quantified the total area of granulation tissue or the area of remaining polymer and newly formed tissu on images of tissue sections. Baynosa *et al.* quantified cell numbers and the number of intersections with a cycloid line to quantify positively stained blood vessels. Pandit *et al.* used the image based analysis system (IBAS) (formerly sold by Kontron, Eching/München, Germany) to quantify contraction, epithelialization, volume fractions of different cell types, and blood vessels on H & E stained sections. This is also possible by using pixel intensities to quantify tissue and fibroblast ingrowth, which can be performed using freely available software like Image J (http://rsbweb.nih.gov/ij/).

The mRNA expression levels of relevant proteins are usually evaluated using microarrays and real-time quantitative reversed transcription polymerase chain reaction (qRT-PCR) like pro-angiogenic VEGF, the urokinase plasminogen activator receptor involved in cell migration, the inflammatory cytokine IL-1β, and MMP- 3 and 9 involved in ECM remodeling. SDS-PAGE in combination with western blotting can be used to assess collagen production of fibroblasts isolated from scar tissue. The location of gene expression can be observed using *in situ* hybridization. Enzyme-linked immunosorbent assay (ELISA) is frequently used to study the role of cytokines and GFs like TGF-β (Schrementi *et al.,* 2008). The localization of enzymatic degradation by MMPs in the tissue can be used *in situ* zymography. Several studies used the transillumination method developed by Egana *et al.* to observe blood vessels in explanted nude mice skin. Removed skin was placed over a transilluminator and digital pictures were taken to calculate vessel area and length in a semi-automated way.

Tissue strength is closely related to its functional performance, and therefore it is remarkable that this important aspect of regenerated skin is often not assessed. Mechanical characteristics can also be studied by different mechanical testing systems like tensile strength, ultimate extension, and stress - strain curves to describe the viscoelastic properties of the healed tissue (Baie & Sheikh, 2000, Balaji *et al.,* 2012). In addition, protein production after co-implantation of a gene expression vector was determined like PDGF, VEGF or endothelial nitric oxide synthase (eNOS) (Lammers *et al.,* 2011). The ASTM International (previously known as the American society for testing and materials, www.astm.org/) and the international organization for standardization (ISO; www.iso.org/iso/home.htm) have developed valuable standards for the classification of therapeutic skin substitutes (ASTM F2311), characterization, and testing of biomaterial scaffolds used in tissue-engineered medical products (TEMPs, ASTM F2150), and testing for irritation and skin sensitization of medical devices (ISO 10993-10:2010). To summarize, much advance has been made in the recent past for curing chronic wounds and active research is in progress (Diana *et al.,* 2019).

CHAPTER 3

3. MATERIALS AND METHODS

In this study, three different lyophilized hybrid scaffolds for use as dermal substitutes were prepared, characterized and evaluated for both *in vitro* tissue engineering and *in vivo* tissue regeneration. In addition, an injectable hydrogel system was developed and tested. The common component used in all scaffolds and hydrogel is biomimetic fibrin-HA matrix, which was combined with a degradable synthetic terpolymer PLGC mat or with natural biomaterials such as decellularized AM or SF. The detailed description of raw materials processing or procurement is described in section # 3.1, followed by section # 3.2 with details of raw material characterization techniques. The section # 3.3 describes fabrication of lyophilized scaffolds and section # 3.4 describes the characterization of hybrid scaffolds. In section # 3.5 formulation of injectable / in situ forming hydrogel system and its characterization is described. In section # 3.6, the differentiation of hADMSCs to fibroblasts and characterization of differentiated cells are described. In section # 3.7, *in vitro* tissue engineering using hADMSC-derived fibroblast on scaffolds is described. In section # 3.8, cell encapsulation in SFFIBHA hydrogel and *in vitro* growth into ECM deposited tissue is described. In section # 3.9, evaluation of lyophilized hybrid scaffold & hydrogel system for guided epidermal/dermal regeneration of full thickness rabbit burn wound is described. In section # 3.10, evaluation of lyophilized hybrid scaffold for guided epidermal/dermal regeneration of full thickness wounds in diabetic porcine model is described. In section # 3.11, toxicological evaluation of hybrid scaffolds is described. Sources of commercial chemicals and reagents used for the study are mentioned in the respective brackets. The commonly used method of statistical analysis in all quantitative experiments is also included at the end.

3.1. Processing of raw materials

3.1.1. Preparation of fibrinogen and thrombin

Clinical grade cryo-precipitated fibrinogen from screened and pooled human plasma as lyophilized powder using in-house method with known concentration as component I of fibrin sealant kit was obtained as gift. Human thrombin purified from cryo-depleted plasma by diethylaminoethyl (DEAE) cellulose ion exchange chromatography as lyophilized powder with known concentration was also obtained as component II of fibrin sealant kit. About 50-100 mg of lyophilized fibrinogen powder was reconstituted with 2 mL sterile deionised water to get a stock solution of 25-50 mg/mL prior to use. About 250 IU/vial lyophilized powder of thrombin was diluted further with sterile water to get the working solution of thrombin.

3.1.2. Preparation of HA

HA was prepared in-house from human umbilical cord (collected from caesarean section delivery after informed consent) according to the published protocol (Kaye and Stacey, 1951, Anilkumar *et al*., 2011). Briefly, human umbilical cord tissue devoid of placenta (~ 250 g) was washed with sterile PBS to remove blood clots and was cut into 2 cm segments and washed with acetone (~ 1 L). After removing acetone, added double distilled water (~2 L) and soaked for 2 to 4 h with intermittent double distilled water change and incubated for 12 to 24 h at 4 ˚C. Grounded the tissue to form a suspension by diluting with double distilled water using a homogenizer/blender. Transferred the suspension of tissue into a beaker and adjusted pH to 2 using 2 N HCl (~ 30 mL), pepsin (~ 100 mg) (Sigma,USA) was added and stirred well and incubated in shaking incubator at 37 ˚C /room temperature (RT) for 24 h /overnight. After incubation, pH was raised to 7.4 using 10 N NaOH (~ 9 mL) and trypsin (~ 100 mg of trypsin or 15 mL of 0.25 % trypsin solution) (Gibco BRL, USA) was added and incubated at 37˚C /RT for 24 h /overnight. After digestion, the mixture was centrifuged for 30 min at 20,000 rpm at 4˚C and the supernatant was collected into a beaker and pH was adjusted to 2.0 using 2 N HCl. Two volumes of 95 % ethanol (~ 3L) was added to the solution and was centrifuged for 30 min at 20,000 rpm at 4˚C. The supernatant was discarded and the precipitate obtained by

ethanol (Sigma, USA) precipitation was suspended in double distilled water (~100 mL) and dialysed against tap water for 24 h. The dialysate was transferred into a beaker (~ 200 mL) and added a mixture containing 900 mL chloroform: 340 mL n-amyl alcohol: 200 mL double distilled water: 60 g sodium acetate: 32 mL glacial acetic acid. The mixture was shaken vigorously in a mechanical shaker for 10 min and the aqueous phase of supernatant containing the HA was collected and again treated repeatedly with the same mixture until no more precipitate appeared at the interface. Added two volumes of 95 % ethanol (~ 400 mL) to the aqueous phase containing the HA and centrifuged for 30 min at 20,000 rpm at 4˚C, the precipitate was dissolved in double distilled water (~ 200 mL) and dialyzed against running tap water for 24 - 48 h with several water changes. The dialysate solution was syringe filtered in a sterile hood into small autoclaved sterile glass vials, deep freezed and lyophilized until completely dry. The yield was calculated and was stored in deep freezer (- 40 ºC) until use. The lyophilized powder was reconstituted in water to get a stock solution of 1mg/mL (Rashmi *et al*., 2020).

3.1.3. Preparation of cell-free AM

Human placenta was collected from mothers who underwent caesarean delivery (with informed consent) who are screened negative for HIV, HBsAg, HCV, syphilis, etc. Placenta was collected in sterile phosphate buffer saline (PBS) containing 0.2 % sodium azide (Sigma, USA) and washed thoroughly in running tap water and in D/W in the laboratory. AM were carefully pulled apart from the chorion, and the chorion along with placental tissue was sent for incineration. The AM was then washed several times with PBS containing 0.2 % sodium azide (Sigma, USA), until all blood and blood clots were washed away and the light pink color of the membrane became vividly apparent and the cleaned membrane was stored in sterile PBS containing 5 x antibiotic-antimycotic (AbAm, Gibco, USA) at 4 ºC until decellularization performed within 12 - 24 h (Rashmi *et al*., 2020).

The cleaned AM was incubated in tris buffer (10 mmol/L, pH 7.6) (Sigma, USA) containing 5x AbAm solution for 24 h at 4 °C. The AM was then transferred into the solution containing 1 % (v/v) triton x-100 (Sigma,USA) and 0.5 % (w/v)

sodium deoxycholate (SD) (Sigma,USA) dissolved in tris buffer (10 mmol/L, pH 7.6) for 24 h at 37 °C with a shaking of 125 rpm. After the incubation, the AM was washed thoroughly under distilled water by rubbing with cotton balls. The decellularisation was confirmed after this step as a quality check for every batch using 4',6-diamidino-2-phenylindole (DAPI) (Sigma,USA) staining. The AM was then washed in distilled water containing 5x AbAm at 4 °C for 12 h with intermittent change in washing solution. The decellularized and washed AM was then loaded and stretched in rings and was air dried in laminar air flow for 4 h. The dried membrane was carefully cut from the ring using a sterile blade, packed and performed plasma (H_2O_2) sterilization (Sterrad 1005 plasma steriliser, USA) at 48 °C and stored at 4°C until use (Rashmi *et al*., 2020).

3.1.4. Synthesis of terpolymer PLGC

The terpolymer PLGC was synthesized by ring opening polymerization with a starting monomer of L-LA, GL (Purac Biomaterials, Purasorb G, Netherlands) and Ɛ-CL (Sigma Aldrich, USA) using the catalyst tin(II)2-ethyl hexanoate/ stannous octoate ($Sn(Oct)_4$) (Sigma Aldrich, USA) in vacuum. Briefly, L-LA, GL and Ɛ-CL in the monomer ratio of 70:10:15 (mol %) were weighed into a round bottomed flask under inert atmosphere of high purity nitrogen and 0.07 % stannous octoate was added as initiator and sealed. The reaction mixture was placed in a medium-sized oil-bath and flushed with high purity nitrogen for 15 min until temperature reached 130 ^{o}C with constant stirring to facilitate homogenous mixing. The temperature was raised to 160 ^{o}C under high vacuum and the reaction was allowed to continue for 24 h. After completion of the reaction, the resultant terpolymer was cooled and purified by dissolving in chloroform and re-precipitating in ice-cold n-hexane. The terpolymer was dried in vacuum oven overnight at RT and lyophilized to remove any residual solvent and stored in vacuum until use (Srisa-ard *et al.,* 2001; Rashmi *et al*., 2019; Rashmi *et al*., 2020).

3.1.5. Preparation of porous PLGC mat

Synthesized terpolymer PLGC of twenty five (w/v) percent was dissolved in dichloromethane (DCM) (Merck, India) for electrospinning (Model-HO NEU-02,

Holmarc Mechanotronics Pvt. Ltd, India). The polymer solution was electrospun at a flow rate of 3 mL/h with 12 - 14 kV voltage at a rotating speed of 1000 rpm to produce fine fibers which resulted in the formation of terpolymer mat. The electrospun fiber matrices were dried under vacuum at RT (~28 ^{o}C) for 24 h, cut into required size.

3.1.6. Preparation of SF solution

SF was processed at IIT Guwahati (IIT-G) as a part of collaborative project. SF was isolated from the cocoons of *Bombyx.mori* (*B. mori*) silkworms purchased from Central Silk Board, Guwahati, Assam, India by degumming to remove sericin and processed further to obtain sericin-free silk fibers. SF solution was prepared from the silk cocoons following the standard procedure (Rockwood *et al.* 2011). The SF pellets obtained from IIT-G was dissolved in sterile water by incubating at 4 ºC overnight. The undissolved particles were removed by centrifuging at 5000 rpm for 10 min. The SF solution was sterilized by autoclaving and stored at 4 ºC and was used for the study.

3.1.7. Preparation of GFs for cell culture

Platelet growth factors (PGFs) was prepared as per the procedures published earlier (Resmi and Krishnan, 2002). Freshly collected platelet rich plasma (PRP) obtained from blood bank was added with 10 % acid citrate dextrose (ACD) solution and centrifuged at 750 ×*g* and cells were washed two more times with ACD-tyrode's buffer. $CaCl_2$ was added to get 2 mM final concentration, and challenged with 1 IU/mL thrombin for 5 min. EDTA (5 mM final concentration) was used to stop further activation. Activated platelets were then centrifuged at 36000 ×*g* for 1 h at 4 ºC , supernatant was dialysed against Ca^{2+} -Mg^{2+}- free Hank's balanced salt solution (HBSS), sterile filtered (0.22 µm) (Millex GP, Millipore, Ireland) and aliquots were stored at -20 ºC until use. The concentration of PGF cocktail was determined by Lowry's protein assay and used for the study.

Bovine hypothalamus extract (BHE) was prepared as per the protocol described by Maciag *et al.,* (1979). Bovine hypothalamus extract has been reported to contain a

cocktail of various GFs and cytokines applicable for the present study such as: BMP4, FGF and VEGF. GFs were isolated from bovine calf brain obtained from the local slaughter house. Briefly, hypothalamus was isolated, homogenized with ice cold saline, stirred for 2 h in ice cold saline and centrifuged at 13000 ×*g* at 4 ℃ for 45 min. Supernatant was collected and mixed with 0.5 w/v % streptomycin sulphate (Sigma Aldrich, USA). The mixture was then incubated overnight at 4 ℃ with stirring to remove the lipid content. After incubation, it was centrifuged at 13000 ×*g* at 4 ℃ for 45 min. The supernatant was then collected and dialyzed against 0.1 M NaCl for 24 h at 4 ℃. Dialyzed solution was filter sterilized using a 0.22 µm filter, lyophilized (Modulyo 4K Freeze dryer, Edwards, UK) and was stored at - 80 ℃ (Sanyo ultralow, Japan) for the cell culture studies. The concentration was estimated using Lowry's method and used for the study.

3.1.8. Isolation of human adipose derived mesenchymal stem cells (hADMSCs)

Collection of human adipose tissue was approved by the Institutional Ethics Committee & Institutional Committee for Stem Cell Research of Sree Chitra Tirunal Institute for Medical Sciences & Technology (IEC-IC-SCTIMST) and Department of plastic surgery, Kerala Institute of Medical Sciences hospital (IEC-KIMS). The isolation of MSCs from adipose tissue was performed according to the modified protocol published by Zhu *et al.*, (2008). Briefly, the adipose tissue (~10 g) was washed thoroughly with HBSS to remove blood stains and was chopped into ~1 mm^3 pieces and in the case of liposuction samples, the chopping section was omitted. Cells were dissociated by treating with 1.5 mg/mL using collagenase NB 4 standard grade (SERVA Electrophoresis, Germany) at 37 ℃ with continuous shaking for 45 - 60 min. The suspension was diluted with an equal volume of serum-containing medium, passed through a 70 µm cell strainer (BD Falcon, USA) and washed by centrifugation. The cell pellet was re suspended in MSC basal medium (BM) consisting of low-glucose Dulbecco's modified eagle's medium (DMEM; Gibco, USA), supplemented with 10 % fetal bovine serum (FBS; Gibco, USA) and AbAm solution. The cells were seeded onto a 25 cm^2 tissue-culture polystyrene (TCPS) flask (Nunc, Denmark) and kept at 37 ℃ and 5 % CO_2; medium change was done at 3 d intervals. When ~ 80 - 90 % confluence was achieved, the cells were passaged

using standard trypsinization protocol. Cells at passages (P) 2 - 4 were used for the MSC markers and also to start differentiation experiments.

3.1.9. Preparation of culture dish for growing human umbilical vein endothelial cells (HUVECs)

For culture of EC, TCPS was coated with fibrin composite as described previously (Chennazhy and Krishnan, 2005). In brief, the dishes were incubated with 5 IU/mL thrombin for 30 min at 37 °C in CO_2 incubator. The solution was then discarded and dishes were coated with a fibrin composite containing 10 mg/mL fibrinogen, 0.2 % gelatin and 50 µg/mL BHE. The clot was allowed to form for 30 mins by incubating the dishes at 37 °C in CO_2 incubator. Following this, the dishes were lyophilized and used for cell culture.

3.1.10. Isolation of HUVECs from umbilical cord

HUVECs were isolated by the previously published method (Jaffe *et al.*,1973). Briefly, umbilical cord was collected from local maternity hospital in Trivandrum (after getting informed consent), in HBSS containing 10 mg/mL glucose and 5x AbAm. The cord was thoroughly cleaned and clots were removed from the ends. The vein was flushed using a cannula with HBSS and then filled with 0.5 % collagenase in serum free medium (DMEM:F12, Gibco, USA). The cord was then placed in beaker filled with HBSS soaked cotton and incubated at 37 °C in 5 % CO_2 incubator for 12 mins. After incubation, the cells were flushed out of the vein by passing serum free medium and simultaneously dislodging the cells by gentle massaging of cord. The cell suspension was collected and centrifuged at 400 ×*g* for 5 min. The pellet was re-suspended in medium containing 20 % FBS and 50 µg/mL BHE and seeded in coated tissue culture dish (# 3.1.9) and was incubated at 37 °C in 5 % CO_2 incubator. Medium change was given after 24 h. Cells were sub-cultured and ECs harvested from P 2- 4 was used for the study.

3.2. Characterization of the raw materials

3.2.1. Purity check of HA

Analysis of HA was done by fourier transform infrared spectroscopy (FT-IR) (JASCO, Model 6300, Japan), nuclear magnetic resonance spectroscopy (NMR) (^{1}H-NMR spectrophotometer, Bruker, USA) and high performance liquid chromatography (HPLC) (Shimanzu, Japan) analysis and it was by compared to the commercially available HA from Sigma, USA to compare its purty (Rashmi *et al*., 2020).

3.2.2. Test for cellular contents in decellularized AM

The total DNA content in the AM was quantified before and after decellularization using Trizol reagent using the manufacturer's manual. Trizol reagent was used for sequential precipitation of RNA, DNA, and proteins from a single sample as per manufacturer's instruction (Chomczynski, 1993). After homogenizing the sample with Trizol reagent, chloroform was added, and the homogenate was allowed to separate into a clear upper aqueous layer (containing RNA), an interphase, and a red lower organic layer (containing the DNA and proteins). DNA was precipitated from the interphase/organic layer with ethanol and washed to remove impurities, then re-suspended for use. Briefly, incubated the sample with Trizol reagent for 5 min to permit complete dissociation of the nucleoproteins complex. Added 0.2 mL of chloroform per 1 mL of Trizol reagent and incubated with sample for 2 - 3 min, and centrifuged the sample for 15 min at 12,000 × g at 4 °C. The mixture separated into a lower red phenol-chloroform, and interphase, and a colourless upper aqueous phase. Added 0.3 mL of 100 % ethanol per 1 mL of Trizol reagent and capped the tube, mixed by inverting the tube several times. Incubated for 2 - 3 min, centrifuged for 5 mins at 2000 × *g* at 4°C to pellet the DNA. Re-suspended the pellet in 1 mL of 0.1 M sodium citrate (Sigma,USA) in 10 % ethanol, pH 8.5, per 1 mL of Trizol reagent and incubated for 30 min, mixing occasionally by gentle inversion. Centrifuged for 5 min at 2000 × g at 4 °C. Discarded the supernatant with a micro-pipette. Re-suspended the pellet in 1.5 - 2 mL of 75 % ethanol per 1 mL of Trizol reagent used for lysis. Incubated for 10 - 20 min, mixing occasionally by gentle inversion. Centrifuged for 5

min at 2000 × g at 4 °C. Discarded the supernatant with a micro-pippete. Vacuum or air dried the DNA pellet for 5 - 10 min. Re-suspended the pellet in 0.3 - 0.6 mL of 8 mM sodium hydroxide (NaOH) (Sigma, USA) by pipetting up and down. Centrifuged for 10 min at 12,000 × g at 4 °C to remove insoluble materials. Transferred the supernatant to a new tube, then adjusted pH as needed with 4-(2-hydroxyethyl)-1-piperazineethanesulfonic acid (HEPES) (Sigma, USA). Determined the DNA yield by measuring absorbance at 260 nm using NanoDrop spectrophotometer (Thermo Scientific™ NanoDrop 2000, USA).

3.2.3. Quantification of total protein content in decellularized AM

Total protein was extracted with radioimmunoprecipitation assay buffer (RIPA buffer, Thermo Fisher Scientific, USA) containing 150 mm NaCl, 1 % NP40, 0.5 % and Lowry's assay was carried out before and after decellularization.

3.2.4. Quantification of total collagen content in decellularized AM

The total collagen was analyzed for AM before decellularization, after decellularization, after drying and the final plasma sterilized AM quantitatively. The total collagen content was quantified using Sirius red assay (according to the published protocol (Choi *et al.*, 2012). Briefly, the membranes were solubilized overnight in an acid-pepsin enzyme solution with a pepsin concentration of 0.1 mg/mL in 0.5 M acetic acid (Sigma, USA). Pepsin/acid soluble collagen was recovered and incubated with Sirius red / direct red-80 (Sigma, USA) reagent for 30 min at RT. The precipitated collagen dye complex was centrifuged at 10,000 × g for 15 min, and the supernatant was discarded. The pellets were dissolved in 0.5 M NaOH (alkali reagent), and the absorbance was measured in a 96-well plate at 555 nm using a microplate reader (iMark Microplate Reader, Biorad ,UK).

3.2.5. Quantification of total elastin content in decellularized AM

The total elastin was analyzed for AM before decellularization, after decellularization, after drying and the final plasma sterilized AM quantitatively.The total elastin content in the membrane was quantified using a fastin elastin assay kit (Biocolor, UK) according to the manufacture's instructions. Briefly, the membranes

were hydrolyzed with 0.25 M oxalic acid at 100 ºC for 1 h. The hydrolysate was centrifuged at 10,000 × g for 10 min. The supernatant was collected, and the extracted elastin was incubated with fastin dye for 30 min. The precipitate was collected by centrifugation at 10000 × g for 15 min and the pellet was dissolved in dye dissociation reagent. The absorbance was measured at 513 nm using a microplate reader (iMark Microplate Reader, Biorad, UK).

3.2.6. Quantification of sGAG content in decellularized AM

The total sulphated glycosaminoglycans (sGAG) was analyzed for AM before decellularization, after decellularization, after drying and the final plasma sterilized AM quantitatively. The total sGAG content was quantified using 1,9-dimethylmethylene blue (DMMB) (Sigma,USA) assay. Briefly, the membranes were digested using papain (Sigma, USA) extraction reagent (pH 6.5) at 65 °C for 4 h for complete digestion and the supernatant was used for the assay. The supernatant was incubated with 1 mL of the GAGs-complexing DMMB solution for 30 mins with gentle shaking. The precipitate was centrifuged (12,000 rpm for 10 min) to sediment the GAGs/DMMB complex. The supernatant, containing un-complexed DMMB and soluble biological molecules, was eliminated. The pellet was then dissolved in 250 µL of the de-complexating solution, vigorously shaken for 30 min, and transferred into a 96 wells microplate for absorbance reading. The absorbance was measured at 656 nm using a microplate reader (iMark Microplate Reader, Biorad, UK).

3.2.7. Identification of ECM molecules in decellularized AM

The decellularized AM was immunostained for ECM molecules like collagen-I (Col-1), collagen-II (Col-2), collagen-III (Col-3), collagen-IV (Col-4), collagen-X (Col-10), elastin and fibrillin-1 antibodies (Abcam, UK). Briefly, the decellularized AM was washed with PBS, blocked with 1% bovine serum albumin (BSA, Sigma,USA) for 30 min, incubated with the respective antibodies (1:100 dilution) for 2 h and developed using flurochrome (alexa flour 488 (AF488) / Texas red (TX)) conjugated secondary antibodies (Abcam,UK). The scaffolds were imaged using fluorescent microscope and Leica Application Suit software (Leica, DMIRB, Germany).

3.2.8. Testing mechanical properties and surface properties of decellularized AM

The mechanical properties of the using the decellularized AM was analyzed using Universal Testing Machine (UTM, Instron 1011, UK) at a crosshead speed of 10 mm/ min (ASTM D 882-97 method). The surface topography and porous nature was analyzed using environmental scanning electron microscope (ESEM, FEI Quanta 200, Netherlands).

3.2.9. Testing cytocompatibility of decellularized AM

Cytotoxicity test was done using direct contact method to identify whether any remnents of dertergent was remaining from the decellularization protocol The sterilized samples were placed on to the top of the confluent layer of L929 fibroblast cells to evaluate cytotoxicity. The cells seeded on cell culture plate (TCPS) were taken as control. The cells were incubated with the samples at 37 ± 2 ºC with 95 % relative humidity and 5 % CO_2 in CO_2 incubator up to 72 ± 2 h and cells was examined under phase contrast optical microscope for morphological changes in cells as well as cellular response around the test samples.

To measure extractable solvent/detergent on cell viability, the decellularized AM was exposed to fibroblast culture for 7 d and using 3-(4, 5-dimethylthiazol-2-yl)-2, 5-diphenyltetrazolium bromide / MTT (Sigma, USA) assay was performed. The cells grown in TCPS was taken as control and compared. The absorbance was measured using microplate reader at 590 nm.

3.2.10. Cell adhesion and spreading on decellularized AM

To evaluate the cell attachment and growth of fibroblasts on decellularized AM, cells were seeded at a density of 5000 cells/cm^2 and cultured under normal conditions for 7 d. The plates were then visualized through phase contrast microscope to observe morphology of attached cells. After 7 d, the decellularized AM with cells was co-stained for actin with Texas red phalloidin (Molecular probes, USA) and vimentin (R & D systems, USA) to confirm cell attachment and growth. Briefly, the scaffold seeded with cells were washed with PBS after removing media, fixed with 3.7 % formaldehyde (Sigma, USA), permeated by 0.2 % triton X 100, washed and stained

with TX conjugated phalloidin (1 : 250 dilution) for 45 min, washed and incubated with primary antibody vimentin (1 : 100) for 1-2 h followed by washing and AF488 secondary antibody (1 : 1000) incubation for 1 h at RT. DAPI was also stained for 5 mins to visualize the cell nuclei. Stained cells were then viewed under fluorescence microscope (Leica, DMIRB, Germany).

3.2.11. Properties of synthesized terpolymer PLGC

The synthesized terpolymer was characterized using FT-IR spectroscopy between 400 - 4000 cm^{-1}, with 40 scans per sample at a resolution of 4 cm^{-1}. NMR spectrum was recorded for the synthesized terpolymer in $CDCl_3$ containing small amount of TMS as internal standard. The molecular weight distribution profile was recorded using gel permeation chromatography (GPC) (Shimadzu Prominence, LC-20, Japan) equipped with a refractive index (RI) detector using tetrahydrofuran (THF) as the mobile phase at a flow rate of 1 mL/min at 40 ºC . The thermal properties were studied using thermogravimetry (DTA-TGA) (Universal V4.5A, TA Instruments Inc, USA). Mass loss of material was determined in the temperature range of 50 - 800 ºC using established procedure (ASTM-E 1131-08). Differential scanning calorimetry (DSC) (Universal V4.5A, TA Instruments Inc, USA) was used to determine the glass transition temperature (Tg), enthalpy of fusion and crystallization using standard procedure (ASTM D 3418-08). Thermograms were recorded at a heating rate of 10 ºC /min in nitrogen atmosphere.

3.2.12. Characterization of electrospun PLGC mat

The surface topography and porous nature of the electrospun PLGC mat was analyzed using ESEM. The fiber diameter distribution was quantitatively analyzed from scanning electron micrographs using Image J software. The mechanical properties of the electrospun PLGC was analyzed using UTM at a crosshead speed of 10 mm/ min (ASTM D 882-97 method).

3.2.13. Detection of surface markers on isolated hADMSCs

Characterization of the hADMSCs was done according to the standards proposed by International Society for Cellular Therapy (ISCT) (Dominici *et al.,* 2006), P3 hADMSCs were characterized using a panel of mesenchymal cell surface markers (CD 105, CD 90 & CD 73) and two hematopoietic stem cell surface markers (CD 45 & CD14) using flow cytometry (BD FACS Aria I). The software flowjo was used for analyzing the FACS data. The sources of the antibodies used for characterization are given in the table 3.

Sl. No	Name	Isotype	Source	Catalog No.
1	CD 105 PE	Mouse IgG	Santa Cruz Biotechnology	SC-18838
2	CD 73 PE	Mouse IgG	Biolegend	344003
3	CD 90 PE	Mouse IgG	BD Biosciences	555596
4	CD 45	Mouse IgG	Beckman Coulter Inc	6607019
5	CD 14	Mouse IgG	Millipore	CBL453F

CD, Cluster of Differentiation; FITC, Fluorescein Isothiocyanate; IgG, Immunoglobin G; PE, Phycoerythrin

Table 3: List of Antibodies

3.2.14. Assessment of multipotency of isolated hADMSCs

Based on the criteria for identification of hMSCs proposed by the ISCT, the ability of MSCs for trilineage differentiation into osteogenic, chondrogenic and adipogenic tissues was tested. The stempro adipogenesis differentiation kit, stempro chondrogenesis differentiation kit and the stempro osteogenesis differentiation kit (Invitrogen, USA) were used to induce differentiation of MSCs into adipogenic, chondrogenic and osteogenic tissues, respectively according to the manufacturer's instructions.

Adipogenic differentiation: P3 hADMSCs were seeded at a density of 10,000 cells /cm^2 and cultured in low glucose DMEM with 10 % FBS and antibiotics for 24 h. The medium was then replaced with adipogenesis differentiation medium and the cells were incubated at 37 $^{\circ}$C with 5 % CO_2. The differentiation medium was replenished every third day for an induction period of 21 d. After induction, the cells were fixed with 3.7 % formaldehyde, rinsed with PBS and the differentiation was confirmed by oil red-O staining.

Osteogenic differentiation: P3 hADMSCs at a density of 10,000 cells/cm^2 were seeded in basal growth medium containing low glucose DMEM with 10 % FBS and antibiotics for 24 h. After 24 h, the medium was replaced with osteogenesis differentiation medium and the cells were incubated at 37 $^{\circ}C$ with 5 % CO_2. Every third day the differentiation medium was replenished till an induction period of 21 d. Post-induction, the cells were fixed with 3.7 % formaldehyde, rinsed with PBS and stained with alizarin red.

Chondrogenic differentiation: P3 hADMSCs were seeded at a density of 5,000 cells/cm^2 in basal growth medium for 24 h. Chondrogenic differentiation medium was supplemented thereafter and the cells were incubated at 37 $^{\circ}C$ with 5 % CO_2. The differentiation medium was replenished every third day for an induction period of 21 d. After induction, the cells were fixed with 3.7 % formaldehyde, rinsed with PBS and stained with toluidine blue.

3.2.15. Expression of CD 31 by isolated HUVECs

The isolated HUVECs was characterized for endothelial cell markers using immunofluorescence of CD 31 and cellular uptake of 1,1'-dioctadecyl-3',3'-tetramethyl-indocarpocyanine perchlorate (dil) labeled acetylated low density lipoprotein (Ac LDL) (Molecular Probes, USA). The cells cultured in EC matrix were washed with PBS. The cells were incubated with 1 % BSA for unspecific binding and incubated with primary antibody against human CD 31 (Abcam, UK) (1:100 dilution) and incubated for 2 h at RT and washed with PBS as described in # 3.2.2.7. Secondary antibody conjugated with AF488 was added and incubated at RT in dark for 1 h. Cells were washed with PBS and fixed with 3.7 % formaldehyde and washed with PBS. Cells were visualized under fluorescence microscope (Leica DM IRB, Germany) and micrographed.

3.2.16. Cellular uptake assay of dil labelled acetylated low density lipoprotein (Ac LDL) by isolated HUVECs

Dil labelled Ac LDL was used for the study. Briefly, the culture medium was changed with fresh medium containing 10 µg/mL of dil labeled Ac LDL and was

incubated for 4 h at 37 °C in a CO_2 incubator. After incubation, the cells were washed with serum-free medium and viewed under fluorescence microscope (Leica DM IRB, Germany) and micrographed.

3.3. Fabrication of biodegradable & hemostatic hybrid scaffolds

Hybrid scaffolds AMFIBHA, PLGCFIBHA and SFFIBHA were prepared in different dimension based on the mould used. For cell culture studies, the hybrid scaffolds were moulded in the tissue culture well of required diameter.

3.3.1. Preparation of FIBHA for hybridization

Different hybrid scaffolds were fabricated in combination with fibrin-HA biomimetic matrix for skin substitution. Concentrations of fibrinogen was diluted to get 40 mg/mL or 20 mg/mL; and thrombin was diluted to get 20 IU/mL or 10 IU/mL. Three different HA concentrations tested were 100 µg/mL, 200 µg/mL and 400 µg/mL. The diluted fibrinogen mixed with required HA is denoted as Component I and diluted thrombin is denoted as Component II. Both components were loaded in separate syringes and were fixed to the Y-connector having separate channels for delivery of components into the needle head to be mixed and delivered to the respective mould. After verifying the clotting efficiency and swelling characteristics, for all hybrid scaffolds, component I comprised 20 mg/mL fibrinogen & 200 ug /mL HA; component II contained 20 IU/mL thrombin. The mixture of both components is denoted as FIBHA.

3.3.2. Fabrication of hemostatic hybrid scaffold AMFIBHA

Sterile decellularized AM was trimmed to the required size. The reconstituted FIBHA components as in # 3.3.1 was delivered to respective mould steadily and slowly to cover the entire surface. Soon after, the trimmed AM was placed, FIBHA was layered using dual syringe applicator. The clot was allowed to stabilize for 20-30 min and was frozen by keeping the entire mould in a sterile container. After overnight freezing at - 80 ºC, the mould was kept in a pre-cooled freeze dryer (Edwards, UK) and lyophilized for 6 to 8 h. After complete drying, the AMFIBHA

wafers were lifted using a forceps and kept sealed in a petriplates at 4 ºC for further evaluations and functional studies (Rashmi *et al.,* 2020).

3.3.3. Fabrication of hemostatic hybrid scaffold PLGCFIBHA

The electrospun PLGC scaffold was trimmed to same size in sterile LAF. The Fib-HA reconstitution and preparation of delivery system was done as described in #3.3.1. The electrospun PLGC was placed on the mould and FIBHA was delivered to the mould steadily and slowly to cover the entire surface of the PLGC. The fibrin clot that penetrated into the pores of PLGC mat was allowed to stabilize for 20 -30 min and was frozen by keeping the entire mould in a sterile container. After overnight freezing at - 80 ºC, the mould and lyophilized for 8 to 12 h (Edwards, UK). After complete drying the PLGCFIBHA wafers were lifted using a forceps and kept sealed in a petriplate at 4 ºC for further evaluations and functional studies.

3.3.4. Fabrication of hemostatic hybrid scaffold SFFIBHA

The lyophilized and processed SF was dissolved in distilled water by incubating at 4 ºC overnight. The concentration of SF was varied to get a final concentration of 1 and 2 % (w/v). The reconstituted Component I was mixed with SF to get 2 - 4 % SF, respectively and is referred as component I. The dual syringe application system was loaded as described in #3.3.1 and both components were delivered to the well of tissue culture plate or SS mould. The volume of the final mixture can be varied based on the volume of the mould, keeping the composition constant. The SFFIBHA which clotted within 1- 2 min was allowed to stabilize for 20-30 min, deep frozen at - 80 ºC and lyophilized for 6 to 8 h. After complete drying the SFFIBHA wafers (4 x 4 cm^2) were lifted using a forceps and kept sealed in a petriplate at 4 ºC for further evaluations and functional studies.

3.4. Characterization of the developed hybrid scaffolds

3.4.1. Chemical analysis

To confirm the deposition of bio mimetic matrix in the fabricated AMFIBHA, PLGCFIBHA and SFFIBHA hybrid scaffolds, FT-IR spectrums were obtained using attenuated total reflectance (ATR) method.

3.4.2 Surface topography analysis of scaffolds

The surface topography of the AMFIBHA, PLGCFIBHA and SFFIBHA hybrid scaffolds was examined using a scanning electron microscope (SEM, Hitachi S2400, Japan) / ESEM and bright field microscopy (Leica, DMIRB). For SEM analysis, the scaffolds were fixed on aluminium stubs, sputter coated with gold and scanned at a voltage of 15 kV. In the case of electrospun scaffolds, the fiber diameter distribution was quantitatively analyzed using scanning electron micrographs and Image J software.

3.4.3 Porosity analysis

Scaffolds were analyzed using micro-CT equipped with a charge-coupled device (CCD) detector. Samples were scanned at 12 µm voxel resolution using X-rays having energy 45 keV and 177 mA intensity. The isotropic slice data obtained by the system was reconstructed to about 300 to 400 two dimensional (2-D) images. The 2D slice images were then compiled and analyzed to obtain the 3-D images. The images were analyzed using an in-built software (Scanco) for estimating pore characteristics such as pore size and pore volume of each scaffold.

3.4.4. Analysis of scaffold swelling

Swelling studies were done in PBS and simulated body fluid (SBF). Briefly, the weights (W_d) of lyophilized scaffolds were noted and were, immersed in petri dishes containing PBS / SBF (pH = 7.4), and placed in an incubator at 37 ºC for 24 h. After 24 h, samples were lifted from solution and the excess fluid was removed by blotting the scaffolds lightly on dry tissue paper and the wet/swollen weight were weighed (W_s).

The percentage swelling was calculated using the equation:

$$\% \text{ Swelling} = [(W_s - W_d) / W_d] \times 100$$

3.4.5. Analysis of water vapour transmission rate (WVTR)

The WVTR was measured according to the published method (Adekogbe & Ghanem, 2005). Briefly, the test dish (2.0 cm in diameter) was filled with distilled water, leaving a space of 25 mm from the top of the dish to the water level. The samples were firmly glued to the mouth of the evaporating dish. The assembled petri dishes were weighed individually using a top loading balance (Sartorious, Germany) and were placed in an incubator at 37 ^{o}C temperature and 50 % humidity for 3 d. The weight loss was plotted against the elapsed time to get a slope with units of g/d. To calculate the WVTR, the slope was divided by the evaporating dish mouth area.

$$\text{WVTR} = \text{Slope (g/d)} / \text{Test Area (m}^2\text{)}$$

3.4.6. Analysis of surface wettability

The surface wettability of the bare and hybrid scaffolds were determined by sessile drop method using a video-assisted contact angle measuring device (Data Physics OCA15 plus, Germany) and imaging software (SCA20 software, Germany). Within 10 seconds of the introduction of the DI/W droplets, the contact angle formed between the sessile droplets and the scaffolds were measured. The contact angle is expressed as average of four independent measurements taken at different sites on each scaffold.

3.4.7. Testing of mechanical properties of scaffolds

The tensile stress at maximum load of PLGCFIBHA hybrid scaffold (10 mm diameter x 40 mm gauge length) was determined using a UTM. The test was conducted uniaxially at crosshead speed of 50 mm/min using a 10 N load cell. Maximum load (N) is obtained from the load-extension curve and knowing the sample cross-sectional area, tensile strength of scaffolds was calculated.

3.4.8. In vitro hydrolytic degradation of hybrid scaffolds

The degradation properties of hybrid scaffolds were studied as per the procedure stipulated in ISO 10993-13. Each scaffold (10 mm diameter) was initially weighed (W_0), and stored separately in 5 mL PBS (pH=7.4) and incubated at 37 ^{o}C for 30 d. The samples were taken out on 30th d, rinsed with deionized water, lyophilized, weighed (W_f) and weight loss was determined. The percentage weight loss was estimated using the equation:

$$\text{Gravimetric weight loss (\%)} = (W_0 - W_f)/ W_0 \times 100.$$

3.4.9. In vivo degradation of hybrid scaffold PLGCFIBHA

The *in vivo* degradation of bare PLGC and hybrid scaffold PLGCFIBHA was evaluated by GPC after subcutaneous implantation in New Zealand white rabbits. The implants were recovered after two time periods; 60 d and 120 d, minced finely, the polymer PLGC was extracted using solvent and GPC analysis was done. Molecular weights of scaffolds before and after degradation were determined using GPC equipped with a RI detector. Twenty micro-litres of 0.1 % solution of scaffolds in THF was injected and THF was used as the mobile phase at a flow rate of 2 mL/minute for each analysis.

3.4.10. Sterilization of the hybrid scaffolds

All the three hybrid scaffolds were sterilized using plasma (H_2O_2) sterilization (Sterrad 1005 plasma steriliser, USA) at 48 °C and stored at 4°C until use. The stability of PLGC was confirmed using SEM analysis for change in morphology of fibres and MW comparison before and after plasma sterilization. The sterility was confirmed by incubating the samples in medium containing serum for 15 d for bacterial and fungal contamination. The functional stability of the hybrid scaffolds were analyzed by comparing growth and proliferation rate of fibroblasts on scaffolds after sterilization with FIBHA scaffold prepared in sterile condition.

3.4.11. Testing hemocompatibilty of hybrid scaffolds

The effect of contact of hybrid scaffold materials with blood was examined using percentage hemolysis assay, which was performed according to ISO 10993-4: *in vitro* blood compatibility of biomaterials for medical use procedure. Free hemoglobin (Hb) liberated into the plasma after exposure was measured for each sample using a diode array spectrophotometer (HP 8453, Hewlett Packard, Germany) and the percentage hemolysis calculated using the equation:

$$\% \text{ Hemolysis} = (\text{Free Hb}/\text{Total Hb}) \times 100.$$

3.5. Fabrication of cell encapsulated SFFIBHA hydrogel

The lyophilized and processed SF was dissolved in distilled water by incubating at 4 ºC to get a final concentration of 4 %. The reconstituted fibrinogen concentrate as in #3.3.1 was mixed with SF and was diluted with distilled water to get a final concentration of 20 mg/mL and 2 % SF respectively. Thrombin (5 IU/mL) was mixed with 200 µg/mL HA and both components loaded in dual syringe applicator was delivered using 21 G needle is connected on the Y connector to the wells of tissue culture plate to a total volume of 0.2 mL.

3.5.1. Checking stability of SFFIBHA hydrogel

The clotting of gel within one min was visible which was further confirmed by preparing SFFIBHA hydrogel in a test tube and polymerization (clotting) with time was monitored by tilting the test tube horizontally till it stops flowing at RT. The stability of the gel was checked in 10 % FBS containing media for up to 7 d.

3.6. Differentiation of hADMSC to fibroblasts

Human ADMSC derived fibroblasts were used for used for the evaluations of scaffold. The establishment of the protocol was done by analyzing morphological changes and marker expressions at the transcriptional and translational level.

3.6.1. Preparation of fibroblast-specific niche

A biomimetic niche was designed for the induction of ADMSCs into fibroblast. The niche comprises of two components: (i) fibrin composite matrix and (ii) the differentiation medium with GF (DM). When cells on TCPS in DM is compared with cells grown on TCPS in basic DMEM-F12 medium (BM), effect of GF on ADMSC induction to fibroblasts is understood. When cells grown on the fibrin composite in DM (niche) is compared to the cells grown on TCPS in DM, the effect of fibrin composite is understood. When both together are exposed to ADMSC, it is called niche. To prepare fibrin composite coating, modified protocol of Unni *et al*., 2014 was adopted with a fibroblast-specific composition of fibrinogen composite comprising of 2 mg/mL human fibrinogen, (~ 0.02 mg) fibronectin, (0.2 %) gelatin (Sigma Chemicals, USA), 100 µg/mL HA (in-house purified; Rashmi *et al.*, 2020), 50 µg/mL human PGFs (in-house isolated) and 10 ng/mL FGF (R&D Systems, USA). Briefly, on a thrombin adsorbed surface, fibrinogen composite was layered to obtain a thin (< 1 µm) fibrin clot by the action of pre-adsorbed thrombin. Fibrin-deposited dishes were lyophilized in a sterile atmosphere, in a freeze-drier. The dishes were then stored at 4 - 6 °C until used. The DM was constituted in DMEM: HAM F12 (1:1) by supplementing 10% FBS, 10 ng/mL FGF, 50 µg/mL L-ascorbic acid (Sigma, USA), 50 µg/mL PGFs and 1× AbAm (Invitrogen, USA) (Rashmi *et al.*, 2020) .

3.6.2. Cell culture and analysis

Characterized human ADMSCs at a seeding density of 5000 cells/cm^2 were seeded onto the plates with complete niche and DM and for the differentiation of ADMSCs into fibroblasts for a time period of 7 and 14 d. The cells grown on complete niche (T1) and on TCPS with DM (T2) was compared with hADMSC grown on TCPS in BM (control) to understand the influence of the designed biomimetic matrix, which was used to set the baseline: (a) in real- time quantitative PCR fold change calculations; (b) in proliferation studies; and (c) in ECM deposition. The cells were examined intermittently under a phase contrast microscope (Leica DMIRB, Germany) to evaluate cell density and morphology.

3.6.3. Proliferation assay

The proliferation of the cells were evaluated by quantifying total DNA content by using the Trizol reagent as described in # 3.2.2.

3.6.4. Estimation of differentiation markers

Cells were harvested after 7 and 14 d of culture by a standard trypsinization method. qRT- PCR was carried out to track and compare differentiation towards fibroblastic lineage in test and control cultures. Total RNA was isolated from cells using Trizol reagent as per the manufacturer's instructions. Approximately 1 mL of Trizol reagent was added to lyse the cells and incubated for 5 min at RT. The RNA pellet was air dried, reconstituted in nuclease free water and quantified using nanodrop spectrophotometry.

Reagent	Volume
5X First strand buffer	4 µL
8 mM DTT	1 µL
RNAase Inhibitor	10 µL
RTase Supersript III	1 µL

Table 4. cDNAreaction mix

Approximately 400 ng of ribonucleic acid (RNA) was used for the complimentary DNA (cDNA) synthesis. Briefly, added 1 µL of 50 µM oligo (dT) primer to PCR tubes containing required volume of RNA solution and reaction mixture was then incubated at 65 °C for 5 min and 4 °C for 1min. After the initial incubation step, 16 µL of reaction mix mentioned in Table 4 was added the reaction volume was made up to 20 µL using nuclease-free water. The contents were then incubated at 50 °C for 1 h, followed by 95 °C for 5 min in a thermocycler (Master cycler, Eppendorff, Germany). Synthesized cDNA was stored at - 40° C until use.

PCR amplification was performed using specific primer pairs designed for gene sequences -fibroblast-specific protein (FSP-1), fibrillin-1, Col-1 and elastin genes, using specific intron-spanning primers. All reactions were carried out for 40 cycles. The cycle threshold (CT) value of the target gene was analyzed -after normalization to the CT value of glyceraldehyde-3-phosphate dehydrogenase

(GAPDH). Fold change ($2^{-\Delta\Delta CT}$) was calculated by comparing the expression levels of mRNA extracted from cells grown on bare TCPS in BM without GF supplements. For each gene, assessment of quality and specificity was performed by examining PCR melt curves. Primer sequences are given in Table 5.

Gene	Forward primer	Reverse primer
GAPDH	GAA ATC CCA TCA CCA TCT TCC AGG	GAG CCC CAG CCT TCT CCA TG
FSP-1	AGCTTCTTGGGGAAAAGGAC	CCCCAACCACATCAGAGG
Fib-1	TGATGGCTCCTACAGATGTG AATGC	GACACGGCTGGCAAGGTTCC
Col-1	CCAAGGGTAACAGCGGTGA	GCTTTCCTTCCTCTCCAG CA
Col-4	GCCTGGCTTGAAAGGTGAT AAG	CCCGCTATACCTTGATCTC
Elastin	CCTCCACCCCTCTCGGCCTG	CAGCGCTGGATAAAAGACTC CTCCA
α-SMA	GAGTTACGAGTTTGCCTGAT	AGACTCCATCCCGATGAA
TGF β-1	AGTTGTGCGGCAGTGGTTGA	GCCATGAATGGTGGCCAGGT
TGF β-2	TAGACATGCCGCCCTTCTTC C	AGCACCTGGGACTGTCTGGA
TGF β-3	AACCCAAAGCAGCAGAAG	CACCTGGAAAGCACTGTAG
CD 31	CAGTCATTACGGTCACAAT	CTGAGGACACTTGAACTTC
FLK-1	CCTCTACTCCAGTAAACCTG ATTGGG	TGTTCCCAGCATTTCACACTA TGG
eNOS	CGGCATCACCAGGAAGAAG A	CATGAGCGAGGCGGAGAT
VECAM	CCTCCTTAATAATACCTGCC ATTG	TCTGTGCTTCTACAAGACTAT ATGA

Table 5. Primers used for gene expression analysis

3.6.5. Analysis of ECM deposited by fibroblasts

To evaluate ECM deposition by cells grown on scaffolds for a time period of 14 d and 28 d, biochemical estimations of the culture surface was carried out after decellularization, as standardized by Divya *et al.* (2007). Briefly, the cells were immersed in sterile water for 3 h at 4 ºC. After 3 h, water was aspirated out and an isotonic solution containing 0.09 % sodium chloride and 0.02 % sodium azide was added and incubated for 1 h at 37 ºC in shaking incubator) at 90 rpm, isotonic solution was removed and wells were incubated for 1 h with a solution containing

1 % triton-x-100, 0.1 % ammonium hydroxide and 0.9 % sodium chloride. The scaffold was then washed three times with PBS and fixed with 3.7 % formaldehyde for 30 min and then washed with PBS. Decellularized scaffolds were used for quantification of collagen, elastin and sGAG. The production of total collagen, elastin and sGAG was quantified as described in # 3.2.4 -3.2 6.

3.7. *In vitro* tissue engineering on AMFIBHA, PLGCFIBHA and SFFIBHA hydrid scaffolds

The characterized human ADMSCs were cultured for 7 d on the designed biomimetic niche for the induction into dermal fibroblast and was trypsinised and used for evaluating the developed hybrid scaffolds. Cell growth potential on the AMFIBHA, PLGCFIBHA and SFFIBHA hybrid scaffolds was demonstrated by qualitative morphology analysis and fibroblast attachment followed by quantification of cell proliferation and ECM deposition.

3.7.1 Direct contact assay

Cytocompatibility of the AMFIBHA, PLGCFIBHA and SFFIBHA hybrid scaffolds were evaluated using direct contact method. The sterilized samples were placed on to the top of the confluent layer of fibroblast to evaluate cytotoxicity. The cells seeded on cell culture plate (TCPS) were taken as control as described in # 3.2.9.

3.7.2. Analysis of cell adhesion

For confirming fibroblast attachment and growth on scaffold, cultured AMFIBHA and PLGCFIBHA hybrid scaffolds were stained for actin with texas red phalloidin after 7 d. Briefly, cell cultured scaffolds were fixed with 3.7 % formaldehyde and then stained with texas red phalloidin as described earlier (# 3.2.10). The scaffolds were then counter stained with hoechst (Sigma, USA) for 10 min and observed and imaged using fluorescent microscope (Leica, DMIRB, Germany). For PLGCFIBHA hybrid scaffold, morphology of bare PLGC and hybrid scaffold PLGCFIBHA were observed by ESEM (FEI Quanta 200, Netherlands).

3.7.3. Quantification of cell adhesion and proliferation

Quantification of fibroblast adhesion and proliferation on the bare and hybrid scaffolds of all the three types were carried out using tritiated (^{3}H) - thymidine (American Radiochemicals, USA) uptake assay for different time periods. Fibroblast in log phase were labelled with ^{3}H-thymidine by adding the nucleotide at a concentration of 5 µCi/mL in the culture media which was then cultured for one week at 37 ^oC and 5 % CO_2 to achieve more than two population doublings. The ^{3}H-thymidine-loaded cells were harvested by trypsinization and 5000 cells/cm^2 were seeded on bare and hybrid scaffolds.

After 2 h of seeding, unattached cells were harvested and DNA was extracted for detecting ^{3}H- thymidine activity as per the reported method (Shivakumar *et al.*, 1992). The cells attached were continued in culture with medium containing ^{3}H-thymidine on alternate day. Cells were harvested from the bare scaffolds and hybrid scaffolds at different time periods. The radioactivity of extracted DNA samples were counted using triathler multilabel tester (Hidex, Finland). ^{3}H- thymidine activity per cell when seeded was used to estimate cell number after culture.

3.7.4. Estimation of ECM deposited by fibroblast on scaffolds

The insoluble ECM laid by cells on the scaffolds was analyzed qualitatively and quantitatively. The decellularization of fibroblast cultured scaffolds was done as described in # 3.6.6. The decellularized scaffolds were stained for Col-1 and 3, elastin and fibrillin-1 with specific monoclonal antibodies. Briefly, the decellularized scaffolds were blocked with 1 % BSA for 30 min, incubated with the respective antibodies (1:100 dilution) for 2 h and developed using flurochrome conjugated secondary antibodies as described in # 3.2.7. The scaffolds were imaged using fluorescent microscope and Leica Application Suit software (Leica, DMIRB, Germany).The total collagen, elastin and sGAG content in the decellularized hybrid scaffolds was quantified as described in # 3.2.4 – 3.2.6.

3.8. Evaluation of SFFIBHA hydrogel for cell growth

3.8.1. Encapsulation of cells in SFFIBHA hydrogel

The hydrogel system was fabricated using the procedure described in # 3.5. Cells at a density of 10,000 cells/100 µL were suspended in component I. A 21 G needle was connected on the Y connector and the both components were delivered to the wells of tissue culture plate to a total volume of 0.2 mL. The gels were allowed to stabilize for about 10 - 15 min in incubator maintained at 37 ºC in 5 % CO_2 incubator and fibroblast basal medium was added. For control, 5000 cells were seeded on SF scaffold and on TCPS for comparison of cell viability and proliferation.

3.8.2. Analysis of cell viability

The cell viability in the cell encapsulated SFFIBHA gel was evaluated after 7 d of culture. After specific time period, the gels were washed with sterile PBS, cut into smaller pieces for the penetration of MTT reagent into the gel. MTT assay was done as described in # 3.2.9.

3.8.3. Analysis of cell proliferation

For analysing proliferation potential of cells in hydrogel, ^{3}H-thymidine loaded cells were used for encapsulation. The assay was done as described in # 3.7.3 for lyophilized scaffolds. The adhesion of fibroblasts on bare SF and hybrid SFFIBHA gel within 2 h and proliferated cell numbers after 7 d of culture were calculated.

3.8.4. Estimation of ECM production

The ECM deposition after 15 d of encapsulation was analyzed for total collagen, elastin and sGAG after decellularisation as described in and # 3.6.6 and # 3.2.4 - 3.2.6.

3.8.5. Co-culture of fibroblasts & ECs in the developed hydrogel

The seeding density of fibroblast and endothelial cells were 1 : 2, respectively. ADMSC-derived fibroblast was harvested after 7 d of culture in the designed biomimetic niche and was used for the study. Cells were harvested simultaneously while preparing gel solutions. Briefly, cells (fibroblasts and ECs) at a density of 10,000 cells/100 µL were suspended in component I and fabricated 0.2 mL clots as described in 3.8.1. The gels were allowed to stabilize for about 10-15 mins in incubator maintained at 37 ºC in 5 % CO_2 incubator and common medium (DMEM:F12) was added. For control, 5,000 cells/cm^2 (fibroblasts and ECs) were seeded on SF discs (containing 0.2 mL SF). The culture was analyzed for a time period of 7, 14 and 28 d.

3.8.6. Analysis of cell proliferation in hydrogel

The proliferation of cells was analyzed by quantifying the total DNA content using Trizol reagent as described in # 3.2.2.

3.8.7. Analysis of cell-specific markers

The co-expression of fibroblasts and ECs were analyzed using qRT-PCR for a time period of 7 and 14 d. The co-expression of fibroblasts and ECs were analyzed for fibroblast and EC specific genes like FSP-1, Fib-1,Col-1, elastin and CD 31, FLK-1, eNOS, VCAM, αSMA and Col-4 respectively as described in # 3.5.1.4. GAPDH was used as the housekeeping gene. Primer sequences, gene accession numbers and amplicon sizes are given in Table 4.

3.8.8. Analysis of ECM synthesis by co-cultured cells

The ECM deposition of the encapsulated cells after 14 and 28 d was analyzed after decellularisation as described in # 3.6.6. The total collagen, elastin and sGAG were quantified using the method described in # 3.2.4 - 3.2.6.

3.9. *In vivo* guided skin regeneration of burn wounds

The developed AMFIBHA, PLGCFIBHA and SFFIBHA hybrid scaffolds were evaluated for their support for skin regeneration in full thickness burn wound models of 4 x 4 cm^2 size. Lyophilized AMFIBHA and PLGCFIBHA were implanted on debrided fresh tissue. In the case of SFFIBHA both lyophilized and hydrogel matrix was applied in separate experiments.

3.9.1. Selection of animals

New Zealand white rabbits with an average weight of 2.34 ± 0.5 kg obtained from the Division of Laboratory Animal Sciences, SCTIMST, India, were used for the study. All animal procedures were conducted with the permission from Institutional Animal Ethics Committee (IAEC) as per Committee for the Purpose of Control and Supervision on Experiments on Animals (CPCSEA) (Govt. of India) guidelines.

Period of study/ Groups	14 d / 28 d
Group I (C)	Control - Untreated/ Sham wound (n=4)
Group II (+ve C)	Positive Control - NeuSkin (n=4)
Group III (Test C)	Test Control - FIBHA Scaffold (n=4)
Group IV (Test C)	Test Control - AM (n=4)
Group V (Test)	AMFIBHA Hybrid scaffold (n=4)
Group VI (Test)	PLGCFIBHA Hybrid scaffold (n=4)
Group VII (Test)	SFFIBHA Hybrid scaffold (n=4)
Group VIII (Test)	SFFIBHA Hydrogel (n=4)

Table 6. Experimental animal groups for burn wound healing evaluation

3.9.2. Burn wound experiment

Adult rabbits of either male or female sex was used for the study. Briefly, the rabbits were anaesthetized using ketamine hydrochloride 50 mg/kg and xylazine 5 mg/kg. The dorsal hair was clipped and was made aseptic using betadine solution and ventilated. Third degree burn injury was induced over the dorsal thorax of the rabbit by applying a 4 x 4 cm^2 template preheated brass plate at 120 ºC for 60 s at two sites per animal. The wound bed was prepared to expose fresh tissue by

surgically debriding the burnt full thickness skin using sterile scalpel blade (size 11) and forceps before applying the test material. The burn was confirmed using histological evaluations. The wound left untreated / sham and positive control commercially available Neuskin (xenogenic collagen - Eucare Pharmaceuticals Pvt Ltd, India) and FIBHA scaffold treated wound was taken as controls. All wounds received standard wound dressing with the help of burn mesh and melolin dressing material to keep the graft material intact to the wound. After recovering from anaesthesia, animals were kept in cages; fed with diet and water. After surgery, ceftriazone (10 mg/kg) was given two times daily for 5 d and meloxican injection (0.3 mg/kg) was also given for 3 d. The controls and tests were given equal care. The wound healing was evaluated upto 28 d (Table 6).

3.9.3. Study design of wound healing

The wound healing efficiency of the regenerated skin was evaluated using gross appearance, wound closure, transcriptional and translational level expression of proteins using qRT-PCR and histological and immunohistological techniques. The wound healing was analyzed in terms of epithelisation, angiogenesis and ECM deposition. The test materials were compared with untreated /sham control (negative control) and NeuSkin (positive control).

3.9.4. Gross tissue analysis

The wound was evaluated by gross observation and photographed periodically till 28^{th} d. The percentage wound closure was evaluated by measuring wound closure area from 0^{th}, 7^{th}, 14^{th}, 21^{st} and 28^{th} d.

3.9.5. Transcriptional level evaluations

After 14 d and 28 d of surgery, the animals were euthanized using carbon dioxide. Part of the excised wound site was incubated in Trizol reagent. Total RNA was isolated from cells using trizol reagent (Invitrogen, USA) as per the manufacturer's instructions as described in as described in # 3.2.2. Approximately 1µg of ribonucleic acid (RNA) was used for the complimentary DNA (cDNA) synthesis.

PCR amplification was performed using specific primer pairs designed for genes using specific intron-spanning primers. GAPDH was used as housekeeping gene. Primer sequences, gene accession numbers and amplicon sizes are given in Table 7.

Gene	Forward primer	Reverse primer	NM Number	A. size
Rabbit GAPDH	TCGGCATTGTGGAGGGGCTC	TCCCGTTCAGCTCGGGGATG	NM_001082253.1	177
Rabbit Col-3	AAGCCCCAGCAGAAAATT G	TGGTGGAACAGCAAAAATCA	XM_002712333.3	160
Rabbit Col-1	GGTTATGATGGAGACTTCTACAG	GGTTGTTCAGAGACTTCAGAG	NM_001195668.1	103
Rabbit Elastin	CTTGGAGTTGGTGCTGGT	CCGTATTTCGCTGCCTTAG	XM_017337950.1	137
Rabbit VEGFR	CTTGCCTTGCTGCTCTAC	ACTTCCATGAACTTCACCAC	XM_017345155.1	104
Rabbit α-SMA	TTCCAGCCCTCCTTCATC	CTGAGAGCACATTGTTAGCA	NM_001101682.2	118
Rabbit IL-6	GAACAGAAAGGAGGCACTGG	CTCCTGAACTTGGCCTGAAG	NM_001082064.2	168
Rabbit TNF-α	GTCTTCCTCTCTCACGCACC	TGGGCTAGAGGCTTGTCACT	NM_001082263.1	336

Table 7. Rabbit primers used for gene expression analysis

3.9.6. Histology evaluation

Wound tissues were explanted on 14 d and 28 d of surgery (4 samples each) along with normal skin on the peripheries were excised and were fixed in 10 % neutral buffered formaldehyde. Tissues were then processed by standard procedure using automated tissue processor, embedded in paraffin wax, thin sections (5 µm) were made using a microtome (Leica RM 2255, Germany). For staining, sections were kept in hot air oven for 60 min and deparaffinised with xylene (3 changes, 15 min each); rehydrated in descending grade of isopropanol series (100 % for 3 min, 95 % for 3 min, 80 % for 3 min and 70 % for 3min); washed in tap water for 5 min; stained with harris's haematoxylin for 15 min; washed in tap water for 5 min, differentiated in 1 % acid alcohol (1-2 fast dip) and blued with 0.2 % ammonia water

for 1 min. It was then washed with tap water for 5 min, counterstained with 1 % eosin Y for 5 min; dehydrated in isopropanol (95 % for 5 min, 100 % ethanol for 5 min - 2 changes); cleared in xylene (3 changes, 15 min each); mounted in DPX and viewed under microscope (Leica, DMIRB, Germany). The inflammatory cells, granulation tissue formation, extent of wound epithelisation and generation of dermal tissue was evaluated using a Leica microscope (DMIRB, Germany). Additionally, the sections were immunostained for the endothelial marker CD 31, epithelialization marker CK 5, elastin deposition and stained with Sirius red (collagen deposition) for evaluation of regenerated wound in terms of epithelialization, angiogenesis and ECM organisation.

3.9.7. Identification of epithelisation marker

The paraffin embedded sections were deparaffinised and rehydrated as described in # 3.9.6. Tissue sections were then incubated with 0.1 % trypsin solution at 37°C for 60 min to retrieve the antigenic sites. Then the peroxidise activity of tissue was blocked by addition of 20 % hydrogen peroxide (Sigma,USA) for 20 min, and washed with tris-buffered saline (TBS) two times. The sections were then incubated with 10% FBS in TBS for 30 min to block nonspecific sites. The primary antibody, CK-5 (Abcam, UK) was added (1:50 dilution), incubated for 1 h at RT and washed with TBS for three times. Horseradish peroxidase (HRP) was added and incubated for 30 min, washed with TBS four times. DAB solutions were added, after 5min, and the reaction was stopped by washing in water. Then the sections were immersed in hematoxylin solution for 1 min and blued with 0.2 % ammonia water for 1 min. It was then washed with tap water for 5 min, dehydrated in isopropanol (95 % for 5 min, 100 % ethanol for 5 min - 2 changes); cleared in xylene (3 changes, 15 min each); mounted in DPX and imaged under light microscope (Leica DMIRB, Germany).

3.9.8. Identification of angiogenic protein marker

The paraffin embedded sections were deparaffinised and rehydrated as described in # 3.9.6. Tissue sections were then incubated with 0.1 % trypsin solution at 37 °C for 60 min to retrieve the antigenic sites. Then the peroxidise activity of tissue was blocked

by addition of 20 % hydrogen peroxide (Sigma,USA) for 20 min, and washed with tris-buffered saline (TBS) two times. The sections were then incubated with 10 % FBS in TBS for 30 min to block nonspecific sites. The primary antibody, CD 31 (Abcam, UK) was added (1:100 dilution), developed with HRP counter stained with eosin-hemotoxylin were embedded and analyzed as described in #3.9.7 (for CK 5).

3.9.9. Identification of collagen deposition/organization

The collagen deposition and organisation was analyzed on 14 and 28 d of wound healing. The sections were deparaffinised with xylene (3 changes, 15 min each); rehydrated in descending grade of isopropanol series (100 % for 3 min, 95 % for 3 min, 80 % for 3 min and 70 % for 3 min); and washed in tap water for 5 min. The nuclei were stained with weigert's haematoxylin for 5 min, and then the slides were washed in running tap water for 10 min. The sections were stained with picro sirius red solution containing 0.1 % Sirius red /direct red 80 (Sigma,USA) in saturated aqueous solution of picric acid for 1h, washed with acidified water and dehydrated the sections with 3 changes of 100 % isopropanol. Cleared in xylene (3 changes, 15 min each); mounted in DPX and viewed under microscope and photo micrographed (Leica, DMIRB, Germany).

3.9.10. Identification of elastin deposition

The paraffin embedded sections were deparaffinised and rehydrated as described in # 3.9.6. Tissue sections were then incubated with 0.1 % trypsin solution at 37°C for 60 min to retrieve the antigenic sites. Then the peroxidise activity of tissue was blocked by addition of 20 % hydrogen peroxide (Sigma,USA) for 20 min, and washed with tris-buffered saline (TBS) two times. The sections were then incubated with 10% FBS in TBS for 30 min to block nonspecific sites. The primary antibody, elastin (Abcam, UK) was added (1:100 dilution), developed with HRP, counter stained with H & E and analyzed as described in # 3.9.7.

3.9.11. Evaluation of regenerated wound for tissue maturation

The long term effect of the hybrid scaffolds AMFIBHA, PLGCFIBHA and SFFIBHA as well as the SFFIBHA hydrogel system on burn wound model was

evaluated for 56 d in terms of its gross appearance, mechanical strength and ECM quantification. The test samples were compared with untreated /sham wound as well as normal rabbit skin. Tensile strength and percentage elongation at break of the regenerated wound on application of the hydrd scaffolds for 56 d were analyzed using Universal Testing Machine (Instron 1011, UK) at a crosshead speed of 50 mm/min (ASTM D 882-97 method). The test samples were compared with untreated/sham control and normal rabbit skin. The ECM estimation of the regenerated skin after 56 d was done using biochemical quantification of total collagen, elastin and sGAG. The methods are as described in # 3.2.4 – 3.2.6.

3.10. *In vivo* guided skin regeneration of wounds in diabetic animals

The developed AMFIBHA, PLGCFIBHA and SFFIBHA hybrid scaffolds were evaluated for their support for skin regeneration in full thickness wound models of 4x4 cm^2 size in diabetic porcine models.

3.10.1. Selection of animals

Yorkshire white pigs with an average weight of 28 ± 1 kg of around 24 - 32 weeks were used for the study. All animal procedures were conducted with the permission from IAEC and CPCSEA (Govt. of India) guidelines.

3.10.2. Development of hyperglycemic pigs

The porcine diabetic model was induced using the administration of two doses of streptozotocin (Sigma, USA). Briefly, the pig was anesthetised with a cocktail of xylazine, ketamine and atropine and jugular vein canulation was done three d prior to the first dose of streptozotocin administration. Twice a day the cannula was flushed with saline containing heparin (1.5 mL / 500 mL saline) with antibiotic (5 mL ampicox / 500 mL saline) to prevent infection and clotting. On the fourth day, first dose of filter-sterilized streptozotocin (100 mg/kg taken as 100 mg/mL in saline) was administrated intravenously (IV) over 10 mins. Weight and baseline blood glucose level was monitored using glucometer (Accu Chek, Roche, Germany) via capillary blood from the ear prior to the streptozotocin administration. Dextrose (5 % w/v) was administered (IV) when blood glucose was below 50 mg/dL to prevent

hypoglycaemic shock. Every 12 h blood glucose was monitored and after 72 h, second dose of streptozotocin (60 mg/kg) was administered intravenously over 10 mins. Dextrose (5 % w/v) was administered (IV) when blood glucose was below 50 mg/dL to prevent hypoglycaemic shock. The animals received special care and standard feed as followed in the animal house. The glucose was monitored twice in a day after the induction. Insulin was administered subcutaneously (SC) once/twice daily when blood glucose levels (BGL) was higher than 350 mg/dL and insulin dose was adjusted accordingly. Enrofloxacin injection (10 % w/v) was given weekly. Two weeks after confirming steady hyperglycaemia, animal experiment was conducted.

Period of study/Groups	28 d
Group I (C)	Control – Untreated/ Sham wound (n=4)
Group II (+ve C)	Positive Control – NeuSkin (n=4)
Group III (Test)	AMFIBHA Hybrid scaffold (n=4)
Group IV (Test)	PLGCFIBHA Hybrid scaffold (n=4)
Group VI (Test)	SFFIBHA Hybrid scaffold (n=4)

Table 8. Experimental animal groups for wound healing evaluation

3.10.3. Diabetic wound experiment

After giving anaesthesia dorsal skin of the pig was shaved and made aseptic using 70 % alcohol and betadine. Full-thickness 4 x 4 cm^2 sized wounds were made on the dorsal skin for the application of test materials. The wound size was marked using a template and full thickness skin was excised to create 4 x 4 cm^2 wound with a sterile blade. The test materials AMFIBHA, PLGCFIBHA and SFFIBHA hybrid scaffolds were applied to the wound bed without any sutures. The test wounds were compared with untreated / sham (negative control) and commercially available NeuSkin (positive control) treated wounds. All wounds received standard wound dressing with the help of mesh and melolin dressing material to keep the graft material intact to the wound. After recovering from anaesthesia, animals were kept in cages; fed with diet and water. The blood glucose level and weight was monitored daily and weekly respectively. The wound dressing was removed weekly, cleaned and monitored the wound healing up to 28^{th} d (Table 8).

3.10.4. Gross evaluation

The wound was evaluated by gross observation and photographed up to 28 d and percentage wound closure was calculated.

Gene	Forward primer	Reverse primer	NM Number	A. size
Porcine GAPDH	CTCAACGACCACTTCGTCAA	TCCAGGGGCTCTTACTCCTT	NM_001206359.1	113
Porcine Col-1	ACCTCAAGATGTGCCACTCC	CCTGTCTCCATGTTGCAGAA	XM_021067155.1	106
Porcine Elastin	GCGGCTTAGGAGTGTCTA	GTACTTTCCCTGGCTTCG	XM_021085799.1	81
Porcine VEGFA	CTTGCCTTGCTGCTCTAC	CGTCCATGAACTTCACCAC	NM_214084.1	100
Porcine α-SMA	ATGGTGGGAATGGGACAA	GGTGATGATGCCGTGTTC	NM_001164650.1	102
Porcine TGF β-1	TGCTAATGGTGGAAAGCGGCAACC	GTTATCTTTGCTGTCACAGGAACAGTGGGC	NM_214015.2	359
Porcine Biglycan	GATGGCCTGAAGCTCAA	GGTTGTTGAAGAGGCTG	XM_003135475.5	406
Porcine CK-14	TGGTGGCCTTGGTACTGGCTTG	GCATTGTCCACTGTGGCTGTGAG	XM_021067000.1	297
Porcine TGF β-3	GAGATCCATAAATTCGACATGATCCAGGGG	ATTTCCAGACCCAAGTTGGACTCTCT	NM_214198.1	359
Porcine Col-3	TAGCAGGAGGAGGAATCG	ACCAGGATGACCAGATACA	NM_001243297.1	86

Table 9. Porcine primers used for gene expression analysis

3.10.5. Transcriptional level evaluations

After 28 d of surgery, the animals were euthanized using carbon dioxide. Part of the excised wound site was incubated in Trizol reagent. Total RNA was isolated from cells using Trizol reagent (Invitrogen, USA) as per the manufacturer's instructions as described in as described in # 3.2.2. Approximately 1µg of ribonucleic acid (RNA) was used for the complimentary DNA (cDNA) synthesis. PCR amplification was performed using specific primer pairs designed for genes using specific intron-

spanning primers. GAPDH was used as housekeeping gene. Primer sequences, gene accession numbers and amplicon sizes are given in Table 9.

3.10.6. Histological analysis

Wound tissues were explanted on 28 d of surgery (4 samples each) along with normal skin on the peripheries were excised and were fixed in 10 % neutral buffered formaldehyde. Tissues were then processed by as described in # 3.9.6. The inflammatory cells, granulation tissue formation, extent of wound epithelisation and generation of dermal tissue was evaluated using a Leica microscope (DMIRB, Germany). Additionally, the sections were immunostained for the endothelial marker CD 31, epithelialization marker CK 5, collagen deposition (Col-1 & 3), and elastin deposition and for evaluation of regenerated wound in terms of epithelialization, angiogenesis and ECM organization.

3.10.7 Identification of epithelialization marker

The paraffin embedded sections were deparaffinised and rehydrated as described in # 3.9.6. Antigen retrieval followed by the steps was done and the sections were stained as described in # 3.9.7.

3.10.8. Identification of angiogenesis marker

The paraffin embedded sections were deparaffinised and rehydrated and sections were stained as described as described in # 3.9.8.

3.10.9. Identification of collagen deposition/organization

The collagen deposition was analyzed by the ratio of collagen-1 to 3. The paraffin embedded sections were deparaffinised and rehydrated and sections were stained as described in # 3.9.7 using col-1 and 3 antibodies (Abcam, UK) (1:50 dilution), mounted in DPX and viewed under microscope and photo micrographed (Leica, DMIRB, Germany).

3.10.10. Identification of elastin deposition

The paraffin embedded sections were deparaffinised and rehydrated as described in # 3.9.10 using primary antibody, elastin (Abcam, UK) (1:50 dilution), mounted in DPX and imaged under light microscope (Leica DM IRB, Germany).

3.10.11. ECM maturation of the regenerated skin

The ECM deposition of the regenerated porcine skin after 28 d of wound healing was evaluated by estimation of total collagen, elastin and GAG as described in # 3.2.4 - 3.2.6.

3.11. Toxicological evaluation of the PLGCFIBHA and AMFIBHA hybrid scaffolds

Toxicological evaluation of PLGCFIBHA and AMFIBHA hybrid scaffold were done according to the OECD guidelines of the good laboratory practices (GLP). Intracutaneous (intradermal) reactivity test and guinea pig maximization test (GPMT) was done for both the scaffolds to meet the requirements of *ISO-10993-10:2010(E) : biological evaluation of medical devices part 10 : test for irritation and skin sensitization test* clause 6.4: animal intracutaneous reactivity test & USP 38/NF33:2015 and clause 7.5: GPMT respectively.

Intracutaneous (intradermal) reactivity test: Intracutaneous (intradermal) reactivity test was done in albino rabbits (n=3) using physiological saline (PS) and cotton seed oil extract from scaffold incubation at 37 ± 1 ºC for a time period of 72 ± 2 ºC at a agitation of 50 rpm. The extracts were aseptically injected (0.2 mL/site) at five different sites which was compared with injections with control solution (PS alone) with scaffold incubation. The grading of erthema of test and control sites of all animals at 24, 48 and 72 h were recorded.

GPMT: GPMT was done in hartley albino guinea pigs (n=15) using PS extract from scaffold incubation at 37 ± 1 ºC for a time period of 72 ± 2 ºC at a agitation of 50 rpm. The PS extract of the tests and control (PS alone) was intradermally injected (0.1 mL/site) and after 7 d it was topically applied. Challenge test was carried out for

14 d on all the animals. The appearance of the challenge skin sites of test and control animals were observed at 24, 48 and 72 h after removal of dressings and patches. The skin reactions for erythema and oedema were scored and recorded the numerical grading as per guidelines.

3.12. Statistical analysis

For all quantitative assays in the above experiments, more than three replicate experiments were carried out and the values were averaged and expressed as the mean ± standard deviation (SD). Statistical analysis using a one-way analysis of variance (ANOVA) and p values showing statistically significant differences were given in the figure legends.

CHAPTER 4

4. RESULTS

The results of the study are illustrated in this chapter; illustrating data on development and evaluation of three different hybrid scaffolds AMFIBHA, PLGCFIBHA and SFFIBHA for application as skin substitutes and SFFIBHA hydrogel system. First section # 4.1 illustrates characteristics of the molecules and biomaterials used for developing different skin substitutes for regenerating wounds that are difficult to heal. Second section # 4.2 demonstrates the properties of all three lyophilized hybrid scaffolds and the cell encapsulated hydrogel system. Third section # 4.3 demonstrates the advantage of lyophilized hybrid scaffolds and hydrogel as *in vitro* tissue engineering scaffold using hADMSC derived fibroblasts. The fourth section # 4.4 presents *in vivo* experimental results demonstrating the advantage of lyophilized hybrid scaffolds as hemostatic skin substitute for healing full thickness burn wounds in rabbit and the fifth section # 4.5 describes the long term evaluation of the regenerated skin. Sixth section # 4.6 illustrates full thickness excision wounds healing responses to the scaffolds in diabetes-induced porcine model and seventh section # 4.7 describes toxicological evaluaton of scaffolds.

4.1. Characteristics of raw materials

4.1.1. Fibrin and HA

Fibrin sealant obtained from biotherapeutic production laboratory of the Institute was reconstituted and used as per the instruction in the user manual (Figure 1). The fibrinogen and thrombin concentrations required was achieved by diluting the reconstituted concentrate.

Figure 3. Fibrin sealant kit

The in-house purified HA appeared as white semi-crystalline powder and yield was found to be ~1.5 g from ~250 g of human umbilical cord tissue (Figure 2 inset). FTIR and NMR spectroscopy showed typical chemical characteristics and HPLC revealed purity of the in-house prepared HA (HA-TRU) to be improved as compared to commercially available HA (HA-Sigma).The FTIR spectrum showed characteristic peaks at 3311 cm^{-1} (broad) corresponding to OH stretching, 2981 cm^{-1} to vibration of C-H stretching, 1608 cm^{-1} (strong peak) to amide carbonyl, 1405 cm^{-1} (strong peak) to acid group of HA (stretching of C00-), 1241 cm^{-1} and 1034 cm^{-1} (strong peak) to stretching linkage of C-OH respectively. The Sigma-HA showed broader peak at 3488 cm^{-1} to the OH and NH stretching compared to TRU-HA which may be due to contamination of protein from the tissue (Figure 4.A). HA is a linear non-sulfated GAGs built of the repeating unit disaccharide β-d-glucuronic acid-(1 → 3)-β-d-N-acetyl-d-glucosamine-(1 → 4). NMR spectrum of in-house purified HA showed signals at δ = 3.7 – 3.5 ppm and δ = 2.1 – 1.9 ppm attributing to $–CH_3$ protons and δ = 3.3 – 3.32 ppm attributing to $-CH_2$ protons in sugar rings (GalNAc). Signal at δ = 4.7 ppm attributes to deuterium oxide (D_2O) solvent (Figure 4.B). The HPLC chromatogram showed similar peaks for retention time. An additional peak was recorded in Sigma-HA at 1.890 minutes which can be due to the protein contamination (Figure 4.C). The purity was calculated from the HPLC data and was ~ 95 % and ~ 83.4 % for HA-TRU and HA-Sigma respectively. Hence, the TRU-HA was proved to have higher purity established by FT-IR & NMR spectroscopy and HPLC (Rashmi *et al.*, 2020).

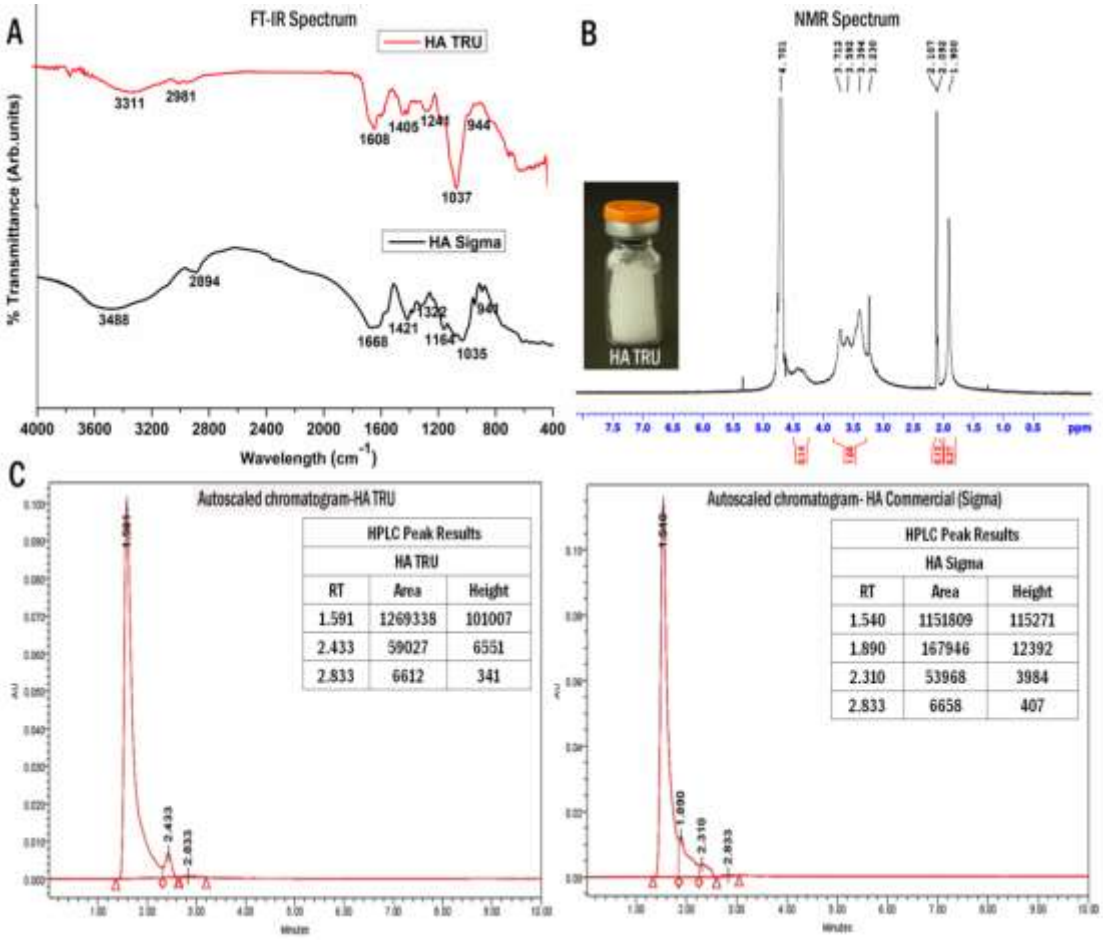

Figure 4. Spectral and chromatographical features of in-house purified HA: A) IR spectrum of HA-TRU and that of commercial source for comparison, B) NMR spectrum of HA-TRU and C) HPLC elution pattern of HA-TRU (inset) and Sigma-HA.

4.1.2. Properties of decellularized AM

Human AM was obtained as white translucent membrane after separating from placenta and cleaning (Figure 5). Different protocols were tried for decellularisation of AM using treatments with detergents, alkali and freeze thawing etc at different temperature, concentration and time period of incubation (Figure 6).

Figure 5. Cleaning of amniotic membrane: A) human placenta, B) Peeling of amniotic membrane, C) Cleaning amnion to remove blood clots and remnents of chorion and D) Cleaned amnion stored in PBS containing 5x antibiotics at 4 ^{o}C.

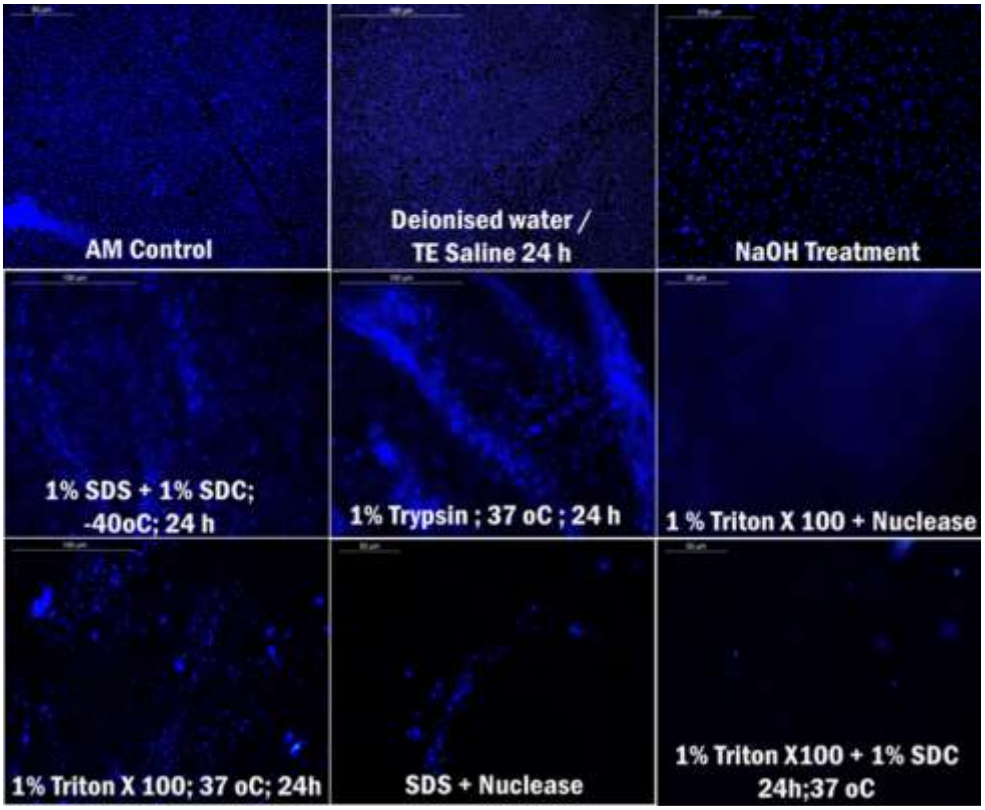

Figure 6. Different protocols attempted for decellularization of AM based on treatments with freeze thawing, alkali, detergents and enzymes with varying concentrations, temperature & time of incubation.

The optimised protocol as described in # 3.1.3 resulted in complete decellularisation confirmed by DAPI staining, which was further air dried and plasma sterilized and stored at 4 ºC until use (Figure 7).

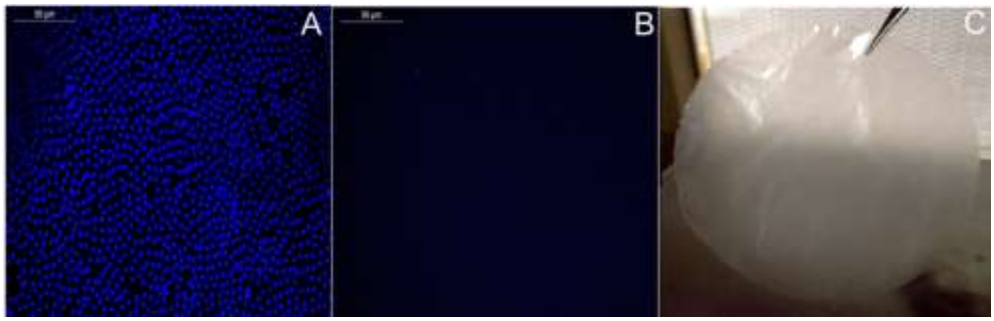

Figure 7. Representative images of decellularized AM: A & B) DAPI staining before and after decellularization; scale bar = 100 µm and C) final decellularized and plasma sterilized AM.

The total DNA content in AM before and after decellularisation was found to be 1458 ± 303 ng/cm² and 120 ± 50 ng/cm² showing significant reduction (P value = 0.0001) indicating successful decellularisation procedure. The total protein content showed 492 ± 91 µg/cm² and 307 ± 38 µg/cm². The reduction in the total protein content can be due to the removal of cellular proteins.

The total collagen, elastin and sGAG content in AM before and after decellulrisation, after drying and after final plasma sterilization was done to access any significant loss of ECM proteins. The total collagen content was found to be was 97.8 ± 11.6 µg/cm^2, 94.3 ± 11.3 µg/cm^2, 94.1 ± 7. 0 µg/cm^2 and 91 ± 10.6 µg/cm^2 respectively. The total elastin content was found to be 201 ± 20 µg/cm^2, 181.9 ± 18 µg/cm^2, 175 ± 20.7 µg/cm^2 and 174 ± 20 µg/cm^2 respectively. The total sGAG content was found to 36.9 ± 4.2 µg/cm^2, 33 ± 3.48 µg/cm^2, 32.2 ± 5.2 µg/cm^2 and 28.9 ± 0.67 µg/cm^2 respectively. There was no significant reduction in the total collagen, elastin and sGAG proteins.

The dAM showed positivity for the ECM molecules like collagen sub types like Col-1, Col-2, Col-3, Col-4 and Col-10, elastin and fibrillin-1 proteins (Figure 8).

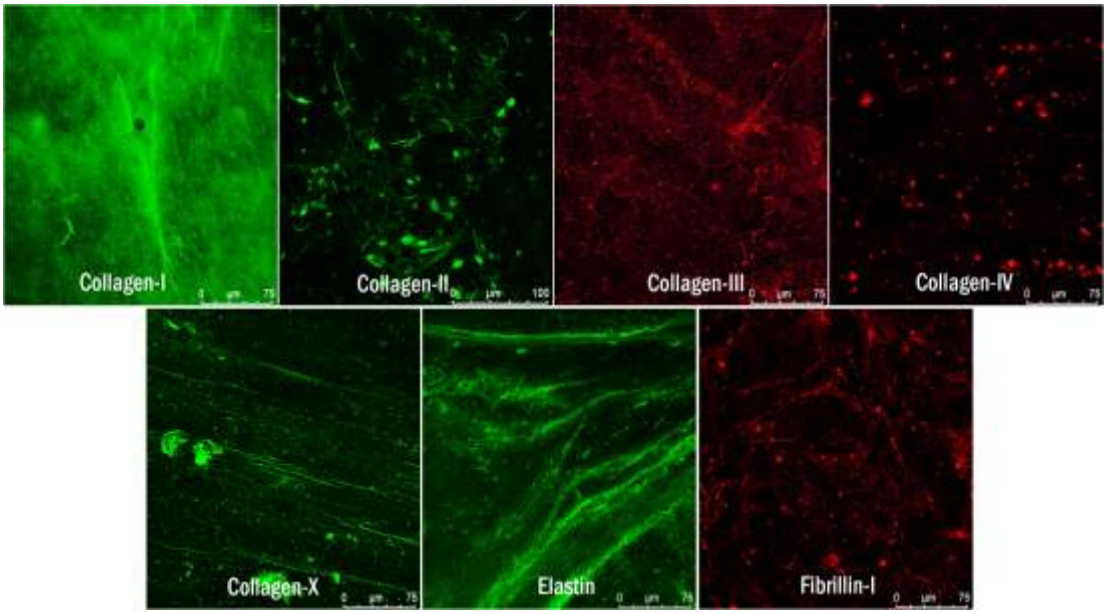

Figure 8. Immunostaining of ECM molecules in the decellulalrized AM: Confocal images showing ECM molecules like Col-1, Col-2, Col-3, Col-4, Col-10, elastin and fibrillin-1 in decellularized AM; scale bar = 75 µm.

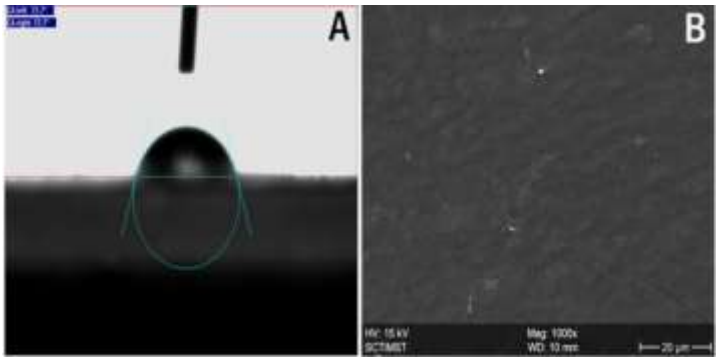

Figure 9. Surface properties of decellularized AM: A) Contact angle showing surface wettability and B) ESEM image showing smooth surface topography; scale bar = 20 µm.

The dAM showed smooth surface topography in ESEM analysis. Surface wettability analysis showed contact angle of 71 ± 2° indicating hydrophilic nature (Figure 9). The mechanical properties of decellularized AM showed tensile strength, tensile modulus and tensile strain of 346 ± 59 MPa, 9.04 ± 0.8 % and 15223 ± 2803 MPa respectively.

Biocompatibility evaluation was done to confirm removal of traces of detergent used in the decellularization protocol. In direct contact assay, the cells

incubated with decelluarized AM were viewed under phase contrast microscopy to observe the morphological and cellular response of the L929 fibroblast cells. There was no cell death and cells were growing near the scaffold (Figure 10).

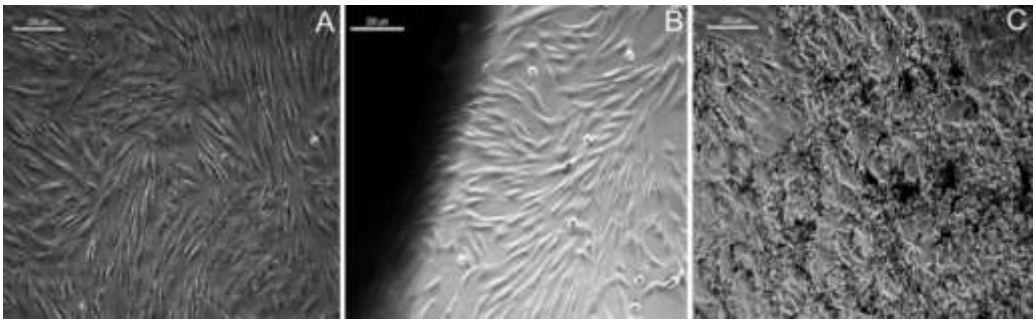

Figure 10. Phase contrast micrographs of direct contact assay of decellularized AM: A) control cells grown on tissue culture dishes (TCPS) and B & C) cells incubated with decellularized AM scaffold for 72 h ; scale bar =200 µm.

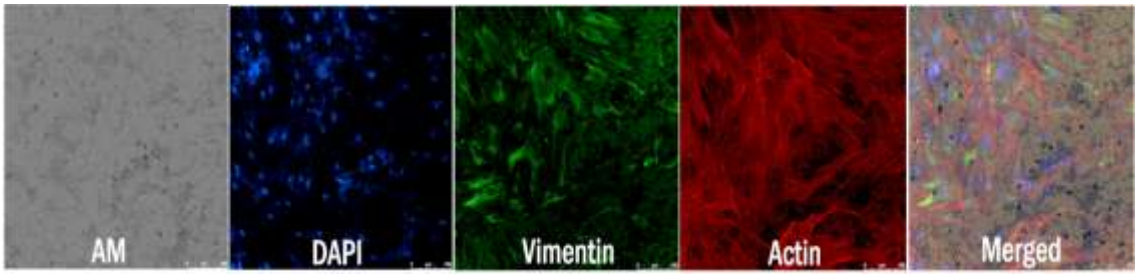

Figure 11. Fluorescent micrographs of actin-vimentin stained fibroblasts on decellularized AM; scale bar =100 µm.

In MTT assay, the dAM showed significant increase in cell viability (~140 ± 10 %) when compared to control cells grown in tissue culture polystyrene cell plate (TCPS). The actin-vimentin co-staining showed entire surface area of the scaffold positive for cytoskeletal actin of cells (Figure 11). These results indicate that the decellularization protocol and the plasma sterilization of dAM have no cytotoxic effect and in fact promote cell proliferation (Rashmi *et al.*, 2020).

4.1.3. Characterisatics of terpolymer PLGC

The terpolymer PLGC was obtained as white coloured blocks. The yield of the terpolymer obtained upon synthesis was found to be 96 ± 2.4 % (Figure 12). The FT-IR spectrum of the synthesized PLGC showed peaks at ~3379 cm^{-1}(OH stretching),

~2954 cm^{-1} and ~2877 cm^{-1}(C–H stretching), ~1720 cm^{-1} (C=O bond stretching, aliphatic esters), ~1457 cm^{-1} (-CH_2- bending), ~1373 cm^{-1} (-COO- stretching) and ~1164 cm^{-1} and ~1095 cm^{-1} (-C-O stretching and -C-H- in plane bending) respectively. The strong monomer peak at ~930 cm^{-1} (-COO- ring breathing mode) characteristic of the cyclic structure of the diketones disappeared in the polymer confirming terpolymer formation (Braun *et al.*, 2006) (Figure 13.A). ^{1}H NMR spectrum of PLGC showed signals at δ = 5.0 - 5.3 ppm attributing to methine proton in lactide unit and at δ = 2.3 - 2.4 ppm and 1.2 - 1.6 ppm attributing to α-CH_2 and ε-CH_2 respectively in caprolactone units. The -CH_2 proton in glycolide units were observed at δ = 4.6 - 4.9 ppm and also at δ = 1.5 ppm of the CH_3 protons in lactide units (Figure 13.B).

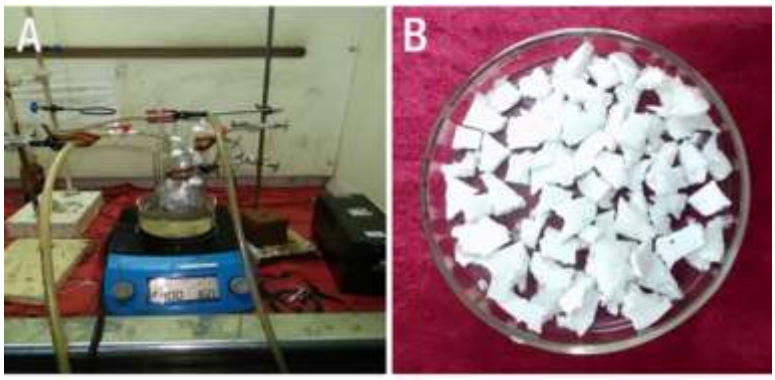

Figure 12. Synthesis of terpolymer PLGC: A) PLGC synthesis set up and B) synthesised terpolymer PLGC.

Molecular weight analysis of the terpolymer using GPC provided a number average molecular weight (Mn) value of 62936, weight average molecular weight (Mw) value of 807944 and polydispersity index (PDI) of 1.3. This polymer was found appropriate for electrospinning into a porous mat. Thermogravimetric analysis showed a single stage decomposition curve from 221 ± 14 º and resulting in total degradation at around 372 ± 6.7º (Figure 13.C). The glass transition temperature (Tg) using DSC was recorded around 28.98 ± 2º. Two thermal transitions were also noticed around 51.33 ± 2.8º and 151.88 ± 5.5º indicating the softening of the caprolactone molecules and subsequently that of the lactide-glycolide linkage respectively confirming terpolymer formation (Figure 13.D). Hence, the PLGC terpolymer formation was evident from FT-IR, NMR and thermal analysis.

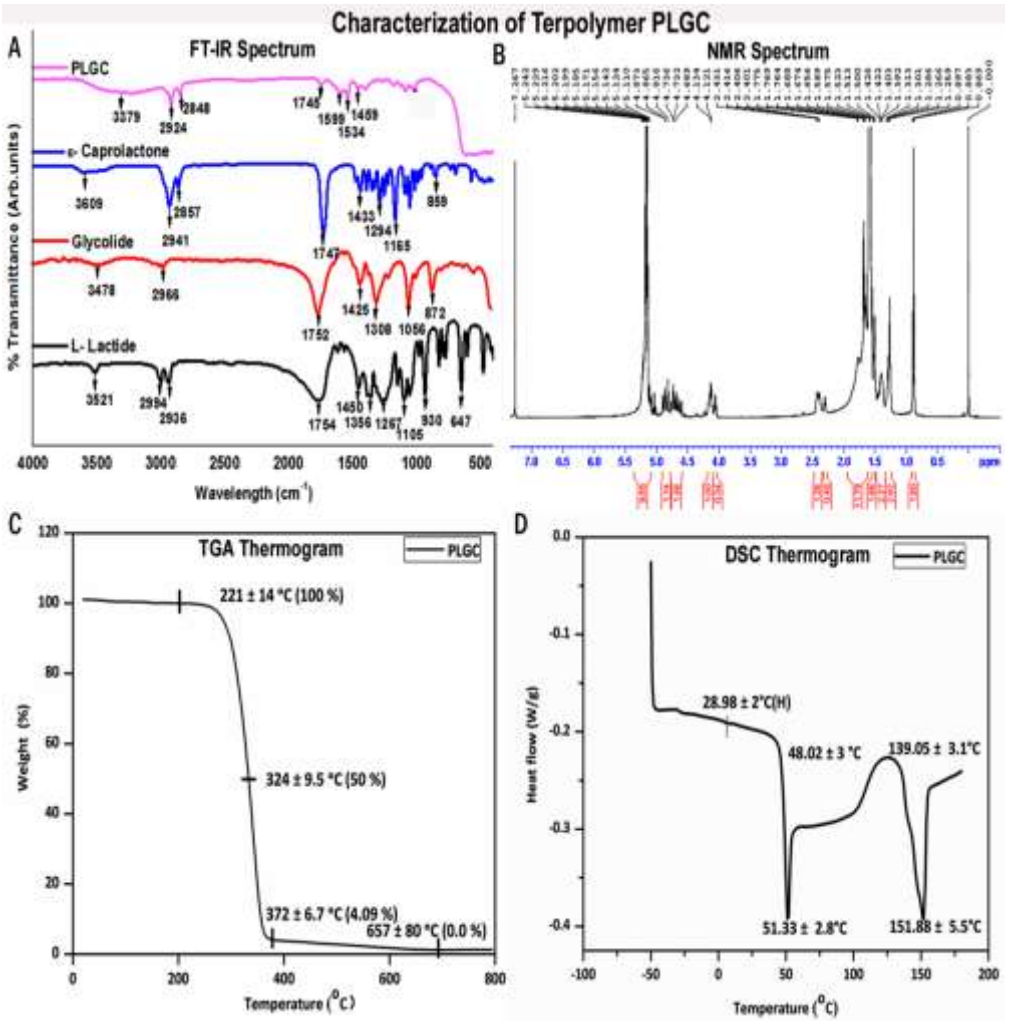

Figure 13. Characterization of synthesized terpolymer PLGC: A) FT-IR spectrum, B) NMR spectrum, C) TGA and D) DSC thermogram of the synthesized terpolymer PLGC.

Electrospinning of PLGC solution resulted in flexible and silky mats. Electrospun PLGC showed randomly aligned fibers upon ESEM analysis with average fiber diameter of 2.02 ± 0.4 µm ranging from 1 to 3 µm (Figure 14). The mechanical properties of electrospun showed tensile strength, tensile modulus and tensile strain of 4.95 ± 0.6 MPa, 7.18 ± 1.4 % and 147 ± 23 MPa respectively.

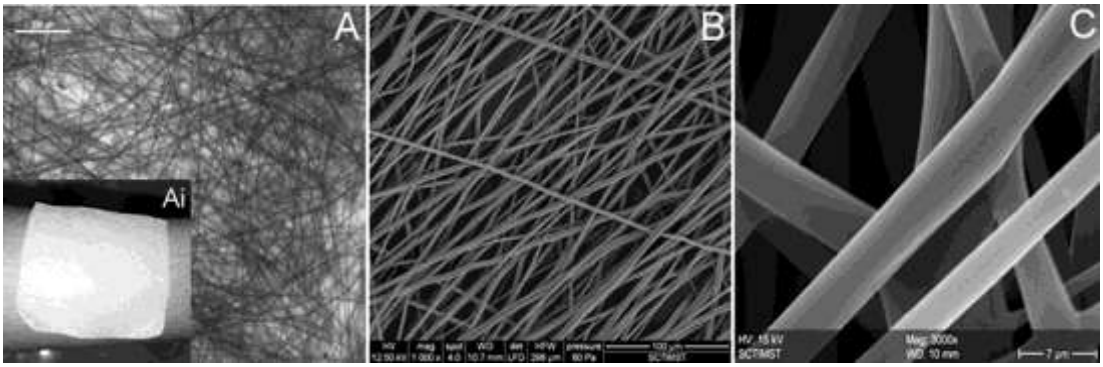

Figure 14. Surface topographical analysis of electrospun PLGC: A) Phase contrast image showing fibrous nature of electrospun PLGC mat (Ai inset showing pliable nature of electrospun PLGC mat), B & C) ESEM image of the bare electrospun PLGC mat at different magnifications.

4.1.4. Characteristics of SF

The final lyophilized SF was obtained as disc (IIT-G). The FT-IR spectrum showed characteristic peaks at characteristic peaks of N-H stretching at ~3275 cm^{-1}, amide I band, amide II and amide III bands at ~1629 cm^{-1}, ~1532 cm^{-1} and ~1245 cm^{-1} respectively (Figure 15).

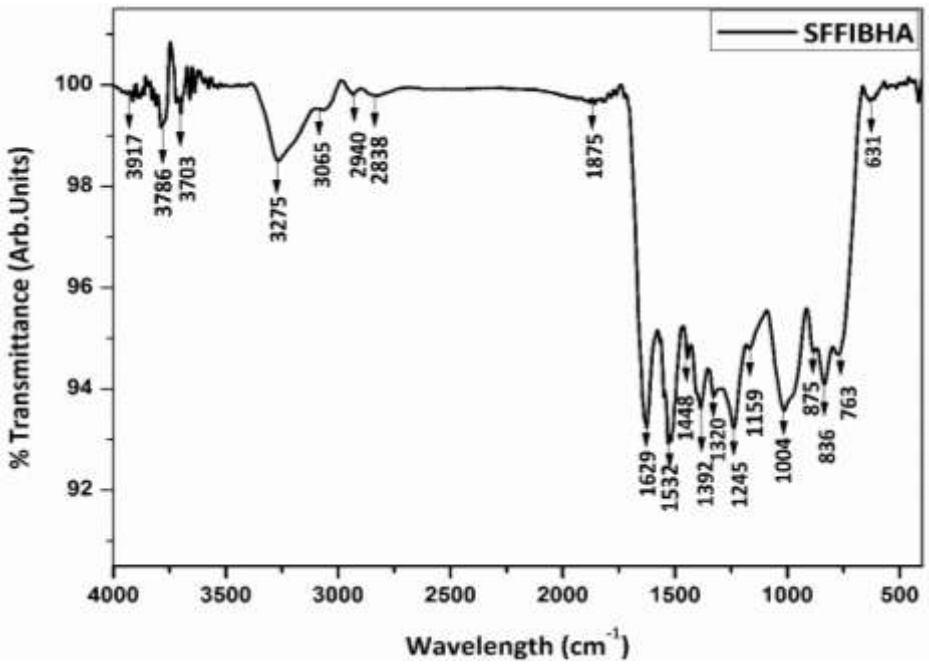

Figure 15. FT-IR spectrum of SF

4.2. Properties of AMFIBHA, PLGCFIBHA and SFFIBHA hybrid scaffolds

Fibrin concentration was determined based on the optimum clotting using claus assay and the ability to get pliable and crack-free lyophilized scaffolds. Varying concentrations of 100, 200 and 400 µg/mL HA was used and based on the optimum swelling characteristics, HA concentration was decided (Figure 16). Hence, the final concentration of the biomimetic matrix was optimised as 20 mg/mL fibrinogen concentrate, 20 IU/mL thrombin and 200 µg /mL HA concentration, which was common for all the hybrid scaffolds used in the study. The lyophilized hybrid AMFIBHA, PLGCFIBHA and SFFIBHA scaffolds were pliable and could be easily handled using forceps.

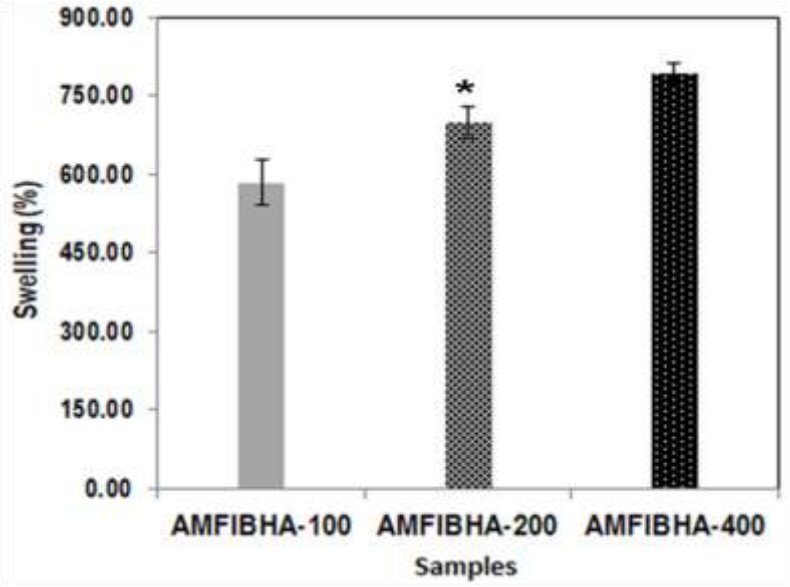

Figure 16. Swelling characteristics of the scaffold with varying concentrations of HA; *p ≥0.05.

4.2.1. Characteristics of AMFIBHA hybrid scaffold

To confirm the deposition of biomimetic fibrin-HA composite on scaffold, FTIR analysis was done using attenuated total reflectance (ATR) method. FTIR spectrum showed characteristic peaks of proteins like N-H stretching, amide I band and amide II band obtained at 3275 cm^{-1}, 1627 cm^{-1},1540 cm^{-1}respectively. The spectrum of hybrid AMFIBHA scaffold was comparable with the biomimetic bare FIBHA sheet and AM (Figure 17).

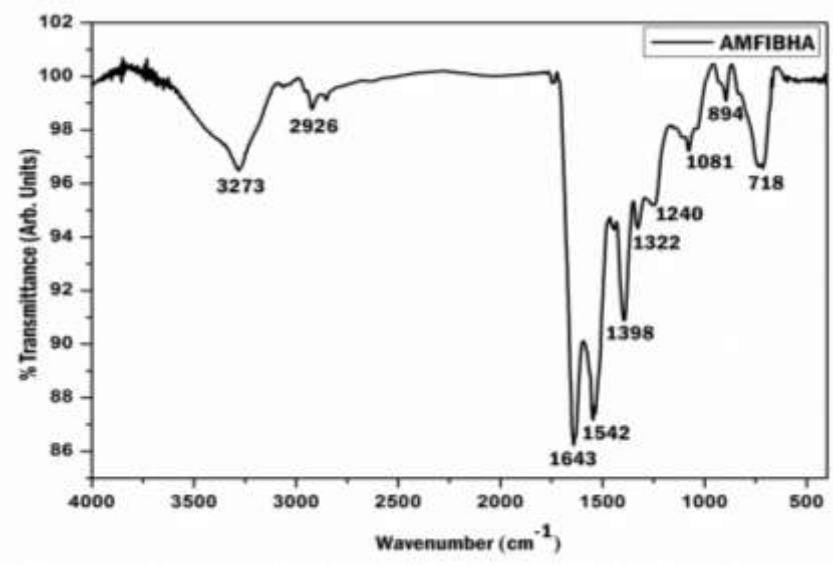

Figure 17. FT-IR spectrum of AMFIBHA hybrid scaffold

Analysis by ESEM showed porous nature of the scaffold. The ESEM images were analyzed using image J software and it showed pore diameter of 39 ± 15 µm. The deposition and distribution of fibrin network is seen uniformly distributed throughout the scaffold (Figure 18).

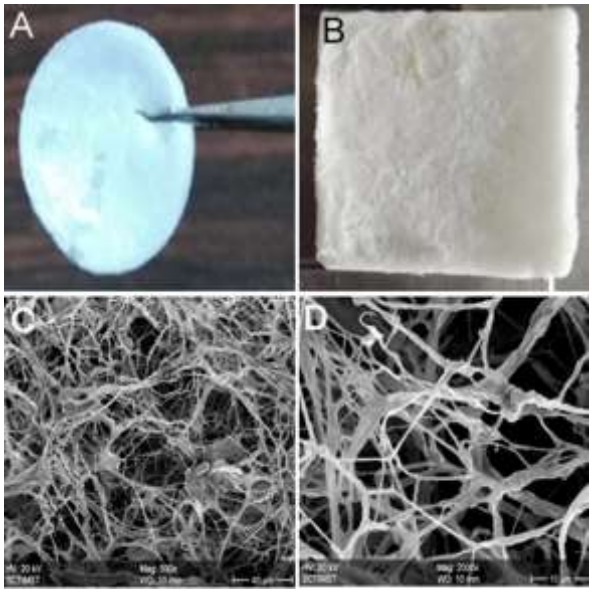

Figure 18. Gross and microscopic image of AMFIBHA hybrid scaffold: A & B) Gross images and C & D) ESEM images at different maginifications of fabricated AMFIBHA respectively.

The distribution of pores within scaffolds was demonstrated by inverted images obtained from micro-CT analysis. Micro-CT analysis demonstrated porosity volume of 70 % with pore size ranging from 6 - 48 µm (Figure 19.A-D). The percentage swelling of AMFIBHA was 647 ± 57 % and 620 ± 53 % in PBS and SBF. The swelling property was highest for the AMFIBHA hybrid scaffold when compared to bare AM and FIBHA scaffolds. The swelling properties in PBS and SBF showed comparable results (Figure 19.E).

The WVTR of the bare AM and the hybrid scaffold AMFIBHA ranged from 2278 to 2301 $g.m^{-2}.day^{-1}$and 2198 to 2407 $g.m^{-2}.day^{-1}$. The values obtained for the scaffold developed falls in the mid-range of loss from injured skin within the recommended range.

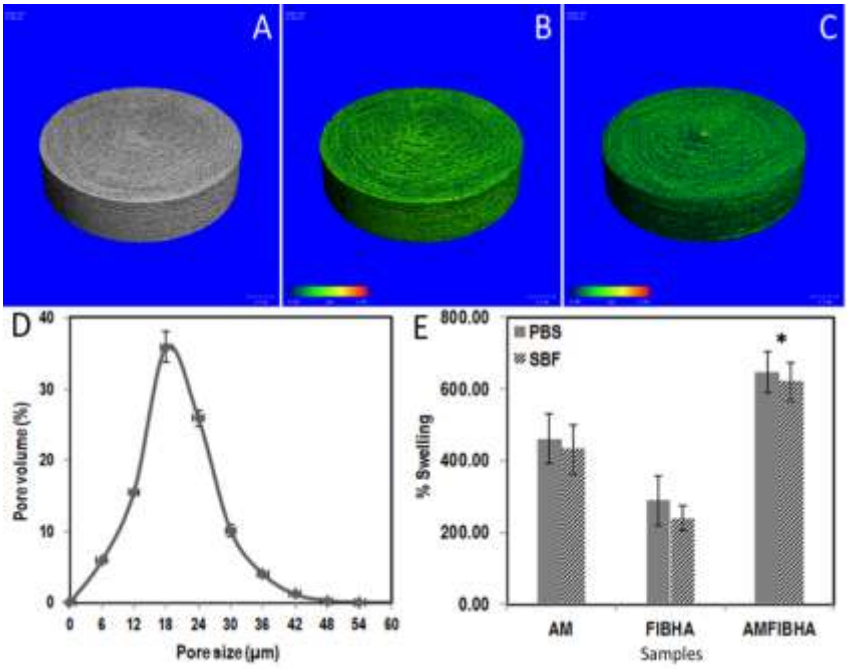

Figure 19. Porosity and swelling of AMFIBHA hybrid scaffold: A, B & C) micro-CT images representing 3D images, colour coded images of thickness distribution and pore size distribution respectively, D) pore size distribution histogram and E) swelling properties of AMFIBHA hybrid scaffold Bars represent means ± SD (n=6); * $p \geq 0.05$.

Contact angle measurement of the AMFIBHA hybrid scaffold showed hydrophilic nature making it difficult to capture the value. Bare AM showed hydrophilic nature with a contact angle measurement of 71 ± 2º. Contact angle

measurement of bare FIBHA scaffold was also not recorded due to its highly hydrophilic nature. *In vitro* hydrolytic degradation studies showed gravimetric weight loss of ~ 90 ± 5 % was seen within 20 d.

4.2.2. Characteristics of PLGCFIBHA hybrid scaffold

The ATR-IR spectrum for PLGCFIBHA scaffold showed characteristic peaks of C–H stretching at 2945 cm^{-1} and 2853 cm^{-1}, amide I band, amide II and amide III bands at 1632 cm^{-1}, 1542 cm^{-1} and 1395 cm^{-1} , C=O bond stretching and aliphatic esters at 1746 cm^{-1} and -C-H- in plane bending at 1016 cm^{-1} respectively representing peaks of HA, fibrin and PLGC (Figure 20).

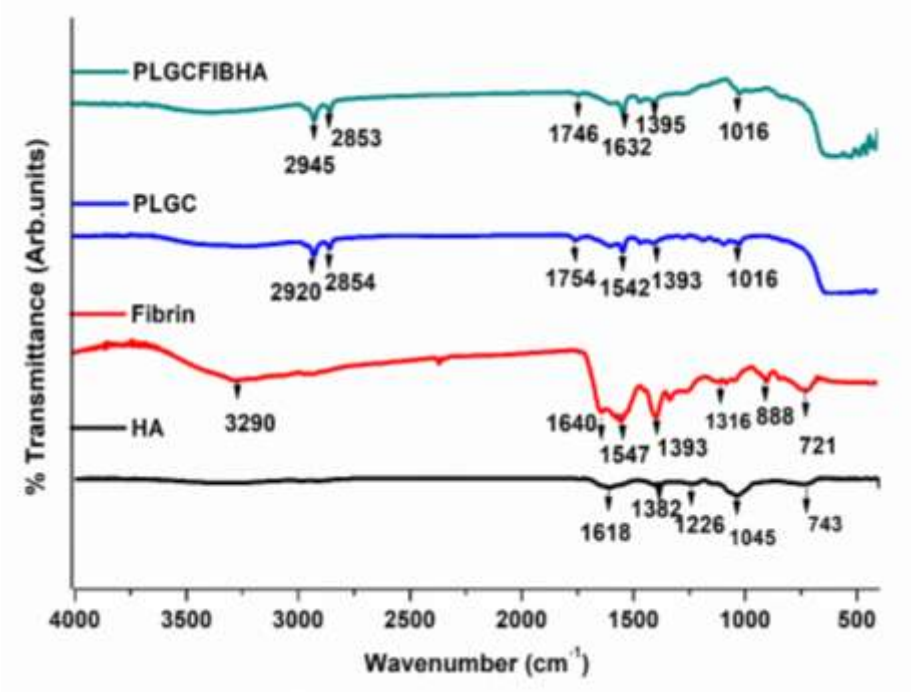

Figure 20. FTIR spectrum of PLGCFIBHA hybrid scaffold

The ESEM analysis showed a porous surface topography with electrospun fibres of PLGC completely covered with FIBHA matrix. The deposition and distribution of fibrin network is seen throughout the scaffold. The ESEM images were analyzed using image J software showed an average pore diameter of 45.45 ± 20 µm (Figure 21).

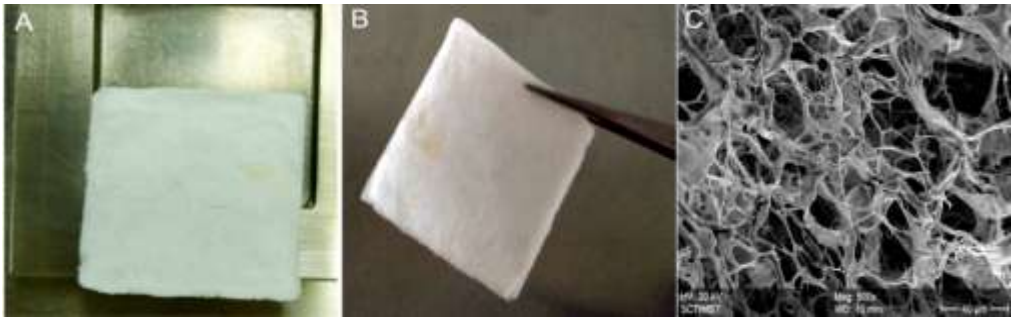

Figure 21. Gross and microscopic images of PLGCFIBHA hybrid scaffold: A & B) Gross images and C) ESEM images of the fabricated hybrid PLGCFIBHA scaffold.

The distribution of pores within scaffolds is demonstrated by inverted images obtained from micro-CT analysis. The porosity measurement using µ-CT of bare PLGC and hybrid PLGCFIBHA scaffold showed total porosity of 70.06 ± 3 % with pore size ranging from 16 to 112 µm and total porosity of 64 ± 2 % with pore size ranging 16 to 128 µm, respectively indicating the porous nature of the polymer and pore-size distribution conducive for cell growth and migration. Probability values indicated ($P<0.05$) reduction of porosity in biologically modified terpolymer compared to bare polymer was insignificant (Figure 22 A-G).

Average swelling percentage of the bare PLGC was found to be 77.3 ± 11.7 % and 69.8 ± 20 % and for hybrid PLGCFIBHA scaffold was 240 ± 38 % and 260 ± 34 % in PBS and SBF respectively. Bare PLGC has no swelling characteristics of its own and the results suggested that bio mimetic matrix deposition enhanced water retaining ability of the PLGCFIBHA scaffold (Figure 22.H).

The WVTR of the bare PLGC and the hybrid PLGFIBHA scaffold ranged from 2639 to 2972 g/m^2/day and 2278 - 2401 g/m^2/day. Statistical analysis showed that WVTR decreased significantly upon fibrin composite deposition still in the normal range for wound healing applications.

The surface wettability analysis using the contact angle measurement showed hydrophobic nature of the bare PLGC with a value of 123 ± 1º whereas, the hybrid PLGCFIBHA scaffold showed hydrophilic character making it difficult to capture

the contact angle. The use of liquid components of fibrin sealant enabled penetration of the components to the pores and formation of fibrin on the internal fiber surfaces.

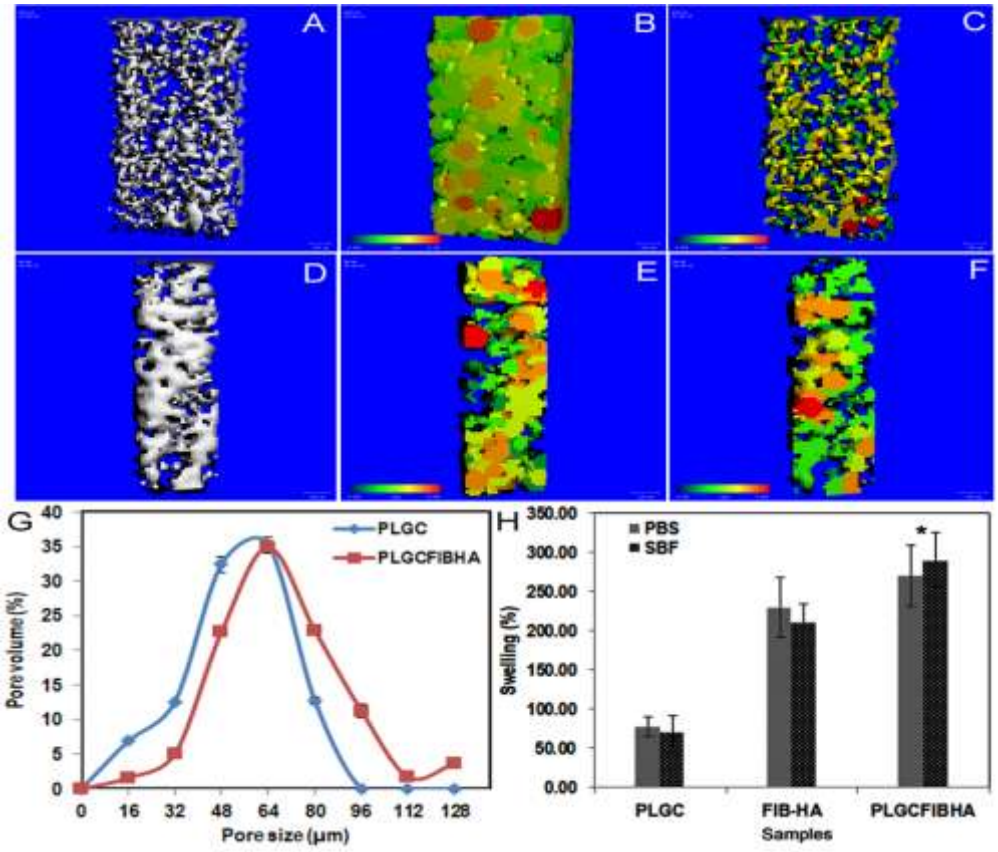

Figure 22. Porosity and swelling chracteristics of PLGCFIBHA hybrid scaffold: A & D) Micro-CT images representating 3D colour coded images, B & E) thickness distribution and C & F) pore size distribution of bare PLGC and hybrid PLGCFIBHA scaffolds respectively, G) pore size distribution histogram showing pore size range and H) swelling properties of PLGCFIBHA hybrid scaffold; Bars represent means ± SD (n=6), * p value < 0.05.

The mechanical properties of the hybrid PLGCFIBHA scaffold was evaluated using UTM. The mechanical properties of electrospun showed tensile strength, tensile modulus and tensile strain of 3.92 ± 0.4 MPa, 10.18 ± 1.4 % and 67.3 ± 19.6 MPa respectively. There was slight reduction in the mechanical properties of hybrid PLGCFIBHA scaffold from bare PLGC scaffold which can be due to the incorporation of FIBHA matrix which tends to break easily.

In vitro hydrolytic degradation showed a gravimetric weight loss of ~ 23 ± 4 % within 30 d. The ESEM analysis showed degradation of FIBHA matrix

components and shrinkage of the fibres from its initial straight fibres and breakage of fibers within the scaffold was seen (Figure 23).

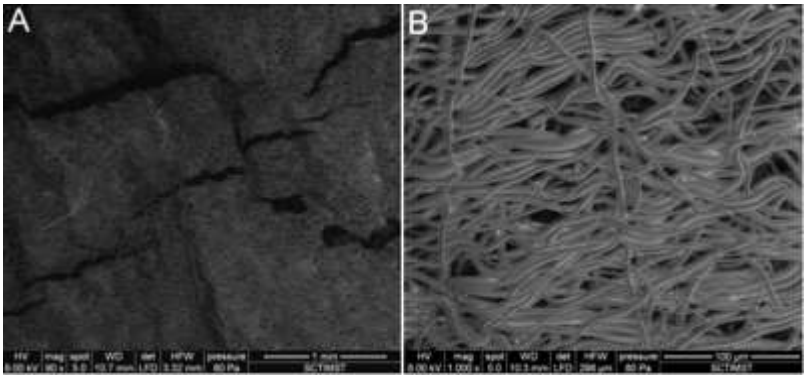

Figure 23. ESEM images of the *in vitro* hydrolytic degraded samples at d 30 at different magnifications.

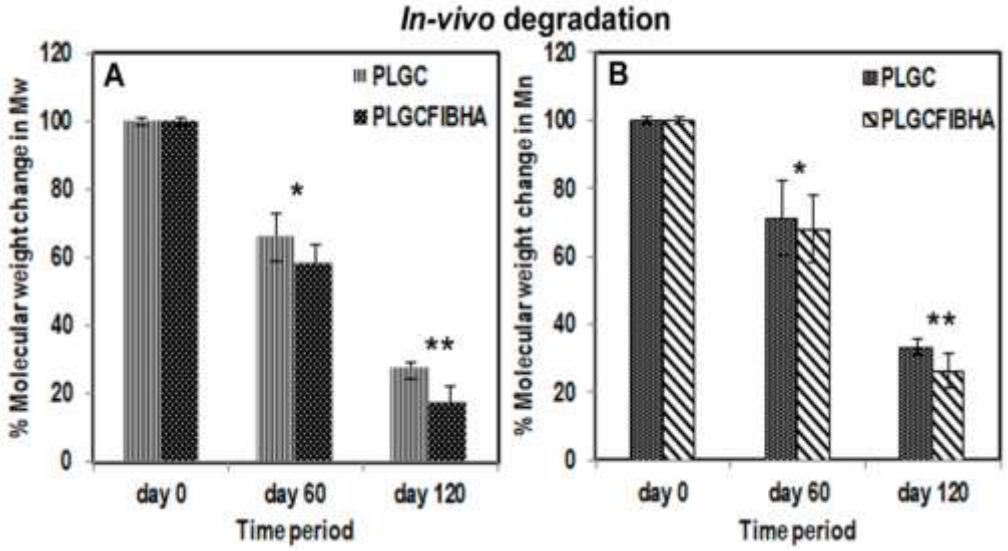

Figure 24. Data on *in vivo* degradation of PLGCFIBHA hybrid scaffold analyzed by GPC: A) number average molecular weight (M_n) of hybrid scaffolds and B,) weight average molecular weight (M_w) of hybrid scaffolds on 0d, 60d and 120d of study respectively. Bars represent means ± SD (n=6), * p value < 0.05, ** p value < 0.01 vs day 0.

In vivo degradation of bare PLGC and hybrid PLGCFIBHA scaffold after 60 d and 120 d of suggest that the degradation was slightly higher for the hybrid PLGCFIBHA than bare PLGC scaffold. The number average molecular weight (Mn) of the bare and hybrid PLGCFIBHA scaffold was decreased by 28.8 ± 11 % and 32

± 10 % within 60 d and 66.7 ± 2.4 % and 73.7 ± 5 % by120 d, respectively (Figure 24.A). The weight average molecular weight (Mw) decreased to and 38 % and 42 % within 60 d and 73 % and 83 % within 120 d, respectively (Figure 24.B).

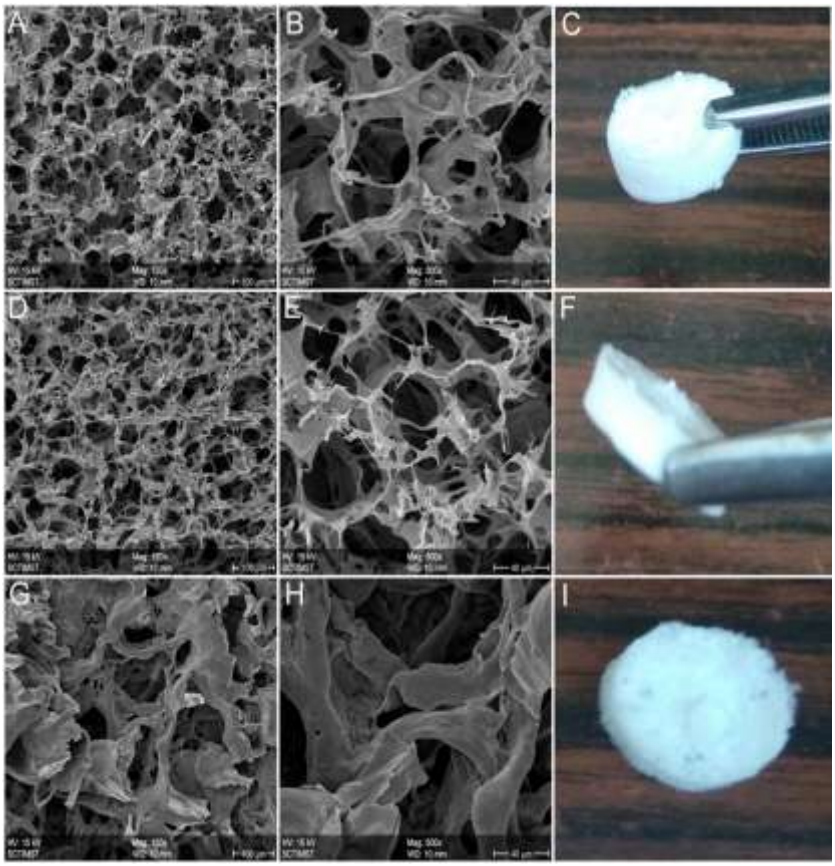

Figure 25. ESEM images at different magnifications and gross image of SFFIBHA hybrid scaffolds: A, B & C) 1 % and D,E & F) 2 % SF and G,H & I) FIBHA scaffold respectively.

4.2.3. Characteristics of SFFIBHA hybrid scaffold

Concentrations of 1 % and 2 % of SF was used for optimising scaffold fabrication. ESEM analysis reveals the porous nature of the scaffold which may support the cell in-growth and migration. Both 1 % and 2 % SFFIBHA showed porous nature and was able to be handled with forceps (Figure 25. A-F). Fibrin alone was also showed pores (Figure 25.G-I). Upon suspending on PBS as well as culture medium, the stability of 1 % SFFIBHA was found to be poor with faster disintegration of the scaffold than 2 % SFFIBHA. Hence, 2 % SFFIBHA gel was used for further studies.

FTIR spectrum showed characteristic peaks of N-H stretching at 3275 cm^{-1}, amide I band, amide II and amide III bands at 1629 cm^{-1}, 1532 cm^{-1} and 1245 cm^{-1} respectively indicating the presence SF, fibrin and HA (Figure 26).

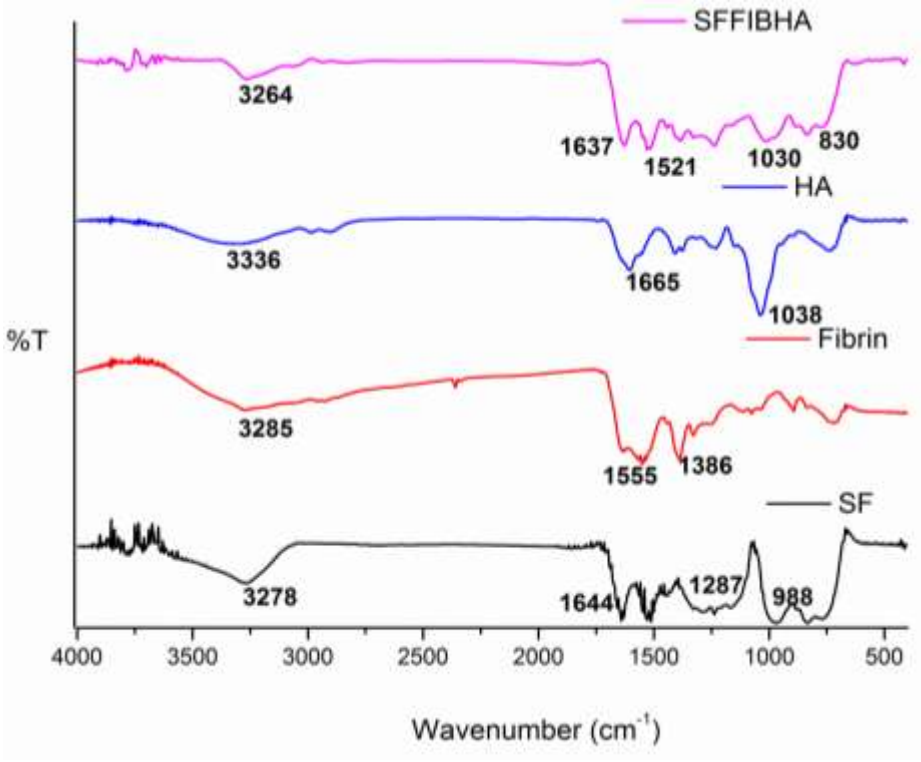

Figure 26. FT-IR spectrum of SFFIBHA hybrid scaffold

ESEM analysis showed porous nature. The distribution of pores within scaffolds was demonstrated by inverted images obtained from micro-CT analysis. The porosity measurement using µ-CT of hybrid SFFIBHA scaffold showed total porosity of 64 ± 2 % with pore size ranging from 6 to 48 µm, respectively indicating the porous nature of the polymer and pore-size distribution conducive for cell growth and migration (Figure 27.A-D).

The bare SF (provided from IITG) showed maximum swelling and SFFIBHA showed swelling between bare SF and FIBHA. Hybrid scaffold showed % swelling of 332 ± 35 % and 301 ± 66 % in PBS and SBF. This can be due to the water soluble nature of SFFIBHA lyophilized scaffold (Figure 27.E). The WVTR of the hybrid SFFIBHA scaffold ranged 2178 to 2301 g/m^2/day optimum for wound healing

applications. The SFFIBHA hybrid scaffold showed hydrophilic nature making it difficult for contact water measurement. *In vitro* hydrolytic degradation studies showed gravimetric weight loss of ~ 90 ± 5 % was seen within 4 d. The SF gets dissolved in water.

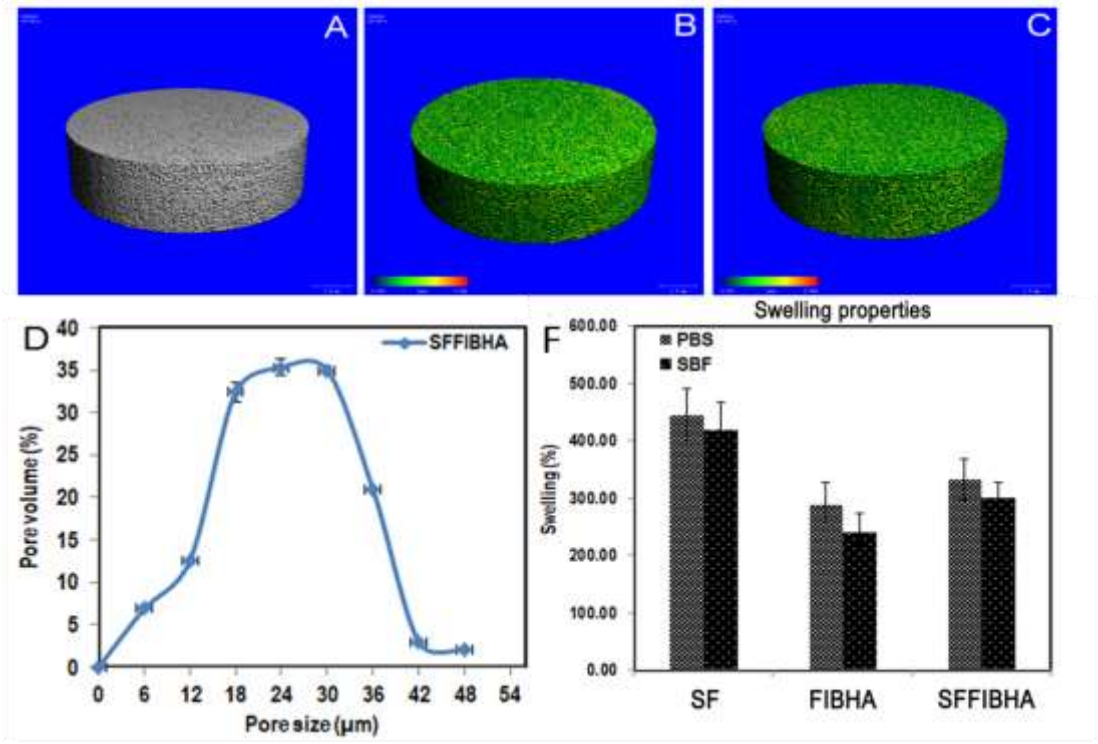

Figure 27. Porosity and swelling chracteristics of SFFIBHA hybrid scaffold: Micro-CT images representating A) 3D images, colour coded images of B) thickness distribution and C) pore size distribution of hybrid SFFIBHA scaffolds respectively, D) pore size distribution histogram showing pore size range and E) swelling properties of SFFIBHA hybrid scaffold; Bars represent means ± SD (n=6).

4.2.4. Validation of sterilization of hybrid scaffolds

The hybrid scaffolds AMFIBHA, PLGCFIBHA and SFFIBHA showed no physically visible shrinkage after plasma sterilization. SEM analysis of PLGC before and after plasma sterilization (psPLGC) showed stable fibre characteristics (Figure 28.A&B). GPC analysis showed variation in number average M_n without much change in weight M_w (Figure 28.C).

There was no contamination observed in the scaffold immersed in the medium incubated for 15 d in sterile ambient conditions. Upon culture of fibroblasts on the plasma sterilized scaffolds, proliferation rate analyzed by total DNA was comparable with FIBHA prepared under sterile atmosphere (Figure 29). The maintenance of the biological function of all hybrid scaffolds is thus established.

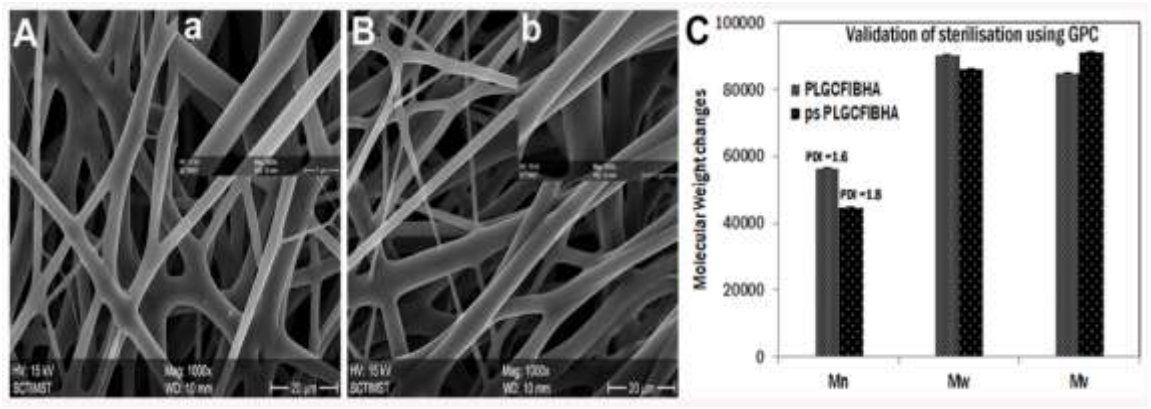

Figure 28. Data demonstrating stability of PLGC and PLGCFIBHA upon plasma sterilization: A&B) SEM Images showing PLGC (a-insert higher magnification image of PLGC) and ps PLGC (b-insert showing higher magnification of ps PLGC) and C) GPC analysis showing the stability of PLGC in terms of molecular weight distribution.

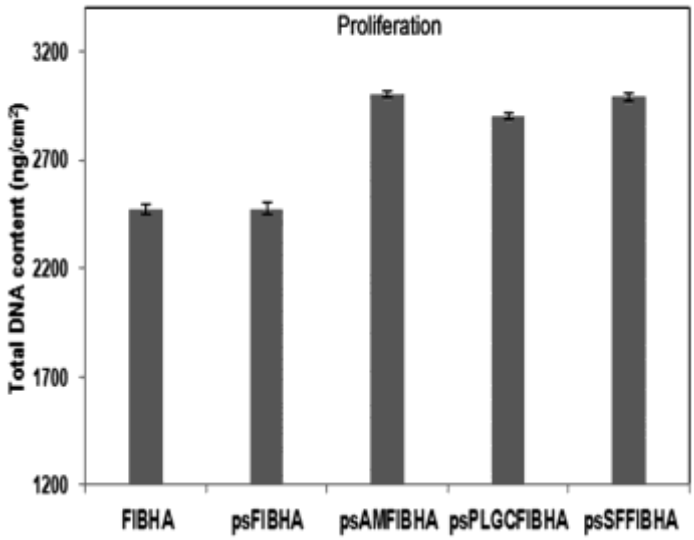

Figure 29. Comparison of proliferation rate of fibroblasts upon seeding and culture on sterile hybrid scaffolds prepared by plasma (H_2O_2) exposure.

4.2.5. Hemocompatibilty of the hybrid scaffolds

Percentage hemolysis estimation has been used as a simple and reliable technique for estimating blood compatibility of materials. In this study, empty polystyrene dishes were used as a reference generating negligible hemolysis < 0.1 %. As per ISO 10993-4:2002 (E), for material to be non-hemolytic, the percentage hemolysis should be less than 0.1 %. All tested samples displayed less than 0.1 % hemolysis. The hybrid scaffolds AMFIBHA, PLGCFIBHA and SFFIBHA showed % hemolysis values of 0.03 ± 0.001, 0.03 ± 0.009 and 0.03 ± 0.007 respectively indicating hemocompatible nature.

4.2.6. Characteristics of hemostatic SFFIBHA hydrogel system

Stability of SSFIBHA gel was evaluated for a time period of 7 d in serum free medium. The gel was stable and remained intact for 7 d, after which pores were seen indicating of degradation .The gelling time was around 1-2 min (Figure 30).

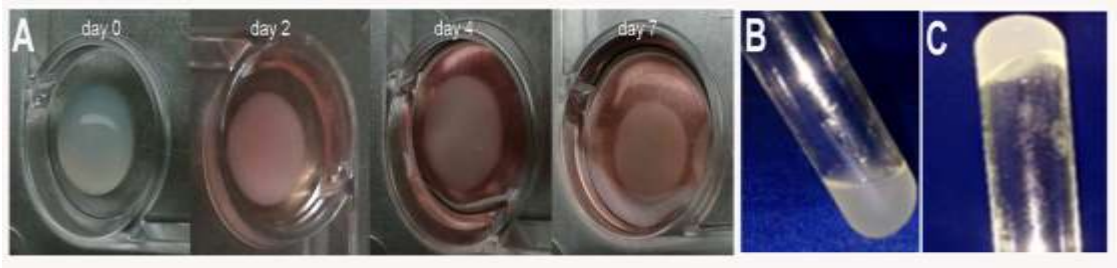

Figure 30. Photographs depicting stability of SFFIBHA hydrogel: A) stability of gel at different time periods, B & C) tilt assay of SFFIBHA hydrogel.

4.3. *In vitro* tissue engineering potential of hybrid scaffolds and SFFIBHA hydrogel

4.3.1. Characteristics of hADMSCs

Isolated hADMSCs showed typical plastic-adherent property with spindle-shaped morphology. The hADMSCs showed > 90 % positivity for MSC markers; CD 90, CD 105 & CD 73 and < 10 % positivity for haematopoeitic stem cell markers; CD 45 and CD 14 (Figure 31).

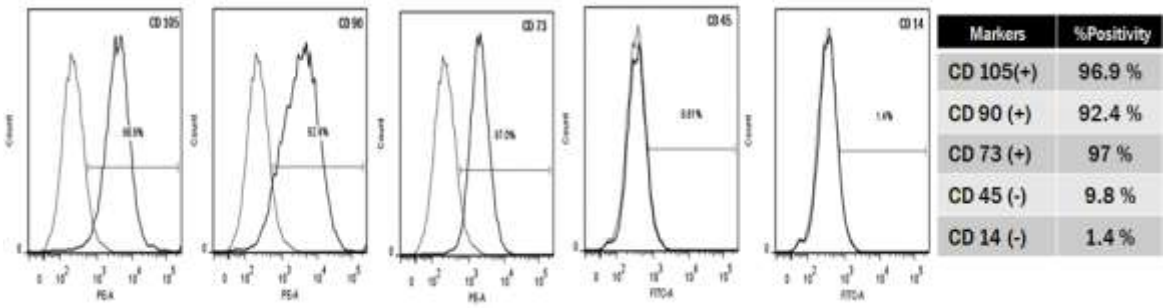

Figure 31. Flow cytometric analysis of hADMSCc for stem cell surface marker expression for positive and negative markers.

Passage 3 hADMSCs cells showed trilineage differentiation potential into adipogenic, osteogenic and chondrogenic lineages after 14 d of induction in their respective medium using immunostaining. The oil red O staining revealed the presence of lipoid substances in adipogenic induced differentiation of hADMSCs, alizarin red staining detected the presence of calcium in osteogenic induced differentiation of hADMSCs and toluidine blue staining identified the presence of acidic proteoglycan present in cartilage tissues for chondrogenic induced differentiation of hADMSCs (Figure 32).

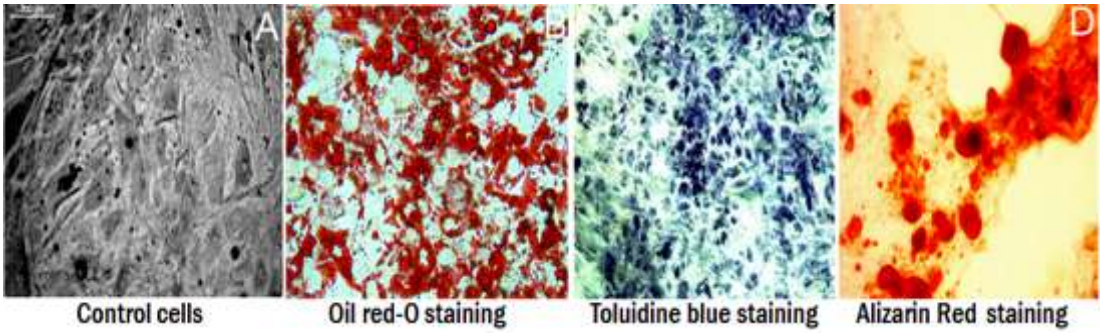

Figure 32. Micrograph depicting trilineage differentiation of hADMSCs: A) control cells, B) oil red-O staining C) alizarin red staining and D) toluidine blue staining for confirming trilineage differentiation potential of hADMSCs.

This result confirmed that, at the time of starting the differentiation experiment, the MSC population was > 90 % homogeneous. At the time of seeding, the mRNA expression for FSP-1 was studied by reverse-transcriptase PCR, but no amplification was found. Therefore, it may be confirmed that there are no fibroblasts in the hADMSC population, which was used for the differentiation experiment.

4.3.2. Induction of hADMSC differentiation to fibroblasts

An increased quantity of DNA indicates proliferation of hADMSCs. In the control, there was a remarkable proliferation between the day of seeding and d 7, but the cell numbers were comparable on d 7 and 14, which was likely due to the characteristic contact inhibition of MSCs. In the case of cells grown with DM and niche, there was significant increase in DNA content. Thus, the higher proliferation rate and multilayered cell growth observed during microscopic analysis complemented the DNA quantification results (Figure 33).

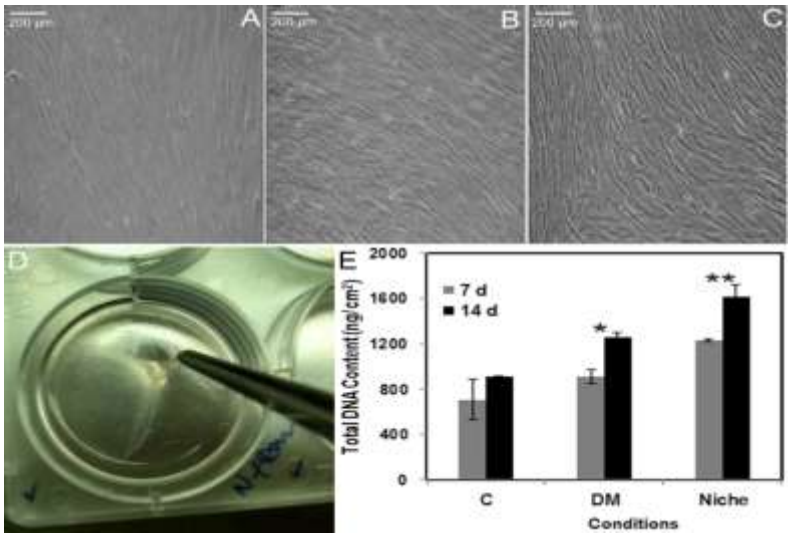

Figure 33. Induction of hADMSC differentiation to fibroblasts: A) control cells on TCPS, B) hADMSC growing on TCPS with DM, C) hADMSC growing on fibroblast specific niche and D) ECM laid by the hADMSC induced fibroblasts after 7 d and E) proliferation assay; scale bar = 200 µm and bars represent means ± SD (n=6), * p value < 0.05, ** p value < 0.01 vs C.

Genes for FSP-I and ECM molecules, such as Fib-1, Col-1 and Ela were amplified using qRT–PCR. Expression of FSP-1 is the most prominent indicator of fibroblastic differentiation. There is increase in the expression of FSP-1 and ECM molecules such as Fib-1, Col-1 and elastin when compared to the control ADMSC in both DM and niche. But in the case of elastin the expression decreases in DM whereas in niche there is slight increase in elastin indicating influence of fibrin matrix for fibroblastic differentiation. The FSP-I and ECM molecules such as Fib-1

and Col-1 increases when compared with two time periods 7 and 14 d. However, there is no exponential increase in the collagen gene expression which indicates that the regulated expression of collagen (Figure 34). The results suggest that 7 d differentiated fibroblasts can maintain the phenotype when transferred to hybrid scaffolds made out of FIBHA matrix.

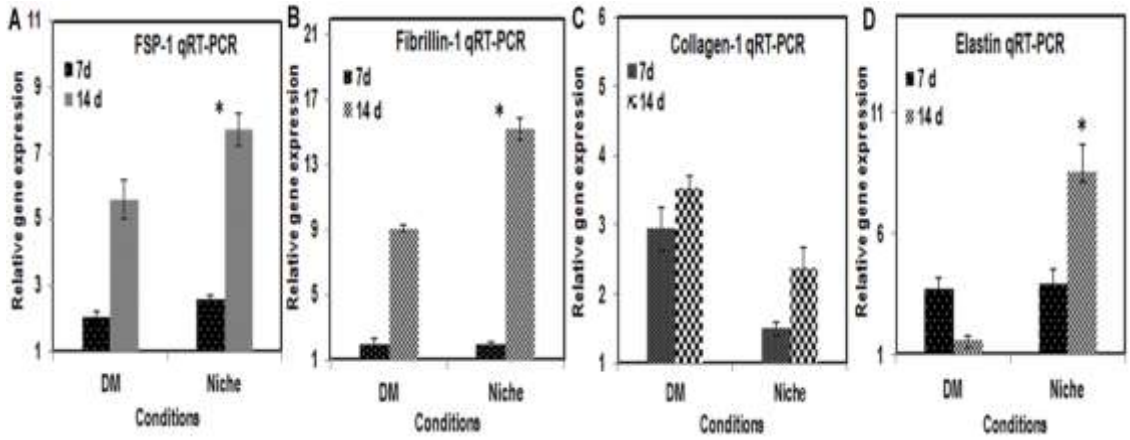

Figure 34. A-D) Relative gene expression of fibroblatic markers at d 7 and 14; data are presented as mean ± SD of replicate experiments using cells from six different donors, *significant difference ($p < 0.05$) between DM and niche.

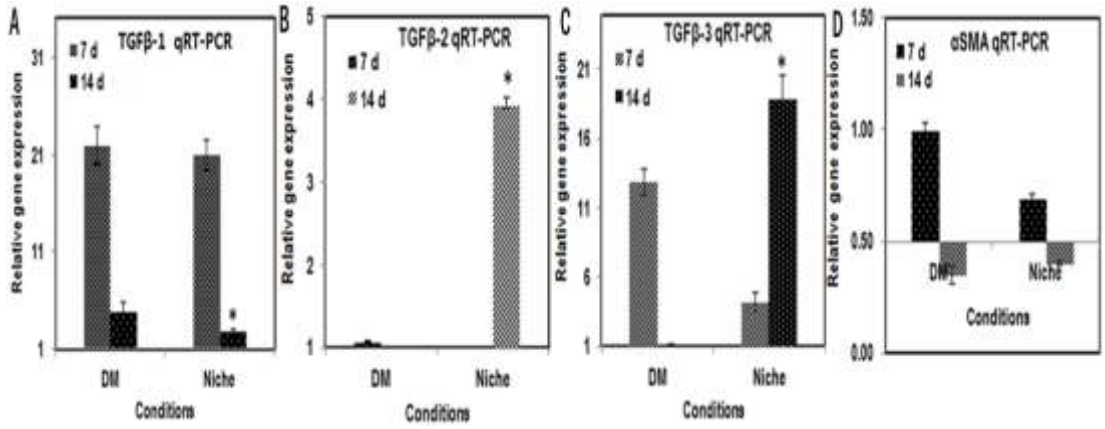

Figure 35. Relative gene expression of non-fibrotic markers of the hADMSCs differentiated fibroblasts : A-B) transforming growth factor -β isoforms (TGF-β1, TGF-β2 and TGF-β3 and D) α-SMA markers for non-fibrotic nature of differentiated cells ; data are presented as mean ± SD of ten replicate experiments, using cells from six different donors, *significant difference ($p < 0.05$) between DM and niche.

The cells grown in niche showed reduced relative gene expression of TGF-β 1 and higher expression of TGF-β2 & TGF-β3 as well as down regulation of myofibroblastic marker, α-SMA indicating non-fibrotic nature of fibroblasts (Figure 35).

ECM formation was visible in the cells grown in the presence of niche and DM, but only traces of ECM was seen in hADMSCs grown control plates. ECM deposition in two different time periods - 14 and 28 d was estimated biochemically. Quantitatively, significant differences in total collagen, elastin and sGAG deposition was evident in niche and DM cells when compared to control. There was no exponential increase in the total ECM molecules in both DM and niche indicating regulated ECM deposition (Figure 36). Henceforth, evident changes was seen when hADMSCs were grown on the designed fibroblast specific niche on d 7 and 14 of culture. Fibroblasts produced are functionally similar to skin fibroblasts by 7-14 d of culture by their ability to grow in multilayer and their ability to produce ECM molecules. As a result, characterized hADMSC derived fibroblast was used for in vitro tissue engineering on hybrid scaffolds.

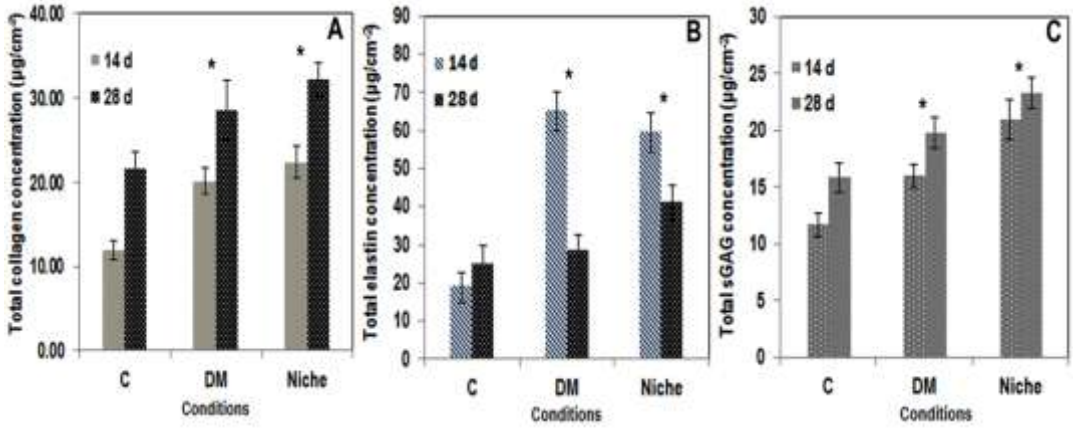

Figure 36. Quantitative data on ECM deposition: A, B & C) Graphical representation of quantified total collagen, elastin (ng) and sGAG from recovered matrix after specified time periods of hADMSCs culture; estimated quantity was normalized per cm^2 culture area in each case; data presented are mean ± SD (n= 4), using cells from six different donors, *significant difference ($p < 0.05$) between control.

4.3.3. In vitro tissue engineering on AMFIBHA

The hybrid scaffold AMFIBHA was stable after lyophilization and could be suspended in the culture medium without delamination of AM for growing cells *in vitro*. In direct contact assay of the AMFIBHA hybrid scaffold, the normal spindle-shaped morphology of fibroblast cells was maintained well which was compared with control cells grown on culture dishes. It also demonstrated that the AMFIBHA hybrid scaffold improved cell density visibly (Figure 37).

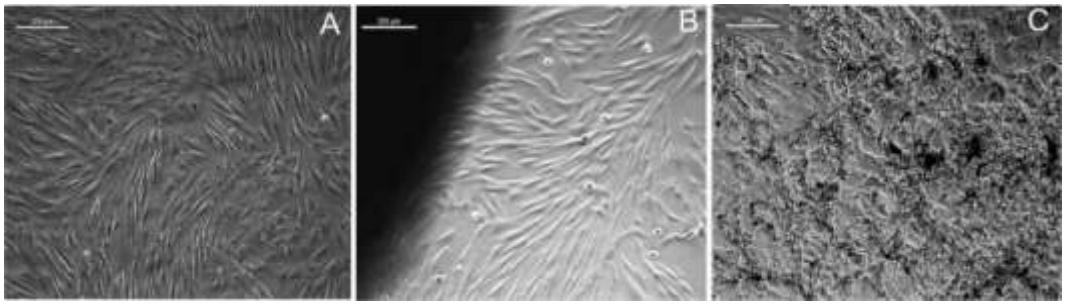

Figure 37. Phase contrast micrographs of fibroblast cells on AMFIBHA hybrid scaffold: A) Control cells growing on TCPS, B & C) cells in contact and growing underneath AMFIBHA hybrid scaffold; scale bar =200 µm.

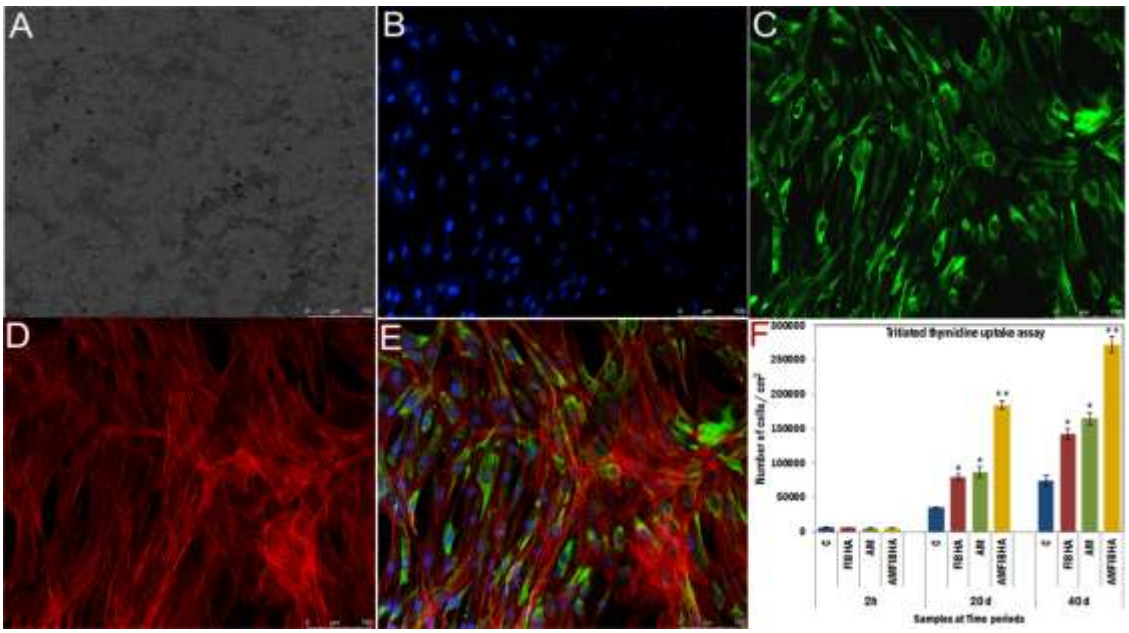

Figure 38. Fluorescent micrographs of vimentin & actin-stained fibroblast on AMFIBHA hybrid scaffold: A) phase contrast images, B) DAPI staining, C) vimentin staining , D) actin staining and E) merged images of fibroblast cultured for 7 d on hybrid AMFIBHA scaffold, scale bar =100µm and F) ^{3}H-thymidine uptake

assay: comparison of cell adhesion and proliferation of fibroblast on TCPC, FIBHA, bare AM and hybrid AMFIBHA scaffolds after 2h, 20 d and 40 d of culture shown graphically. Bars represent means ± SD, * p value < 0.05, ** p value < 0.01.

For confirming fibroblast attachment and growth on scaffolds, fibroblast seeded scaffolds were stained for vimentin and actin with TX phalloidin for fibroblast and cytoskeletal staining respectively after 7 d of culture. The entire surface area in the hybrid scaffold was found to be positive for vimentin and cytoskeletal actin of cells. When counter stained with DAPI, blue coloured nuclei seen in actin stained regions confirmed the specificity of fibroblast vimentin and actin stained cytoskeleton. The results suggest that the biomimetic matrix deposition enhanced the fibroblast attachment and proliferation (Figure 38 A-E).

Quantification of cell adhesion and proliferation on the scaffolds was done by ^{3}H thymidine uptake assay. The number of cells present after 2 h, 20 d, and 40 d are compared and significantly high cell proliferation was observed on the hybrid scaffold AMFIBHA when compared to bare AM and control TCPS on all d of analysis (Figure 38.F).

Deposition of ECM molecules like Col-1 & 3, elastin and fibrillin-1 after long term culture of fibroblast was analyzed qualitatively using immunostaining and quantitatively by estimation of total collagen, elastin and sGAG molecules after decellularization. The immunostaining of decellularized scaffold after 20 d of cell culture showed deposition of Col -1 & 3, elastin and fibrillin-1 throughout the hybrid scaffold compared to bare AM (Figure 39). Quantitative analysis of collagen on d 20 and d 40 showed ~4 fold increase in hybrid scaffold when compared with the bare scaffold. Similar pattern of deposition was observed for the elastin and sGAG on hybrid scaffold (Figure 40). There was no exponential increase between collagen, elastin or sGAG deposition between 20 d and 40 d of fibroblast culture on hybrid scaffold.

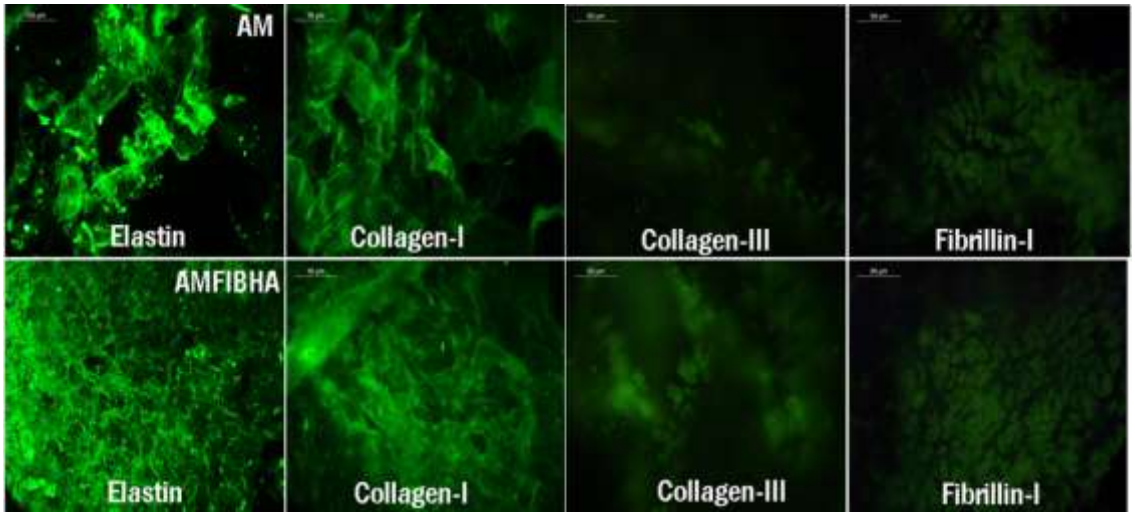

Figure 39. Representative fluorescent images of ECM molecules like elastin, collagen subtypes - collagen 1, collagen-3 and fibrillin-1 on decellularized bare AM and hybrid AMFIBHA scaffolds after 20 d of fibroblast culture, scale bar = 200 µm.

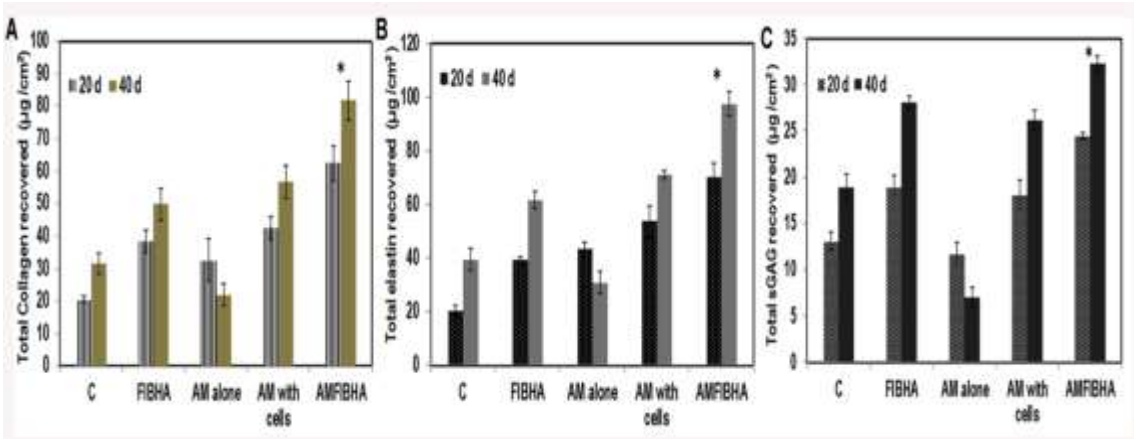

Figure 40. Quantitative analysis of ECM estimated on decellularized scaffolds after long term fibroblast culture : A) total collagen, B) total elastin and C) total sGAG recovering after 20 and 40 d of fibroblast culture; data presented is mean ± SD (n = 4); *p < 0.05 vs C.

In summary, the hybrid scaffold showed significantly higher cell adhesion, improved cellular growth and proliferation with regulated ECM deposition, which was evident from fluorescent staining, tritiated thymidine uptake assay and biochemical estimations.

4.3.4. In vitro tissue engineering on PLGCFIBHA

Both bare PLGC and hybrid scaffold PLGCFIBHA did not induce any toxic effects and scaffolds were found to be cyto-compatible upon growing L929 cells on the

scaffold. The normal spindle-shaped morphology of fibroblast cells was compared with control cells grown on culture dishes. Culture of hADMSC-derived fibroblasts evidenced improved cell density on PLGCFIBHA (Figures 41).

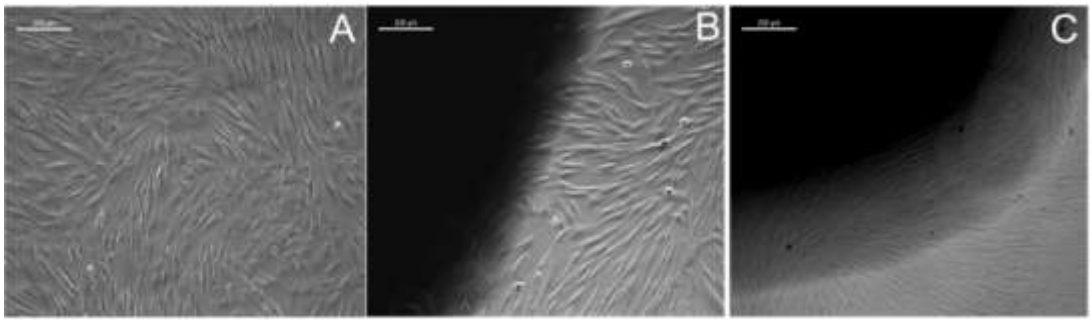

Figure 41. Phase contrast micrographs of fibroblast cells on contact with PLGCFIBHA hybrid scaffold: A) cells on TCPS and B & C) cells in contact with bare PLGC and hybrid PLGCFIBHA scaffold respectively; scale bar =200 µm.

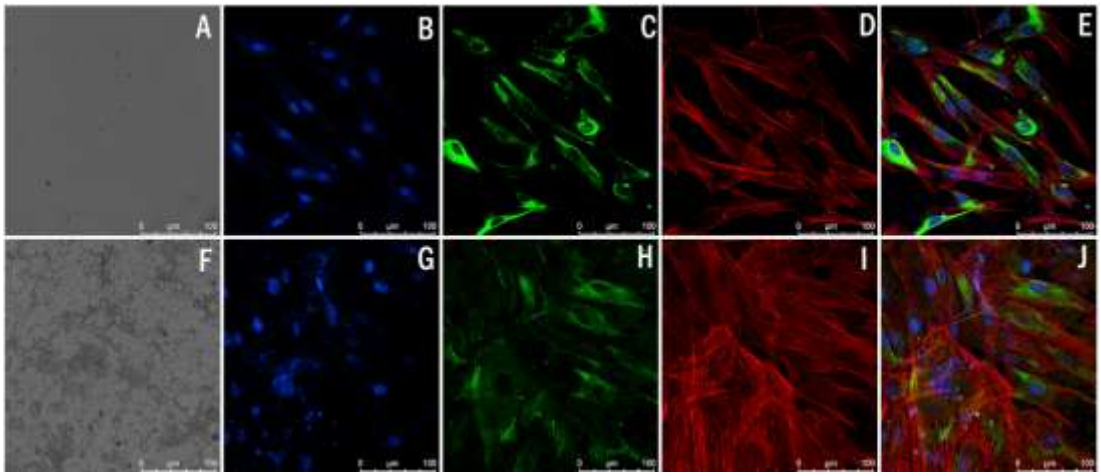

Figure 42. Fluorescent micrographs of vimentin & actin-stained fibroblast on PLGCFIBHA hybrid scaffold: A & F) phase contrast images, B & G) DAPI staining, C & H) vimentin staining, D & I) actin staining and E & J) merged images of fibroblast cultured for 7 d on bare PLGC and hybrid PLGCFIBHA scaffolds respectively, scale bar =100 µm.

Cell adhesion on the hybrid scaffold was found to be higher than that on bare PLGC. The entire surface area in the hybrid scaffold was found to be positive for vimentin and cytoskeletal actin of cells when compared to bare PLGC scaffold. When counter stained with Hoechst, blue coloured nuclei seen in actin stained

regions confirmed the specificity of fibroblast vimentin and actin stained cytoskeletons. The results suggest that the biomimetic matrix deposition enhanced the fibroblast attachment and proliferation (Figure 42).

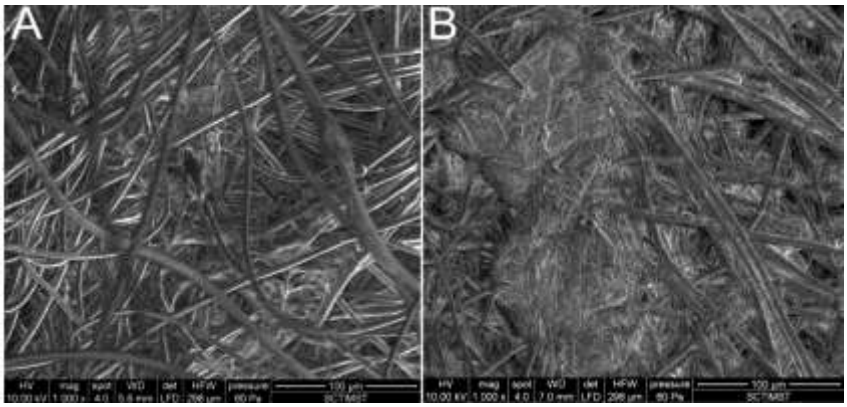

Figure 43: ESEM images of scaffolds grown with fibroblast after 20 d: A) Bare PLGC and B) PLGCFIBHA, scale bar = 100μm.

ESEM analysis after 14 d further confirmed better fibroblast coverage on the scaffold surface of the combination scaffold indicating that the cells are not only spread on the outer surface but also probably penetrated into the pores and proliferated. Fibroblast covered fibre to fibre distance and the entire scaffold surface was found to be covered with a canopy of fibroblast cells, whereas in the case of bare PLGC only few patches of fibroblast cells were observed. The increased cell numbers may be attributed to biological cues from fibrin-HA components (Figure 43).

The number of cells present after 2 h, 25 d and 50 d of culture on bare PLGC and hybrid PLGCFIBHA scaffolds was analyzed and plotted and comparative data is presented in figure 41. The cell adhesion on the hybrid scaffold was found to be higher than that on bare PLGC. The cell proliferation analysis on 25 d and 50 d shows a significant increase in cell number in the hybrid scaffold when compared with the bare scaffold on all days of analysis (Figure 44).

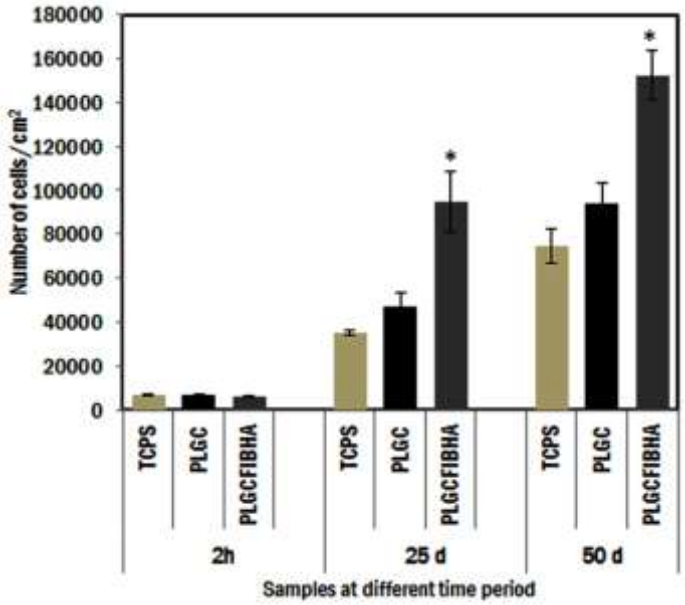

Figure 44. Data on ^{3}H-thymidine uptake assay on PLGCFIBHA hybrid scaffold: The cells adhesion and proliferation of fibroblast on bare PLGC and hybrid PLGC scaffolds after 2h, 25 d and 50 d of culture are shown graphically. Bars represent means ± SD, * p value < 0.05 vs TCPS & bare PLGC.

The decellularized scaffolds after 25 d of cell culture showed deposition of collagen types-1 & 3, elastin and fibrillin-1 throughout the hybrid scaffold upon immunostaining. But in bare scaffold, only patches of elastin and collagen deposition were observed (Figure 45).

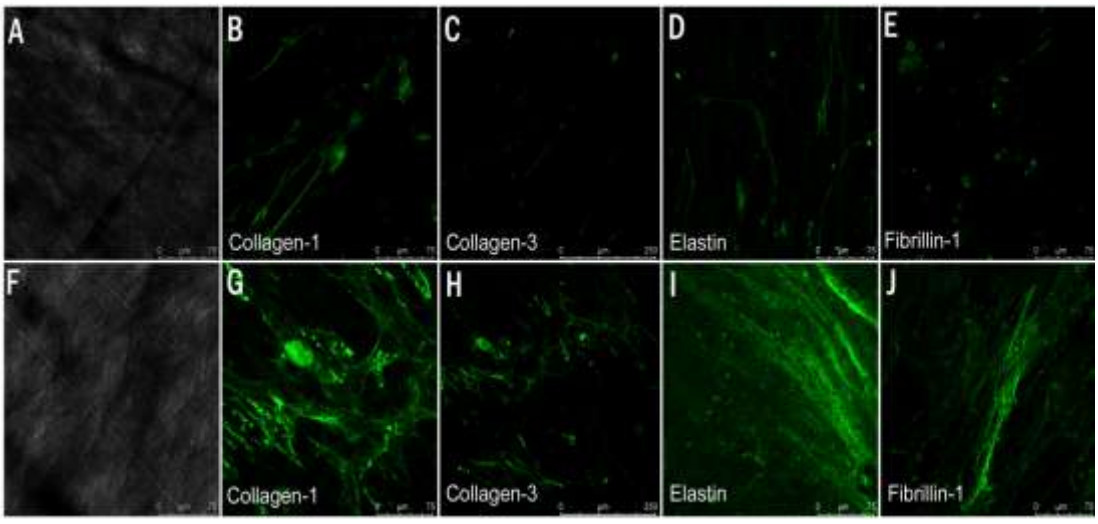

Figure 45. Representative fluorescent images of collagen subtypes, elastin and fibrillin-1 recovered after 20 d of fibroblast culture: A & F) phase contrast

images, B & G) collagen-1, C & H) collagen-3, D & I) elastin and E & J) fibrillin-1 stained images on decellularized bare PLGC and hybrid PLGCFIBHA scaffolds respectively, scale bar = 75 & 250 µm.

Quantitative analysis of collagen on 25 and 50 d showed ~4 fold increase in hybrid scaffold when compared with the bare scaffold. Similar pattern of deposition was observed for the elastin on hybrid scaffold. There was no exponential increase in ECM deposition when compared between 25d and 50d, indicating regulated ECM deposition (Figure 46).

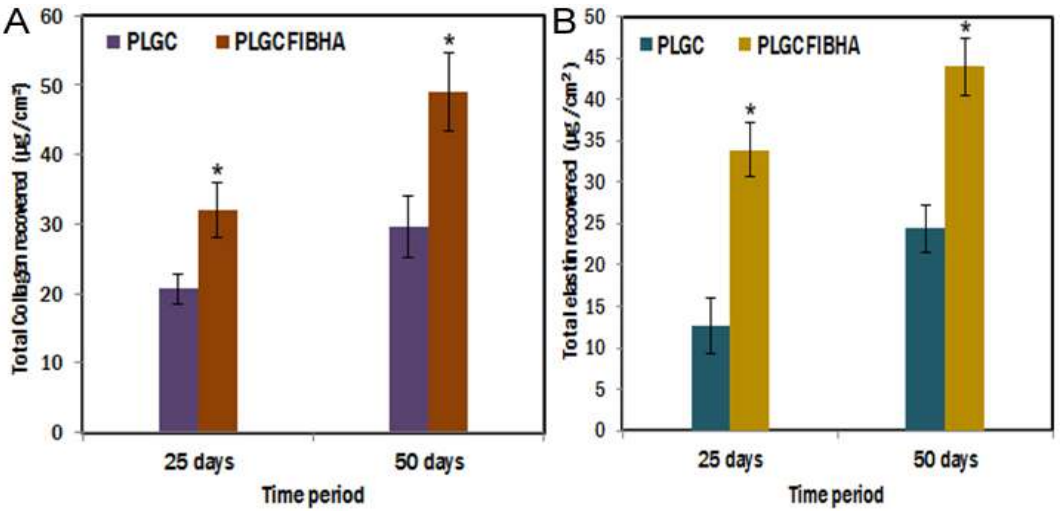

Figure 46. Quantitative analysis of ECM on PLGCFIBHA hybrid scaffold: A) total collagen and B) total elastin estimated on decellularized scaffolds after long term fibroblast culture. Data presented is mean±SD,(n = 4). *p < 0.05 vs bare PLGC.

In summary, the PLGCFIBHA showed significantly higher cell adhesion, improved cellular growth and proliferation when compared with the bare scaffold with regulated ECM deposition.

4.3.5. In vitro tissue engineering on SFFIBHA

In direct contact assay of the SFFIBHA hybrid scaffold, the normal spindle-shaped morphology of fibroblast cells around the scaffold was maintained and was comparable with control cells grown on culture dishes (Figure 47.A & B). The number of cells present after 2 h and 15 d of culture presented in Figure 47.C shows

significantly high cell proliferation on SFFIBHA scaffold when compared to bare SF and control TCPS (C).

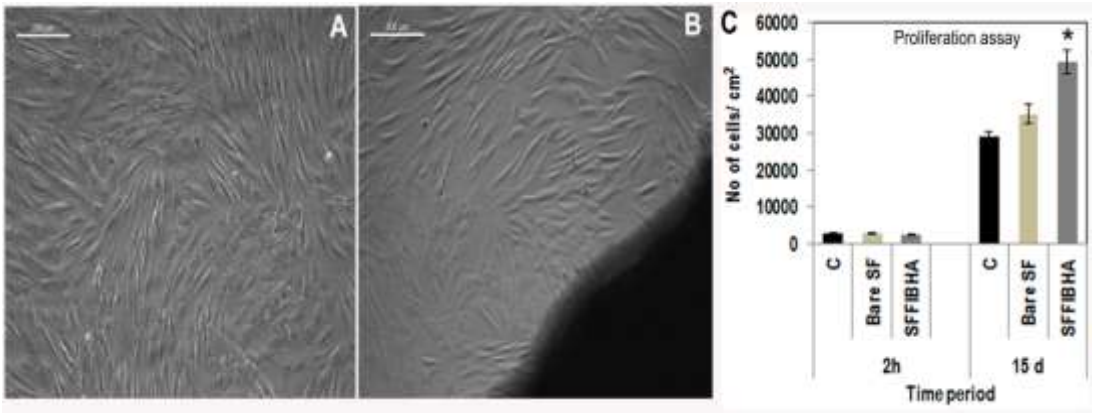

Figure 47. Evidence for cell growth on SFFIBHA hybrid scaffold: A&B) phase contrast image showing direct contact assay ; scale bar = 200 µm and C) proliferation assay using ^{3}H-thymidine uptake assay: The adhesion of fibroblasts on bare SF and hybrid SFFIBHA scaffolds within 2 h and proliferated cell numbers after 15 d of culture are shown graphically. Bars represent mean – SD, (n = 4). *p < 0.05 vs C & bare SF.

The SFFIBHA disintegrated visibly from 4th to 12th d; cell culture was terminated on 15th d. Proliferated cell number on 15th d was only ~ 25 % of the cell number in AMFIBHA on 20th d and only ~ 50 % PLGCFIBHA on 25th d. Since the SFFIBHA scaffold was not stable in the medium, the *in vitro* cell construct is not transferrable to the wound and therefore a modified system was developed for further *in vitro* tissue engineering using the same components.

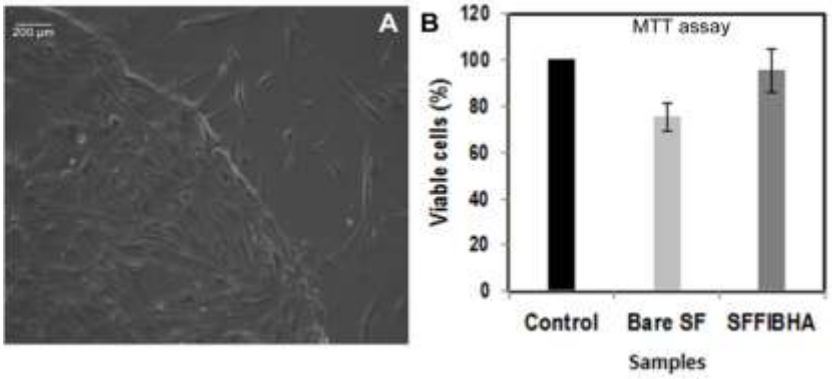

Figure 48. Cell survival on SFFIBHA hydrogel: A) phase contrast image showing cells migrating from the SFFIBHA encapsulated gel on 7 d; scale bar =

200 µm and B) cell viability assay of the cell encapsulated SFFIBHA hydrogel Bars represent mean – SD, (n = 4).

4.3.6. In vitro tissue engineering by cell encapsulation in SFFIBHA hydrogel

Viability of the encapsulated cells after 7 d of culture was comparable with control cells grown on TCPS. There is significant difference in viability when compared with bare SF which showed only about 80 % cells viability (Figure 48). The adhesion of ADMSC-derived fibroblasts on bare SF and hybrid SFFIBHA gel within 2 h and proliferated cell numbers after 7 d of culture were calculated. There was significant fold increase in cell numbers in the hybrid SFFIBHA gel when compared to bare SF scaffolds. The fold change in the cell number in bare SF scaffold was 2 and in hybrid SFFIBHA gel was ~ 6 in 7 d. Cells were migrating out of the gel by 7 d indicating favourable condition for cell growth and proliferation. Cell proliferation was better with gel system mainly because the cells are well distributed within the gel at the start of the experiment. The SFFIBHA scaffold disintegrated limiting the penetration of the cells across the scaffold leading to restricted 3-D growth. The gel system is more stable, may be because cells distributed and produced more ECM to hold the scaffold components together to enable cellular growth and proliferation 3-dimensionally (Figure 49).

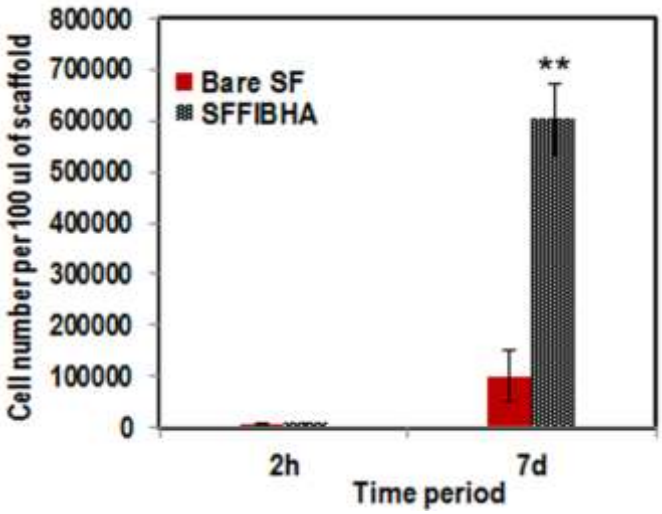

Figure 49. Cell proliferation on SFFIBHA hydrogel using ^{3}H-thymidine uptake assay; bars represent mean – SD, (n =4). **p < 0.01 vs bare SF.

The ECM (total elastin, collagen and sGAG) deposition was found to be proportionate with increase in cell numbers in the SFFIBHA hydrogel. This confirms that uniform deposition of ECM by cells may be the cause for stability of hydrogel (Figure 50).

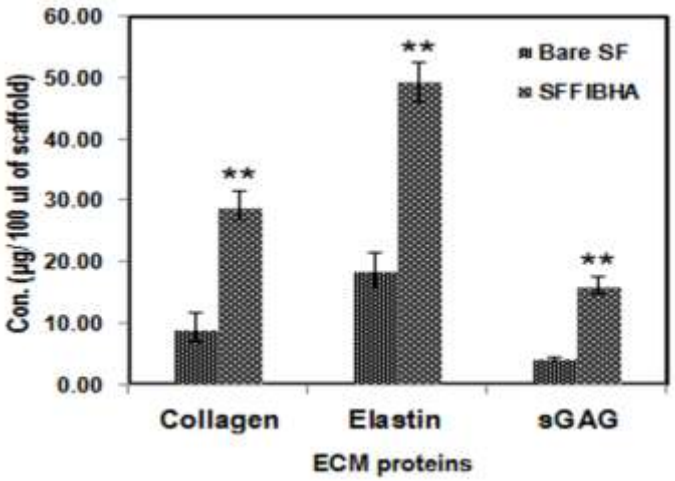

Figure 50. Quantitative analysis of ECM on SFFIBHA hydrogel: for total collagen, elastin and sGAG estimated on decellularized bare SF and SFFIBHA after 15 d of fibroblast culture. Data presented is mean±SD, (n = 4). **p < 0.01 vs bare SF.

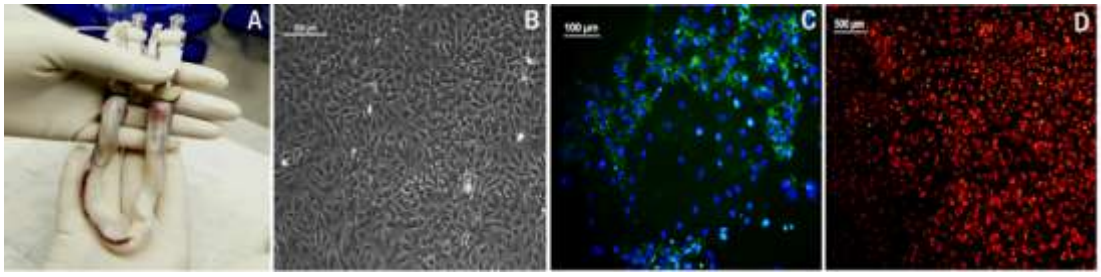

Figure 51. Characterization of human umbilical cord endothelial cells (HUVECs): A) human umbilical cord used for HUVEC isolation, B) HUVECS at passage 2, C & D) fluorescent staining of endothelial markers - CD 31 and Dil-Ac-LDL uptake assay confirming EC phenotype respectively.

4.3.7. *In vitro* tissue engineering in SFFIBHA with angiogenic activity

Well characterized HUVECs with typical cobble-stone morphology (Figure 51.A & B) was encapsulated with hydrogel to induce angiogenic activity. Detection of CD31

and uptake of acetylated low-density lipoprotein (Dil-Ac-LDL), upon immunocytochemistry confirmed endothelial phenotype (Figure 51.C&D).

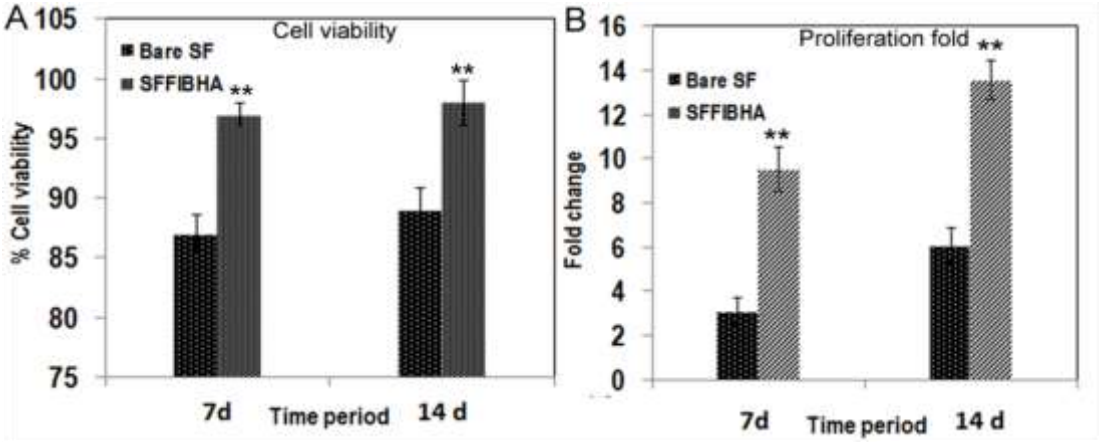

Figure 52. Proliferative ability of cells encapsulated inside the hydrogel: A) cell viability analysis using MTT assay and B) quantification of proliferation fold in 7 and 14 d time period of study. Data presented is mean ± SD, (n = 4); **p < 0.01 vs bare SF.

Viability of the cells in hydrogel system was confirmed using MTT assay. Proliferative ability of the cells encapsulated in the gel system was higher in SFFIBHA gel and proliferation was significantly higher in the SFFIBHA hydrogel when compared to bare SF (Figure 52).

Transcriptional level gene expression of both fibroblast and EC markers was up regulated in SFFIBHA as compared to when co-cultured on bare SF. Dermal collagen-I and basal membrane collagen-IV were significantly up regulated in SFFIBHA grown cells. eNOS did not express when co-cultured on bare SF at both 7d and 14 d (Figure 53).

Parallel to proliferation, the ECM (elastin, collagen and sGAG) deposition was also found to be proportionate with increase in cell numbers in the SFFIBHA hydrogel (Figure 54).

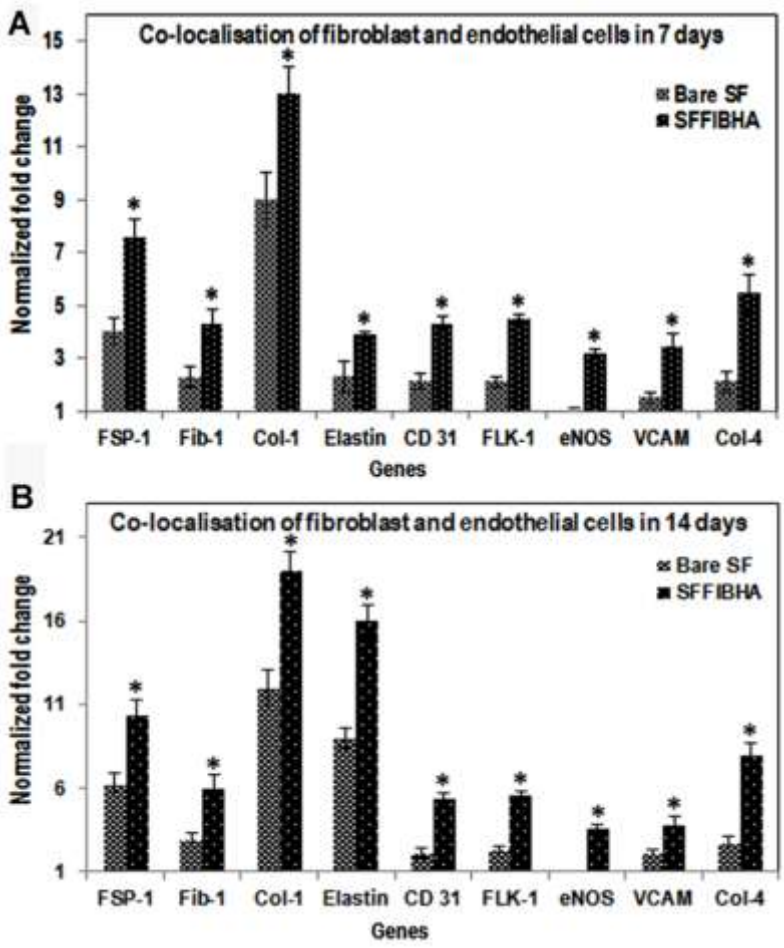

Figure 53. Transcriptional level co-expression of EC and fibroblast markers using qRT-PCR:A&B)Relative expression of both fibroblast and EC markers during two time periods, baseline was calculated by the control cells seeded on 0 d.

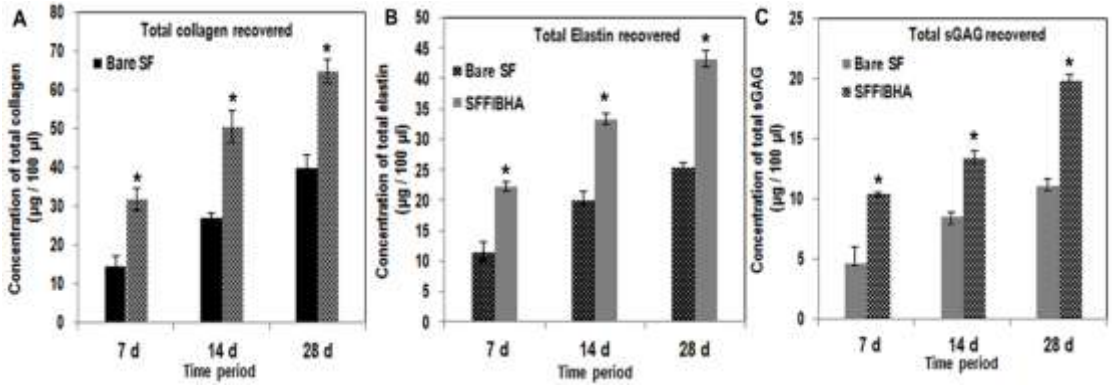

Figure 54. Quantitative analysis of ECM on co-cultured SFFIBHA hydrogel for total collagen, elastin and sGAG estimated on decellularized bare SF and SFFIBHA after 7, 14 and 28 d of co-culture. Data presented is mean±SD,(n = 4). *$p < 0.05$.

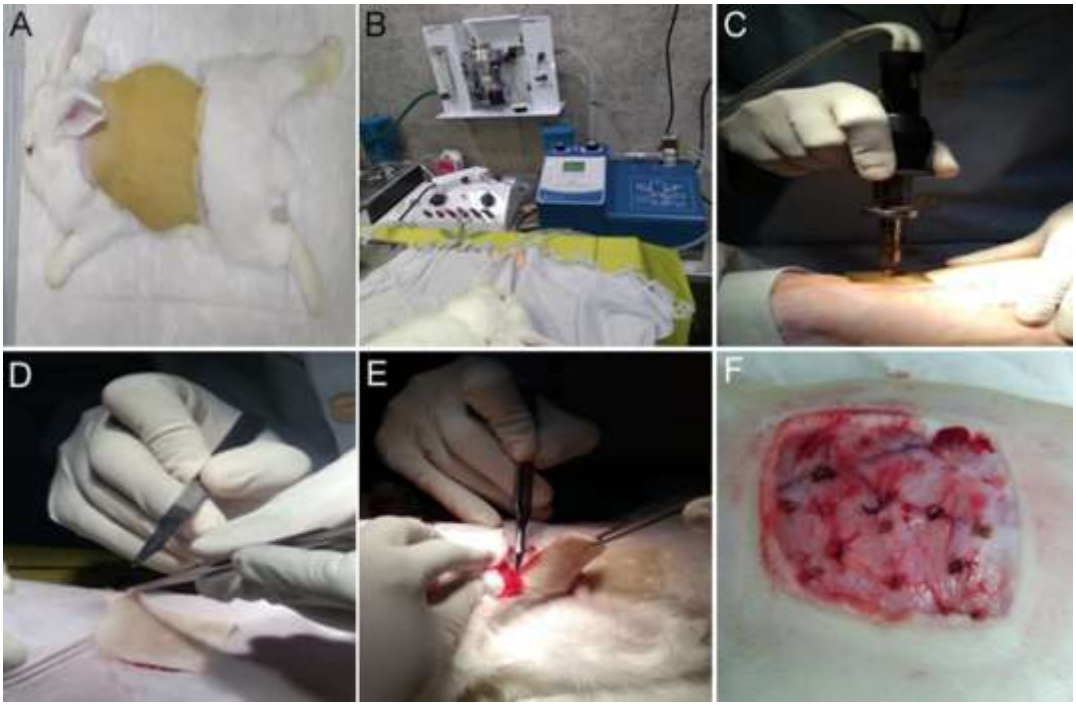

Figure 55. Development of rabbit full thickness third-degree burn wound model: A) anasthestized rabbit, B) intubated with endotracheal tube and maintained under isoflurane and positive ventilation, C) third-degree burn induction, D) burnt full-thickness skin, E) surgical debridement of burnt full-thickness skin and F) full-thickness burnt wound bed ready for application of dermal substitute/scaffold.

4.4. *In vivo* effects of hybrid scaffold for wound regeneration

4.4.1. Effect of scaffold in rabbit burn wound

After burning, the skin appeared dry and hard (Figure 55). Histology analysis of burnt skin revealed that in epidermis, the stratified layers were not seen. Condensed nucleus was seen with coagulated protein. Dermal layer was completely coagulated. Skin appendages like hair follicles, glandular structure could be seen, but were are coagulated. Panniculus carnous muscle layer was observed but completely lost striations and appeared as a homogenous structure. Hence, these results suggested that skin was completely burnt affecting all the three layers of skin making it a full thickness burn wound model.

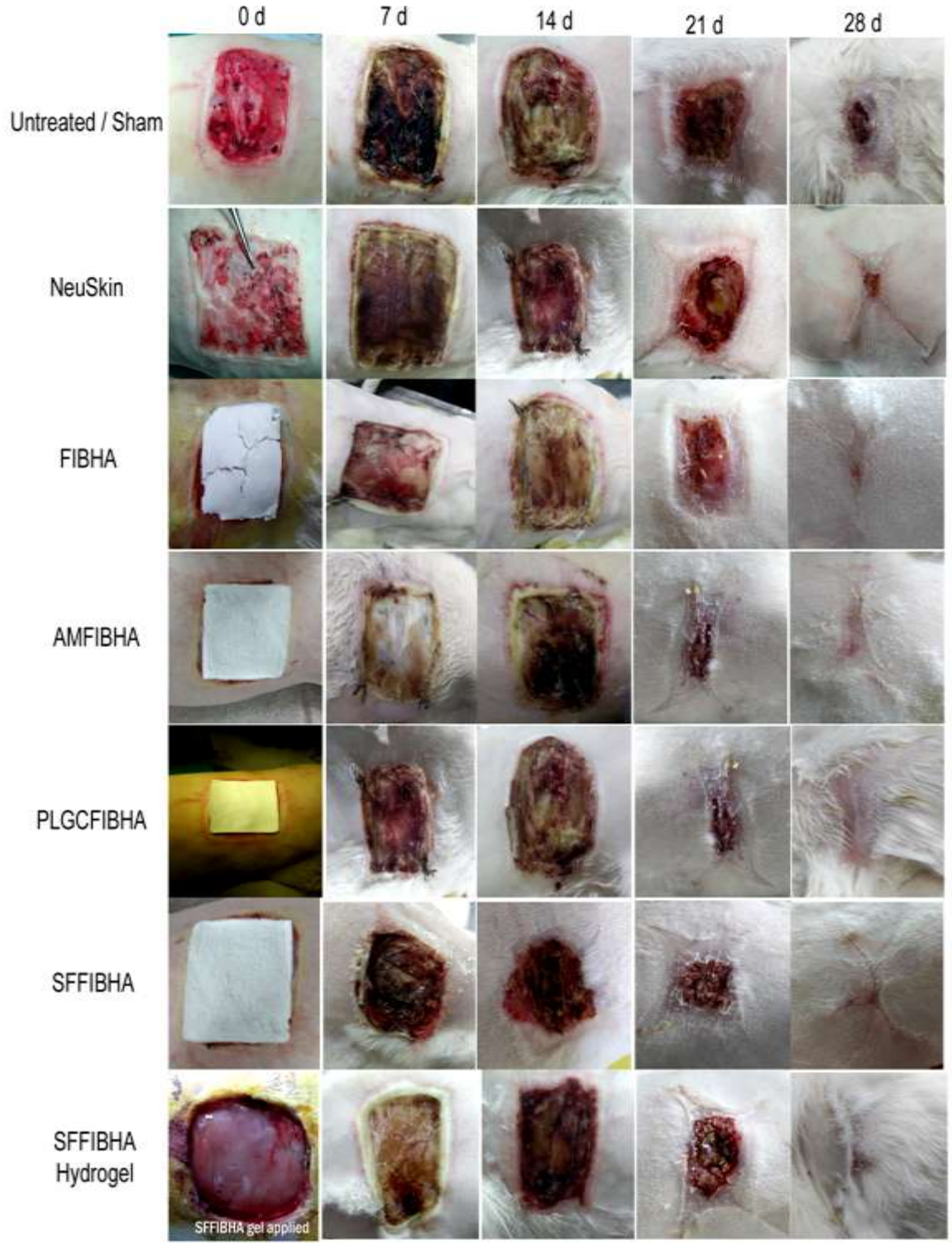

Figure 56. Gross images of wound healing treated with different scaffolds; Untreated/sham control; wound treated with NeuSkin (Positive control (commercial), FIBHA scaffold, AMFIBHA, PLGCFIBHA, SFFIBHA hybrid scaffolds and SFFIBHA hydrogel from d 0- d 28.

4.4.2. Gross evaluation of wound closure

Burnt skin was completely debrided surgically for the application of the test materials. The wound size was 4 x 4 cm^2 full thickness burn wound. Wound healing of the test groups (AMFIBHA, PLGCFIBHA and SFFIBHA hybrid scaffolds and SFFIBHA hydrogel) was compared with untreated / sham wounds (control) and commercially available NeuSkin (positive control). The FIBHA scaffold was also mechanical support has any synergistic or deleterious effect on wound regeneration as compared to the common biological matrix used in all hybrid scaffolds and hydrogel system. After the application of haemostatic hybrid scaffolds, the bleeding was stopped and scaffold was found to be firmly attached to the wounds and covered the wound bed without any help of sutures. The scaffold material was on the wound bed up to 7 - 14 d. Gross evaluation showed that the wound closure was better in treated wounds when compared with the untreated sites. The SFFIBHA in lyophilized and hydrogel form showed comparable results. On 28^{th} d, scar formation was evident in both the control groups (untreated & NeuSkin) and comparatively less scaring seen in the treated groups (Figure 56).

4.4.3. Expressions of wound healing markers

Pro-inflammatory response: The NeuSkin treated wounds showed significantly higher pro-inflammatory response for both markers at 14 d and 28 d as detected by gene expressions of TNF-α and IL-6. Compared to FIBHA, test scaffolds treated wound sites did not show significant inflammatory gene expressions and the order of expression was SFFIBHA hybrid scaffold > SFFIBHA hydrogel > AMFIBHA > PLGCFIBHA. Least relative gene expressions of TNF-α and IL-6 was seen in PLGCFIBHA treated sites indicating the least inflammatory response by 14^{th} day (Figure 57).

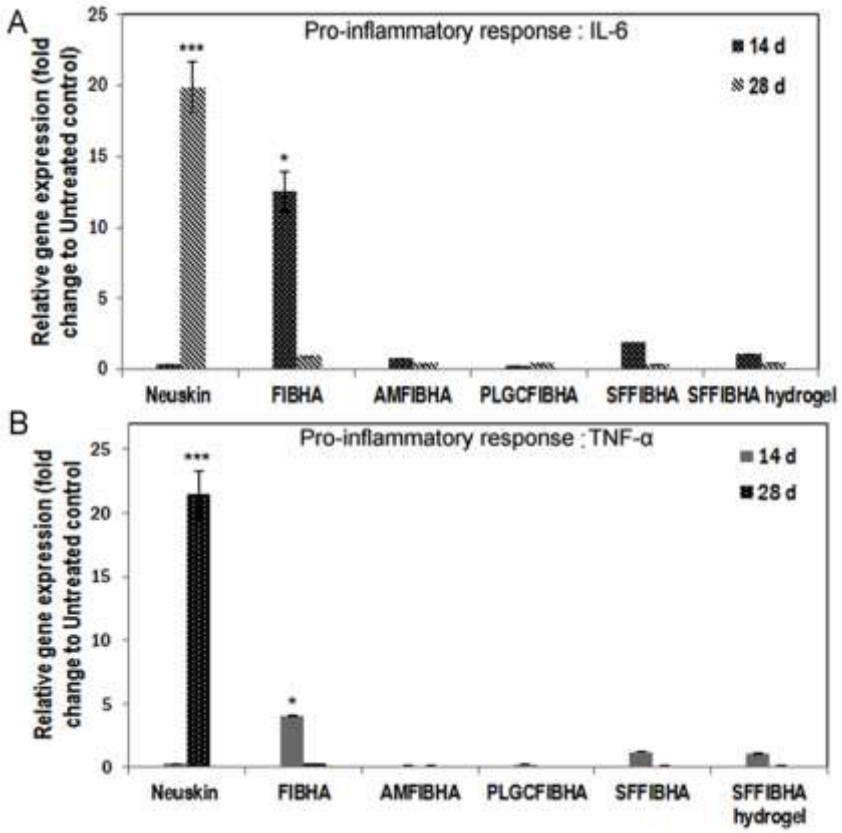

Figure 57. Relative gene expression of IL-6 and TNF-α on 14 and 28 d of wound healing; data presented is mean ± SD,(n = 4). *p < 0.05, **p < 0.01 & ***p < 0.001.

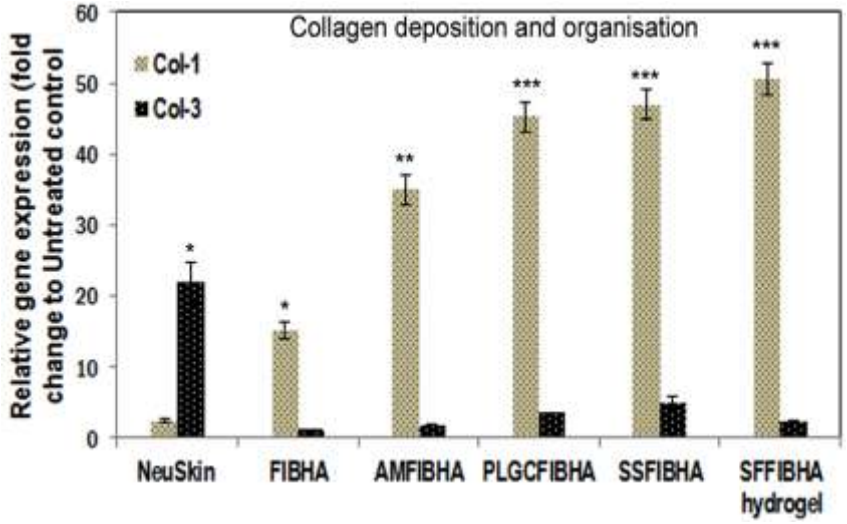

Figure 58. Relative gene expression of collagen-1 & 3 on 28 d of wound healing; data presented is mean ± SD, (n = 4). *p < 0.05, **p < 0.01 & ***p < 0.001.

Collagen deposition: The two dominant types of collagen in wound repair are Col-1 and Col-3. The Col-3 expression was significantly higher in NeuSkin treated wounds and least expression was found in SFFIBHA hybrid scaffold > PLGCFIBHA > SFFIBHA hydrogel > AMFIBHA treated wounds. Col-1 expression was significantly higher in SFFIBHA hydrogel > SFFIBHA > PLGCFIBHA > AMFIBHA > FIBHA > NeuSkin treated wounds. The lower Col-1 and higher Col-3 in NeuSkin treated wound indicates that collagen organization is in the earlier stage of deposition in these wounds and that in all test scaffolds treated wounds collagen in the organized form of Col-1 (Figure 58).

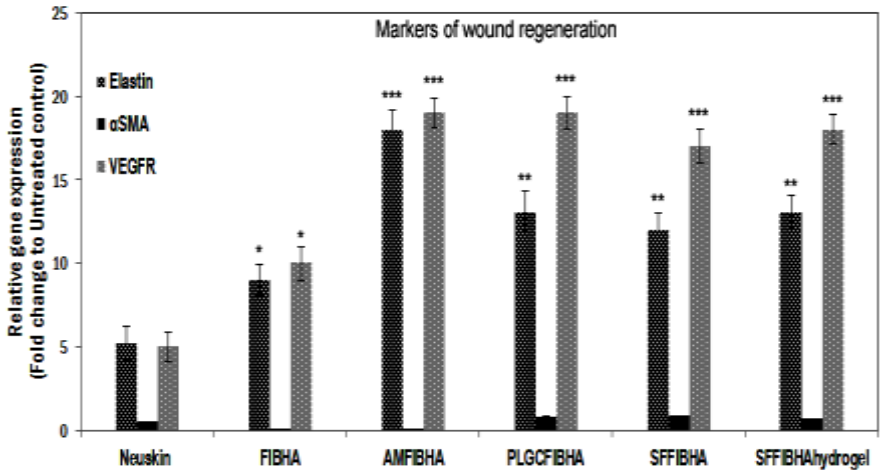

Figure 59. Relative gene expression of elastin, αSMA & VEGFR on 28th d of wound healing; data presented is mean ± SD,(n = 4). *p < 0.05, **p < 0.01 & ***p < 0.001.

Elastin deposition: The expression of elastin in the wounds were found to be in the order AMFIBHA > SFFIBHA hydrogel > PLGCFIBHA > SFFIBHA > FIBHA > NeuSkin treated wounds. αSMA expression was found to be higher in PLGCFIBHA > SFFIBHA > SFFIBHA hydrogel > NeuSkin > AMFIBHA > FIBHA treated wounds. VEGFR was found to be higher in AMFIBHA > PLGCFIBHA >SFFIBHA hydrogel > SFFIBHA > FIBHA > NeuSkin treated wounds (Figure 59).

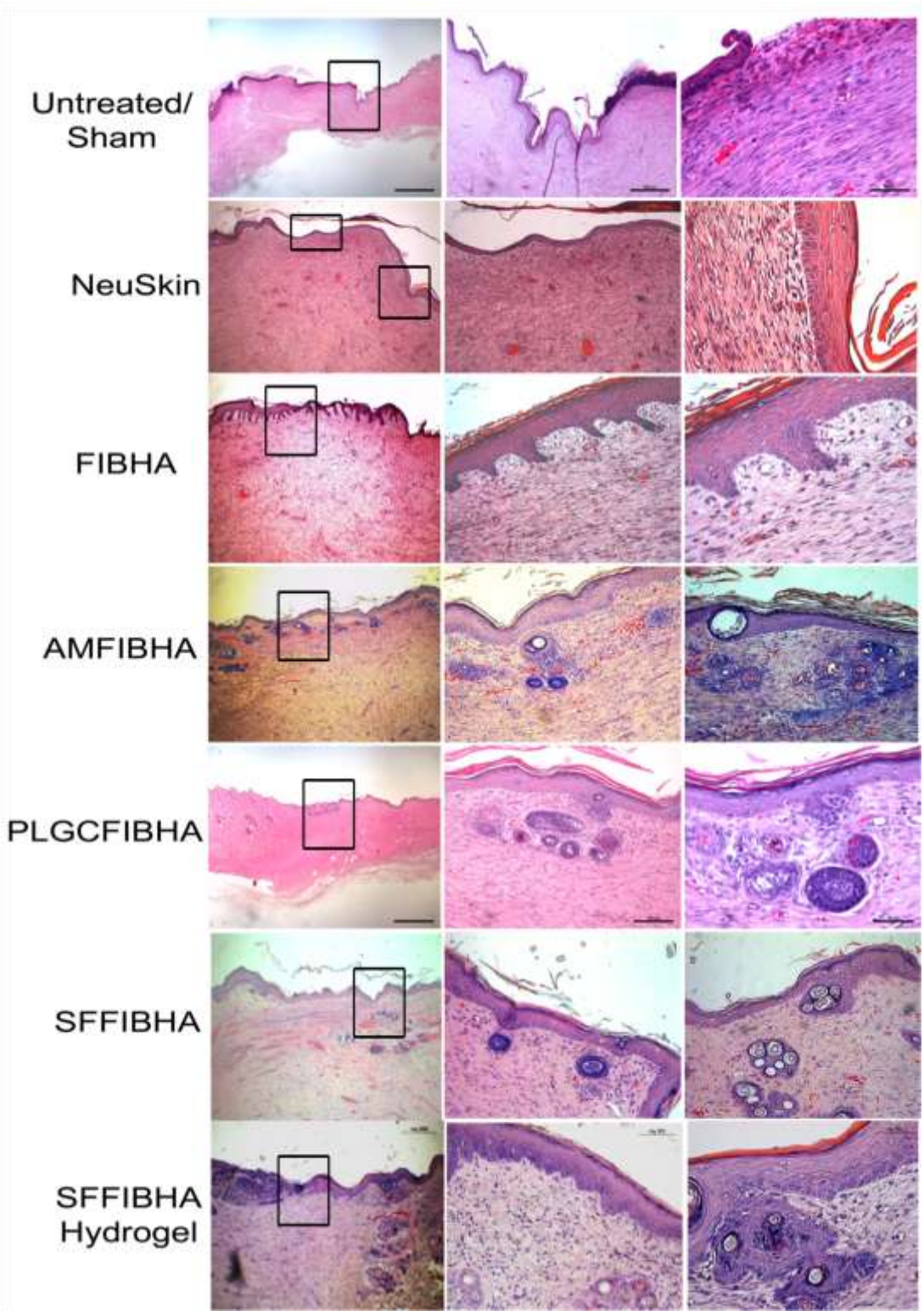

Figure 60. Representative H & E images of wound sections on 28th d of wound healing at different magnifications, the test treated wounds healed with fully matured epithelium and dermis with rete pegs and skin appendage formation.

4.4.4. Histological proof of wound healing

Histopathology analysis on 14th d sample showed thick scab and large number of inflammatory cells were also observed in the untreated group. The inflammatory cells were comparatively less in both the treated groups. By 28th d, all hybrid scaffold treated wounds were completely healed. Complete epithelialization and healing was observed in controls and scaffold treated wounds. Epithelialization was complete with uniformly thick neo-epithelium with intact basal cell layer and superficial keratinocytes and multiple layers of keratohyalin were noted. Dermal closure was complete throughout the wound area, fibrocytes and collagen arranged in multiple layers is noted. Angiogenesis is observed throughout the healed region of dermis. Hair follicle-like structures was observed in the tissue regenerated on 28th day and regenerated tissue was comparable to the architecture of normal skin. Peripheral healed wound region revealed focal region of hair follicle papilla and rete pegs. The control groups also healed with epithelisation, but none of the control groups (untreated / NeuSkin) showed skin appendage formation which was an added advantage to the scaffold treated groups. All the three hybrid scaffolds (AMFIBHA, PLGCFIBHA and SFFIBHA) and the hydrogel SFFIBHA treated groups showed skin appendage development and were comparable (Figure 60).

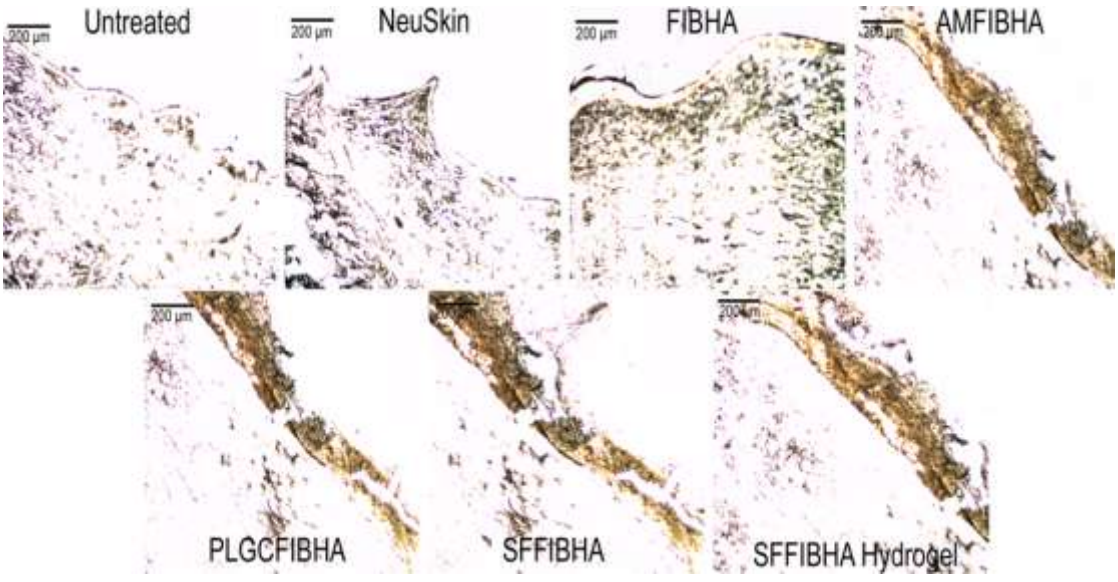

Figure 61. Immunohistochemical staining of CK5 proving epithelialization on 28th d of wound healing: brown colour is positive for CK 5 which stains basal keratinocytes in the epithelium of the regenerated wounds; scale bar = 200 µm.

4.4.5. Extent of epithelialization

Epithelialization was complete with uniformly thick neo-epithelium with intact basal cell layer and superficial keratinocytes and multiple layers of keratohyalin were noted in hybrid scaffolds treated wounds proved by histological evaluation. Epithelial marker, CK 5 are expressed by basal cells of skin epithelium. Immunohistochemistical staining showed positivity for all the test hybrid scaffolds AMFIBHA > PLGCFIBHA > SFFIBHA > SFFIBHA hydrogel > FIBHA > NeuSkin > Untreated wounds (Figure 61).

4.4.6. Proof of angiogenic response to the hybrid scaffolds

Angiogenesis was evaluated by immune staining of regenerated wound sections on 28th d for CD31, an endothelial marker which stains the blood vessels. The results suggested that number of blood vessels was significantly higher in the wound treated with hybrid scaffolds and hydrogel (Figure 62).

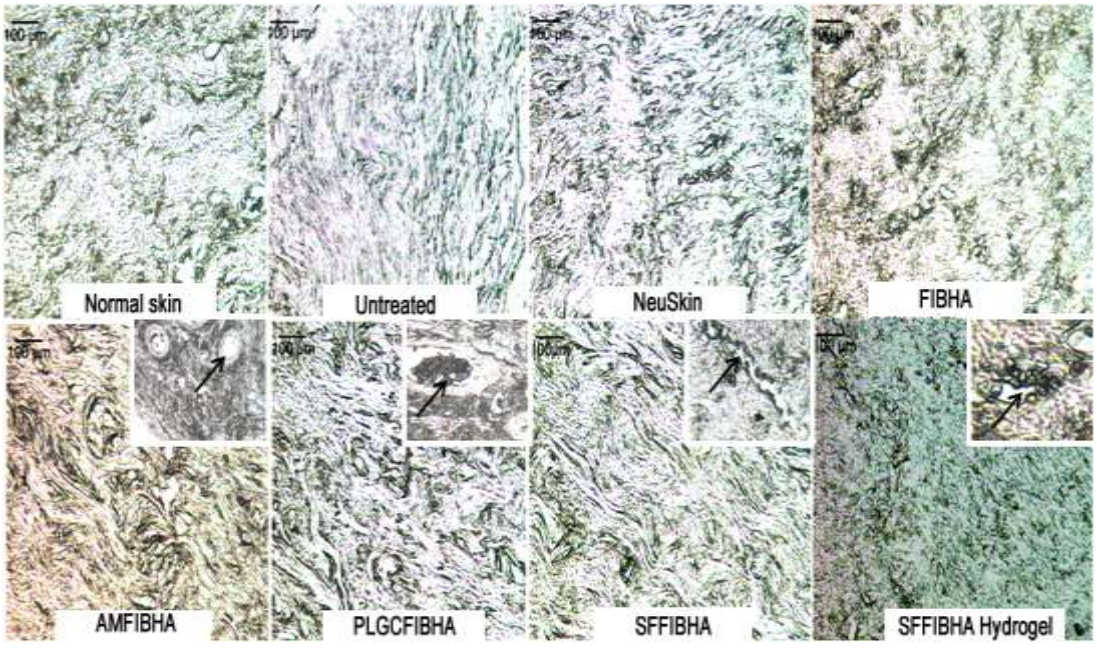

Figure 62. Representative images of immunohistochemical data of angiogenesi on 28th d of wound healing, the wound sections were stained for CD31, brown colour is positive for CD31 which stains the endothelial cells lining blood vessels, arrow in the inset shows blood vessels seen in the dermis; scale bar = 100 µm.

4.4.7. Evidence for collagen deposition

The collagen deposition on the regenerated tissue was evaluated by staining with Picro-Sirius red. The collagen stained tissue sections on 14th d and 28th d of analysis are depicted in the figure 63 & 64. Collagen deposition in the hybrid scaffold and hydrogel treated group was significantly higher than the untreated control on 14th d of analysis.

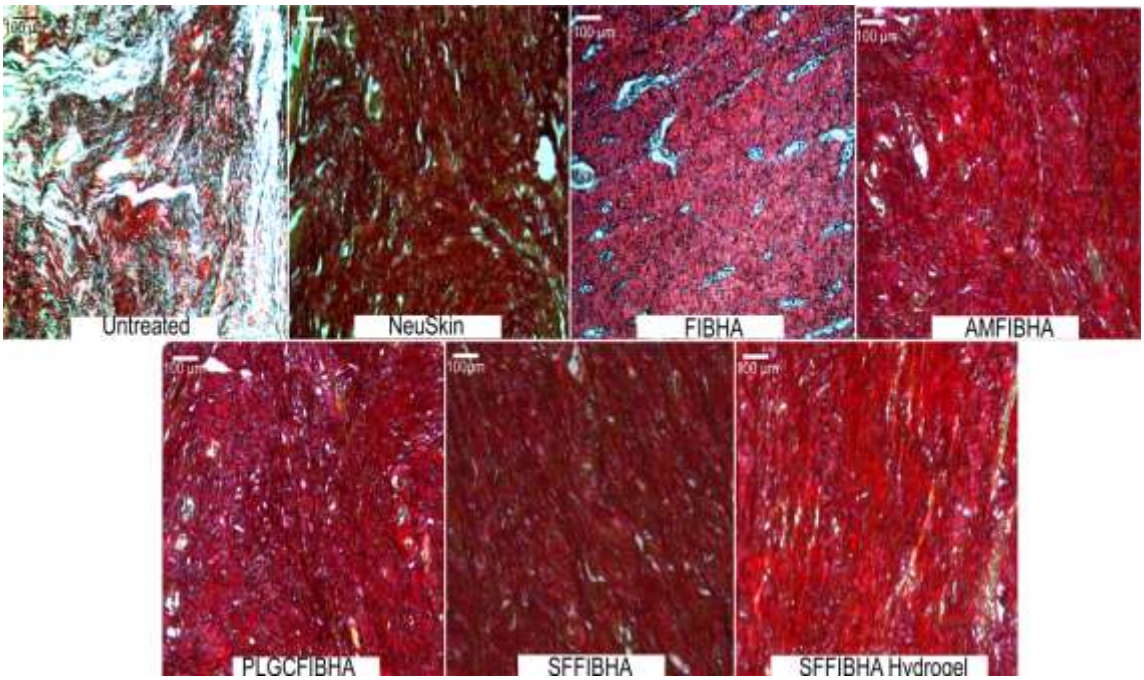

Figure 63. Representative images showing pattern of collagen deposition on 14th d of wound healing: Picro-Sirius red staining of collagen in the dermis- the stained collagen fibers are arranged in a more organized fashion in the test groups than the untreated/sham (negative control) wound. Red colour is the collagen and all other components are green in colour; scale bar = 100 µm.

Within 28th d, more collagen got deposited in the untreated control and the NeuSkin treated group; but the pattern of deposition was found to be irregular. On the other hand, in the hybrid scaffold and hydrogel treated group appreciable collagen reorganization occurred and showed a bundle-like pattern similar to th normal skin on the 28th day (Figure 64).

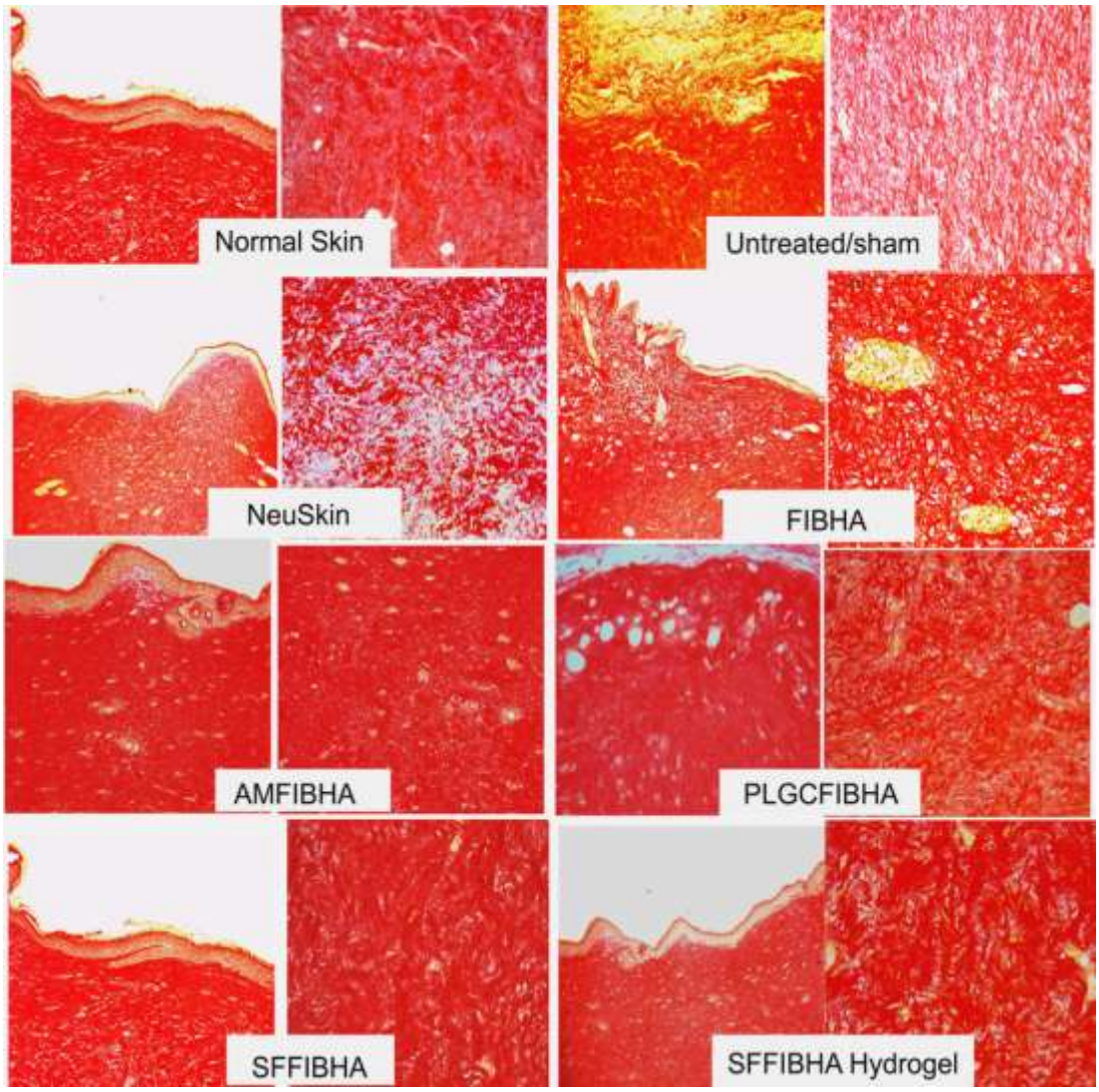

Figure 64. Representative images of collagen deposition on 28th d of wound healing; wound sections were stained with Picro-Sirius red (red colour is the new collagen), collagen fibers are arranged in a more organized fashion in the test groups than the untreated/sham (negative control) and NeuSkin (positive control) treated wound when compared to normal rabbit skin; scale bar = 200 & 50 µm.

4.4.8. Evidence of elastin deposition

The elastin deposition on the regenerated tissue 28th d of analysis was evaluated by immunohistochemistry. Elastin deposition in the hybrid scaffold and hydrogel treated group was significantly higher than the untreated control and NeuSkin treated groups. The pattern of elastin deposition was similar to that of normal rabbit skin (Figure 65).

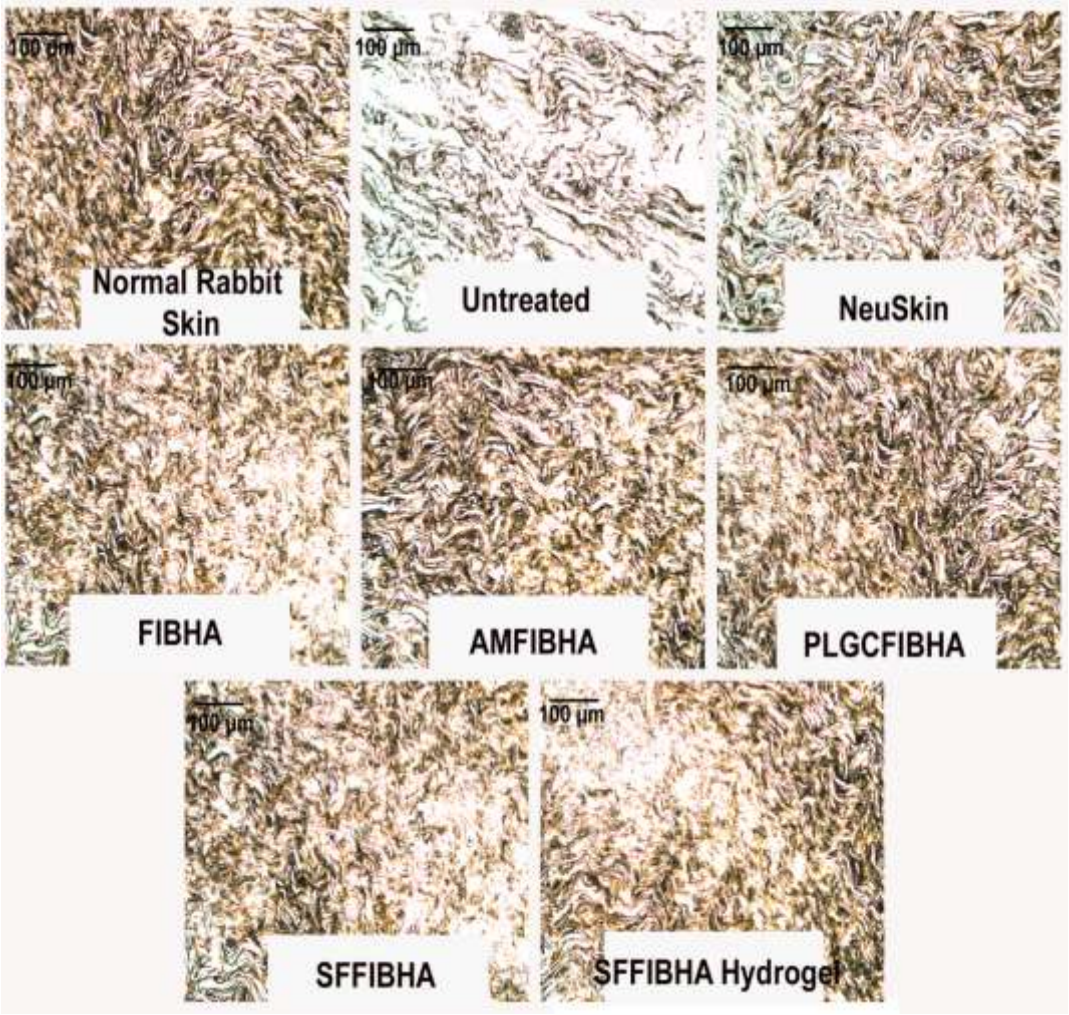

Figure 65. Pattern of elastin deposition on 28th d of wound healing. The wound sections on 28th day were stained for elastin, brown colour is the positive for elastin deposition in the dermis; scale bar = 100 µm.

4.5. Long term evaluation of wound regeneration

4.5.1. Evaluation of ECM molecules in the regenerated skin after 56 d ofwounding

Higher collagen and elastin deposition on hybrid scaffold was due to better cell survival and growth. ECM deposition was evaluated by quantification of total collagen, elastin and sGAG and was compared with ECM quantified from normal skin. The untreated wound showed significantly higher collagen deposition. Hybrid scaffolds showed total collagen deposition as Untreated > SFFIBHA hydrogel > SFFIBHA > PLGCFIBHA > AMFIBHA. Elastin deposition was in the order

SFFIBHA > PLGCFIBHA > SFFIBHA hydrogel > AMFIBHA > untreated. sGAG deposition was in the order was found comparatively higher than hybrid treated wounds. Hybrid scaffold treated wounds showed similar deposition as of normal skin (Figure 66).

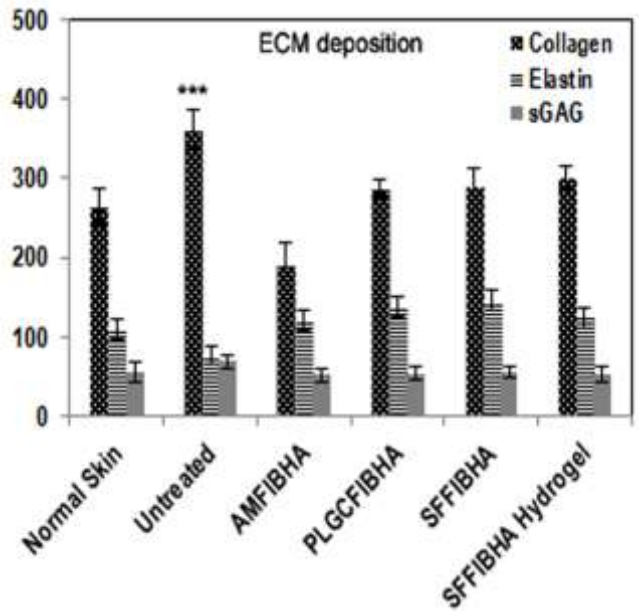

Figure 66. ECM deposition after 56 d of wound healing on application of hybrid scaffolds and hydrogel.

4.5.2. Mechanical properties of the regenerated skin

The mechanical properties of regenerated skin 56 d after application of hybrid scaffolds were measured using UTM. The properties was compared to normal rabbit skin and regenerated skin of the untreated sham wounds. The tensile strength of thehybrid scaffolds was comparable with normal skin whereas the untreated regenerated skin showed significant reduction. The percentage elongation of hybrid scaffolds showed comparable results with AMFIBHA, PLGCFIBHA and SFFIBHA hydrogel treated regenerated skin with normal skin, whereas the untreated and lyophilized SFFIBHA treated wounds showed similar results. The tensile modulus was higher for hybrid scaffold treated wounds PLGCFIBHA > SFFIBHA > SFFIBHA hydrogel > AMFIBHA > Untreated. The improved mechanical property may be attributed to the organized ECM molecules on hybrid scaffolds (Figure 67).

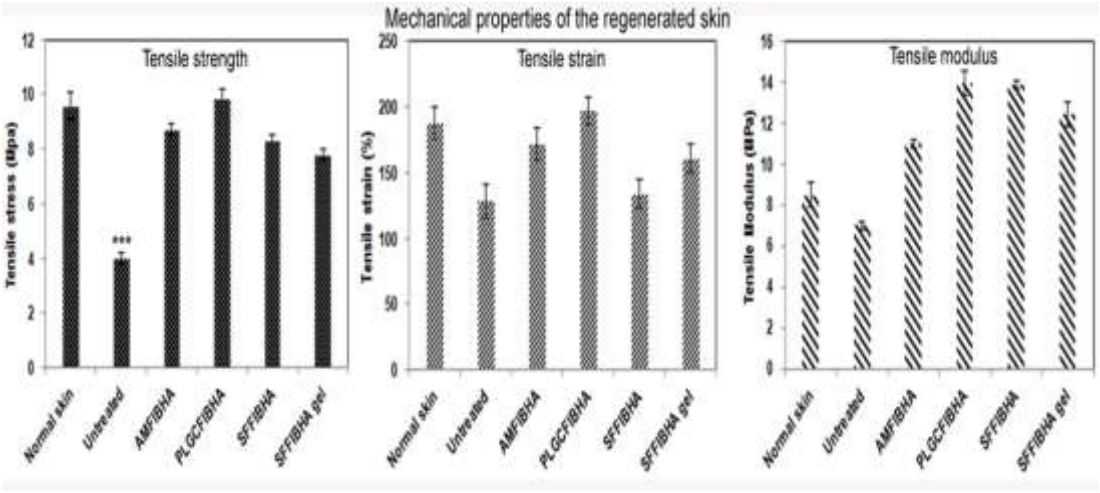

Figure. 67. Data on mechanical strength of regenerated skin after 56 d of wound healing: A) tensile strength, B) tensile strain(percentage elongation) and tensile modulus of the regenerated skin of hybrid scaffolds. Bars represent means ± SD,*** p value < 0.001.

Figure 68. Porcine diabetic wound model design: A) wound made (4 x 4 cm^2) using sterile blade using a template, B) surgically removing full thickness skin & C) wound bed ready for application of test materials.

4.6. *In vivo* evaluation in porcine diabetic wound model

4.6.1. Gross evaluation of wound healing and wound closure

Full-thickness excisional wounds were made on hyperglycemic pigs for the application of the test materials (Figure 68). The wound size was 4 x 4 cm^2 full-thickness wound. Wound healing of the test groups (AMFIBHA, PLGCFIBHA and SFFIBHA hybrid scaffolds) was compared with untreated / sham wounds (control) and commercially available NeuSkin (positive control). Upon application of haemostatic hybrid scaffolds, the bleeding was stopped and scaffold was found to be

firmly attached to the wounds and covered the wound bed without needing sutures. The scaffold material was on the wound bed up to 7-10 d. Gross evaluation showed that the wound closure was better in treated groups when compared with the untreated wound (Figure 69).

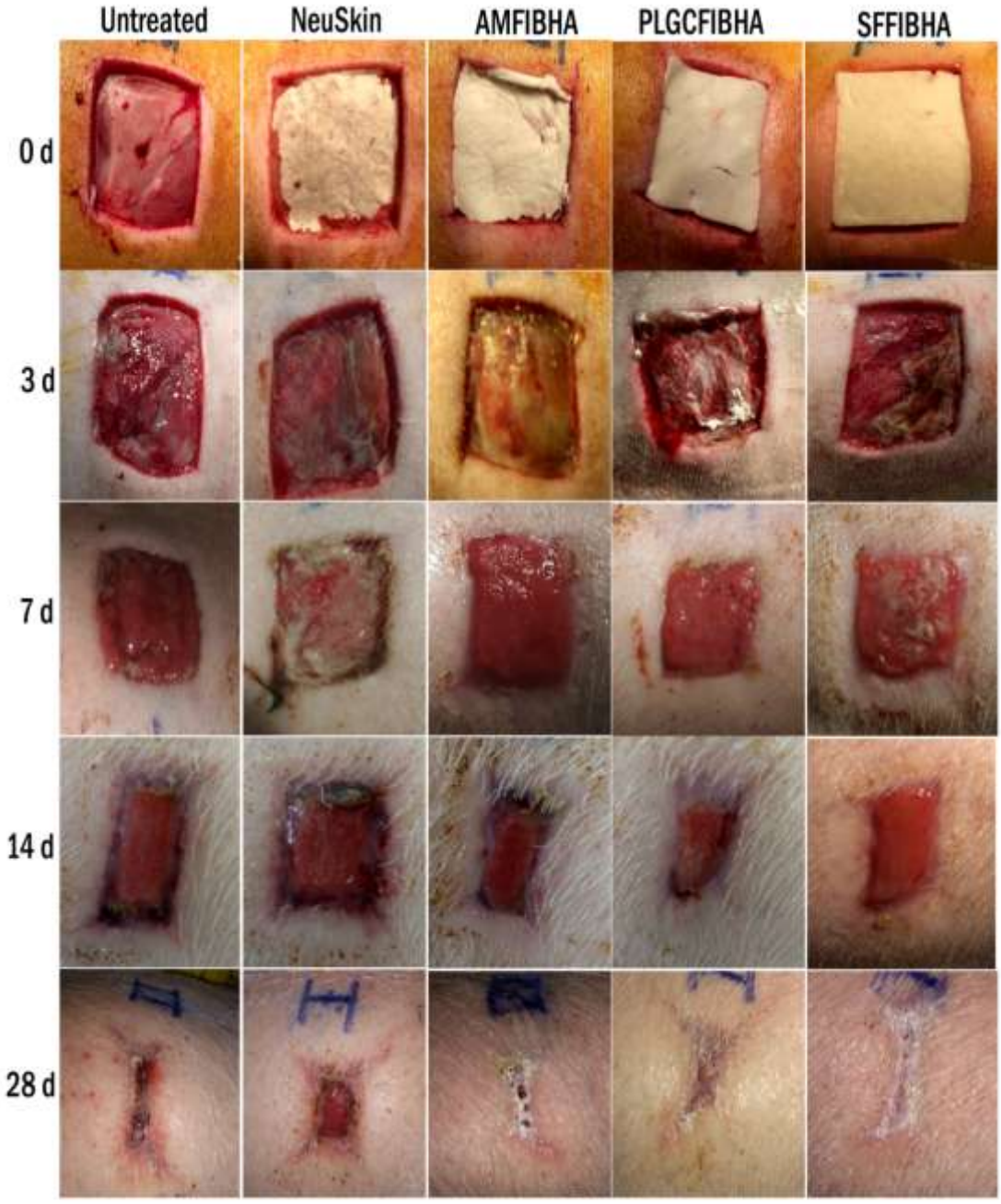

Figure 69. Gross images showing comparison of wound closure from d 0 – d 28 on diabetic pig wound model; untreated/sham control; wound treated with NeuSkin (Positive control, commercial), FIBHA scaffold, AMFIBHA, PLGCFIBHA and SFFIBHA hybrid scaffolds from d 0- d 28.

4.6.2. Gene expression of wound healing markers

Angiogenesis and epithelialization: CK 14 (basal keratinocyte marker) expression in the wounds was found in the order AMFIBHA > PLGCFIBHA >SFFIBHA > NeuSkin treated wounds. In NeuSkin treated wound CK14 expression was very low. VEGF-A indicating angiogeneiss was found to be higher in AMFIBHA > PLGCFIBHA > SFFIBHA > NeuSkin treated wounds (Figure 70).

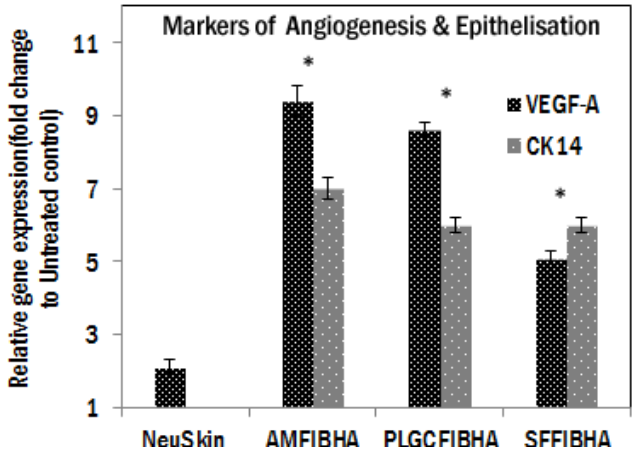

Figure 70: Relative gene expression of angiogenic and epithelialization markers at d 28 wounds; data presented is mean±SD, (n = 4). *p < 0.05.

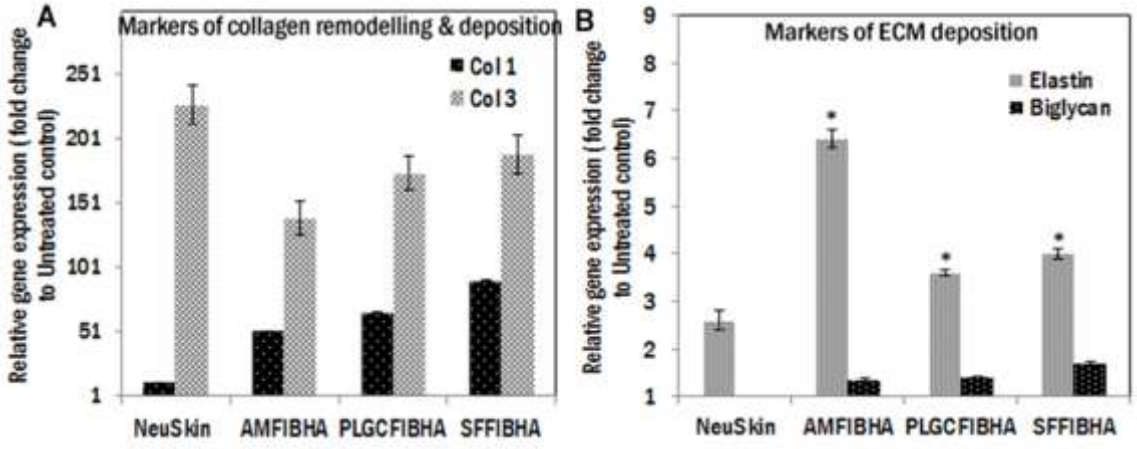

Figure 71. Relative gene expression of ECM markers at d 28 wounds : A) Collagen remodeling and organization and B) elastin and biglycan gene expression, Data presented is mean±SD,(n = 4). *p < 0.05.

Collagen remodeling: The Col-3 expression was significantly higher in NeuSkin > SFFIBHA > PLGCFIBHA > AMFIBHA treated wounds. Col-1 expression was significantly higher in SFFIBHA > PLGCFIBHA > AMFIBHA > Neuskin treated wounds. This indicates that the NeuSkin treated wound is in the earlier stage of collagen organization (Figure 71.A). The elastin expression in the wounds were found to be in the order AMFIBHA > SFFIBHA hydrogel > PLGCFIBHA > SFFIBHA > FIBHA > NeuSkin treated wounds. Glycosaminoglycan expression was found to be higher in SFFIBHA > PLGCFIBHA > AMFIBHA> NeuSkin treated wounds (Figure 71.B).

4.6.3. Histological evidence of wound healing

Histological analysis was done on 28^{th} d of experiment. The untreated/sham and NeuSkin treated wounds showed similar results. The wounds showed incomplete epidermal healing. Epithelialization was complete at periphery of wound, variably thick stratified squamous epithelium with basal cell layer and superficial keratinocytes and multiple layers of keratohyalin was noted. At the centre of the wound, focal area of fibrokeratinocyte layers or absence of epithelium was noted. Healing under scab was noted. Dermal layer was formed with fibrocytes and collagen. Granulation tissue is noted at the center of the wound. Dermal and subepidermal region revealed mild degree of inflammation with infiltration of few polymporphonuclear (PMN) cells and lymphocytes. Foci of macrophages and mononuclear cells collection are noted in deep dermal region. Whereas, the hybrid scaffold wounds showed complete epithelialization. Epithelialization was complete, variably thick stratified squamous epithelium with intact basal cell layer and epithelium with basal cell layer and superficial keratinocytes and multiple layers of keratohyalin was noted. Dermis was completely formed with fibrocytes and collagen. Granulation tissue is noted at the center of the wound. Dermal and subepidermal region revealed mild degree of inflammation with infiltration of polymporphonuclear (PMN) cells and lymphocytes. Angiogenesis is observed throughout the healed region of dermis. Peripheral healed wound region revealed rete pegs. Histological evaluation showed efficient healing when compared to untreated and NeuSkin

treated wounds. All three scaffolds were comparable w.r.t. regenerative capacity (Figure 72).

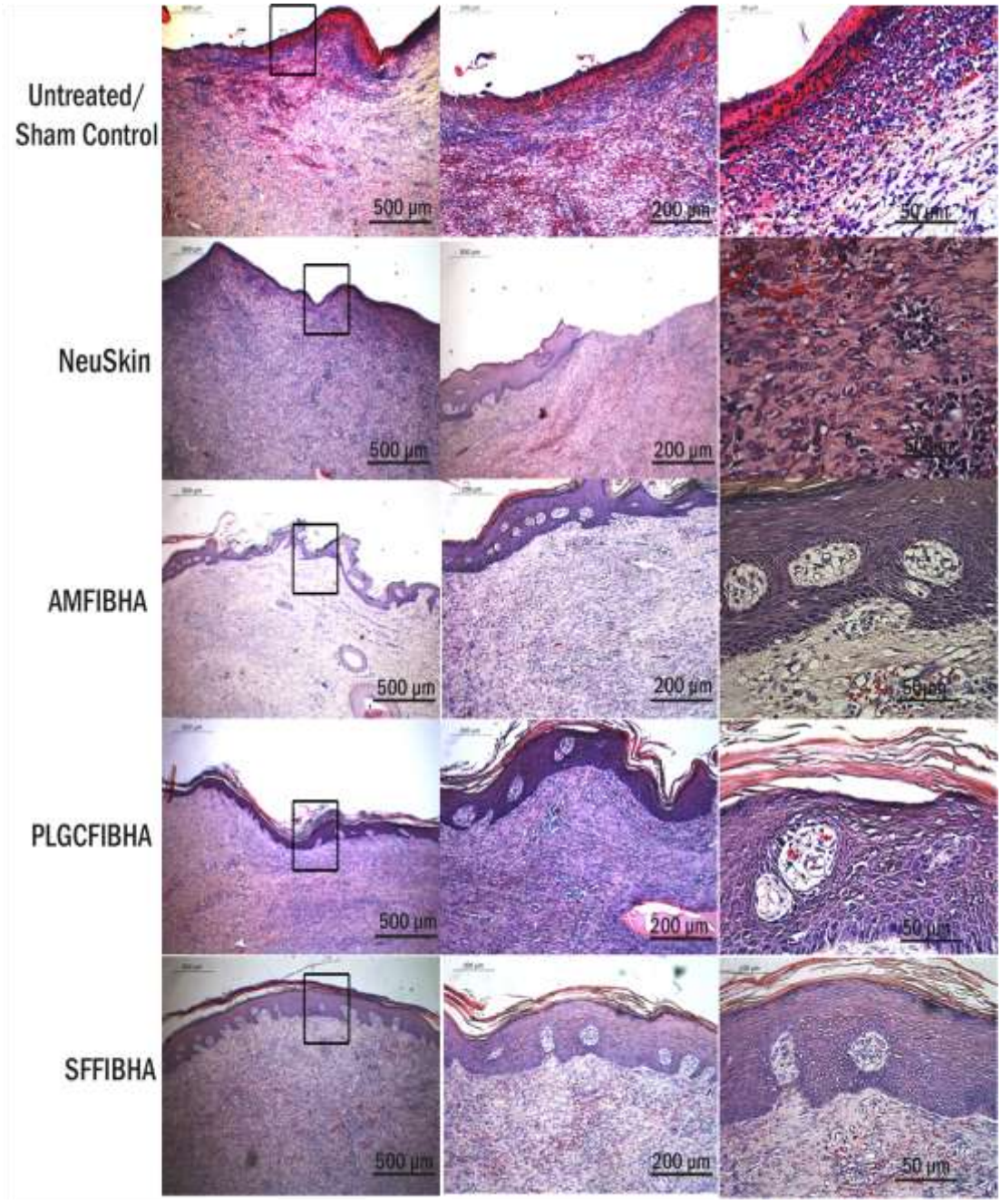

Figure 72. H & E staining showing wound healing on 28th d at different magnifications: the insets shown in the first column are magnified and shown in lower magnifications in the next columns. Both the control wounds showed incomplete epithelialisation, whereas AMFIBHA, PLGCFIBHA & SFFIBHA treated wounds healed with fully formed mature epithelium along with rete peg formations and dermis with angiogenesis.

4.6.4. Proof of epithelialization in response to scaffolds

Epithelialization was proved by histological evaluation. Epithelial marker, CK 5 is expressed by basal cells of epithelium of skin. Immuno-histochemical staining showed positivity for all the test hybrid scaffolds, whereas it was absent in both untreated and NeuSkin treated wounds (Figure 73).

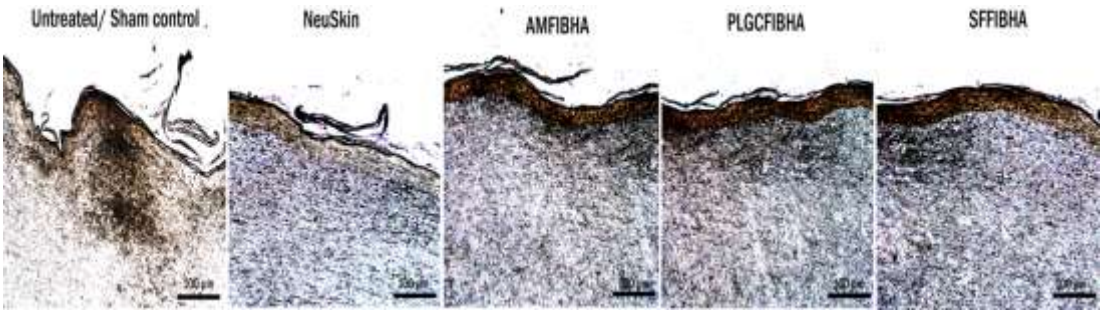

Figure 73. Immunohistochemical staining of CK5 for proving epithelialization on d 28 on diabetic pig wound model: The wound sections on 28th day were stained for CK 5, brown colour is the positive for basal keratinocytes marker expression.

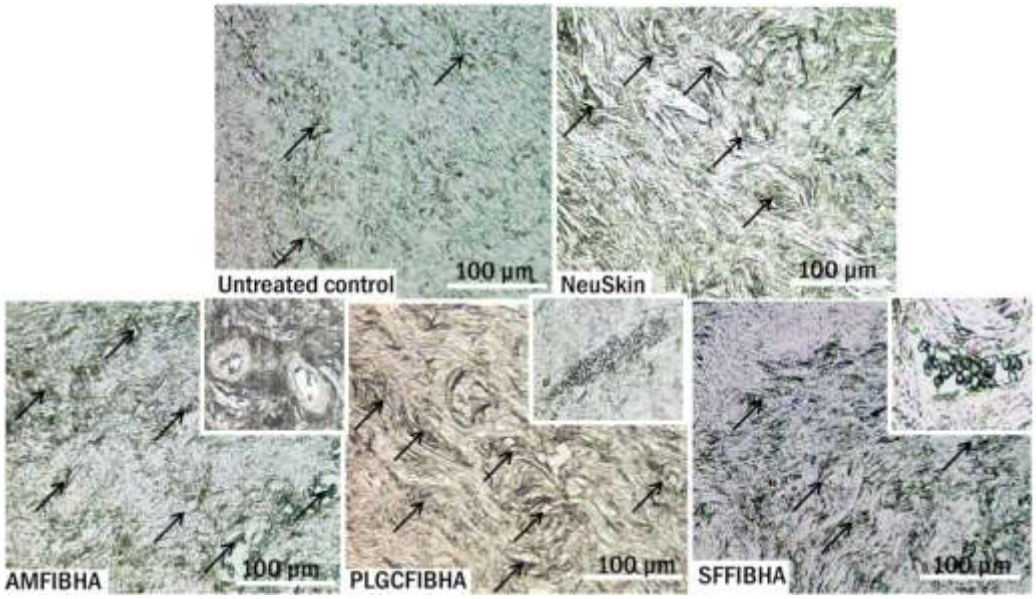

Figure 74. Immunostaining of endothelial cell marker CD31 on wounds treated with different scaffolds and their controls: The wound sections on 28th d were stained for CD 31, brown colour is the positive for CD 31 staining endothelial cells lining blood vessels, inset shows blood vessels in dermis; scale bar = 100 µm & 50 µm.

4.6.5. Effect of hybrid scaffolds on wound angiogenesis

Angiogenesis was evaluated by immune staining of regenerated wound sections on 28th d for CD31, an endothelial marker which stains the blood vessels. The results suggested that number of blood vessels was significantly higher in the wound treated with hybrid scaffolds and hydrogel. Angiogenesis was seen in the order AMFIBHA > PLGCFIBHA > SFFIBHA > NeuSkin > Untreated control (Figure 74).

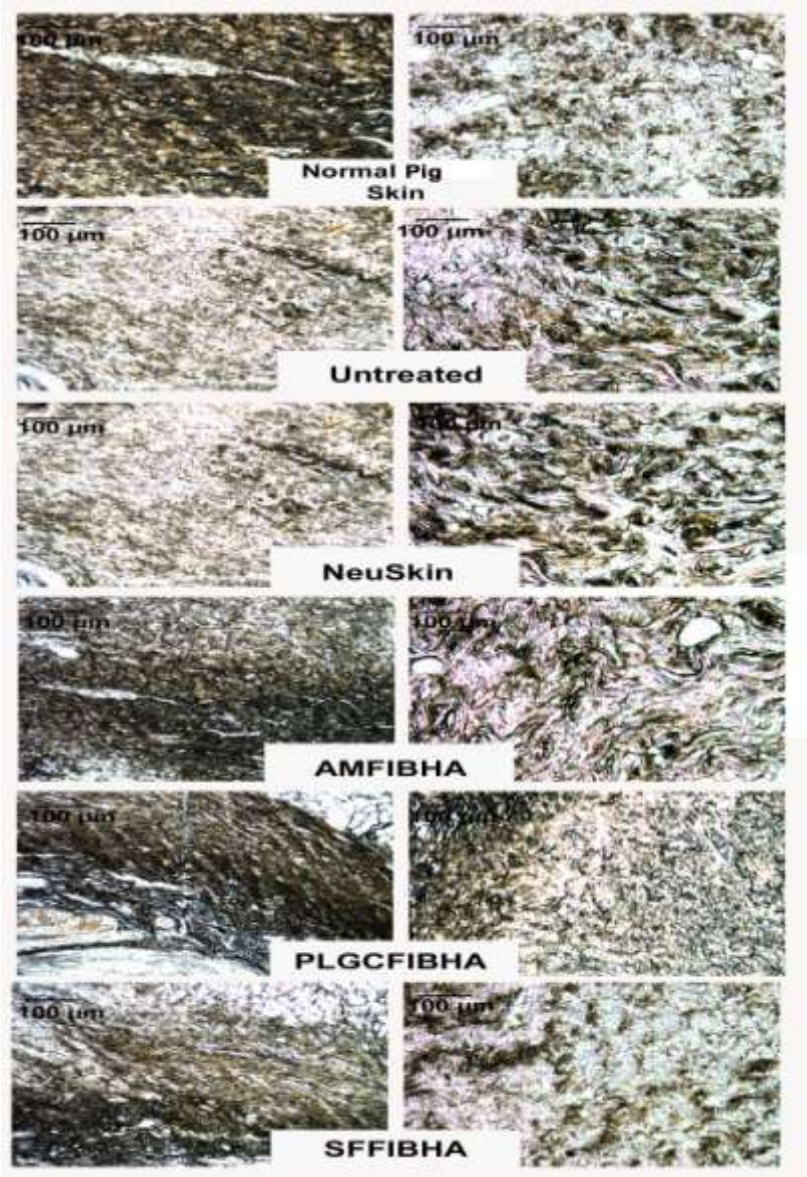

Figure 75. Representative immuno histochemistry data of collagen deposition: The wound sections on 28th day were stained for Col-1 & 3, brown colour is the positive for collagen deposition.

4.6.6. Proof of ECM deposition in response to scaffolds

Collagen deposition and organisation: The two dominant types of collagen in wound repair are Col-1 and 3. The Col-3 expression was higher in NeusSkin followed by treated wounds and least expression was found in hybrid scaffolds treated wounds. Col-1 expression was significantly higher in the hybrid scaffold treated groups than both untreated and NeuSkin treated wounds. The lower Col-1 and higher Col-3 in NeuSkin treated wound indicates that collagen organization is in the earlier stage of deposition in these wounds and that in all test scaffolds treated wounds collagen in the organized form of Col-1. The results correlated with the RT-PCR data (Figure 75).

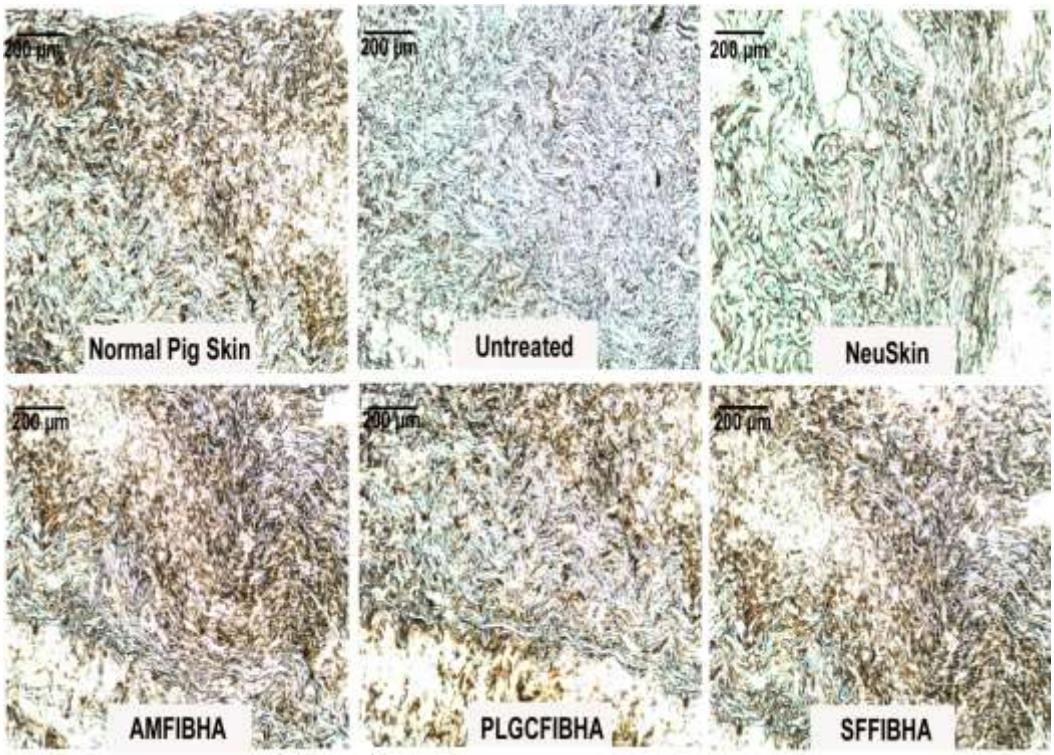

Figure 76. Pattern of elastin deposition on 28th d of wound healing. The wound sections on 28th d were stained for elastin, brown colour is the positive for collagen deposition.

Elastin deposition: The elastin deposition on the regenerated tissue 28th d of analysis was evaluated by immunohistochemistry. In untreated and NeuSkin treated groups elastin deposition was less whereas, the elastin deposition in the hybrid scaffold

treated groups was significantly higher than both control groups. The pattern of elastin deposition was similar to that of normal pig skin (Figure 76).

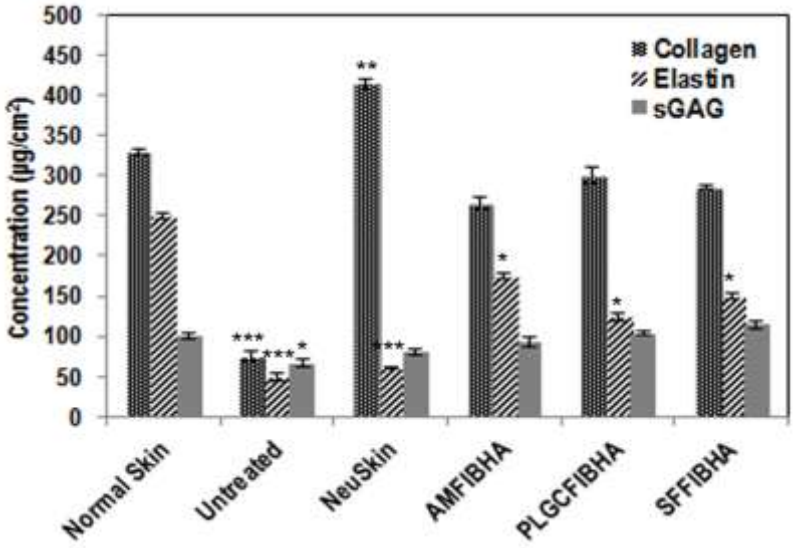

Figure 77. ECM deposition after 28th d of wound healing on application of hybrid scaffolds.

Quantification of ECM molecules in the regenerated skin: Higher collagen and elastin deposition on hybrid scaffold was due to better cell survival and growth. ECM deposition was proven based on quantification of total collagen, elastin and sGAG as compared to that in normal skin. The untreated wound showed significantly low levels of ECM molecules. NeuSkin treated sample showed significantly higher collagen deposition. Hybrid scaffold treated wounds showed similar deposition as of normal skin (Figure 77).

4.7. Toxicological evaluation of the PLGCFIBHA and AMFIBHA hybrid scaffolds

Intracutaneous (intradermal) reactivity test: The results indicated that PS and cotton seed oil extract of AMFIBHA and PLGCFIBHA hybrid scaffolds induced a total mean score of 0.22 and 0 in physiological saline respectively and 0.33 and 0.89 in cotton seed oil extract respectively following intradermal injection confirming no adverse reaction to the test solutions. In both cases, there was no reduction of body weight seen.

Guinea pig maximization test (GPMT): GPMT did not show any adverse sin reaction during the induction or challenge period and confirmed that PS extract of test materials (AMFIBHA and PLGCFIBHA hybrid scaffolds) is non-irritant at the laboratory conditions simulated. In both cases, there was no reduction of body weight seen.

CHAPTER 5

5. DISCUSSION

The important results of the study that are illustrated in chapter 4 are discussed in this chapter. Major findings of the study are correlated to recently published literature in the relevant field and interpretations are made. The limitations of the study are listed and future prospects are outlined.

5.1. Identification of biomaterials for skin regeneration

The development of effective, affordable and durable techniques for rapid wound closure is a priority for health care systems. Recent advances in tissue engineering using biocompatible materials and cells have led to more complex biological skin equivalents that may yield better treatment options for patients. However, major hurdles involving cell-based tissue engineering and associated cell-based therapies are their complicated regulatory and financial difficulties causing delayed clinical translation and commercialization. Such limitations have led to the quest of non-cellular dermal substitutes for regenerative medical applications in general and skin wound healing application in particular. Such products could be designed to enable migration of cells from neighbouring native tissue and promote cell growth. Primary specification of such products should target minimal immune rejection, be biodegradable- and resorbed by body's natural proteolytic pathways, be easy to apply, promote scar-less healing, stable during storage, and most importantly should be cost effective. Unfortunately, none of the currently available commercial product meets all these properties in a single system. Hence absorbable and non-immunogenic matrix as skin substitute that can guide wound regeneration pose scope in the wound care product market.

This study conceptualized design of a suitable combination scaffold, meeting defined primary requirements and comprising biomimetic matrix for improved cell adhesion/migration supported by a mechanically strong, biocompatible scaffold. Three combination strategies are exploited combining a common biomimetic matrix with different non-immunogenic biomaterials in defined combinations to compensate

for the limitation of each one of them. Fibrin and HA has been identified as the key ingredient for the skin substitutes developed in this study. Fibrin is a critical blood component causing hemostasis, which has been used extensively as soft tissue sealant, drug delivery vehicle and a matrix component for tissue engineering. Fibrin has remarkable skin repair and wound healing properties generating good *milieu* at the site of application (Ahmed *et al.,* 2008, Krishnan *et al.*, 2004). HA is a naturally occurring GAGs present within the skin having important modulating effects on the wound healing (Price *et al.,* 2005, Anilkumar *et al.,* 2009). Fragile and non-pliable nature of fibrin and HA preventing easy positioning on wound bed was identified as a drawback. Therefore, this study exploited the advantages of fibrin and HA to produce user-friendly, cell-free skin substitutes by integrating with human AM, terpolymer PLGC and SF. Other than the wound regeneration potential, combining fibrin with biomaterial scaffolds can offer hemostatic, self-adhesive and suture-less combination products. However, careful selection of biomaterials is essential for preventing adverse effects of materials. So, this study describes three combination products, compensating for the limitation of each of them.

Human AM has been reported to possess remarkable therapeutic potential for wound healing due to its inherent bioactive and biocompatible properties that allow the wound to heal in a much faster and efficient way (Daniel *et al.,* 2006). Moreover, the lyophilized material is found to retain all physical and biological characteristics of the fresh membrane which can be easily processed into a sterile and stable product in dry form and can be stored for longer duration. Despite having these excellent biocompatibility and bioactive nature, the poor mechanical and handling characteristics of AM have limited its clinical use as a standalone product on wounds of different dimensions, thus needing modifications.

Biodegradable terpolymers synthesised using combinations of glycolide (GL) / L-lactide (L-LA) / Ɛ-caprolactone (Ɛ-CL) monomers which are FDA approved are frequently employed for skin tissue engineering. They are biocompatible and possess excellent mechanical properties which can be varied based on requirements by altering their composition. Electrospinning was employed to produce electrospun

scaffold to ensure porosity and 3-D architecture to support dermal tissue generation. The nano and micro architectural fibres of electrospun scaffolds mimic the normal ECM-like architecture of tissue and have properties such as controlled evaporative water loss, oxygen permeability, and enhanced fluid drainage and inter connected pores (Bhattarai *et al.,* 2004, Boudriot *et al.,* 2006). Major limitation of this polymer scaffolds are their hydrophobic nature and lack of cell attachment sites; and therefore requires modification to increase regeneration potential.

SF is a natural biomaterial which has been explored for tissue engineering and regenerative medicine applications due to its excellent biological and mechanical properties. But lack of cell attachment sites is a drawback; therefore, biological modification could produce a better skin substitute.

However, the morphology of all three biomaterial scaffolds is different requiring different protocols for combining with fibrin-HA. The electrospun PLGC mat is highly porous with inter connectivity and therefore, by covering with liquid fibrin-HA, the biomimetic matrix could penetrate into the pores and the fibrin network could get intercalated with the polymer. Both AM and SF are not so porous requiring a sandwiching strategy to combine the scaffolds with fibrin-HA mixture. The pores of AM and SF are not wide enough for free flow of liquid fibrin and thus even cell penetration into the biomaterial compartment of the combination scaffold may be limited. However, the roughness of AM and SF is found to be sufficient for the FIBHA to adhere stably even after lyophilisation.

5.2. Physicochemical properties of the hybrid scaffolds

Deposition of bio mimetic fibrin composite on decellularized AM, electrospun PLGC and SF scaffold was confirmed by analyzing the ATR-IR spectrum of bare components and hybrid scaffolds. The ATR-IR spectral peaks of the bio mimetic fibrin-HA were prominent in hybrid scaffold spectral recording; so, it confirms successful and stable incorporation of bio mimetic fibrin composite matrix on the scaffolds. In AMFIBHA and SFFIBHA, the peaks were mainly of $–NH_2$ stretching

and amine peaks. In the case of PLGCFIBHA, characteristic peaks of PLGC was absent in the hybrid scaffold probably because fibrin composite covered the polymer surface and efficiently masked the spectral characteristics of the polymer as reported earlier for PCL-fibrin hybrid scaffold (Pankajakshan *et al.,* 2008).

Surface topography and porosity analysis using ESEM and micro-CT confirmed porous nature of the hybrid scaffolds developed. Water absorption ability reflects capability of the scaffold for holding aqueous medium which is necessary for the cell growth and wound healing (Luangbudnark *et al.,* 2012). All the hybrid scaffolds exhibited optimum swelling capacity, mainly contributed by the HA component of the bio mimetic matrix. Enormous amount of water can be absorbed by HA and this property of HA produces swelling pressure in ECM and allows rapid diffusion of water-soluble molecules. Decreasing HA during aging imply shrinkage accounting for dried and wrinkled appearance of aged skin (Fleischmajer *et al.,* 1972). HA incorporation can in turn aid healing. In case of AMFIBHA and SFFIBHA hybrid scaffolds, AM and SF also plays a significant role in swelling.

WVTR for an injured skin can range from 279 ± 26 g/m^2/day for first-degree burn to 5138 ± 202 g/m^2/day for a granulating wound (Lamke *et al.,* 1977). Water vapour permeability of scaffold for wound healing should prevent both build-up of exudates and excessive dehydration. It has been recommended that a rate of 2000 - 2500 g/m^2/day would provide an adequate level of moisture without wound dehydration because it falls in the mid-range of loss rates from injured skin (Mi *et al.,* 2001). All hybrid scaffolds showed required WVTR. The bare PLGC showed more WVTR than PLGCFIBHA indicating that FIBHA has penetrated and closed the pores; however, the swelling property of the biodegradable matrix enabled water vapour transmission.

Biodegradation of the scaffold is a desirable prerequisite in tissue engineering endeavours for facilitating natural tissue formation. Ideally, the rate of scaffold biodegradation and the tissue growth may be correlated. The scaffold should provide sufficient mechanical support in the physiological conditions immediately upon implantation. As scaffold degrades, its mechanical strength should be gradually

transferred to the growing tissue such that the integrity of the construct should be maintained *in vivo* (Dong *et al*., 2009). *In vitro* and *in vivo* degradation of the hybrid scaffolds showed biodegradable nature. AMFIBHA and SFFIBHA hybrid scaffold showed significant hydrolytic degradation. Mass loss and molecular weight loss of the PLGCFIBHA hybrid scaffold indicate that they degrade by bulk degradation kinetics as reported for PCL (Lam *et al*., 2007). There was significant *in vivo* reduction in MW of PLGC when analyzed by GPC which is due to polymer chain cleavage. Thus the biomaterial clearance from the wound site with time could pave way for regenerated tissue. However, poor stability of SFFIBHA in *in vitro* tissue engineering was a concern. The observation indicated that the SF degrades too quickly *in vitro* and due to poor porosity of the scaffold, the cells do not penetrate and bridge through ECM deposition. Therefore, the utility of lyophilized SFFIBHA hybrid scaffold for *in vitro* tissue engineering seemed limited due to poor mechanical stability upon suspending in the culture medium.

5.3. Hydrogel system developed for wound healing applications

The water solubility and miscibility of SF with FIBHA was exploited in this study to produce cell encapsulated SFIBHA hydrogels which is stable in the medium. The viability, proliferation and ECM deposition was better when compared to bare SF. Compared to lyophilized SFFIBHA scaffold, hydrogel system showed better stability and excellent cell proliferation due to the intercalation fibrin and SF. The fibroblasts encapsulated and grown in the gel system produced ECM. Co-cultured cells in the hydrogel maintained both fibroblast and EC phenotypes expressing cell-specific markers. Within 15 d of cell culture, the gel seemed degrading with pores seen with naked eyes. Therefore, cell encapsulated gel system is not stable enough for transfer or transplantation. Other than stability, properties like cell growth, phenotype maintenance and ECM deposition was found good. Therefore, it may be suitable for cell transplantation to wound site which needs to be evaluated. The hydrogels can protect the cells from the host immune system and high molecular weight complexes like immunoglobulin. Furthermore, the softness and flexibility rendered by hydrogels reduces the mechanical stress and friction on cells and also on adjacent tissue upon transplantation (Wilson, 2013). Not only that, the highly hydrophilic

nature of hydrogels lead to high water content, providing a tissue like environment to the attached cells . Therefore, potential of SFFIBHA as a cell transplantation vehicle is considered to be high; however, it was not attempted during this study.

5.4. *In vitro* skin tissue engineering efforts

Effort to establish these scaffolds as an off-the-shelf *in vitro* tissue engineering scaffold was attempted using primary fibroblasts. Many research groups have studied skin regeneration using hADMSCs, but only a few have undertaken fibroblastic differentiation of hADMSCs, which resulted in varying stages of success (Lee *et al.,* 2005). Autologous mesenchymal stem cells (MSCs) may be the most favourable source for differentiation into dermal and epidermal lineages due to their non-immunogenic and immune-modulatory properties and multipotency. Human ADMSCs were first identified in progressive osseous heteroplasia patients and their ability to differentiate to multiple lineages was described (Kaplan *et al.,* 1994). MSCs can be easily isolated from adipose tissue, making it an attractive source of stem cells for regenerative applications (Romanov *et al.,* 2003; Schaffler and Buchler, 2007). Schaffler and Buchler (2007) reviewed the clinical implications of tissue engineering in relation to cell-specific differentiation of hADMSCs into adipogenic, chondrogenic, osteogenic, myogenic, cardiomyogenic, neurogenic, pancreatic, hepatic, haematopoietic and ECs. To circumvent disadvantage of hADMSC leading to undesired lineage, pre-differentiation of the cells into dermal fibroblast-like cells is a promising option.

It has been well established that for homing and differentiation, stem cells need a microenvironment which includes different soluble and insoluble biological factors (Watt and Hogan, 2000; Zhang *et al.,* 2011). Most of the differentiation studies employed soluble GFs and cytokines to induce differentiation. Evidence for matrix-directed differentiation of hADMSCs into dermal cells is demonstrated in this study using modified protocol (Unni *et al.,* 2014). So fibrin based biomimetic matrix with GFs was employed for pre-differentiation of hADMSC. The hADMSC - derived fibroblasts populated on scaffolds and important components of ECM including elastic fibres were deposited. hADMSC - derived fibroblasts also

established non-fibrotic phenotype by regulated expression of TGF-β isoforms and α-SMA expression.

5.5. *In vitro* evaluation of the hybrid scaffolds and hydrogel developed

Bio mimetic matrix coating provided biological cues for cell adhesion and also favour migration and proliferation of cells as described earlier (Chen *et al.*, 2005). On analysis of PLGCFIBHA hybrid scaffold seeded with cells appeared that individual polymer fibres in the hybrid scaffold could not be distinguished due to the extended cell spreading on the scaffold surface. This was due to the long term survival of cells on hybrid scaffold and its ability to support tissue generation. Highly porous nature of the electrospun scaffold which allowed oxygen and nutrient exchange into the deeper layers of the scaffold might have enhanced cell viability and adhesion. Sprouting and migration of cells from the scaffold into the culture dish area suggests that upon transplantation, tissue engineered constructs may easily integrate into surrounding tissue.

Collagen and elastin deposition on hybrid scaffold was proportionate to cell survival and growth. However, the SFFIBHA scaffold was not stable in culture and was not found suitable for *in vitro* tissue engineering. In AMFIBHA and PLGCFIBHA hybrid scaffolds cell numbers or ECM content were not doubled by doubling culture period, indicating that after certain growth there is auto-regulation and thereby, fibrotic tendency is limited. This may be due to modulation of cell growth by bio mimetic matrix or media components especially HA. It has been reported that HA can modulate proliferation and cellular activity such as synthesis of collagen by fibroblasts (Mast *et al.*, 1993). The study thus established that both lyophilized AMFIBHA and PLGCFIBHA are suitable as off-the-shelf scaffolds for *in vitro* tissue engineering by seeding autologous or allogenous hADMSC-derived fibroblasts. Depending on the area of skin coverage required, the period of skin tissue construction *in vitro* may vary. Also, regulatory approvals for implantation of *in vitro* engineered constructs may be difficult because even when cells used are autologous, *in vitro* manipulation can make changes in the cell karyotype; therfore, before using the cells for implantation as tissue construct, several safety aspects needs to be

addressed. Therefore, use of cell-free scaffolds for guiding *in vivo* tissue regeneration holds better scope for translational purposes.

5.6. *In vivo* wound healing experiments

The objective of this experiment was to establish suitability of suture-less application of developed hemostatic hybrid scaffolds for guiding regeneration of large-sized (4 x 4 cm^2) wounds. Creating animal models with similar chronic human wound pathology is difficult; therefore large sized wound was used. Compared to total skin area of rabbits and porcine, 16 cm^2 is a reasonable large size wound to be evaluated and ECM in the wound area was completely removed before treatment with test material. Healing of larger wounds demonstrate contribution by the ECM-like properties of hybrid scaffolds causing cell migration and deposition of new collagen and elastin, producing suppleness in the regenerated tissue.

Chronic wounds are burdensome in terms of both the deleterious effects on the patient quality of life and the financial costs associated with their treatment. Wound healing in the human has many unique aspects that depend on the physiology, aging, and regional characteristics. Even though there is considerable biological variation of the wound healing as well as its anatomy, animal models remain the best available alternative to study the complex mechanisms that occur during the wound healing process in a biologically relevant environment. No single animal model is capable of fully recapitulating each clinical scenario considering the heterogeneity and complexity of human chronic wounds, a combination of models may be employed. Full thickness wound model involves the complete removal of epidermis and dermis to the depth of fascial planes or subcutaneous fat. Healing occurs from the margins and the base of the wound by the formation of a fibrin clot that is invaded by granulation tissue and by the migration of an epidermal tongue along the interface between granulation tissue and clot (eschar). The actual wound depth, as in partial thickness wounds, is dependent on species, the mouse having the thinnest skin, while the pig and other large domestic animals having dermis which is as thick as or thicker than that of humans. Healing rates are often monitored on the basis of total excisional volume (or cross-sectional area) filled with granulation tissue

(neodermis), extent of re-epithelialization, histological organization of connective tissue, angiogenesis, and biochemical content of collagen or proteoglycans (Davidson, 1998). This study employed rabbits for studying burn and pigs for diabetic full thickness wound models.

Rabbits are a potentially overlooked, manageable species for wound healing experiments (Wang *et al.*, 2010). By 28 d, in terms of Col-3 expression NeuSkin was just in the early stage whereas both AM-based and PLGC-based scaffolds already was in collagen maturation/reorganization phase. This observation indicates that both these biomaterials integrated FIBHA scaffolds induce wound regeneration at a faster pace and inflammation was also subsided much faster as seen by marker expression. Out of the three lyophilized scaffolds AMFIBHA and PLGCFIBHA promoted elastin deposition also. In terms of angiogenesis marker expressions also, AMFIBHA and PLGCFIBHA showed better performance. Both faster degradation and the GFs and ECM present in AM could be responsible for better regenerative effect of hybrid scaffold based on this natural biomaterial. In the case of PLGCFIBHA the high scaffold porosity even in the initial implantation phase may be permitting improved cell penetration into the 3-D architecture of the scaffold promoting regenerative responses. In the case of SFFIBHA most of the responses are similar to FIBHA alone indicating that there is no added contribution of SF even though it is also a natural protein. It is interesting to note that physical form also contributes to the wound regeneration because in both the SFFIBHA lyophilized scaffold and hydrogel the composition is same but the wound regeneration responses are different.

In histology analysis, both controls did not show any formation of rete pegs and skin appendages whereas, the scaffold treated wounds showed better wound healing with rete pegs and skin appendage formation. The rete pegs are more frequently seen in FIBHA treated wounds suggesting that the biological properties of the composite and its degradation products promote cellular migration and maturation into basal cells. In immunohistochemical analysis, vascular density was in the order AMFIBHA > PLGCFIBHA > SFFIBHA hydrogel > SFFIBHA> NeuSkin > negative control. Collagen organization and elastin deposition was in the order AMFIBHA > PLGCFIBHA ≥ SFFIBHA > SFFIBHA hydrogel >

NeuSkin > negative control. Interestingly, hair follicle like structure was observed in the test treated healed wound which was absent in controls. Large number of micro vessel was also observed in the scaffold transplanted wound, whereas only few micro vessels were observed in the untreated control wound or NeuSkin treated wound. Mechnaical strength evaluated after 56 d also showed similar trend. The mechanical properties was better for test treated than untreated wounds when compared to normal rabbit skin. ECM deposition was also better. Hence all the test material showed effective wound healing in terms of all wound healing parameters as well as re-gaining its mechanical integrity when compared to both the controls.

The most common lesions formed in diabetic wound are those in the lower extremity and the foot, and they are the result of a chronic diabetic state and poor glucose control. However, wound model appropriate for testing diabetic wound healing is not easily available. Pigs have tight skin adherence with thick epidermis and dermis layers, sparse hair, apocrine glands and heal their wounds through re-epithelialization (Seaton *et al.,* 2015). Therefore, diabetic porcine was considered as the closest model for studying diabetic wound healing; however, the exact pathology of human diabetic wound is not expected in this model. Large sized excisional wounds of 4 x 4 cm^2 full thickness wounds was made for applying test materials. In both untreated and NeuSkin treated control wounds, epithelialization was incomplete and rete pegs was not seen. Complete wound epithelialization with collagen deposition, angiogenesis and rete peg formation was observed only in the test treated group (AMFIBHA, PLGCFIBHA & SFFIBHA). In test treated groups, collagen bundles were well organized and the wound was also covered with a continuous epidermis and well-formed basement membrane. The test-treated wounds healed with minimum scarring. The ECM components in the scaffolds could have played a role in the generation of well-structured basement membrane, to regulate keratinocyte differentiation and to normalize epithelial and dermal tissue architecture.

Thus in both burn and diabetic models, hybrid scaffold attached firmly to the bleeding wound without any suture because the blood/body fluid which penetrated into the fibrin reacted with excess thrombin in the scaffold and clotted with the help

of interpenetrating fibrin network. If the scaffold implantation without suturing is intended, chronic wounds may be debrided to generate fresh bleed enabling self-adhesion of haemostatic scaffold to the wound site. The scaffold help in the adherence of cells, protect the wound, and provide the provisional matrix components and a moist environment, until the formation of epidermis. Normally, as the wound is healed the scab gets peeled off. Similarly, in this study scaffold was found to be detached partially from the wound once the wound was healed.

In the international market most of the wound care products available are based on xenogenic acellular collagen. Both porcine and bovine collagen/ gelatin materials are plenty and are used extensively showing wound healing effects clinically. In this study also, a commercially available product Neuskin which is based on bovine collagen was found to have closed the wound in 28 d in burn wounds. However, when the wound tissue regeneration was evaluated the response was very poor as compared to any of the three lyophilized fibrin based products. The collagen organization was slow. There was no rete pegs formation in both the animal models and angiogenesis was low. In porcine model, epithelialization was incomplete and poor in the case of Neuskin applied wounds as compared to fibrin based test materials. Therefore, this study highlights significant difference in terms of wound regeneration upon using the fibrin based products.

Biodegradable polymer based skin substitutes are rarely seen in the market and in clinical use. Two such polymer based products are available internationally but are not being used in India owing to the high cost of the products. Cerafix Dura Substitute (Acera Surgical, St. Louis, MO, USA) is a synthetic, porous polymer matrix composed of electrospun poly (lactic-co-glycolic acid) (PGLA) and poly-p-dioxanone (PDS) that has been FDA-approved for the treatment of dural defects of 12.5 cm^2 or less in area. It is available in sizes ranging from 2.5 x 2.5 cm, up to 10 x 12.5 cm, and may be cut to shape (Schmalz *et al.,* 2018). Suprathel (PolyMedics Innovations GmbH, Germany) is a synthetic copolymer membrane fabricated from a tripolymer of polylactide, trimethylene carbonate, and s-caprolactone. It is used to provide temporary coverage of superficial dermal burns and wounds. Suprathel is covered with gauze and a dressing that is left in place until the wound has healed. It

is FDA approved (Rashaan *et al.*, 2017). The only commercially available fibrin based product is EVARREST which is a fibrin sealant patch indicated for use with manual compression as an adjunct to hemostasis in adult patients undergoing surgery, when control of bleeding by conventional surgical techniques (such as suture, ligature, and cautery) is ineffective or impractical (Matonick *et al.*, 2014).

Suprathel and Cerafix are tripolymer made from FDA approved monomers, consisting mainly lactide which is similar to the synthetic component of PLGC produced in this study. However, Suprathel is indicated for skin and Cerafix is indicated for dural repair. Both these products are purely synthetic product with no biological contribution to wound healing. This study demonstrates advantage of combining degradable polymer with fibrin-HA in regeneration of wounds. No similar products are available in the global market.

Human AM is a unique biomimetic material used for a variety of reconstructive surgical procedures since the early 1900s. There are many AM based products in the market (Brantley *et al.*, 2015, Haugh *et al.*, 2017). The wound healing property of AM has been explored and the decellularized and lyophilized AM has been a major attraction in the wound care industry (Mrugala *et al.*, 2016). AM based products are dehydrated / decellularized / cryopreserved / injectable membranes like Amniograft (BioTissue), Graftjacket, AmnioFix, GraFix (OsirisTherapeutics), EpiFix (MiMedx), AmnioExcel (Derma Sciences), AmnioClear (Liventa Biosciences), Surgenex, Neox (Amniox Medical), Bioplex (NovastepInc), Biovance **(**Alliqua**)** for wound healing. But a combination product is not available. The major reason for the popularity of AM is due to the presence of various inherently present ECM molecules and GFs that are able to promote skin regeneration. Compositions having a combination of specific biological components have been found to exert a number of useful effects in mammalian cells, including modulating TGF signalling, apoptosis, and proliferation of mammalian cells, as well as decreasing inflammation in mice. However, the hemostatic adhesion of AMFIBHA described in this study much superior to the products available in the market. In all aspects of the study, AMFIBHA showed very significant outcome in terms of wound regeneration.

SF-based wound care products can also be used as carriers for delivering drugs, GFs, and bioactive agents to the wound area, while providing appropriate support for complete healing (Wang *et al.*, 2019). Three SF-based medical products have obtained regulatory approval for clinical use in the world: SeriScaffold (Allergan Medical, Inc.) from the U.S. FDA, TymPaSil (CG Bio Inc.) form the Ministry of Food and Drug Safety of South Korea and Sidaiyi (Suzhou Soho Biomaterial Science and Technology Co., Ltd) from the China Food and Drug Administration (CFDA). Of the three SF-based medical products, SeriScaffold is a knitted silk mesh intended for hernia repair; TymPaSil is a SF patch used as a tympanic membrane; but only Sidaiyi, a SF sponge-silicone two-layered scaffold, is indicated for skin wound healing (Zhang *et al.*, 2017). Other SF based products include: fibroheal (Fibroheal Woundcare Pvt. Ltd, Bangalore, India) is a silk protein based surgical wound cover available in different dimensions for wound healing. The SSFIBHA hydrogel developed in the study can be used for injectable cell-delivery system for faster wound healing.

The handling properties and ease of positioning were similar with all three hybrid scaffolds developed in this study. Healing of large size full thickness- diabetic porcine wound was slower as compared to debrided burn wounds. Both burn wounds and diabetic animal wound healed well with epithelialization, dermal regeneration and angiogenesis. In all analysis the efficiency was in the order AMFIBHA > PLGCFIBHA > SFFIBHA lyophilized and hydrogel > NeuSkin > Untreated wounds. Both the AMFIBHA and PLGCFIBHA hybrid scaffolds met the requirements as per ISO-10993-10:2010(E): biological evaluation of medical devices part 10: test for irritation and skin sensitization test clause 6.4: animal intracutaneous reactivity test & USP 38/NF33:2015 and clause 7.5: guinea pig maximization test respectively. Therefore, considering the cost of production and availability PLGCFIBHA could be a more viable option. Product scaling up is also easy. Since fibrin sealant is a pharmacopoeia approved and monomers of PLGC are FDA approved; therefore regulatory approvals could be easier. AMHIBHA production involves more regulatory challenges, large scale collection of placenta may be easier in India but cost of production may be higher as compared to PLGC.

Overall, this study suggests both products can be used in limited clinical trial for donor wound sites and further chronic wounds. Considering the cost : benefit ratio after limited clinical trials, appropriate product may be translated into clinic and commercialized.

5.7. Limitations of the study

The study evaluated post sterilization stability and function of scaffolds for *in vitro* and *in vivo* tissue engineering. However, a breathable package for the product was not designed. Also, scaffolds larger than 16 cm^2 were not evaluated in animals. The *in vitro* tissue engineering was successfully done on AMFIBHA and PLGCFIBHA using hADMSC-derived fibroblasts; however no animal study was conducted to evaluate if engineered dermal construct would perform faster wound regeneration. In the evaluation of the in situ forming hydrogel system for angiogenic potential, hADMSC-derived endothelial progenitor cells (EPCs) could have been cultured instead of HUVEC to improve translational potential. The cell encapsulated SFFIBHA hydrogel seemed to be an excellent system for delivering cells to the wound but no animal experiments were done to evaluate feasibility of cell transplantation using the hydrogel. Study result can be extrapolated to clinical conditions only after chronic wound model is evaluated.

CHAPTER 6

6. SUMMARY AND CONCLUSION

6.1. Summary

Chronic wound healing is compromised in situations like severe burns and diabetic foot resulting in non-healing ulcers which currently has no effective pharmacologic remedy. Principles of regenerative medicine gives a ray of hope in such conditions, which is an emerging technology - based on biomaterials, stem cells or a combination of both. A wide variety of biomaterials are commercially available for wound care which are based on natural materials; mainly xenogenic or allogenic collagen products with or without allogenic cells. Therefore, uses of currently available products are prone to cause immune rejection, which is a major concern in the field of skin regenerative approaches. The use of stem cells alone is another strategy which gives option of using autologous cells thus limiting the immune-rejection. However, stem cells are unlikely to survive in the *milieu* of chronic wounds because of the infection, inflammation and matrix degradation causing lack of cell survival, proliferation and differentiation required for tissue regeneration. Therefore, one potential approach that may be developed is *in vitro* tissue engineering which means having a suitable degradable, non-immunogenic and mechanically strong scaffold with molecules that can support stem cell growth and differentiation resulting a suitable tissue construct for implantation, after long term culture of cells. Another suitable strategy is to develop a biomimetic scaffold that is mechanically compliant with native skin and having biological cues that can mobilize stem cells, keratinocyte precursors, fibroblasts and vascular cells from neighbouring tissue to promote proliferation and differentiation of cells to bridge the gap, heal the epidermal and dermal wound and produce vascularity and thus bringing out continuity of native tissue with regenerated tissue. In the case of *in vitro* tissue engineering, the major problems are requirement of long term culture of cells on

scaffold to produce mechanically strong constructs that can be transplanted by suturing to the wound bed. But since the *in vitro* produced constructs lack proper vascularity, it gets rejected and do not get integrated easily to the surrounding native tissue. Therefore, *in vivo* guided tissue engineering seems more promising for translational purpose. Once the requirements of cell adhesion, proliferation, and maintenance of differentiated cells are met by the physicochemical nature of the scaffold, the cells, including stem cells may migrate from the neighbouring tissue and grow resulting in automatic bridging or integration taking place.

Therefore, this study focused on development of three similar products that can be implanted at wound site without cells to promote the native tissue cells to migrate and regenerate the wound. Here, fibrin and HA was identified as the common biological compartment in all three scaffolds. Fibrin has remarkable skin repair and wound healing properties; whereas, HA has excellent swelling properties and helps cell migration and growth. This study exploited the advantages of fibrin and HA to produce easy to use, off-the shelf, cell-free skin substitutes by integrating with human decellularized AM, electrospun terpolymer PLGC and fabricated-freeze dried SF matrix. The purpose of combining with biomaterial was to reduce the fragile nature of Fibrin-HA wafer. The process of hybridization was expected to impart biological cell growth properties to biomaterials; thus both biological and biomaterial compartments could mutually benefit providing an additive or synergistic property to the hybrid scaffold contributed by both.

The *in vivo* guided tissue engineering scaffolds can function properly only if the *in vitro* cell growth on these is found appropriate with good dermal cell population, stability enhancement supported by ECM deposited by fibroblasts showing regulated non-fibrotic cell survival. Both AMFIBHA and PLGCFIBHA were found to possess all these qualities upon using them as *in vitro* tissue engineering scaffold by growing hADMSC-derived fibroblasts. The tissue constructs made on these scaffolds showed regulated cell growth, collagen/ elastin deposition and were stable for several days in culture. But the third hybrid scaffold SFFIBHA was found to be unstable after 4 - 7 d of culture indicating that cells are not penetrating well into the 3-D architecture of the biomaterial matrix, or enough ECM

is not produced to imbibe stability to the construct. However, considering the properties of water solubility of SF, the biomaterial was integrated with FIBHA to produce an injectable hydrogel with encapsulated dermal fibroblast. This method yielded a stable tissue construct upon long term culture of the encapsulated cells within the hydrogel scaffold

The lyophilized test materials AMFIBHA, PLGCFIBHA and SFFIBHA were compared with untreated / sham (negative control) and commercially available NeuSkin (positive control). All three hybrid scaffolds attached firmly to the bleeding wound in both case of burnt and acute incisions wounds without any help of sutures. This can be due to the interaction of blood/tissue fluids with the excess thrombin present in the scaffold and clotted with the support of interpenetrating fibrin network. In rabbit burn wound histology analysis, both the controls did not show any formation of rete pegs and skin appendages whereas, the scaffold treated wounds showed better wound healing with rete peg and skin appendage formation. The wound healing and regeneration efficiency was in the order AMFIBHA > PLGCFIBHA > SFFIBHA & SFFIBHA hydrogel > NeuSkin (positive control) > Untreated (negative control). Interestingly, hair follicle like structure was observed in the test scaffold treated wound, but was absent in both controls. Mechanical strength and ECM deposition evaluated after 56 d also showed similar trend. In porcine diabetic wounds, complete epithelialization with organized collagen deposition, angiogenesis and rete peg formation was observed only in the test scaffold implanted wounds but not in both negative/positive controls. The test scaffold-treated wounds healed with minimum scarring and a layer of basal cells were seen below the epithelial layer. Thus the common role played by FIBHA in tissue regeneration is evident. Despite wound closure, the inefficiency of collagen matrix based commercial, clinically used product (Neuskin) to promote wound tissue regeneration is also clear. Therefore, the developed hybrid scaffolds score much higher than the commercially available collagen based products. No cells were seeded on the scaffold at the time of implantation; however, the tissue regeneration was complete within 28 d with basal cell layer, vascularity etc., and guided cell migration from the native tissue is indicted which is a remarkable achievement.

6.2. Conclusions

1. Human fibrin was identified as the key component enabling hybridization with three different biomaterial matrices.
2. Human HA was isolated successfully and concentration that produced optimal scaffold swelling was identified.
3. Human AM was processed and characterized into sterile cell-free dry membrane and was hybridized with FIBHA producing hemostatic scaffold with desirable properties for guided tissue engineering.
4. Terpolymer PLGC was synthesised and electrospun into a mechanically strong porous mats and was hybridized with FIBHA producing hemostatic scaffold with desirable properties for guided tissue engineering.
5. SF was processed into lyophilized pellets and SF solutions were prepared; allowing integration with FIBHA to produce lyophilized hemostatic scaffolds.
6. Human ADMSCs were differentiated into non-fibrotic fibroblasts with regulated ECM deposition using a fibrin niche directed approach.
7. Supporting role of the hybrid scaffold for dermal tissue engineering with regulated ECM deposition was proven *in vitro* by long term culture of hADMSC-derived fibroblast.
8. The water solubility and miscibility of SF with FIBHA was exploited to produce stable cell encapsulated SFIBHA hydrogels.
9. Full thickness large sized wounds in rabbit burn and porcine diabetic wound models were shown to regenerate to mature skin with biological and mechanical similarity with native skin.
10. In burn wound healing, and skin tissue regeneration efficiency was in the order AMFIBHA > PLGCFIBHA > SFFIBHA & SFFIBHA hydrogel > NeuSkin (positive control) > Untreated (negative control).
11. In porcine diabetic wound healing, complete wound epithelialization with collagen deposition, angiogenesis and rete peg formation with minimum scarring was observed only in the test scaffold treated group; in both

untreated (negative control) and NeuSkin (positive control) treated control wounds, epithelialization was incomplete and rete pegs was not seen.

12. In both wound models, commercially available bovine collagen-based Neuskin did not produce much regenerative effects, as compared to test materials.
13. AMFIBHA supersedes other two hybrid scaffolds w.r.t wound regeneration potential.
14. Ease of processing : PLGCFIBHA > SFFIBHA > AMFIBHA
15. Availability : PLGCFIBHA > SFFIBHA > AMFIBHA
16. Cost : PLGCFIBHA < SFFIBHA < AMFIBHA
17. Both the AMFIBHA and PLGCFIBHA hybrid scaffolds met the requirements as per ISO-10993-10:2010 (E) standards for biological evaluation of medical devices part 10 for irritation and skin sensitization test.
18. Hydrogel SFFIBHA is a value addition as an injectable or in situ foring matrix for cell delivery which may result in faster wound regeneration.

6.3. Future Perspectives of the study

1. The package design, validation and shelf life studies of both AMFIBHA and PLGCIBHA may be conducted systematically.
2. Cell based therapy may be evaluated in animal model using SFFIBHA as injectable cell delivery system.
3. Since the preclinical evaluation of both AMFIBHA and PLGCFIBHA has shown promising results, regulatory approvals may be taken for limited clinical trial to prove the efficiency of the scaffolds for human wound care.
4. Study of acute wounds that are formed at the donor site during clinical skin grafting is proposed as an ideal site for preliminary evaluation.
5. Once found efficient in acute wounds, the scaffold may be tested in other surgical wounds that are difficult to heal to prove efficiency of guided wound regeneration.
6. In the third stage, limited number of patients may be recruited for testing efficiency of chronic wound regeneration.

7. Once proven the production of hybrid scaffolds may be scaled up and commerciali

BIBLIOGRAPHY

Ahmed TA, Dare EV, Hincke M (2008) Fibrin: a versatile scaffold for tissue engineering applications. *Tissue Eng Part B Rev* 14: 199-215.

Anilkumar TV, Muhamed J, Jose A, Jyothi A, Mohanan PV,Krishnan LK (2011) Advantages of hyaluronic acid as a component of fibrin sheet for care of acute wound. *Biologicals* 39: 81-8.

Ansell DM, Campbell L, Thomason HA, Brass A, & Hardman MJ (2014) A statistical analysis of murine incisional and excisional acute wound models. *Wound repair and regeneration* 22(2): 281-287. doi:10.1111/wrr.12148.

Atala A (2012) Regenerative medicine strategies. *Journal of Pediatric Surgery* 47(1):17–28. doi: 10.1016/j.jpedsurg.2011.10.013.

Baie SH, Sheikh KA (2000) The wound healing properties of Channa striatus-cetrimide cream - tensile strength measurement. *Journal of Ethnopharmacology* 71: 93-100.

Baie SH, Sheikh KA (2000) The wound healing properties of Channa striatus-cetrimide cream- tensile strength measurement. *J Ethnopharmacol* 71(1-2):93.

Balaji S, Vaikunth SS, Lang SA, Sheikh AQ, Lim FY, Crombleholme TM, Narmoneva DA (2012) Tissue-engineered provisional matrix as a novel approach to enhance diabetic wound healing. *Wound Repair Regen* 20: 15-27.

Bazzoni G and Dejana E (2002) Keratinocyte junctions and epidermal barrier. *J cell boil* 156 (6):947-949.

Benson HAE (2011) Skin Structure, Function, and Permeation. *Topical and Transdermal Drug Delivery: Principles and Practice.* John Wiley Sons, Inc. https://doi.org/10.1002/9781118140505.ch1

Bhattarai SR, Bhattarai N, Yi HK, Hwang PH, Cha DI, Kim HY (2004) Novel biodegradable electrospun membrane: scaffold for tissue engineering. *Biomaterials* 25: 2595-602.

Bonnans C, Chou J, & Werb Z (2014). Remodelling the extracellular matrix in development and disease. *Nature reviews. Molecular cell biology* 15(12):786–801. doi:10.1038/nrm3904.

Boudriot U, Dersch R, Greiner A,Wendorff JH (2006) Electrospinning Approaches Toward Scaffold Engineering-A Brief Overview. *Artificial Organs* 30: 785-792.

Brantley JN, & Verla TD (2015) Use of Placental Membranes for the Treatment of Chronic Diabetic Foot Ulcers. *Advances in wound care* 4(9):545–559. doi:10.1089/wound.2015.0634.

Breen A, Mc Redmond G, Dockery P, OBrien T, Pandit A (2008) Assessment of wound healing in the alloxan-induced diabetic rabbit ear model. *J Invest Surg* 21: 261-9.

Briggaman RA, Wheeler CE (1975) The epidermal-dermal junction. *J Invest Dermatol* 65(1):71-84.

Burnouf T, and Radosevich M (2001) Affinity chromatography inthe industrial purification of plasma proteins for therapeuticuse. *J. Biochem. Biophys. Methods* 49:575.

Chan LS (1997) Human skin basement membrane in health and in autoimmune diseases. *Frontiers in Bioscience* 2:343-352.

Chardack W, Brueske D, Santamauro A, Fazekas G (1962) Experimental studies on synthetic substitutes for skin and their use in the treatment of burns. *Ann Surg* 155:127.

Chen G, Sato T, Ohgushi H, Ushida T, Tateishi T,Tanaka J (2005) Culturing of skin fibroblasts in a thin PLGA-collagen hybrid mesh. *Biomaterials* 26: 2559-66.

Chen MF, Zhang M, Wu ZF (2010) Toward delivery of multiple growth factors in tissue engineering. *Biomaterials* 31:24, 6279-6308.

Choi JS, Kim JD, Yoon HS, Cho YW (2013) Full-thickness skin wound healing using human placenta-derived extracellular matrix containing bioactive molecules. *Tissue Eng Part A* 19: 329-39.

Chomczynski Piotr (1993) A Reagent for the Single-step Simultaneous Isolation of RNA, DNA and Proteins from Cell and Tissue Samples. *BioTechniques* 15. 532-4, 536.

Chu DH (2008) Overview of biology, development and structure of skin. *Fitzpatrick's dermatology in general medicine* 7:57-73.

Clark RA, Ghosh K,Tonnesen MG (2007) Tissue engineering for cutaneous wounds. *J Invest Dermatol* 127: 1018-29.

Colazzo F, Chester AH, Taylor PM and Yacoub MH (2010) Induction of mesenchymal to endothelial transformation of adipose-derived stem cells. *Journal of Heart Valve Disease*, 19:6:736–744.

Davidson J (1998) Animal models for wound repair. *Arch Dermatol Res* 290:1:S1. https://doi.org/10.1007/PL00007448.

Diana GS, Hana HH, Ahmed A (2019) Wound healing models: A systematic review of animal and non-animal models. 24:1: 8-17.

Diegelmann RF, Evans MC (2004) Wound healing: an overview of acute, fibrotic and delayed healing. *Front Biosci* 1(9):283-9.

Dietrich Ntoukas T, Hofmann Rummelt C, KruseF E et al. (2012) Comparative analysis of the basement membrane composition of the human limbus epithelium and amniotic membrane epithelium. *Cornea* 31:564-9.

Dimple C, Piyali D, Naresh T, Samit KN, My Hedhammar, Biman BM (2019) Silkworm Silk Matrices Coated with Functionalized Spider Silk Accelerate Healing of Diabetic Wounds. *Biomater Sci Eng* .2019573537-3548 https://doi.org/10.1021/acsbiomaterials.9b00514.

Din S (2017) Non-animal models of wound healing in cutaneous repair: in silico, in vitro, ex vivo, and in vivo models of wounds and scars in human skin. *Wound Repair Regen* 25:164-176, 10.1111/wrr.12513.

Dominici M, Le Blanc K, Mueller I (2006) Minimal criteria for defining multipotent mesenchymal stromal cells.*Cytotherapy* 8: 315–317.

Douglas MPM et al.,(1993) Cellular origin of the dermal-epidermal basement membrane. *Developmental Dynamics* 197:4:255–267.

Dusko Ilic, Ljiljana Vicovac, Milos Nikolic, Emilija Lazic Ilic (2016) Human amniotic membrane grafts in therapy of chronic non-healing wounds. *British Medical Bulletin* 117:1:59-67. https://doi.org/10.1093/bmb/ldv053.

ElHeneidy H, Omran E, Halwagy A, AlInany H, AlAnsary M, Gad A (2016) Amniotic membrane can be a valid source for wound healing. *Int J Womens Health* 8:225-31. doi:10.2147/IJWH.S96636.

Enoch S, Grey JE,Harding KG (2006) Recent advances and emerging treatments. *BMJ* 332: 962-5.

Fleischmajer R, Perlish JS,Bashey RI (1972) Human dermal glycosaminoglycans and aging. *Biochem Biophys Acta* 279: 265-75.

Flick MJ, Du X,Degen JL (2004) Fibrin(ogen)-alpha M beta 2 interactions regulate leukocyte function and innate immunity in vivo. *Exp Biol Med* 229: 1105-10.

Franco R, Nguyen T, Lee BT (2011) Preparation and characterization of electrospun PCL/PLGA membranes and chitosan/gelatin hydrogels for skin bioengineering applications. *Journal of Materials Science: Materials in Medicine* 22: 2207-2218.

Frese L, Dijkman PE, Hoerstrup SP (2016) Adipose Tissue-Derived Stem Cells in Regenerative Medicine. *Transfus Med Hemother* 43(4):268-274.

Gajiwala K, Gajiwala AL (2004) Evaluation of lyophilized, gamma-irradiated amnion as a biological dressing. *Cell Tissue Bank.*

Garoufalis M, Nagesh D, Sanchez PJ, Lenz R, Park SJ, Ruff JG, Tien A, Goldsmith J, Seat A (2018) Use of dehydrated human amnion/chorion membrane allografts in more than 100 patients with six major types of refractory nonhealing wounds. *J Am Podiatr Med Assoc* 108(2):84-89. doi: 10.7547/17-039.

Griffiths M, Ojeh N, Livingstone R, Price R,Navsaria H (2004) Survival of Apligraf in acute human wounds. *Tissue Eng* 10: 1180-95.

Gunatillake PA,Adhikari R (2003) Biodegradable synthetic polymers for tissue engineering. *Eur Cell Mater* 5: 1-16.

Haugh AM, Witt JG, Hauch A, Darden M, Parker G, Ellsworth WA, & Buell JF (2017) Amnion Membrane in Diabetic Foot Wounds: A Meta-analysis. *Plastic and reconstructive surgery. Global open 5*(4):e1302. doi:10.1097/GOX.0000000000001302.

Horan JT and Francis CW (2001) Fibrin degradation products,fibrin monomer and soluble fibrin in disseminated intravascular coagulation. *Semin Thromb Hemost.* 27:657.

Irena P, Liang L, Andrew PS, Wikramanayake TC et al. (2018) Preclinical models for wound-healing studies.*Skin tissue models* Elsevier BV.

Jaffe EA, Nachman RL, Becker CG, Minick CR (1973) Culture of human endothelial cells derived from umbilical veins. Identification by morphologic and immunologic criteria. *J Clin Invest* 52:2745–2756. doi: 10.1172/JCI107470.

Jaianand K et al. (2017) Amniotic membrane as a scaffold in wound healing and diabetic foot ulcer: an experimental technique and recommendations. *International Journal of Research in Medical Sciences* 4:8:3654-3660. doi:http://dx.doi.org/10.18203/2320-6012.ijrms20162206.

James WD, Berger TG, Elston DM (2006) Andrews diseases of the skin: Clinical dermatology (10th ed.): Philadelphia: Elsevier Saunders.

Jansen LH, Rottier PB (1958) Comparison of the mechanical properties of strips of human abdominal skin excised from below and from above the umbilic. *Dermatology* 117: 252-258.

Kanczler JM, Barry J, Ginty P, Howdle SM, Shakesheff KM, Oreffo RO (2007) Supercritical carbon dioxide generated vascular endothelial growth factor encapsulated poly(DL-lactic acid) scaffolds induce angiogenesis in vitro. *Biochem Biophys Res Commun* 5;352(1):135-41.

Kanitakis J (2002) Anatomy, histology and immunohistochemistry of normal human skin. *Eur J Dermatol* 12(4):390-9.

Kaplan FS, Hahn GV, Zasloff MA (1994) Heterotopic ossification: two rare forms and what they can teach us. *J Am Acad Orthop Surg* 2: 288–296.

Kaye Mag, Stacey M (1951) Chemistry of tissues; methylation studies on hyaluronic acid. *Biochem J* 48: 249–255.

Kolarsick PAJ, Kolarsick MA, Goodwin C (2011) Anatomy and Physiology of the Skin. Dermatology Nurses' Association 3(4):1-11.

Koster A, Sanger S, Knorig FJ, Kuppe H, Hetzer R and Loebe M (2002) Autologous plasma and platelet sequestrationat the beginning of cardiopulmonary bypass: a pilot investigationin five patients undergoing extended vascular surgeryin deep hypothermia. *ASAIO J* 48:106.

Kotler EV, Sharma V, Kang VN, and Gareta EG (2018) A universal classification system of skin substitutes inspired by factorial design. *Tissue Engineering Part B: Reviews* 24:4. http://doi.org/10.1089/ten.teb.2017.0477

Krishnan LK, Mohanty M, Umashankar PR,Vijayan Lal A (2004) Comparative evaluation of absorbable hemostats: advantages of fibrin-based sheets. *Biomaterials* 25: 5557-5563.

Kubo M, Sonoda Y, Muramatsu R, Usui M (2001) Immunogenicity of human amniotic membrane in experimental xenotransplantation. *Invest Ophthalmol Vis Sci* 42(7):1539-46.

Kumar TR, Krishnan LK (2002) A stable matrix for generation of tissue-engineered nonthrombogenic vascular grafts. *Tissue Eng* 8: 763-70.

Kumar V, Khan A, Nagarajan K (2013) Animal Models for the Evaluation of Wound Healing Activity. 3. 93-107.

Kumbar SG, Nukavarapu SP, James R, Nair LS, Laurencin CT (2008) Electrospun poly(lactic acid-co-glycolic acid) scaffolds for skin tissue engineering. *Biomaterials* 29: 4100-7.

Kumbar SG, Nukavarapu SP, James R, Nair LS, Laurencin CT (2008) Electrospun poly(lactic acid-co-glycolic acid) scaffolds for skin tissue engineering. *Biomaterials* 29: 4100-7.

Kundu B, Rajkhowa R, Kundu S & Wang X(2012) Silk fibroin biomaterials for tissue regeneration. *Advanced drug delivery reviews.* 65. 10.1016/j.addr.2012.09.043.

Lamke LO, Nilsson GE,Reithner HL (1977) The evaporative water loss from burns and the water-vapour permeability of grafts and artificial membranes used in the treatment of burns. *Burns* 3: 159-165.

Lammers G, Pauline DHM Verhaegen, Magda M.W. Ulrich, Joost Schalkwijk, Esther Middelkoop, Daniela Weiland, Suzan T.M. Nillesen, Toin H. Van Kuppevelt, and Willeke F. Daamen (2011) An Overview of Methods for the In Vivo Evaluation of Tissue-Engineered Skin Constructs. *Tissue Engineering Part B* 17:1.http://doi.org/10.1089/ten.teb.2010.0473

Langer R,Vacanti JP (1993) Tissue engineering. *Science* 260: 920-6.

Laurens N, Koolwijk P, Maat PMP DE (2006) Fibrin structure and wound healing. *Journal of Thrombosis and hemostasis* 4:5:932-39.

Leblond CP, Inoue S (1989) Structure, composition, and assembly of basement membrane. *Am J Ana* 185(4):367-90.

Lee JA, Conejero JA, Mason JM, Parrett BM, Wear-Maggitti KD, Grant RT,Breitbart AS (2005) Lentiviral transfection with the PDGF-B gene improves diabetic wound healing. *Plast Reconstr Surg* 116: 532-8.

Lee KO, Kim SN, Kim YC (2014) Anti-wrinkle effects of water extracts of teas in hairless mouse. *Toxicol Res* 30:283-289. 10.5487/TR.2014.30.4.283.

Lee PY, Chesnoy S,Huang L (2004) Electroporatic delivery of TGF-beta1 gene works synergistically with electric therapy to enhance diabetic wound healing in db/db mice. *J Invest Dermatol* 123: 791-8.

Lesher AP et al., (2011) Effectiveness of Biobrane for treatment of partial-thickness burns in children. *J Pediatr Surg* 46 (9): 1759–1763.doi: 10.1016/j.jpedsurg.2011.03.070.

Li J, Chen J, Kirsner R (2007) Pathophysiology of acute wound healing.*Clinics in Dermatology*. 25: 9 – 18.

Li WJ, Laurencin CT, Caterson EJ, Tuan RS,Ko FK (2002) Electrospun nanofibrous structure: a novel scaffold for tissue engineering. *J Biomed Mater Res* 60: 613-21.

Litwiniuk M, Krejner-Bienias A, S Speyrer M, Gauto A, Grzela T (2016) Hyaluronic Acid in Inflammation and Tissue Regeneration.*Wounds : a compendium of clinical research and practice* 28. 78-88.

Lobmann R, Ambrosch A, Schultz G, Waldmann K, Schiweck S, Lehnert H (2002) Expression of matrix-metalloproteinases and their inhibitors in the wounds of diabetic and non-diabetic patients. *Diabetologia* 45: 1011-6.

Luangbudnark W,Viyoch J, Laupattarakasem W, Surakunprapha P,Laupattarakasem P (2012) Properties and biocompatibility of chitosan and silk fibroin blend films for application in skin tissue engineering. *ScientificWorld Journal* 697201.

Ma L, Gao C, Mao Z, Zhou J, Shen J, Hu X,Han C (2003) Collagen/chitosan porous scaffolds with improved biostability for skin tissue engineering. *Biomaterials* 24: 4833-41.

MacNeil S (2007) Review article progress and opportunities for tissue-engineered

Maja Olsson RN, Krister Järbrink, Ushashree Divakar, Ram Bajpai, Zee Upton, Artur Schmidtchen MD, Josip CaR (2018) The humanistic and economic burden of chronic wounds: A systematic review. *Wound Repair and Regeneration* 27:1:114-125. https://doi.org/10.1111/wrr.12683.

Mast BA, Schultz GS (1996) Interactions of cytokines, growth factors, and proteases in acute and chronic wounds. *Wound Repair and Regeneration* 4: 411-420.

Matonick JP, Hammond J (2014) Hemostatic efficacy of EVARREST™, Fibrin Sealant Patch vs. TachoSil® in a heparinized swine spleen incision model. *J Invest Surg* 27(6):360-5. doi: 10.3109/08941939.2014.941444.

McGrath JA and Uitto J (2010) Anatomy and organisation of human skin. *burns*. Rooks

McLafferty E, Hendry C and Alistair F (2012) The integumentary system: anatomy, physiology and function of skin. Nursing standard (Royal College of Nursing (Great Britain): 1987)27. 35-42. 10.7748/ns2012.09.27.3.35.c9299.

Meaume S (2002) Chronic wound scars *Wound Repair and Regeneration*. 10(2):103–106.

Metcalfe AD, Ferguson MW (2007) Tissue engineering of replacement skin: the crossroads of biomaterials, wound healing, embryonic development, stem cells and regeneration. *J R Soc Interface* 4: 413-37.

Mi FL, Shyu SS, Wu YB, Lee ST, Shyong JY, Huang RN (2001) Fabrication and characterization of a sponge-like asymmetric chitosan membrane as a wound dressing. *Biomaterials* 22: 165-173.

Michel D, Harmand MF (1990) Fibrin seal in wound healing: effect of thrombin and [Ca2+] on human skin fibroblast growth and collagen production. *J Dermatol Sci* 1:5:325-33.

Mohammed HK, Hanan J, Abdalla A (2016) Synthetic Biomaterials for Skin Tissue Engineering. *Skin Tissue Engineering and Regenerative Medicine* Elsevier BV.

Mrugala A, Sui A, Plummer M, Altman I, Papineau E, Frandsen D, Hill D, Ennis WJ (2016) Amniotic membrane is a potential regenerative option for chronic non-healing wounds:a report of five cases receiving dehydrated human amnion/chorion membrane allograft. *Int Wound J* 13:485–492.

Muguregowda Honnegowda, Thittamaranahalli & Kumar, Pramod & Udupa, Padmanabha & Rao, Pragna. (2018). Epidemiological study of burn patients hospitalised at a burns centre, Manipal. *International Wound Journal* 16. 10.1111/iwj.12995.

Murphy GF (1997) Histology of the skin: Levers histopathology of the skin: Philadelphia: Lippincott Williams & Wilkins 8: 5-45.

muscle cells into a biodegradable, elastomeric fiber matrix. *Biomaterials* 27: 735-44.

Nayak S, Nalabothu P, Sandiford S, Bhogadi V, Adogwa A (2006) Evaluation of wound healing activity of Allamanda cathartica. L. and Laurus nobilis. L. extracts on rats. *BMC Complementary and Alternative Medicine* 6: 12.

Nunery WR (2001) Risk of prion transmission with the use of xenografts and allografts in surgery. *Ophthal Plast Reconstr Surg* 17:389-394.

Padol AR., Jayakumar K, Shridhar NB, Narayana Swamy HD, Narayana Swamy M., and Mohan K (2011) Safety evaluation of silk protein film (a novel wound healing agent) in terms of acute dermal toxicity, acute dermal irritation and skin sensitization. *Toxicology international* 18(1):17–21. doi:10.4103/0971-6580.75847.

Pankajakshan D, Philipose LP, Palakkal M, Krishnan K,Krishnan LK (2008) Development of a fibrin composite-coated poly(epsilon-caprolactone) scaffold for potential vascular tissue engineering applications. *J Biomed Mater Res B Appl Biomater* 87: 570-9.

Pham QP, Sharma U, Mikos AG (2006) Electrospun poly(ε-caprolactone) microfiber andmultilayer nanofiber/microfiber scaffolds: characterization of scaffolds and measurement of cellular infiltration. *Biomacromolecules* 7: 2796-805.

Prasad Chennazhy, Krishnan LK (2005) Effect of passage number and matrix characteristics on differentiation of endothelial cells cultured for tissue engineering. *Biomaterials* 26: 5658-5667.

Price RD, Berry MG, Navsaria HA (2007) Hyaluronic acid: the scientific and clinical evidence. *Journal of Plastic, Reconstructive & Aesthetic Surgery* 60: 1110-1119.

Prodicimi M, Bevilacqua C (2012) Exogenous hyaluronic acid and wound healing: an up-dated vision. *Panminerva Med* 54 : 129-135.

Rashaan ZM, Krijnen P, Allema JH, Vloemans AF, Schipper IB, & Breederveld RS (2017) Usability and effectiveness of Suprathel® in partial thickness burns in children. *European journal of trauma and emergency surgery : official publication of the European Trauma Society*, *43*(4), 549–556. doi:10.1007/s00068-016-0708-z.

Rashmi R, Amita Ajit, Santhosh KR, Manesh S, Lissy KK (2020) Generation of niche tuned anti-fibrotic fibroblasts and nonviral mediated endothelial commitment using adipose stem cells for dermal graft development. *J Biomed Mater Res B* 1-13. DOI: 10.1002/jbm.b.34611.

Rashmi R, Harikrishnan VS, Arya A, Sabareeswaran A, Prashanth V, Manesh S, Lissy KK(2020) Human derived scaffold components and stem cells creating immuno-compatible dermal tissue ensuing regulated non-fibrotic cellular phenotypes. *ACS Biomater Sci Eng* 6: 2740−2756. DOI.org/10.1021/acsbiomaterials.9b01961.

Rashmi R, Lissy KK, Renjith PN, Kalliyanakrishnan V (2019) Reinforcement of amniotic membrane with fibrin coated poly-[Lactide-co-Glycolide-co-Caprolactone] terpolymer containing silver nanoparticles for potential wound healing applications. *Int J Polym Mater* 69(12):810-819, DOI:10.1080/00914037.2019.1626388.

Rashmi R, Mohanan PV, Lissy KK (2020) Potential Skin Substitute of Biomimetic Proteins and Terpolymer with Proven Immuno-Compatible and Biodegradable Properties. *Paripex- Indian Journal of Research* 9(2):140-141. DOI : 10.36106/paripex.

Resmi KR, Krishnan LK (2002) Protease action and generation of β-thromboglobulin-like protein followed by platelet activation. *Thromb Res* 107: 23–29.

Rheinwald JG,Green H (1975) Serial cultivation of strains of human epidermal keratinocytes: the formation of keratinizing colonies from single cells. *Cell* 6: 331-43.

Romanov YA, Svintsitskaya VA, Smirnov VN (2003) Searching for alternative sources of postnatal human mesenchymal stem cells:candidate MSC-like cells from umbilical cord. *Stem Cells* 21: 105–110.

Roy S, Biswas S, Khanna S, Gordillo S, Bergdall V, Green J, Marsh CB, Gould LJ, Sen CK (2009) Characterization of a preclinical model of chronic ischemic wound *Physiol. Genomics* 211-224. 10.1152/physiolgenomics.90362.2008.

Sahoo S, Ang LT, Goh JC, Toh SL (2010) Growth factor delivery through electrospun nanofibers in scaffolds for tissue engineering applications. *J Biomed Mater Res* A 93: 1539-50.

Schaffler A, Buchler C (2007) Concise review:adipose tissue-derived stromal cells – basic and clinical implications for novel cell based therapies. *Stem Cells* 25: 818–827.

Schmalz P, Griessenauer C, Ogilvy CS, & Thomas AJ (2018) Use of an Absorbable Synthetic Polymer Dural Substitute for Repair of Dural Defects: A Technical Note. *Cureus 10*(1), e2127. doi:10.7759/cureus.2127.

Schreiter J, Meyer S, Schmidt C, Schulz RM, Langer S (2017) Dorsal skinfold chamber models in mice *Interdiscip Plast Reconstr Surg* 6 : 10.3205/iprs000112.

Schrementi ME, Ferreira AM, Zender C, DiPietro LA (2008) Site-specific production of TGF-beta in oral mucosal and cutaneous wounds. *Wound Repair Regen* 16(1):80-6.

Schultz GS, Ladwig G, Wysocki A (2005) Extracellular matrix: review of its roles in acute and chronic wounds. Worldwide wounds.

Seaton M, Hocking A, Gibran NS (2015) Porcine models of cutaneous wound healing *ILAR J* 56:127-138. 10.1093/ilar/ilv016.

Shevchenko RV, James SL, James SE (2010) A review of tissue-engineered skin bioconstructs available for skin reconstruction. *J R Soc Interface* 7: 229-58.

Shivakumar K, Nair RR,Valiathan MS (1992) Paradoxical effect of cerium on collagen synthesis in cardiac fibroblasts. *J Mol Cell Cardiol* 24: 775-80.

Silver FH, Wang MC, and Pins GD (1995) Preparation offibrin glue: a study of chemical and physical methods. *J. Appl. Biomater* 6:175.

Singer AJ,Clark RA (1999) Cutaneous wound healing. *N Engl J Med* 341: 738-46.

Sivamuthu TC (2019) Epidemiological study of 100 cases of burn injuries. *Int Surg J* 6:(2):428-431. DOI: http://dx.doi.org/10.18203/2349-2902.isj20190025.

Spotnitz WD, Mintz PD, Avery N, Bithell TC, Kaul S, and Nolan SP (1987) Fibrin glue from stored human plasma An inexpensive and efficient method for local blood bank preparation. *Am Surg* 53, 460.

Sreerekha PR, Menon D, Nair SV,Chennazhi KP (2013) Fabrication of electrospun poly (lactide-co-glycolide)-fibrin multiscale scaffold for myocardial regeneration in vitro. *Tissue Eng Part A* 19: 849-59.

Srisa-ard M, Molloy R, Molloy N, Siripitayananon J and Sriyai M (2001) Synthesis and characterization of a random terpolymer of L-lactide, -caprolactone and glycolide *Polym Int* 50:891-896. DOI:10-1002/pi.713.

Stankus JJ, Guan J, Fujimoto K, Wagner WR (2006) Microintegrating smooth muscle *Biomaterials* 27(5):735-44. DOI: 10.1016/j.biomaterials.2005.06.020.

Starcher B, Aycock RL, Hill CH (2005) Multiple roles for elastic fibers in the skin. *J Histochem Cytochem* 53(4)431-43.

Sundaramurthi, D, Uma MK, and Swaminathan S (2014) Electrospun Nanofibers as Scaffolds for Skin Tissue Engineering. *Polymer Reviews* 54:2, 348-376, DOI: 10.1080/15583724.2014.881374.

Swaim SF, Hinkle SH, Bradley DM (2001) Wound contraction: basic and clinical factors. *Compend contin educ pract* 23:20-24.

Takeuchi Y, Ueno K, Mizoguchi T, Samura M, Harada T, Oga A, Murata T, Hosoyama T, Morikage N, Hamano K (2017) Development of novel mouse model of ulcers induced by implantation of magnets. *Sci. Rep*. 7:10.1038/s41598-017-05250-y.

Thakur R, Nitika J, Raghvendra P, and Sardul SS (2011) Practices in wound healing studies of plants. *Evidence-based complementary and alternative medicine* 438056:17.https://doi.org/10.1155/2011/438056.

Tobin DJ (2006) Biochemistry of human skin-our brain on the outside. *Chemical Society Reviews.* 35(1): 52-67.

Trengove NJ, Stacey MC, Macauley S, Bennett N, Gibson J, Burslem F, Murphy G,Schultz G (1999) Analysis of the acute and chronic wound environments: the role of proteases and their inhibitors. *Wound Repair and Regeneration* 7: 442-452.

Unnikrishnan S, Jayakumar K, Krishnan LK (2014) Matrix-directed differentiation of human adipose-derived mesenchymal stem cells to dermal-like fibroblasts that produce extracellular matrix. *Journal of tissue engineering and regenerative medicine*. https://doi.org/10.1002/term.1865.

Venetia L and Elena P (2009) Amniotic membrane use in dermatology. *International Journal of Dermatology* 48:935-940.

Verhaegen PD, van Zuijlen, PP, Pennings, NM, et al (2009) Differences in collagen architecture between keloid, hypertrophic scar, normotrophic scar, and normal skin: An objective histopathological analysis. *Wound Repair Regen* 17:649.

Vig K, Chaudhari A, Tripathi S, Dixit S, Sahu R, Pillai S, Singh SR(2017) Advances in Skin Regeneration Using Tissue Engineering. *International journal of molecular sciences* 18(4):789. doi:10.3390/ijms18040789.

Wang J,Wan R, Mo Y, Zhang Q, Sherwood LC, Chien S (2010) Creating a long-term diabetic rabbit model. *Exp Diabetes Res* 10.1155/2010/289614.

Wang Q, Han G, Yan S, & Zhang Q (2019) 3D Printing of Silk Fibroin for Biomedical Applications. *Materials (Basel, Switzerland) 12*(3):504. doi:10.3390/ma12030504.

Watt FM, Hogan BL (2000) Out of Eden:stem cells and their niches. *Science* 287: 1427–1430.

William J Lindblad (2008) Considerations for selecting the correct animal model for dermal wound-healing studies. *Journal of Biomaterials Science* Polymer Edition, 19:8, 1087-1096, DOI: 10.1163/156856208784909390.

Wilson JL, & McDevitt TC (2013) Stem cell microencapsulation for phenotypic control, bioprocessing, and transplantation. *Biotechnology and bioengineering* 110(3):667–682. doi:10.1002/bit.24802.

Wood FM, Stoner ML, Fowler BV, Fear MW (2007) The use of a non-cultured autologous cell suspension and Integra dermal regeneration template to repair full-thickness skin wounds in a porcine model: a one-step process. *Burns* 33: 693-700.

Wooldridge M, Surveyer JA (2000) Skin grafting for full-thickness burn injury. *Am J Nurs* 80(11):2000-4.

Yin A, Zhang K, McClure MJ, Huang C, Wu J, Fang J, Mo X, Bowlin GL, Al-Deyab SS,El-Newehy M (2013) Electrospinning collagen/chitosan/poly(L-lactic acid-co-epsilon-caprolactone) to form a vascular graft: mechanical and biological characterization. *J Biomed Mater Res A* 101: 1292-301.

Zhang H, Dai S, Bi J (2011) Biomimeticthree-dimensional microenvironment for controlling stem cell fate. *Interface Focus* 1: 792–803.

Zhang W, Chen L, Chen J, Wang L, Gui X, Ran J, Xu G, Zhao H, Zeng M, Ji J, Qian L, Zhou J, Ouyang H, Zou X (2017) Silk Fibroin Biomaterial Shows Safe and Effective Wound Healing in Animal Models and a Randomized Controlled Clinical Trial. *Adv Healthc Mater* 6(10). doi: 10.1002/adhm.201700121

Zhu Y, Liu T, Song K, et al. (2008) Adipose-derived stem cell: a better stem cell than BMSC. *Cell Biochem Funct* 26: 664–675.

Zuk PA, Zhu M, Ashjian P, de Ugarte DA, Huang JI, Mizuno H, Alfonso ZC, Fraser JK, Benhaim P, Hedrick MH (2002) Human adipose tissue is a source of multipotent stem cells. *Mol Biol Cell* 13:4279-4295.

LIST OF PUBLICATIONS

1. Rashmi Ramakrishnan, Harikrishnan V S, Arya Anil, Sabareeswaran A, Prashanth Varkey, Manesh Senan, Lissy K. Krishnan. Human derived scaffold components and stem cells creating immuno-compatible dermal tissue ensuing regulated non-fibrotic cellular phenotypes. *ACS Biomaterial Science and Engineering*. 2020 : 6 : 2740 - 2756. DOI.org/10.1021/acsbiomaterials.9b01961 (IF - 4.5).

2. Rashmi Ramakrishnan, Amita Ajit, SanthoshKumar Retnabai, Manesh Senan, Lissy Krishnan. Generation of niche tuned anti-fibrotic fibroblasts and nonviral mediated endothelial commitment using adipose stem cells for dermal graft development. *Journal of Biomedical Materials Research: Part B - Applied Biomaterials*. 2020: 1-13. DOI: 10.1002/jbm.b.34611 (IF - 2.8).

3. Rashmi Ramakrishnan, Mohanan PV, Lissy K. Krishnan. Potential Skin Substitute of Biomimetic Proteins and Terpolymer with Proven Immuno-Compatible and Biodegradable Properties. *Paripex- Indian Journal of Research*. 2020: 9(2):140-141. DOI : 10.36106/paripex (SIF - 6.9).

4. Rashmi Ramakrishnan, Lissy K. Krishnan, Renjith P. Nair & V. Kalliyana Krishnan. Reinforcement of amniotic membrane with fibrin coated poly-[Lactide-co-Glycolide-co-Caprolactone] terpolymer containing silver nanoparticles for potential wound healing applications. *International Journal of Polymeric Materials and Polymeric Biomaterials.* 69(12):810-819. DOI:10.1080/00914037.2019.1626388 (IF - 2.2).

MANUSCRIPTS UNDER COMMUNICATION & PREPARATION

Rashmi Ramakrishnan, Harikrishnan VS, Arya Anil, Sabareeswaran A, Lissy K. Krishnan. Combination scaffold comprising amniotic membrane-hyaluronic acid-fibrin sealant regenerates large full-thickness rabbit burn wounds upon single application.

Rashmi Ramakrishnan, Kalliyana Krishnan V, Harikrishnan VS, Aishwarya Lekshman, Sabareeswaran A, Lissy K. Krishnan. Biodegradable and hemostatic skin substitute of biomimetic proteins deposited on terpolymer for *in vivo* large full-thickness rabbit burn wound regeneration.

Rashmi Ramakrishnan, Dimple Chouhan, Harikrishnan VS, Arya Anil, Sabareeswaran A, Biman Mandel, Lissy K. Krishnan. Silk fibroin-fibrin-hyaluronic acid based skin graft for guided regeneration of rabbit full-thickness burn wounds.

Rashmi Ramakrishnan, Dimple Chouhan, Harikrishnan VS, Arya Anil, Sabareeswaran A, Biman Mandel, Lissy K. Krishnan. Hemostatic *in situ* forming silk fibroin-fibrin-hyaluronic acid based hydrogel system for functional and guided regeneration of full-thickness burn wounds in rabbits.

Rashmi Ramakrishnan, Sachin J Shenoy, Dimple Chouhan, Arya Anil, Kalliyana Krishnan V, Sabareeswaran A, Biman Mandel, Lissy K. Krishnan. Comparative study of different biomimetic acellular skin substitutes for functional and guided regeneration of full-thickness diabetic porcine wounds.

PATENTS APPLIED

1. Rashmi Ramakrishnan & Lissy Kalliyana Krishnan; An absorbable skin substitute with a combination matrix of Amnion, Fibrin and Hyaluronic acid (AMFIBHA) for wound regeneration and the process there of. (Complete Specification File No: 201841038669; Ref No: IPTRU120.Y18).

2. Rashmi Ramakrishnan, Lissy Kalliyana Krishnan, Dimple Chouhan & Biman Behari Mandel; A porous injectable freeze-dried hydrogel scaffold for aiding dermal regeneration and the process there of. (Complete Specification File No: 201941022982; Ref No: IPTRU121.Y18).

CONFERENCES PAPERS & PROCEEDINGS

1. R. Rashmi, K. V, P. Varkey, L. K. Krishnan. Biomimetic combination graft of amnion, fibrin and PLGC for accelerated burn wound healing. 29th Annual Meeting of the Wound Healing Society, SAWC-Spring/WHS Joint Meeting: San Diego Convention Center, San Diego, California, USA, April 5–9, 2017. ***Wound Repair and Regeneration***. 25: A1–A47. DOI:10.1111/wrr.12573.
2. R. Rashmi, V. S. Harikrishnan, V. Prashanth, L. K. Krishnan. Combination of Amnion and Fibrin as a Potential Hybrid Matrix for Guided Wound Regeneration Applications. ***Tissue Engineering Part A***. December 2017, 23(S1): S-1-S-159.
3. R. Rashmi, V. K. Krishnan, V. S. Harikrishnan, L. K. Krishnan. Hybrid Degradable Scaffold supports Functional Skin Tissue Generation upon Seeding Adipose Derived Mesenchymal Stem Cells committed to Dermal Lineage. ***Tissue Engineering Part A***. December 2017, 23(S1): S-1-S-159.
4. Rashmi R, Harikrishnan VS, Lissy K Krishnan. Development of a novel human tissue derived skin substitute and its preclinical evaluation in animal wound models. ***Best paper award category - Proceedings of 31st Kerala Science Congress (KSC)***, Fatima Mata National College, Kollam, Kerala, India.
5. Rashmi R, Prashanth Varkey, Lissy K Krishnan. Novel amnion-fibrin matrix for accelerated and guided burn wound regeneration. Poster - ***Proceedings of national seminar on frontiers in biotechnology- molecular, epigenetic and genomic research platforms in healthcare and food security***, Inter University Centre for Genomics Gene Technology, Kariavattom Campus, University of Kerala, India.
6. Rashmi R, Lissy K Krishnan and Kalliyana Krishnan V. Novel terpolymer supported biological membrane scaffold for dermal burn wound applications. ***Best paper award category - Proceedings of 29th Kerala Science Congress (KSC)***, Thiruvalla, Pathanamthitta, Kerala, India.

CURRICULUM VITAE

Ph.D. Scholar (August, 2016 - 2020) at Biomedical Technology Wing, Sree Chitra Tirunal Institute for Medical Sciences and Technology (SCTIMST), Thiruvananthapuram, Kerala - 695012, India.

Master of Philisophy (M.Phil) in Biomedical Technology (2014 - 2015) at Sree Chitra Tirunal Institute for Medical Sciences and Technology (SCTIMST), Thiruvananthapuram, Kerala - 695012, India (First class with distinction).

Master of Science (M.Sc) in Medical Biochemistry (2010 - 2013) at School of Medical Education, Mahatma Gandhi University, Kottayam - 686008, Kerala, India (First class with distinction).

ACHIEVEMENTS

Secured M.G.University SECOND RANK in MSc Medical Biochemistry.

Qualified KSCSTE Research Fellowship 2015.

APPENDIX

PBS (1000 mL) pH 7.4

NaCl	-	8 g
KCl	-	0.2 g
Na_2HPO_4	-	1.44 g
KH_2PO_4	-	0.24 g

(Added distilled water to a final volume of 1000 mL, solution is filtered and stored at RT).

HBSS (1000 mL) pH- 7.4

KCl	-	0. 4 g
KH_2PO_4	-	0.06 g
NaCl	-	8 g
Na_2PO_4	-	0.0482 g

(Added distilled water to a final volume of 1000 mL, solution was filtered autoclaved and stored at 4 ºC).

SBF (1000 mL) pH- 7.4

NaCl	-	8.035 g
$NaHCO_3$	-	0.355 g
KCl	-	0.225 g
$KH_2PO_4.3H_2O$	-	0.231 g
$MgCl_2.6H2O$	-	0.311 g
1 M HCl	-	39 mL
$CaCl_2$	-	0.292 g
Na_2SO_4	-	0.072
Tris	-	6.118
1 M HCl	-	0 - 5 mL

(Added distilled water to a final volume of 1000 mL, solution was filtered autoclaved and stored at 4 ºC; Shelf life-1 month).